

The Origin and Evolution of the Tasmanian Dolerites

by

Janet M. Hergt

Thesis submitted for the degree of

DOCTOR OF PHILOSOPHY

THE AUSTRALIAN NATIONAL UNIVERSITY

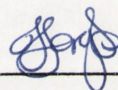
August 1987

STATEMENT

This thesis is based on experimental work carried out at the Research School of Earth Sciences and the Department of Geology, Australian National University between March, 1984 and August, 1987.

The data obtained by X-ray fluorescence and instrumental neutron activation techniques are the result of collaboration between Dr. B.W. Chappell and myself. Similarly, the ion-microprobe dating was done under the guidance of Drs. I.S. Williams and J.J. Foster. Dr. A.R. Chivas performed the stable-isotope mass spectrometry.

Unless otherwise acknowledged, all other analytical work, and the conclusions presented in this thesis are those of the author.



Janet Margaret Hergt
Research School of Earth Sciences
Australian National University

ACKNOWLEDGEMENTS

During the course of my studies at the ANU, I was in receipt of a Commonwealth Postgraduate Scholarship for which I am grateful. Through the generosity of the Research School of Earth Sciences and the Department of Geology, additional funds were made available for both fieldwork, and attendance at scientific meetings.

Special mention must go to my two supervisors, Drs. B. W. Chappell and I. McDougall for their help, advice and cooperation during my endeavours. I am very grateful to Bruce for his support, both in the lab, and in arranging additional finances for me to attend the ICOG conference in 1986. I should like to express my gratitude to Ian, for his prompt and critical reviews of first, second..., drafts of this thesis.

I also thank Ian, Bruce and Malcolm McCulloch for their help in collecting my samples in the first place! Material provided by the Tasmanian Department of Mines, the Hydroelectric Commission, Prof. Dave Green, and Prof. Gunter Faure are also greatly appreciated.

In the last three and a half years, I have had the privilege of working with many helpful and friendly people, including many who have instructed me in the 'whys and wherefores' of numerous analytical techniques. For their friendly advice and instruction I thank (in alphabetical order): Bruce Chappell, Allan Chivas, Maurie Cowen, John Foster, Ross Freeman, Les Kingsley, Elainor Laing, Roland Maas, Keith Massey, Malcolm McCulloch, Bill McDonough, Dave Nelson, Pat Oswald-Sealy, Mike Shelley, Roy, Suresh, Roberta Rudnick, Shen-Su Sun, Nick Ware, Jack Wasik, Liz Webber, Ian Williams and Dave Young. Limitation of space does not permit more personal thanks to these colleagues.

I would also like to take this opportunity of thanking Warrington Cameron, Dave Ellis, Malcolm McCulloch, Chris Gray, Robert Hill, Bill McDonough, Shen-Su Sun, Stewart Turner, and Ian Williams, for their careful and helpful reviews of parts of this thesis.

Finally, I thank my close friends and family for having the faith in me to finish this thing! I am particularly grateful to Paul, who, through his hours of faithful service (the "above and beyond the call of duty" type), has worked as hard at making my thesis a success, as he did his own!

ABSTRACT

The Mesozoic continental tholeiites of Gondwanaland have been extensively studied over several decades, often with much debate over the interpretation of some of the more unusual signatures observed. The Jurassic dolerites of Tasmania represent a small part of the widespread Mesozoic magmatism of Gondwanaland, and possess some of the most extreme isotopic and elemental signatures observed in tholeiitic rocks. The Tasmanian Dolerites are well exposed, and considerable in extent, providing an excellent opportunity for the investigation of the magma genesis and its evolution subsequent to emplacement.

In this study, the post-emplacement differentiation of some of the larger intrusions is examined, and detailed modelling of the possible petrogenetic history is presented. Comparison between selected Tasmanian Dolerites, and Jurassic tholeiites from southern Australia, and the Ferrar province of Antarctica is also made.

It appears that a mechanism of differentiation involving *in situ* crystallization at the floor of the larger intrusions, with the convective removal of residual liquids, is compatible with the chemical and mineralogical data. However, crystal settling models, although considered less likely, cannot be completely discounted.

The remarkable chemical uniformity of the magma at the time of emplacement is demonstrated (confirming earlier work), and includes a large amount of trace element and isotopic data previously unavailable for these rocks. Many of the trace element and isotopic characteristics show remarkable similarities to continental crustal rocks rather than mantle signatures, indicating the dominance of a crustal component in the petrogenetic history of these tholeiites. Difficulties in reproducing the trace element signatures of the dolerites by crustal assimilation models, and the unreasonable isotopic compositions required of the contaminant, make such models unlikely.

The more favoured model presented here, involves the introduction of a small quantity of sediment (≤ 3 wt.%) into a depleted mantle source by the process of subduction. It is envisaged that the crustal signatures dominate the trace element and isotopic compositions of the mantle source (owing to the low abundance of incompatible trace elements originally present), and are inherited by magmas produced during partial melting.

Comparison between the results obtained for the Tasmanian Dolerites, and tholeiites from other areas in southern Australia, and the Ferrar province of Antarctica, confirms the existence of a single, large magmatic province during the Jurassic. The source contamination model briefly outlined above is applied on a regional scale, and some speculation is made on the possible implications of this model for other continental tholeiitic provinces of Gondwanaland.

CONTENTS

	Page
STATEMENT	(i)
ACKNOWLEDGEMENTS	(ii)
ABSTRACT	(iii)
TABLE OF CONTENTS	(iv)
CHAPTER 1. INTRODUCTION	1
CHAPTER 2. GENERAL GEOLOGY	5
2.1 Geological setting	5
2.2 Relationship with Gondwanaland	8
2.3 Previous work on the dolerites of Tasmania	11
2.3.1 Intrusive style	11
2.3.2 Petrography	12
2.3.3 Geochemistry	13
2.3.4 Petrogenesis	14
CHAPTER 3. POST-EMPLACEMENT DIFFERENTIATION IN THE TASMANIAN DOLERITES	16
3.1 Mineral Compositions	16
3.1.1 Compositional variation in the pyroxenes	16
3.1.2 Compositions of other phases	21
3.2 Geochemical Variation	22
3.3 Fractionation Models	25
3.3.1 The important phases and their compositions	25
3.3.2 Least-squares mixing calculations	26
3.4 Mechanisms of Differentiation	
3.4.1 Some aspects of settling versus in situ crystallization methods	30
3.4.2 Application to the Tasmanian tholeiites	33

CHAPTER 4. THE MAGMA COMPOSITION OF THE TASMANIAN DOLERITES	37
AND ITS PETROGENESIS	
4.1 Geochemistry	38
<i>4.1.1 Chemical variability of the chilled margin tholeiites</i>	38
<i>4.1.2 Major element composition</i>	40
<i>4.1.3 Ba, Rb, Sr, Cs</i>	41
<i>4.1.4 Sc, Co, Mn, V, Zn, Cu and Ga</i>	44
<i>4.1.5 Ni and Cr</i>	45
<i>4.1.6 The pre-intrusion evolution of the melt</i>	46
<i>4.1.7 Rare earth elements (REE)</i>	51
<i>4.1.8 Primitive mantle normalised (PMN) pattern</i>	52
<i>4.1.9 Elemental ratios: a comparison with mantle and crustal reservoirs</i>	54
4.2 Isotope geochemistry	55
<i>4.2.1 Sr isotopic composition</i>	55
<i>4.2.2 Nd isotopic composition</i>	56
<i>4.2.3 Pb isotopic composition</i>	58
<i>4.2.4 Oxygen isotopic composition</i>	59
4.3 Magma Genesis	61
<i>4.3.1 Crustal-level contamination</i>	63
<i>4.3.2 Mantle source contamination</i>	72
4.4 Summary	77
CHAPTER 5. RELATED THOLEIITES FROM ANTARCTICA AND	80
SOUTHERN AUSTRALIA	
5.1 A review of previous work on Antarctic tholeiites	80
<i>5.1.1 Distribution and age</i>	80
<i>5.1.2 Petrological work</i>	81
<i>5.1.3 Magma genesis</i>	83
5.2 Analytical results from the dolerites of Portal Peak	85
<i>5.2.1 Geochemical composition</i>	85
<i>5.2.2 Isotopic composition</i>	90
5.3 Analytical results for basalts from Kangaroo Island	92
and western Victoria	

5.3.1 <i>Geochemical composition</i>	93
5.3.2 <i>Isotopic composition</i>	96
5.4 Distribution of magmatic clan	97
CHAPTER 6. CONTINENTAL THOLEIITES- A COMPARISON	101
6.1 The major provinces	101
6.1.1 <i>The Karoo, southern Africa</i>	101
6.1.2 <i>The Paraná, South America</i>	105
6.1.3 <i>The Deccan traps, India</i>	106
6.2 General characteristics	110
6.3 Possible petrogenetic implications	115
CHAPTER 7. SYNTHESIS	117
BIBLIOGRAPHY	120
<u>APPENDICES</u> (see accompanying volume)	
APPENDIX 1.SAMPLE LOCALITIES	1
APPENDIX 2.SAMPLE PREPARATION AND ANALYTICAL TECHNIQUES	7
2.1 Crushing	7
2.2 Determination of H₂O⁺, H₂O⁻, CO₂ and FeO	7
2.3 Preparation of glass discs and pressed powder pellets and their analysis by XRF spectrometry	8
2.4 Determination of trace element concentrations by INAA	9
2.5 Determination of trace element concentrations by SSMS	12
2.6 Determination Sr and Nd isotopic compositions	12

2.7 Determination of Pb isotopic compositions	13
2.8 Determination of oxygen isotopic compositions	14
APPENDIX 3. DETERMINATION OF ANALYTICAL PRECISION AND ACCURACY	15
3.1 Determination of analytical precision and accuracy	15
3.1.1 Precision	15
3.1.2 Accuracy	17
3.1.3 Isotopic data	20
3.2 Comparison between concentration data obtained by different instrumental techniques (XRF, INAA and ID)	23
APPENDIX 4. GEOCHEMICAL DATABASE	29
4.1 Database of Tasmanian samples	31
4.1.1 XRF and wet-chemical analyses of chilled and differentiated dolerites, as well as country-rocks sampled from contacts	32
4.1.2 XRF, INAA and wet-chemical analyses of chilled margin dolerites	66
4.1.3 XRF, INAA and wet-chemical analyses of differentiated dolerites	79
4.2 Database of Ferrar samples	88
4.3 Database of western Victorian and Kangaroo Island samples	98
APPENDIX 5. ISOTOPIC DATA	100
APPENDIX 6. ELECTRON MICROPROBE DATA	104
APPENDIX 7. ION-MICROPROBE U-Pb DATING OF ZIRCONS AND BADDELEYTTES	108
7.1 Age data	110
7.2 Concentration data	113
7.3 Summary	114
APPENDIX 8. ESTIMATE OF MAGMA TEMPERATURE DURING INTRUSION	115

CHAPTER 1

INTRODUCTION

Continental flood basalt petrogenesis has received close attention in recent years. This large-scale magmatism attests to major mantle-melting episodes, particularly in the case of the Mesozoic provinces of Gondwanaland where millions of cubic kilometres of magma were generated across distances of thousands of kilometres. Such magmatic events are important in evaluating the role and composition of mantle reservoirs underlying continents.

The recognition and characterisation of a variety of mantle reservoirs from studies of basalts from the oceanic environment (e.g. Hofmann and Hart, 1978; Hart, 1984; Sun and McDonough, 1987) allows the re-evaluation of signatures observed in continental tholeiitic rocks. Many of the world's continental tholeiitic provinces have recently been studied using detailed isotopic and geochemical data (e.g. the Karoo of southern Africa, the Paraná of South America, the Deccan Traps of India and the Columbia River Basalts of the United States). Geochemical and isotopic signatures are broadly similar in many of these basalts, but there remains considerable controversy as to how these signatures were derived.

The Jurassic tholeiites of Tasmania represent a small part of the enormous magmatic episode across Gondwanaland. Although extrusive flows have recently been recognised in Tasmania, the tholeiites are almost entirely represented by intrusive rocks which form large sheets, sills and dyke-like bodies. Previously reported geochemical and isotopic data on dolerites from Tasmania have revealed several important features: 1) Although the thicker sheets show marked differentiation, chilled margin samples from different localities have remarkably uniform major element compositions (Edwards, 1942; McDougall, 1962); 2) The chemistry of the dolerites is similar to many continental tholeiites but with higher SiO_2 , CaO and Al_2O_3 , and lower FeO , TiO_2 , Na_2O , K_2O and P_2O_5 contents compared with other Mesozoic tholeiites of Gondwanaland. An important exception is the Ferrar Group of Antarctica, where the match with the Tasmanian Dolerites is very close (Edwards, 1942; Walker, 1961; Gunn, 1962); 3) Some characteristics of the chemistry (K/Rb, Th/K, U/K) and isotope composition (initial $^{87}\text{Sr}/^{86}\text{Sr} = \sim 0.710$) are more typical of continental crust than of mantle-derived melts (Heier *et al.*, 1965; Compston *et al.*, 1968).

This third observation has been further reinforced by rare-earth element (REE) data (obtained for a single sample of dolerite from Tasmania) which show a chondrite normalised pattern of light rare-earth element (LREE) enrichment and a depletion in Eu (Philpotts and Schnetzler, 1968). Also, additional isotopic data including Sr, Pb and Nd results (Allègre *et al.*, 1982) were interpreted as more akin to continental crust than mantle in character. In contrast, the limited oxygen isotope data available in the literature are close to mantle compositions for the samples measured (Brooks and James, 1978).

In the present study, two major questions of continental tholeiitic magmatism are explored. First, the compositional variation caused by differentiation in many of the intrusions is examined. Sheets exceeding 200-300 m in thickness commonly show a broad zone of high

MgO content (relative to the MgO content of the original magma) towards the base and progressive Fe-enrichment above this zone. In this study, the chemical variation has been studied using both whole rock and mineral compositions, and the mechanisms controlling the differentiation are considered. Over 200 samples of dolerite from Tasmania have been analysed to investigate the post-emplacement evolution of the intruding magmas. These include several vertical sections obtained from drill-core, as well as the strongly differentiated felsic members from Red Hill previously documented by McDougall (1962).

Second, using the results obtained from the range of rock-types, chilled margin samples were chosen for study, in an attempt to obtain information on the petrogenetic history of the dolerite magma. The chilled margin rocks are believed to be quenched liquids judging from their glassy texture and low abundance of microphenocrysts. As the pyroxene microphenocrysts in these chilled dolerites have the most magnesian compositions obtained from the samples analysed, they are likely to provide a close approximation to the most primitive magma composition at the time of intrusion, prior to differentiation.

The results summarised in this thesis have been divided into these two main topics and are preceded by a brief discussion of some of the general geology of Tasmania in Chapter 2. Following this, parts of the geological history of Tasmania are placed in a wider perspective through comparison with events in other areas of Gondwanaland. A review of previous work including the petrography and field relations of the Tasmanian Dolerites is also included in Chapter 2.

The major contribution of this study is the documentation and interpretation of detailed geochemical and isotopic data obtained on a large number of samples from many localities in Tasmania (Fig. 1.1), as well as related samples from western Victoria and Kangaroo Island, and a suite of samples from Portal Peak in Antarctica. Geochemical analyses of close to 300 samples, together with isotopic compositions for nearly 50 of these, are presented in the accompanying volume of appendices. These data have been separated from the text for the readers' convenience.

Discussion of the geochemical and isotopic results is divided into four parts:

1. In Chapter 3, some of the thicker differentiated sheets in Tasmania are examined. The chemical variation from whole rock analyses is combined with electron-probe data obtained on minerals to evaluate the phases controlling the fractionation. Possible mechanisms responsible for the differentiation within these intrusives are also discussed.
2. An estimate of the compositional characteristics of the intruding magma is made in Chapter 4. This includes a study of the possible evolution of the magma after leaving its source but prior to emplacement, and the interpretation of the petrogenetic implications of the magma signatures.
3. The similarities between the tholeiites of Tasmania and those of the Ferrar province in Antarctica are examined, using the results of previous investigations carried out in Antarctica (presented as a review in the first part of the chapter), and additional analytical data obtained in this study on

dolerites from Portal Peak. Results from several samples from western Victoria and Kangaroo Island in southern Australia are also compared with the Tasmanian Dolerites and an estimate of the extent of this clan of magmatism is made (Chapter 5).

4. Comparison of the data presented for the Tasmanian Dolerites (in Chapter 4) is made with similar data from selected continental flood basalt provinces after a review of some of the main features of these larger provinces (Chapter 6).

The thesis concludes with a summary of the main points presented. Included in the accompanying appendices are details of the sample localities (Appendix 1) and analytical techniques employed in obtaining the data (Appendix 2). A detailed discussion of the precision and accuracy of many of the techniques is included to illustrate the quality of the data. This study has employed many different analytical techniques to obtain the results presented in the database. Thus, a comparison between the results obtained for the same elements determined by different methods has also been possible (Appendix 3). The large database is located in Appendix 4, and has been divided into subgroups for easy reference. Isotopic and mineralogical (electron probe) data obtained from selected samples are given in appendices 5 and 6 respectively. Dating of the Red Hill intrusion of Tasmania by ion-probe U-Pb analysis of zircon and baddeleyite separates is presented in Appendix 7. Finally, the methods used in estimating the temperature of the Tasmanian Dolerite magma at the time of emplacement are outlined in Appendix 8.

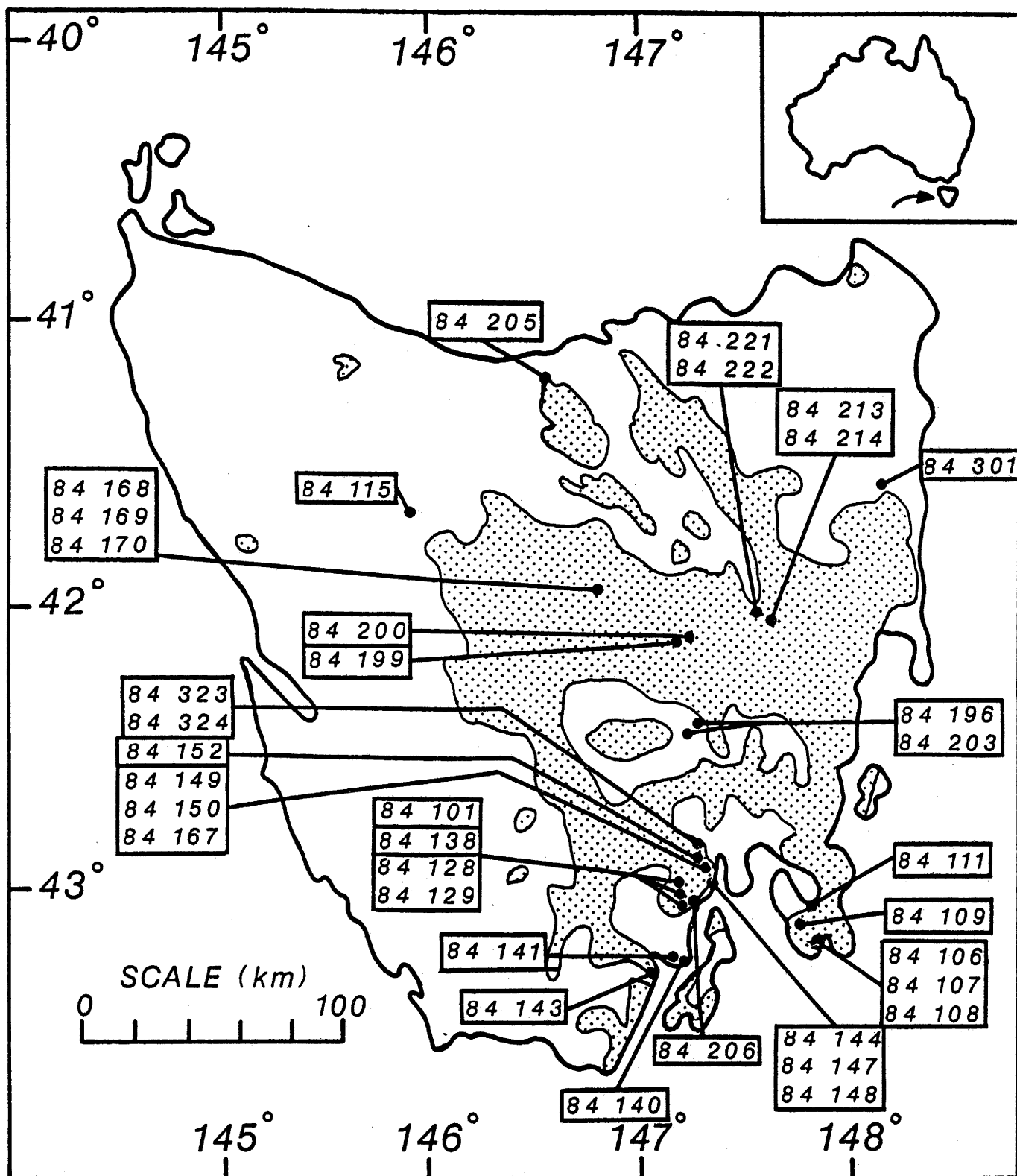


Fig. 1.1 Sketch map of Tasmania indicating the sample localities of chilled margins (identified by catalogue numbers) and differentiated dolerites. The stippled pattern gives a generalised representation of the dolerite outcrop (Modified from Spry, 1962).

CHAPTER 2

GENERAL GEOLOGY

In the first part of this chapter some aspects of the geology of Tasmania are discussed. The basement geology is briefly reviewed as a guide to the composition of the crust through which the magma migrated prior to emplacement. The sedimentary sequences into which the majority of the dolerites were emplaced are also described; these give an indication of the geological environment in Tasmania shortly before the widespread magmatism.

Tasmania probably was originally part of, or adjacent to, the Pacific margin of Gondwanaland prior to sea-floor spreading. It is, therefore, useful to place Tasmania in a wider geological perspective by examining the geology of other areas along the ancient Pacific margin of Gondwanaland. It is evident that some major episodes of tectonism are shared by continents believed to be adjacent at the time. These sections are intended to provide a basis for discussion of the widespread magmatic activity which occurred throughout the Gondwanide continents during the Mesozoic.

Previous research on the Tasmanian Dolerites is also reviewed under four headings. An outline of the mechanism of intrusion of the magmas is followed by a review of earlier petrographic and geochemical studies of these rocks. Finally, the interpretation of the geochemical and isotopic data in terms of magma petrogenesis is reviewed.

2.1 GEOLOGICAL SETTING

Surface exposure in Tasmania indicates a change in basement lithologies in the east compared with the west. Lithologies in the eastern one-third of Tasmania are strongly folded but virtually unmetamorphosed Ordovician to Devonian greywackes and shales, termed the Mathinna Beds (Banks, 1962a). These are intruded by Devonian granites (McDougall and Leggo, 1965; Cocker, 1982). In contrast, the basement in western Tasmania consists of two Precambrian blocks separated by the Cambrian Dundas Group. The Precambrian blocks include deformed and metamorphosed quartzites and pelites (with minor amphibolite), as well as comparatively unmetamorphosed orthoquartzite-mudstone, turbidite and dolomite sequences. These and the overlying Ordovician-Devonian sedimentary sequences (Banks, 1962b) are intruded by granites ranging in age from the Precambrian (restricted to King Island) to younger bodies emplaced throughout much of the Palaeozoic (McDougall and Leggo, 1965), as well as Precambrian dolerites. The Dundas Trough contains the Mt. Read calc-alkaline volcanics, and turbidite and shallow marine sediments (Spry, 1962; Banks, 1962c). The composition and structure of Ordovician sediments on the east and west banks of the Tamar River are markedly different, indicating a well defined boundary between the two parts of Tasmania in this area (Williams, 1978a).

Recent studies of granitic rocks indicate that the subdivision of Tasmania into two distinct provinces based on surface geology also extends to the depth of granite genesis, and the two separate geochemical zones have been termed the Bassian (east) and Taswegian (west) terranes

(Stump *et al.*, 1986). These terranes are believed to represent two microplates of different geological history that have subsequently been juxtaposed (A.J.R. White pers. comm., 1987), possibly along the Tamar Fracture System, which is a major tectonic feature dividing east and west Tasmania (Williams, 1978a).

Although the location of the Tamar Fracture System is well constrained in the northern part of Tasmania (indicated by the Tamar Graben), it is not obvious where it extends to in the south. There is some suggestion from an electrical conductivity survey that it may continue east to a position somewhere near Maria Island (Hermanto, 1985), (Fig 2.1). This may be a subordinate fracture system branching off the main structure however, and it has been suggested that the Tamar Fracture System may be located much further to the west, possibly closer to Hobart (Williams, 1978a).

The results of a seismic survey across northern Tasmania have been interpreted as indicating that the Tamar Fracture System extends to the Moho (Richardson, 1980). This model also calculates a remarkably thin crust for Tasmania (22.3-27.4 km); however, this assumes that the sharp increase in compressional wave velocity (from ~6 to ~8 km/s) represents the crust-mantle interface. A recent comparison between the geological Moho (defined as the transition between felsic-mafic crustal rocks and a dominantly ultramafic upper mantle) and the Moho interpreted from seismic data is given in Griffin and O'Reilly (1987). These authors argue that a lower crust with a significant amount of mafic cumulates or frozen magmas may be interpreted as "mantle" in geophysical profiles. In addition, it is also argued that the increase in compressional wave velocity of mafic granulites during cooling could result in these rocks being seismically defined as mantle. Using these arguments, if there is a significant amount of mafic material in the lower crust of Tasmania, the crustal thickness may be as great as ~35-40 km, more typical of continental crust in general.

The data used in Richardson's model were obtained along a traverse from Savage River (north-west) to St Helens (north-east) using several quarry blasts (Fig. 2.1) combined with results from previous studies. Although the actual crustal thicknesses are open to alternative interpretation, the proposed model yields a crustal profile which bulges to a maximum (with an increase of 4 km above the average thickness) at the Tamar Fracture System. The increase in the thickness of the crust at the Tamar Fracture System has been interpreted by Richardson as strong evidence that this structure is a major break in the crust.

It appears that geological and geochemical data are consistent with a change in the crust between east and west Tasmania. This division may be defined by the Tamar Fracture System, and possibly extends to the crust-mantle boundary.

If Tasmania comprises two microplates with separate histories, there can be no doubt that they were juxtaposed prior to the Late Carboniferous. The evidence for this is provided by widespread occurrence across both terranes of a near flat-lying Late Carboniferous-Triassic sedimentary sequence termed the Parmeener Supergroup (Banks, 1973). The Parmeener Supergroup is relatively thin (~1000 m, not including the tillites at the base of the sequence which vary in thickness) and unconformably overlies the two terranes previously described. The lower part of the sequence is Late Carboniferous to Permian and alternates between marine and

freshwater sequences (Clarke and Banks, 1975).

The lowermost part of the Parmeener Supergroup consists of a tillite sequence, and from microflora and fauna preserved at different levels, tillite deposition is believed to have persisted from the Late Carboniferous through to the Early Permian. Above this, shallow-marine deposits rich in Permian faunas grade upwards into a thin freshwater sequence containing coal measures, before returning to shallow-marine sedimentary rocks. The types of fauna preserved in the marine sequences attest to a cold-water shallow-marine environment of deposition. The Permian section of the Parmeener Supergroup is terminated with the deposition of the Upper Freshwater Sequence which contains *Glossopteris* flora as well as microfloras of Permian age.

The upper part of the Parmeener Supergroup is Triassic in age and composed entirely of freshwater sedimentary rocks consisting of sandstones, siltstones, mudstones and coal measures. The thickness of these lacustrine and fluvial sediments varies between approximately 450 and 600 m (Hale, 1962).

Sedimentation ceased in the Late Triassic or possibly Early Jurassic and was followed by the intrusion of a large volume of tholeiitic magma at 175 ± 8 Ma (Schmidt and McDougall, 1977; recalculated using the recommended decay constants of Steiger and Jäger, 1977) which is Mid-Jurassic according to the timescale of Harland *et al.* (1982). The dolerites are relatively scarce in the basement lithologies and occur almost exclusively within the nearly flat-lying sediments of the Parmeener Supergroup. The present estimate of around 15,000 km³ for the volume of magma emplaced in Tasmania is based on the extent of outcrop and average thickness of sheets. Although extrusive tholeiites of Jurassic age are almost entirely absent in Tasmania, a small area believed to contain Jurassic flows has recently been located ~70 km SSW of Hobart (Banks *et al.*, in prep). The estimated volume is therefore likely to be a minimum, especially if considerable extrusive material has been stripped by erosion.

Despite the widespread intrusion of magmas throughout Tasmania, the sedimentary rocks of the Parmeener Supergroup remain essentially flat-lying. It has been shown that instead of significant tilting and distortion of the sedimentary beds, intrusion was facilitated by extensive block-faulting, the dolerite having made room for itself by lifting the sediments (Carey, 1961a,b).

Reactivation of Jurassic structures, and additional block-faulting occurred during a period of extension in the Tertiary-Recent (Solomon, 1962). This is exemplified by three dominant horst features, the western coastal range, the central highlands, and the eastern horst represented by Ben Lomond. Between the latter two horsts is the complex graben structure of the Midland Valley extending from Launceston to Hobart, which has been referred to as the Tamar Fracture System in the earlier part of this discussion. During this tensional phase there was only limited sedimentation in restricted basins, but a considerable outpouring of Tertiary-Recent basalts.

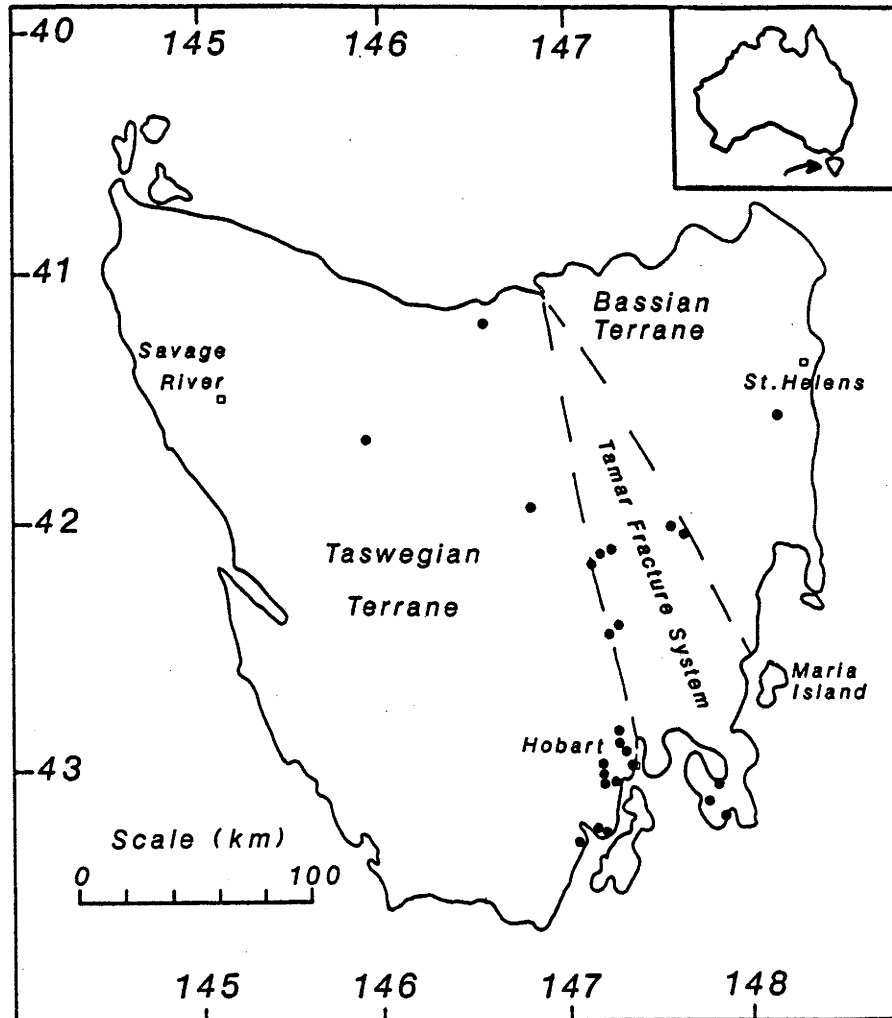


Fig. 2.1 Map of Tasmania illustrating the possible location of the Tamar Fracture System, the two granite terranes, and some of the landmarks referred to in the text.

2.2 RELATIONSHIP WITH GONDWANALAND

Despite early reluctance by the scientific community to believe in the existence of a protocontinent (Gondwanaland) combining the continents of the southern hemisphere (and India), this concept has become widely accepted owing to the wealth of supporting evidence now available. This includes the remarkable fit of continental margins, similarities in lithological and tectonic units across adjacent continental boundaries, continuity in glacial and fossil records between continents, paleomagnetic direction data, contemporaneous magmatism throughout the major fragments during the Mesozoic, and marine magnetic anomaly records.

Many attempts at reassembling all or parts of Gondwanaland have been made (e.g. Wegener, 1912; Du Toit, 1937; Carey, 1955; Bullard *et al.*, 1965; Craddock, 1975; and many others). In all such reconstructions, Tasmania is situated close to the Pacific margin of the Gondwana landmass. Craddock (1975, 1982) provided a detailed review of the tectonic evolution of the Pacific margin of Gondwanaland and suggested that this area was an active continental margin from the Late Precambrian until the fragmentation of Gondwanaland in the Mesozoic.

Craddock (1982) suggested that three major orogenic episodes in this region represent peaks in tectonic activity during the Early Palaeozoic, Middle Palaeozoic, and Permo-Triassic,

and are defined by deformation, igneous activity and regional metamorphism. These orogenic episodes took place prior to the breakup of Gondwanaland; however, they are not developed (or exposed) in all fragments of Gondwanaland (Fig. 2.2).

With the close of this activity, a comparatively stable period resulted in extensive sedimentation along the Pacific margin (Craddock, 1982). The Parmeener Supergroup of Tasmania exemplifies this sedimentation and has been discussed in section 2.1. Correlatives of this sequence have been identified in Antarctica (Beacon Supergroup), southern Africa (Karoo System), in the Paraná Basin of South America (Tubarao and Santa Maria sequences), and also in India, Madagascar and the Falkland Islands. The similarity between these sequences is remarkable indicating that the environments in these areas of Gondwanaland were comparable shortly prior to widespread magmatic activity.

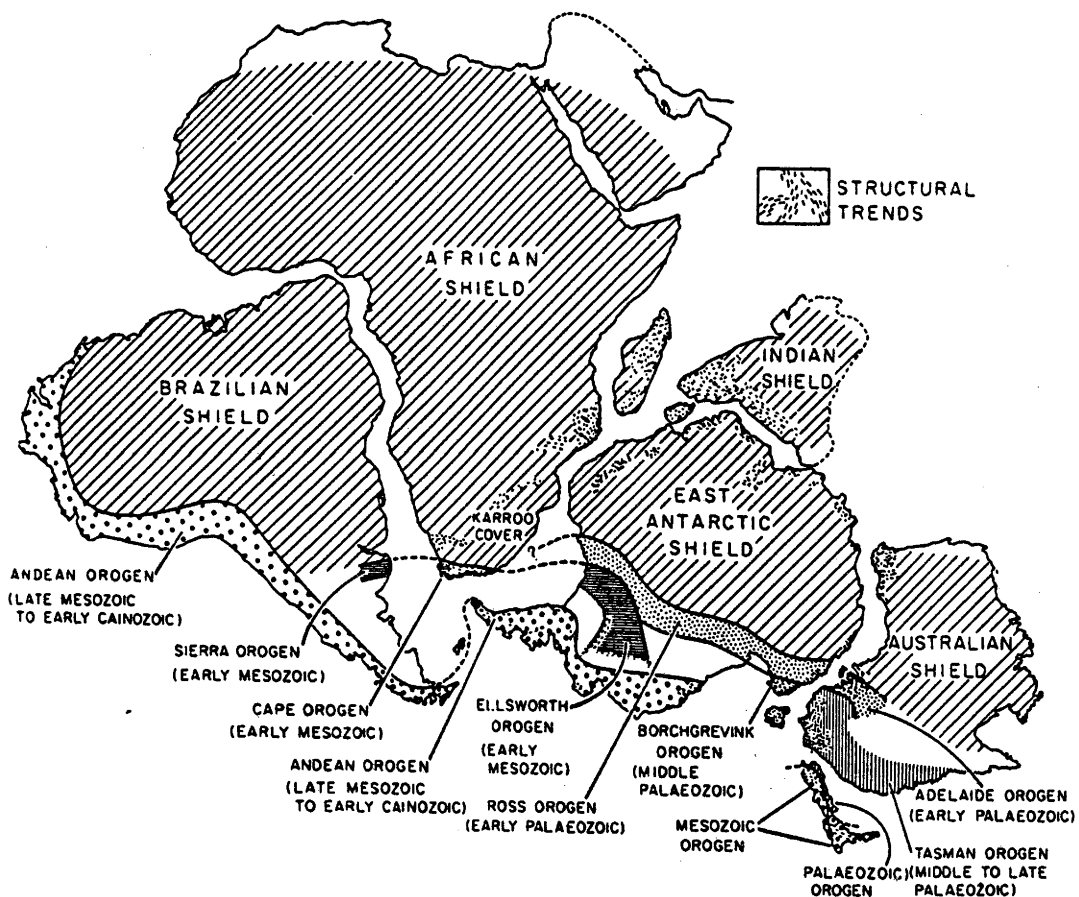


Fig. 2.2 Reconstruction of Gondwanaland showing the correlation of geological events across adjacent coastlines (From Craddock, 1975).

During the Mesozoic, Gondwanaland ceased to act as a single supercontinent. One of the first indications of fragmentation was heralded by the vast outpouring and intrusion of continental tholeiitic magma, resulting in huge magmatic provinces such as the Karoo of southern Africa (Fig. 2.3). Igneous activity occurred throughout Gondwanaland but was not entirely synchronous and preceded separation of continental blocks by ~50-75 million years or so in some cases.



Fig. 2.3 Reconstruction of Gondwanaland (from Craddock, 1975) showing the extent of continental tholeiitic magmatism. The oldest occurrences include the Karoo, Dronning Maud Land, Ferrar and Australian tholeiites, which span a period from the Early-Middle Jurassic. Some members of the Karoo province, and the volcanics of the Paraná Basin are Cretaceous; and the Deccan Traps are Late Cretaceous-Tertiary in age. (Refer to Chapter 6 for details and sources of these ages).

Veevers *et al.* (1981) gave a model of fragmentation involving several stages, based upon marine magnetic anomalies.

Stage 1. 150-125 Ma: East (South America, Africa, Madagascar and India) and west (Antarctica, Australia and New Zealand) Gondwanaland separate.

Stage 2. 125-105 Ma: India becomes separated and Madagascar is brought to its present position.

Stage 3. 105- 90 Ma: Sea-floor spreading between Australia and Antarctica, South America and Africa, and Australia and New Zealand is initiated. No further movement occurs between Africa, Madagascar and India. After stage three, India and Madagascar separate and India migrates rapidly towards its present position.

A more detailed account of the separation of Antarctica and Australia has been outlined in Mutter *et al.* (1985). Their reconstruction gives complete closure between the continents at around 100 Ma with the oldest marine magnetic anomaly corresponding to anomaly 34 time (~85 Ma ago) and rift-to-drift transition between ~60-110 Ma.

Mutter *et al.* (1985) suggested that the margin between Antarctica and Australia experienced an extraordinarily slow initial spreading rate (< 5 mm per year half rate) and believe that this is supported by evidence from subsidence patterns in the sedimentary basins of the southern margin of Australia. These authors also documented a west-east progression of subsidence patterns and truncation of magnetic anomalies, and suggested that fragmentation therefore proceeded from west to east. Their calculated propagation rate is approximately 2 cm per year beginning at the end of rifting, at the commencement of sea-floor emplacement.

2.3 PREVIOUS WORK ON THE DOLERITES OF TASMANIA

2.3.1 *Intrusive style*

Much of the landscape of Tasmania is dominated by Jurassic dolerite owing to its marked resistance to erosion. Hills and mountains are commonly capped by unroofed intrusions of dolerite, and there are many spectacular exposures (ranging up to ~300 m high) of vertical pillars of columnar jointed dolerite. The dolerite is well exposed as a result of uplift during extensive block-faulting both contemporaneous with, and post-dating emplacement (Carey, 1961a), followed by considerable subsequent erosion.

The Jurassic tholeiites of Tasmania crop out over an area of about 30,000 km² and as previously noted are generally confined to the essentially flat-lying Permo-Triassic sediments of the Parmeener Supergroup (with very little occurring in the basement rocks). The intrusive form includes sills and discordant sheets typically 100-400 m thick, as well as dykes and dyke-like protrusions (up to 1 km or more wide) from sheets.

Carey (1961a, 1961b) showed that the dolerite intrusions occur as large cone sheets rising from a restricted number of feeders. He suggested that the basaltic magma rose through most of the continental crust confined to relatively narrow conduits. On encountering the horizontal sediments of the Parmeener Supergroup however, lateral migration could be easily accommodated. Carey suggested that because of the higher density of the magma relative to the sedimentary sequence, less work was required in lifting the sedimentary pile than would be necessary in transporting the magma to the surface.

This mode of intrusion was confirmed by Leaman (1972) after a detailed gravity survey covering an area of 2,300 km² in southeastern Tasmania located numerous feeders and traced the dolerite extending from them. The centres appear to be pipes up to 1.6 km in diameter, however a few are dyke-like. A number of feeders were shown to continue to significant depth (at least 11-12 km in one case), and the dolerite feeders occupy major fractures in the crust which may have been used as a means of conveying the magma from its source.

Jaeger and Green (1961) found that within differentiated intrusions, samples from various levels show a range in density (~2.85 to ~3.00 g/cm³). These authors constructed a model based on the measurement of the density of drill-core samples through a differentiated sheet, in order to relate the results to other localities where part of the intrusion was unavailable for sampling. It was suggested that this type of comparison could help: 1) estimate the depth to the lower contact in drill-cores which had failed to penetrate the bottom of sheets, 2) determine the throw of faults causing displacement in intrusions, and 3) calculate the thickness of dolerite

lost by erosion from the tops of exposed sheets.

Palaeomagnetic work also indicated that the dolerites were normally polarised with steep directions indicative of the position of Australia relative to the southern pole at the time of emplacement (Irving, 1963; Schmidt and McDougall, 1977).

2.3.2 Petrography

The intrusive contacts between dolerite and its host sediment are sharply defined, even where mobilization of sediment has occurred and rheomorphic veining is observed. In the more siliceous hosts, hornfelsing is only evident for a metre or so from the contact, however the calcareous sediments may be noticeably affected for several tens of metres. Closely spaced jointing is common in the chilled margin dolerite but there is no difficulty in obtaining petrographically fresh material.

Detailed petrographic descriptions of Tasmanian Dolerites have been given by several workers. Careful modal and textural analyses were performed by Edwards (1942) and Joplin (1957). Although the mineral assemblages described in these reports are similar to those of many other provinces, the Tasmanian Dolerites have an unusually high proportion of fine-grained material (mesostasis) between the main phases (Walker, 1961). Additional work by McDougall (1961, 1962 and 1964) on differentiated intrusions included a detailed investigation of the Red Hill intrusion, a large dyke-like body in southern Tasmania. This intrusion contains the most felsic members of the differentiation suite yet documented in Tasmania including fayalite-bearing dolerites and silicic differentiates with a high proportion of quartz and feldspar.

The strong chemical differentiation within a body is reflected in the change in composition and modal abundance of the mineral phases present. The dominant phases are pyroxene and plagioclase although mesostasis is common throughout. When fresh, the mesostasis contains quartz, alkali feldspar, rods of plagioclase, and opaques, and when altered appreciable chlorite is observed. The three pyroxene series occur in the dolerites, i.e. augites, orthopyroxenes and pigeonites. To summarise the literature, descriptions from several reports (referred to above) have been combined to give an idealised section through a hypothetical sheet. The compositions of minerals quoted have been obtained in this study by electron microprobe analysis, and are consistent with many of the results obtained in earlier studies by optical techniques.

Chilled margin samples are very fine-grained to glassy and contain less than a few per cent microphenocrysts. Primary orthopyroxene is restricted to a narrow zone at the chilled margins, and when present it occurs as blocky crystals of bronzite (En_{75-83}). Also present as rare microphenocrysts in the chilled margins are irregular augites, pigeonites and stumpy plagioclases (An_{75-80}). In the most glassy dolerites the plagioclases have forked terminations indicative of rapid quenching. Olivine has not been positively identified in the Tasmanian chilled margin dolerites.

Away from the contacts, the dolerite is medium-grained and dominated by pyroxene, plagioclase and iron oxide, usually with an appreciable amount of mesostasis. Over much of the crystallization history, two pyroxenes occur together, a Ca-rich variety of the augite series and a

Ca-poor variety of the pigeonite series. In the lower (approximately) one-third of the dolerite sheets, pigeonite has often inverted to orthopyroxene and exsolution textures are observed.

The early crystallizing pyroxenes are Mg-rich and are concentrated in the lower parts of the bodies so that the remaining magma becomes Fe-enriched. Thus later pyroxenes become more Fe-rich in the upper levels of the intrusions. The abundance of pyroxene and plagioclase decreases in later differentiates, being balanced by a marked increase in the amount of mesostasis. In those bodies where extreme fractionation and differentiation has occurred, fayalitic olivine (Fa_{95}) enters as a crystallizing phase at the expense of the Ca-poor pyroxene, and coexists with ferroaugite and more sodic plagioclase (An_{50}). In the Red Hill intrusion, the fayalite-bearing dolerite passes upward into a granophyre in which the mafic minerals are ferrohedenbergite and iron oxide, with quartz and alkali feldspar comprising more than 50% of the rock.

Accessory phases include chlorite, biotite, minor carbonate, pyrite, chalcopyrite, magnetite (with up to one third of the crystals invaded by ilmenite), prismatic hornblende and apatite. In the present study, the felsic differentiates from Red Hill were also found to contain zircon and baddeleyite.

2.3.3 Geochemistry

Detailed geochemical investigations of the Tasmanian Dolerites, mainly utilizing major element analyses, were undertaken by Edwards (1942) and McDougall (1962, 1964) on a number of sheets and dyke-like intrusions. Some trace element data were also provided by McDougall and Lovering (1963). These studies showed that the magma was remarkably homogenous on emplacement, and enriched in SiO_2 , Al_2O_3 and CaO with lower abundances of FeO , TiO_2 , Na_2O , K_2O and P_2O_5 compared with other tholeiites of mainly Mesozoic age in the southern (Gondwana) continents, although a close match was demonstrated with the Ferrar Dolerites of Antarctica.

From the geochemistry, Edwards (1942) showed that marked differentiation had occurred within the sheets and dyke-like bodies, and explained it in terms of fractional crystallization with settling of Mg-rich pyroxene towards the floor of the bodies under gravity, resulting in Fe and alkali enrichment in the residual liquid, especially in the sheets. Although Edwards (1942) did not find Fe enrichment in the dolerites from Gunnings Sugarloaf (a dyke-like body), the study of the Red Hill Dyke by McDougall (1962) showed that in such bodies similar trends occur in the higher levels.

The range of dolerite compositions was greatly extended by the study of samples from the Red Hill Dyke, in which coherent chemical trends were found through to rocks with SiO_2 contents greater than 65 wt.% with high alkalies and MgO contents of less than 0.5 wt.% (McDougall, 1962). Arguments were advanced favouring the view that the extreme compositions were produced by differentiation of the dolerite magma, rather than being the result of metasomatism of SiO_2 -rich sedimentary roof rocks of the intrusion, a conclusion further buttressed by isotopic data presented by Heier *et al.* (1965).

The study of the Red Hill samples allowed a better comparison to be made with other

well documented differentiated tholeiitic intrusions, and McDougall (1962) compared the iron enrichment trend with that of the Skaergaard rocks. Although the Fe enrichment is not as marked in the Tasmanian tholeiites, the trends are similar to each other, and distinct from that observed in calc-alkaline suites.

There is wide agreement that the differentiation revealed by the geochemical data is controlled by fractional crystallization with relative movement of phases, including residual liquids under the influence of gravity. In other occurrences of differentiated intrusions this is often accompanied by macroscopic layering, a feature absent in the Tasmanian Dolerites.

2.3.4 Petrogenesis

Another aspect of the Tasmanian Dolerites which has been addressed relates to the origin of the voluminous magma which gave rise to these rocks. Geochemical data, especially the measurement of trace elements and isotopic ratios, have provided a wealth of somewhat enigmatic information. These measurements reveal that the Tasmanian Dolerite magma possessed a most unusual geochemical signature with characteristics more akin to those of continental crust rather than upper mantle, from where such large volumes of magma might be expected to have been derived.

Heier *et al.* (1965) found that initial $^{87}\text{Sr}/^{86}\text{Sr}$ ratios of samples from the Red Hill Dyke and the Great Lake Sheet lay in the range 0.7106-0.7123, remarkably high values for basaltic magma. Brooks and James (1978) and Allègre *et al.* (1982) confirmed the high initial $^{87}\text{Sr}/^{86}\text{Sr}$ values for the Tasmanian Dolerites, extending the range to a lower value of ~ 0.7095 . Lead and neodymium data reported by Allègre *et al.* (1982) were also regarded as more typical of continental crust. In contrast, oxygen isotopic values in the range $\delta^{18}\text{O} = +6.2$ to $+6.4\text{‰}$, were interpreted by Brooks and James (1978) as consistent with upper mantle values. Philpotts and Schnetzler (1968) analysed a single sample of Tasmanian Dolerite and showed that it possessed a light rare-earth element enriched pattern (when normalised to chondrites) with a depletion in Eu. Although this pattern is similar to those observed in other continental tholeiites, the depletion in Eu is unusually large.

Virtually all of these geochemical features emphasise the continental crustal type signature for the Tasmanian Dolerites. In addition, the major element data show that the magma was silica-saturated on emplacement and is most unlikely to have been derived unmodified by partial melting of typical upper mantle compositions, as olivine would be expected to be a liquidus phase. Alternative explanations presented by previous workers include derivation from an atypical upper mantle source (strongly enriched in incompatible elements over a long period of time to allow the isotopic systems to evolve), derivation from a normal upper mantle source with marked fractionation and removal of olivine concomitant with thorough-going contamination by crustal materials (with either bulk or selective addition of crustal components), or by partial melting of crustal rocks.

In addition to the petrogenesis of the magma, the relationship between the magmatism and the break-up of Gondwanaland is also of interest. As early as 1968, Compston *et al.* showed that $^{87}\text{Sr}/^{86}\text{Sr}$ initial ratios similar to the Tasmanian Dolerites characterised the Jurassic

Ferrar Dolerites of Antarctica and interpreted these results as reflecting a common source and history for the magmas prior to the break-up of Gondwanaland when the two provinces were adjacent.

CHAPTER 3

POST-EMPLACEMENT DIFFERENTIATION IN THE TASMANIAN DOLERITES

A general account of the textural, mineralogical and geochemical variation observed in the Tasmanian Dolerites has been presented in Chapter 2.3. The lithologies vary from pyroxene-rich rocks to the silicic granophyres, and in the earlier studies, Edwards (1942) and McDougall (1962) explained the variety of rock-types as resulting from *in situ* differentiation caused by fractional crystallization of an originally homogeneous magma (represented by the chilled margins).

In the present study, a large number of samples were analysed from different intrusions for two purposes. Additional information documenting the range in composition of the rocks and their constituent minerals is presented, with a discussion of the possible mechanisms responsible for the development of compositional variation. Further study of the most magnesian rocks also relates to modelling the magma genesis. In the earlier studies mentioned, the authors argued that the chilled margins represented quenched liquids which were parental to the differentiates; this was based on the homogeneity of the chilled dolerites sampled from different intrusions, and the low abundance of microphenocrysts. The more magnesian compositions (i.e. dolerites with $> \sim 7$ wt.% MgO) were interpreted as being cumulates from the differentiation process.

A significant part of the present study involves modelling the magma genesis (Chapter 4). Therefore, although the chilled margins are texturally consistent with being quenched liquids, it is essential to confirm either that the chilled margins represent the most primitive liquids involved with the formation of the dolerites of Tasmania, or locate (or deduce from mineral compositions) the more magnesian parents.

A progressive change in the pyroxene compositions with differentiation appears to be closely linked with the geochemical evolution of the magma chamber (McDougall, 1961), and may be expected to provide information regarding the differentiation history. Therefore, before applying the bulk-rock chemistry to the problem of the differentiation history, it is worth examining the chemistry of the dominant mineral phases more closely. The discussion is mainly focussed on the pyroxene compositions; however, some comment will be made regarding the plagioclase and oxide compositions.

3.1 MINERAL COMPOSITIONS

3.1.1 Compositional variation in the pyroxenes

The probe analyses of pyroxenes from selected samples of this study (comprising rocks from Red Hill, Fingal, and various chilled margins) are illustrated on the pyroxene quadrilateral in Figure 3.1, and the spectrum of compositions obtained is almost identical to that previously documented (McDougall, 1961). The most magnesian low-Ca pyroxenes are En_{80-83} , and the most Fe-rich are En_{27} . It is possible that olivine ceased to be a liquidus phase only shortly prior

to emplacement, owing to the high magnesium content of the earliest pyroxenes (i.e. the cross-over to olivine-bearing assemblages occurs at $\sim\text{En}_{75}$ for the Palisades Sill, Walker *et al.*, 1973). The miscibility gap between the two pyroxene series converges with Fe-enrichment; however, the disappearance of pigeonite results in a marked increase in the Ca concentration in the clinopyroxenes.

There have been many studies of the causes for the chemical variation in pyroxenes formed by slow cooling of tholeiitic intrusions, and these will be examined in detail shortly. Importantly, the *pyroxenes from rocks sampled away from chilled margins have compositions either similar to, or less magnesian than pyroxenes measured in chilled margin samples*. This includes rocks with substantially higher MgO contents compared with the average of 6.7 wt.% for the chilled margin dolerites, and indicates that the pyroxenes from rocks with higher bulk-rock MgO contents crystallized from a liquid with similar, or lower MgO/FeO, than the chilled margins. Thus, the rocks with MgO contents greater than the chilled margins, are cumulates rather than products from liquids of higher magnesium content, confirming that *the chilled margins represent the most primitive liquid compositions available for studying the genesis of the Tasmanian Dolerites* (Chapter 4).

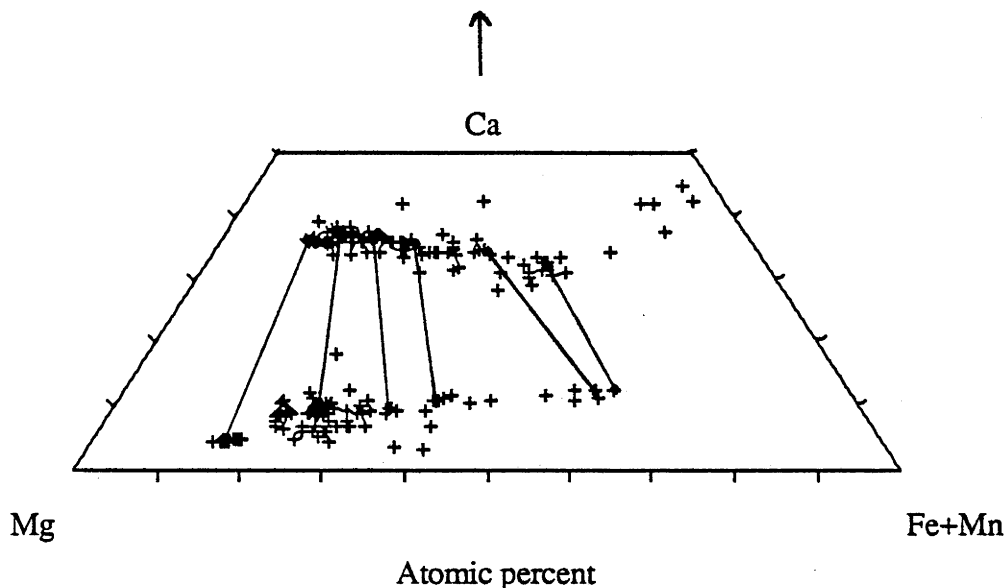


Fig. 3.1 Pyroxene quadrilateral showing the range in compositions of the pyroxene series with progressive differentiation (N = 210). Some scatter is likely to have resulted from exsolution during cooling. Representative tie lines joining coexisting phases are shown.

The minor element contents of pyroxenes have been documented by numerous workers (e.g. Hess, 1949; Muir, 1951; Kushiro, 1960; McDougall, 1961; Campbell and Borley, 1974). McDougall (1961) noted that the Al contents of pyroxenes from the Red Hill intrusion are low compared with pyroxenes from Skaergaard; also, the Al contents decrease with differentiation, and the pigeonite separate was found to contain less Al than the coexisting augite. These features have also been observed in the present study.

In addition, McDougall (1961) described the behaviour of Ti and Mn in the same separates. He found that the concentration of Ti and Mn increased with fractionation, and that

the pigeonite analysis showed a greater abundance of these elements compared with the coexisting augite. The results of the present study are the same in most respects; however, the Ti content in the pigeonites is always lower than that in coexisting augites (Fig 3.2). The lower Ti content in the pigeonites is consistent with other studies (e.g. Campbell and Borley, 1974), and it is not clear why the single pigeonite-augite pair analysed by McDougall (1961) showed the reverse behaviour.

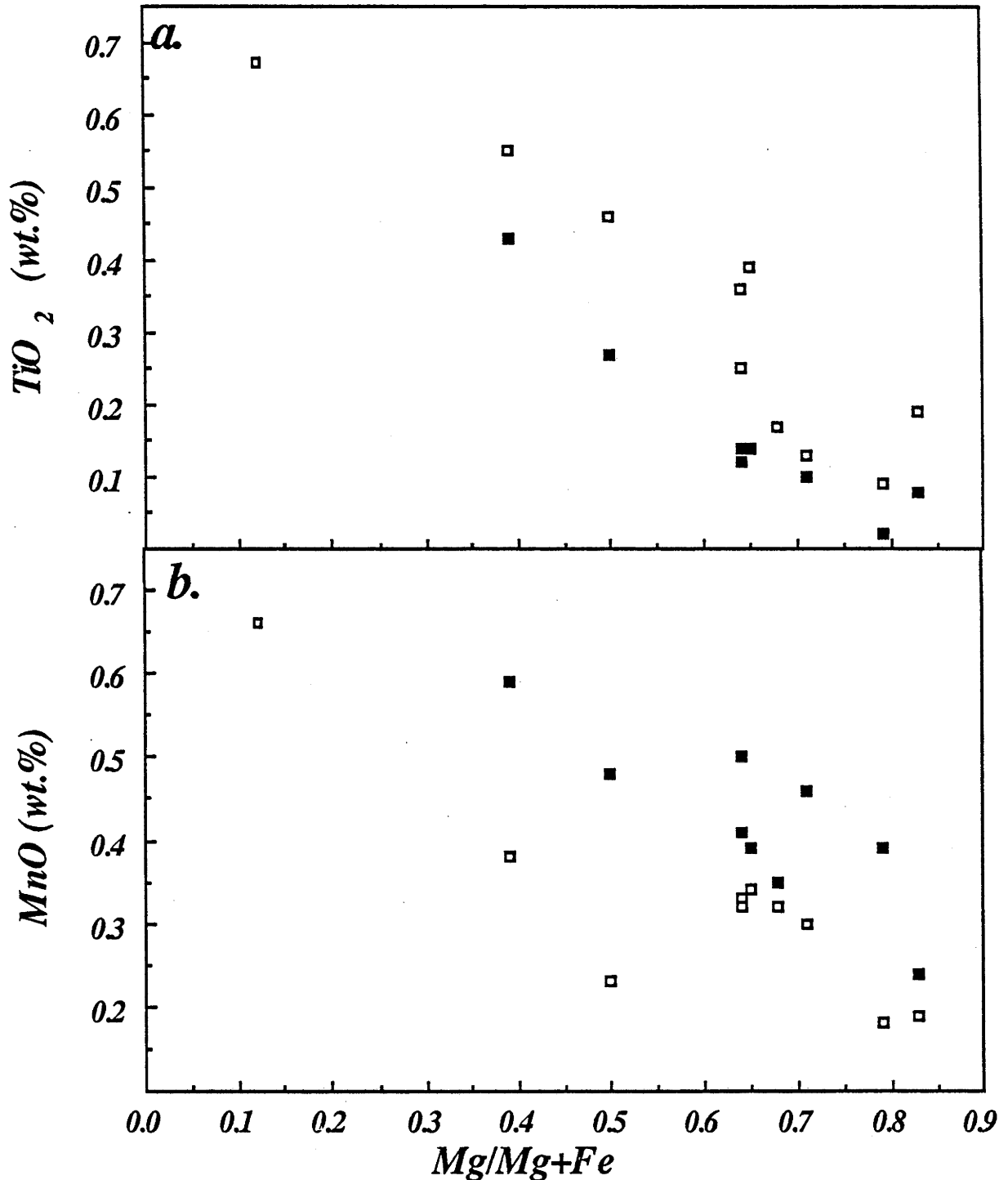


Fig. 3.2 Plots of minor element variation in analysed pyroxenes against the Mg/Mg+Fe of the clinopyroxenes. a. TiO₂ versus Mg/Mg+Fe. b. MnO versus Mg/Mg+Fe. In both diagrams the clinopyroxenes are represented by the open squares, and the pigeonite data are plotted as filled squares.

Some doubt has been cast on the reliability of mineral compositions in recording the chemical changes in magmas during crystallization (e.g. Campbell and Borley, 1974; Barnes, 1986). Barnes (1986) demonstrated that an apparent Fe-enrichment trend in pyroxenes could be produced by diffusion processes, for a sequence in which the pyroxenes were originally homogeneous. He proposed that although the residual melt trapped between magnesian liquidus pyroxenes would initially be in equilibrium with the minerals, with cooling the trapped melt could crystallize more Fe-rich pyroxenes as overgrowths around pre-existing crystals. If diffusion between the core and margins occurred, the resultant pyroxene composition analysed would be an average based on the relative contributions from the original liquidus composition and the more evolved pyroxenes.

Barnes (1986) calculated that the shift towards more Fe-rich compositions (termed the "trapped liquid shift") was relatively insensitive to the original composition of the pyroxene, but increased with an increase in the quantity of trapped liquid, and/or a decrease in the total FeO+MgO of the initial cumulus assemblage. The amount of trapped liquid was probably significant in the Tasmanian cumulates because the proportion of mesostasis is quite high, and increases in the more differentiated rocks, (see McDougall, 1962 Fig. 6, and section 2.3.2). It is notable however, that the absolute increase in Fe in rocks with decreasing MgO requires that the crystallizing pyroxenes were also more Fe-rich. Therefore, the change in the pyroxenes towards more Fe-rich compositions is consistent with fractionation, even if it may have been enhanced by later diffusion involving trapped intercumulus liquid.

Much research has been carried out on the role of pyroxenes during the differentiation of large tholeiitic intrusions (e.g. Brown, 1957; Brown *et al.*, 1963; Atkins, 1969; Walker *et al.*, 1973, and numerous others). Of particular interest has been the cause of the limit to the two-pyroxene field. In differentiated tholeiitic intrusions, the Ca-rich and Ca-poor pyroxene series crystallize together for much of the fractionation history; however, in many intrusions, a single Fe-rich clinopyroxene continues to crystallize after the disappearance of the pigeonite. In some intrusions the loss of pigeonite is accompanied by the appearance of fayalitic olivine (e.g. Skaergaard, Poldervaart and Hess, 1951; Red Hill, McDougall, 1961).

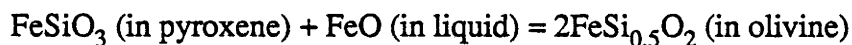
The loss of Ca-poor pyroxene from the crystallizing assemblage has been related to a decrease in the activity of silica by several workers, and Lindsley and Munoz (1969) suggested that the appearance of fayalitic olivine at a similar time to the disappearance of pigeonite observed in the Skaergaard and Bushveld intrusions may therefore be related by the reaction:



with the loss of Ca-poor pyroxene resulting from a decrease in silica activity in the melt. Carmichael *et al.* (1970) suggested a strong interdependence of silica activity and oxygen fugacity resulting from the crystallization of titanium-bearing magnetites. These authors argued that this interrelationship denies the choice between silica activity and oxygen fugacity as the main cause for the disappearance of pigeonite. Subsequent work has demonstrated the stability field of Ca-poor pyroxene is further increased at higher pressure (e.g. Lindsley, 1965, 1981).

The importance of silica activity, oxygen fugacity and pressure on the origin of the two-pyroxene minimum has been examined by Campbell and Nolan (1974). They concluded that the Fe/Mg in Ca-poor pyroxenes could be extended to higher values with an increase in both temperature and pressure. It was shown that the influence of silica activity on the stability of Ca-poor pyroxenes is dependent on the order of crystallization of minerals within the magma. In agreement with Lindsley and Munoz (1969), Campbell and Nolan (1974) demonstrated that an increase in the silica activity results in stabilization of Ca-poor pyroxenes with higher Fe/Mg, but this is only important in magmas which crystallize fayalitic olivine before quartz. For magmas in which quartz precedes the appearance of olivine, the activity of silica is so high, that any increase will not influence the stability field of the Ca-poor pyroxenes.

Campbell and Nolan (1974) suggested that the replacement of Ca-poor pyroxene by fayalitic olivine could only be achieved if the activity of FeO was high enough to satisfy the relation:



In this case the effect of oxygen fugacity on the stability of Ca-poor pyroxenes is indirect. Campbell and Nolan (1974) noted that the higher FeO (relative to Fe_2O_3) generated by a low oxygen fugacity would favour the production of fayalite at the expense of Ca-poor pyroxene. Also, the influence on the silica activity of the melt resulting from the formation of cumulus magnetite would be important (i.e. as proposed by Carmichael *et al.*, 1970), but only in cases where the silica activity is involved controlling the stability of Ca-poor pyroxene (i.e. where fayalite is crystallized before quartz).

Thus, the limit to the two-pyroxene stability field in tholeiitic intrusions is related to the chemical evolution of the magma during differentiation, which in turn is reflected in the mineralogy. Using the observation that modal quartz occurs before the disappearance of pigeonite in the Tasmanian Dolerites, the silica activity is likely to have had little effect on the position of the two-pyroxene minimum. This is consistent with the low En value of the last pigeonite to crystallize.

In addition to differences in the limit of the two-pyroxene field, the changeover from orthopyroxene to pigeonite, and the miscibility gap between the two pyroxene series differs between tholeiitic intrusions (Fig. 3.3). A narrowing of the miscibility gap, and an increase in the En content of the orthopyroxene-pigeonite changeover is generally attributed to higher magma temperatures (e.g. Campbell and Borley, 1974; Lindsley, 1983). The changeover from orthopyroxene to pigeonite in the Tasmanian Dolerites is at $\sim\text{En}_{75}$ which is consistent with the high magma temperature (at the time of emplacement) estimated from melting experiments, phase equilibria calculations, and the compositions of the chilled margin pyroxenes ($\sim 1200\text{-}1250^\circ\text{C}$; Appendix 8).

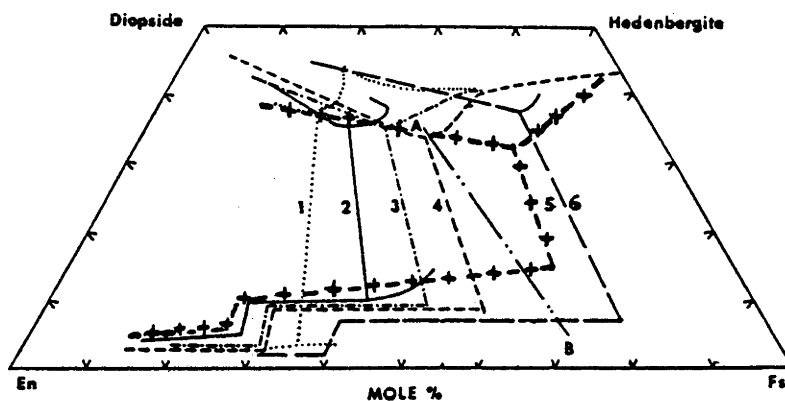


Fig. 3.3 Pyroxene quadrilateral illustrating the differences in pyroxene fractionation trends from various intrusions. 1. Sudbury, 2. Jimberlana, 3. Skaergaard, 4. Bushveld, 5. Tasmanian dolerites, 6. Bjerkrem-Sogndal. The line AB gives the limit to the two-pyroxene field for the Palisades Sill (Modified from Campbell and Nolan, 1974). Note that the Tasmanian dolerites have the highest Mg-pigeonites and the smallest miscibility gap.

3.1.2 Compositions of other phases.

Although McDougall (1962) documented a well defined progression towards more sodic plagioclase with differentiation, the probe results of the present study indicate that a remarkably wide range in compositions can be obtained in each sample, with only a general decrease in the An-content for increasing differentiation (Fig. 3.4a). Although the cores of the largest feldspars are typically more calcic compared with their rims, this relationship is not strict and a wide variation in An-contents can be obtained from the cores, rims and smaller plagioclases in any one section. Obtaining a representative composition for plagioclase is therefore impossible from these data, and an estimate has been obtained using the bulk-rock normative An-content (Fig. 3.4b).

The compositions of some magnetite-ilmenite pairs were also obtained by electron probe; however, these do not appear to reflect original compositions. Using the composition- fO_2 -T model for coexisting iron-titanium oxides of Spencer and Lindsley (1981), the oxide pairs consistently plot near the magnetite-ulvospinel miscibility gap, giving temperatures of 500-550°C compared with temperatures $\geq 750^\circ\text{C}$ obtained from pyroxenes in the same rocks (determined using the model of Lindsley, 1983). The intergrowth of these pyroxenes and oxides indicates that they are likely to have crystallized together; therefore, the oxides have evidently experienced sub-solidus re-equilibration, and do not give a measure of the T or fO_2 at the original time of growth.

As mentioned in Chapter 2.3.2, zircons and baddeleyites have been observed in the most differentiated rocks from Red Hill. Several of these have been dated using the ion microprobe, and, although more fully described in Appendix 7, the results indicate that these phases are likely to have crystallized from the fractionated magmas in the later stages of differentiation. Consistent with earlier geochemical and isotopic studies (i.e. McDougall, 1962; Heier *et al.*,

1965) no evidence was found to suggest that assimilated roof material was incorporated into these granophyres (i.e. no xenocrystic crystals or cores were found).

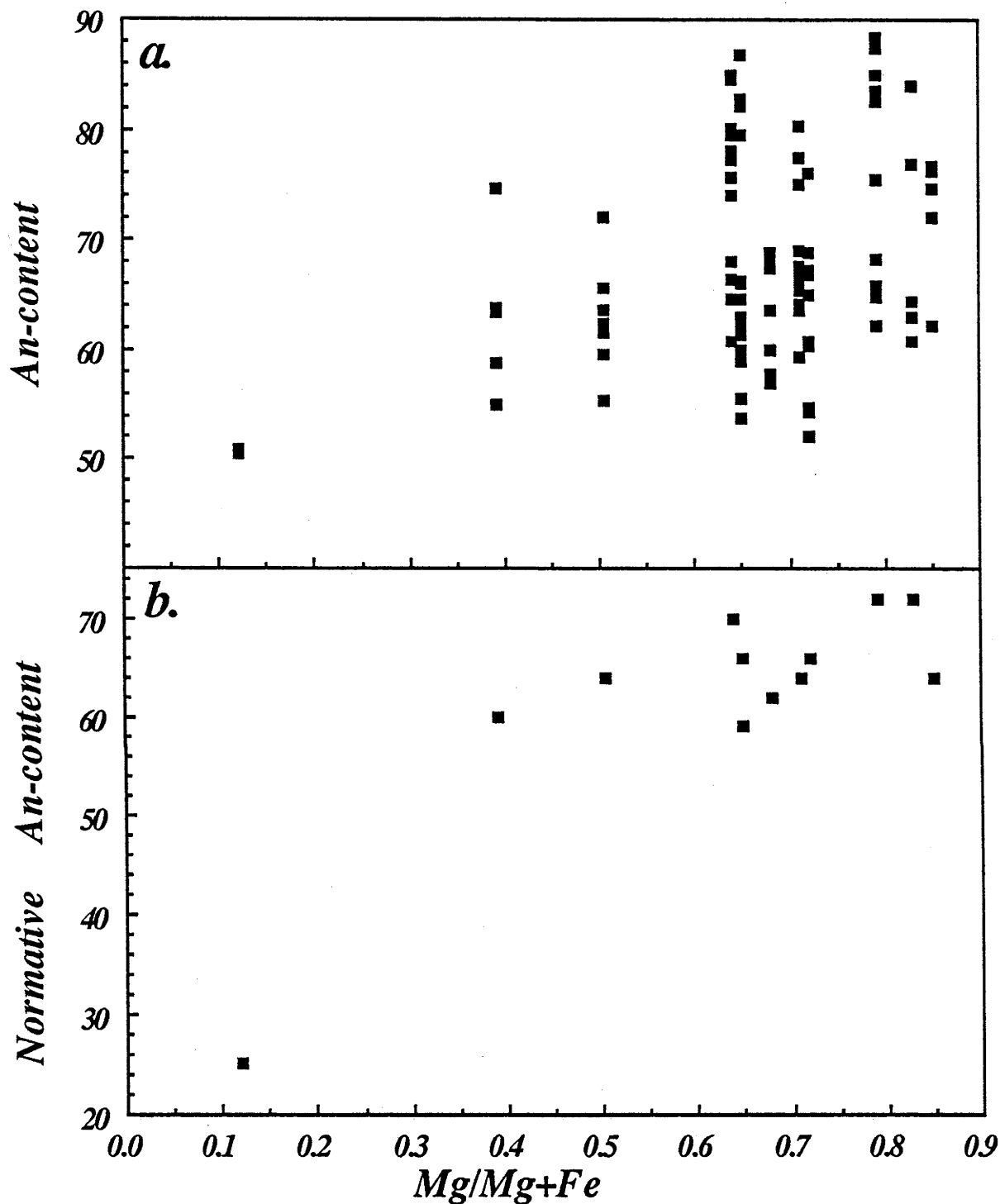


Fig. 3.4 Plot of plagioclase compositions obtained by a. electron probe and b. the bulk-rock CIPW norm, against the Mg/Mg+Fe content of coexisting clinopyroxenes for selected samples.

3.2 GEOCHEMICAL VARIATION

The whole-rock compositions obtained in the present study show a considerable range, from dolerites with ~53 wt.% SiO₂ and 12 wt.% MgO, to rocks with ~67 wt.% SiO₂ and less than 0.5 wt.% MgO; much of this range can be observed within a single intrusion.

McDougall (1961, 1962) illustrated the progressive enrichment in Fe relative to Mg in the bulk-rocks from Tasmania (in a plot similar to Fig. 3.5), and noted that the relative enrichment in Fe was accompanied by an absolute increase in Fe with differentiation.

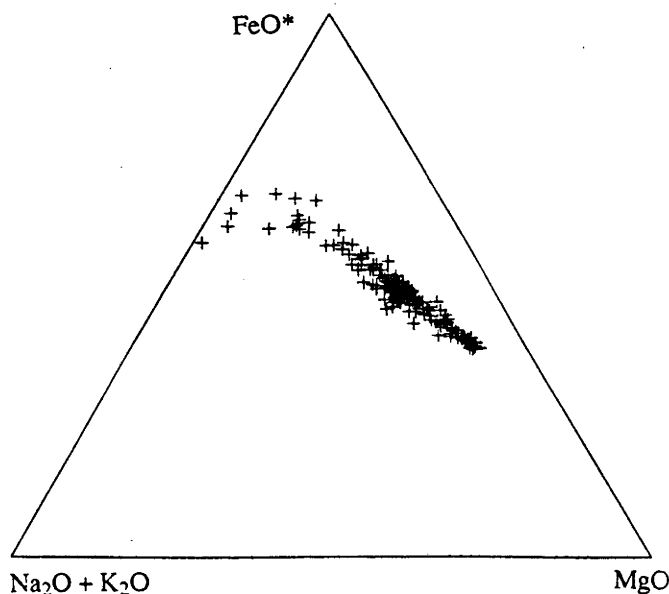


Fig. 3.5 FeO*-Na₂O+K₂O-MgO plot of the Tasmanian dolerites analysed in this study.

Most "element vs MgO" diagrams plotted for the differentiated dolerites show considerable coherence between samples from widely separated localities throughout Tasmania. Four examples of these diagrams, showing a range in chemical behaviour during differentiation are chosen as a means of illustration (Fig. 3.6). Chilled margins plot in a tight cluster approximately midway between the most and least magnesian endmembers, confirming the major element homogeneity noted by Edwards (1942) and McDougall (1962). The curves are defined by samples from a number of localities (Fig. 1.1), and in most cases the intrusions sampled have been eroded. Therefore, no single section has samples that span the entire differentiation trend; however, the coherence of the curves illustrated in Figure 3.6 suggests that study of the differentiation history using a combination of sections from different localities may be justified.

Much of the discussion that follows is based on a suite of 26 samples chosen for detailed analysis using INAA (Appendix 4.1c), and the average chilled margin composition (Chapter 4); however, the XRF geochemical data obtained on the rest of the Tasmanian dolerite samples (Appendix 4.1a) are consistent with the results discussed here. The 26 samples chosen include a suite of rocks from Red Hill (MgO from 0.20-3.10 wt.%), Mt. Wellington (MgO from 1.57-9.08 wt.%), and Fingal (MgO from 5.07-11.04 wt.%), as well as the average (N = 36) chilled margin composition (MgO = 6.7 wt.%).

Variation diagrams plotting "element (or oxide)" against wt.% MgO, chosen to illustrate the range of dolerite compositions, can be divided into three groups:

1. Those in which the concentration of the element or oxide increases with decreasing MgO. This group includes SiO₂, Zr (Fig. 3.6), K₂O, Na₂O, Ba, Rb, Th, Pb, Nb, Y and the REE (La, Ce, Nd, Sm, Eu, Gd, Tb, Ho, Yb and Lu; Fig. 3.7). Of this

group, SiO_2 is almost constant above ~ 3 wt.% MgO, Na_2O is approximately linear over the entire range in MgO, and all other elements show an inflexion with a dramatic increase in their enrichment below $\sim 2-3$ wt.% MgO.

2. Those in which the concentration of the component decreases with decreasing MgO. This group includes CaO, Ni (Fig. 3.6) Cr, V and Sc (Fig. 3.8). Of these, Ni and Cr have almost linear correlations with MgO down to their detection limit, with Cr disappearing earlier than Ni in the fractionation history (~ 1.5 wt.% MgO in the case of Ni cf. ~ 5 wt.% MgO for Cr). The correlation of CaO with MgO has a gentle slope, and the concentrations of V and Sc are almost constant for rocks with $> \sim 3$ wt.% MgO; however, all show a more dramatic decline at higher degrees of fractionation.
3. Those in which an initial increase in the concentration of the component is followed by a subsequent decrease, with decreasing MgO. This includes Al_2O_3 , TiO_2 , P_2O_5 , Sr, Ga, Cu, and U. The sharp decrease in Al_2O_3 , Sr, and Ga occurs in a small interval between $\sim 2-3$ wt.% MgO, which is close to the change in slope in the TiO_2 and Cu plots. In contrast, the plots for P_2O_5 and U show a progressive increase with decreasing MgO until very low MgO contents (~ 0.5 wt.%) where a dramatic decrease in concentration occurs (Fig 3.9).

Components such as FeO^* (total Fe as FeO), Mn, Cs and Zn show only poor correlation with MgO and have not been categorised. The scatter in these elements (particularly Cs), may be the result of alteration processes.

Figures 3.6-3.9 indicate that most elements display curved trends with MgO. It is significant that this curvature almost invariably occurs at around 2-3 wt% MgO which indicates a marked difference in the fractionation in this interval. The steep decline in Ni and Cr, accompanied by the negative correlation of CaO with Al_2O_3 down to the 2-3 wt.% MgO level (Fig. 3.10) strongly supports the dominance of clinopyroxene fractionation in controlling the chemistry in this interval (Dupuy and Dostal, 1984). In contrast, below ~ 3 wt.% MgO, the dramatic change in direction from progressive enrichment to depletion in Al_2O_3 , Sr, Ga and an increase in the gradient of the depletion in CaO, all support a control of plagioclase in the fractionation in this interval. This is consistent with the results of McDougall (1962), who noted a sharp change in the assemblage controlling the dolerite composition from a mafic composition, to something more felsic in the later stages of differentiation in the Red Hill Dyke.

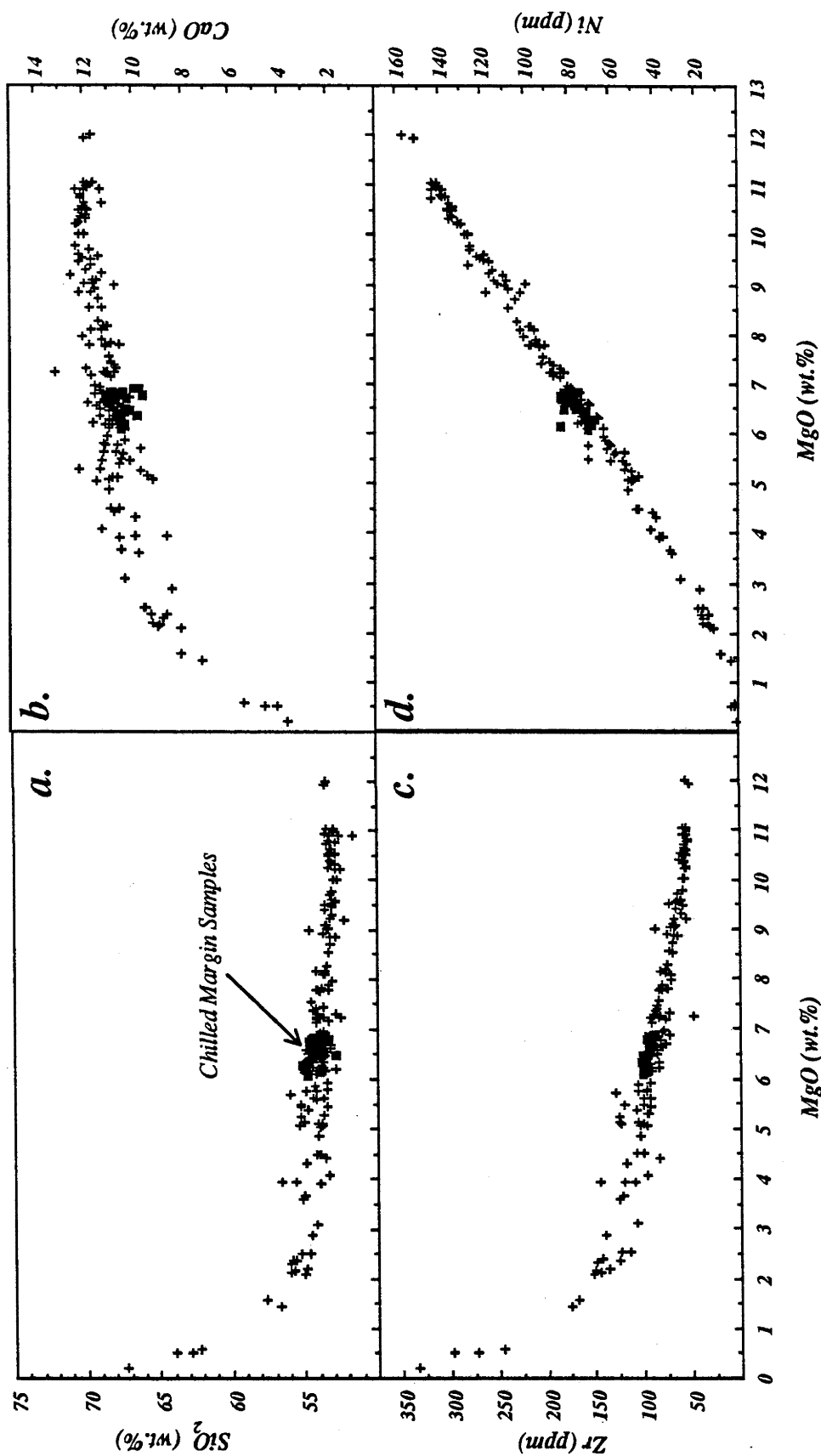


Fig. 3.6 Variation diagrams illustrating the correlation between chemical components caused by differentiation of dolerite magmas throughout Tasmania. a. Although silica shows a gradual increase down to MgO = ~3 wt.%, a sharp increase in silica occurs at lower MgO concentrations. b. In contrast with silica, the concentration of CaO progressively decreases with decreasing MgO throughout much of the differentiation history. At an MgO content of ~3 wt.%, the decline in CaO becomes steeper, and the rocks with lowest MgO also have low CaO contents. c. During differentiation, Zr acts as an incompatible element and shows a steady increase in abundance as MgO decreases. Like silica, Zr is strongly enriched in the least magnesian rocks (particularly those with less than 2.3 wt. % MgO). d. Ni parallels the behaviour of MgO. The correlation between these components is essentially linear down to an MgO value of ~1.5 wt.%, at which point negligible Ni remains.

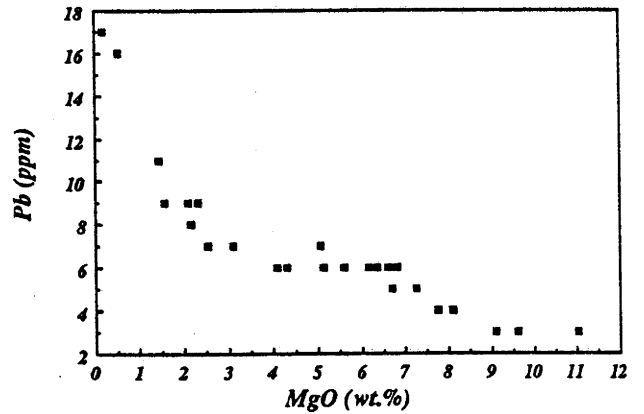
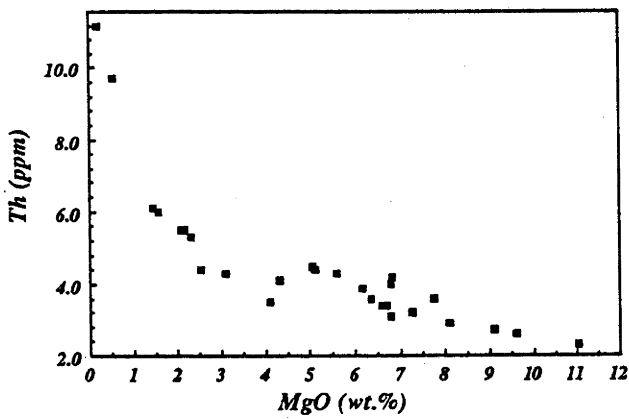
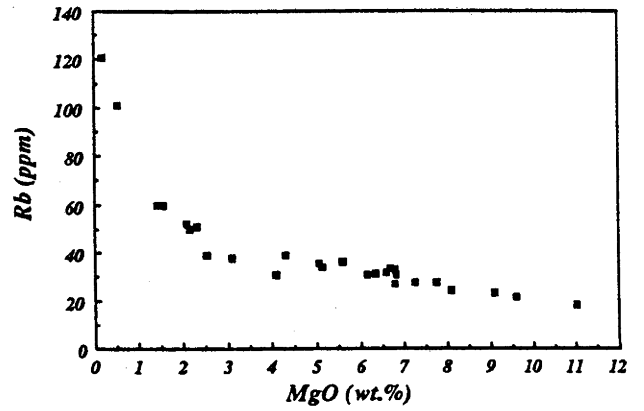
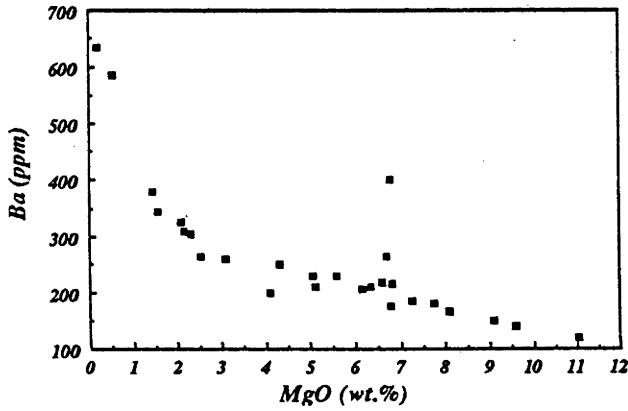
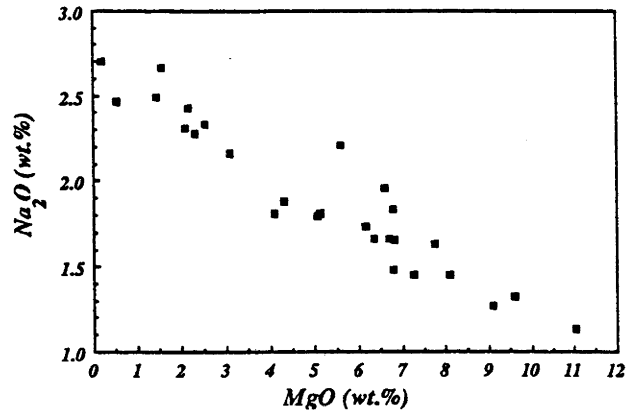
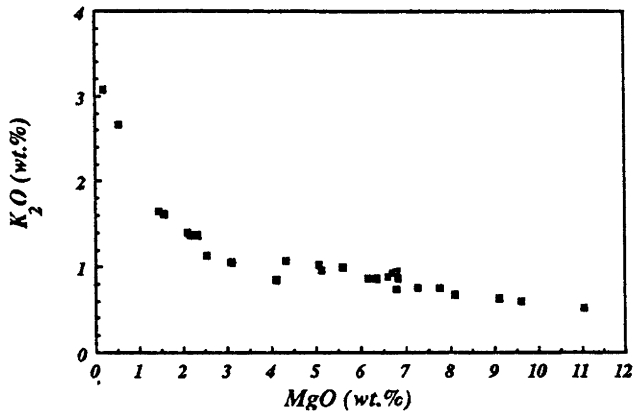


Fig. 3.7 Group 1: Elements and oxides which become progressively enriched with decreasing MgO content (particularly for $MgO < \sim 3$ wt.%).

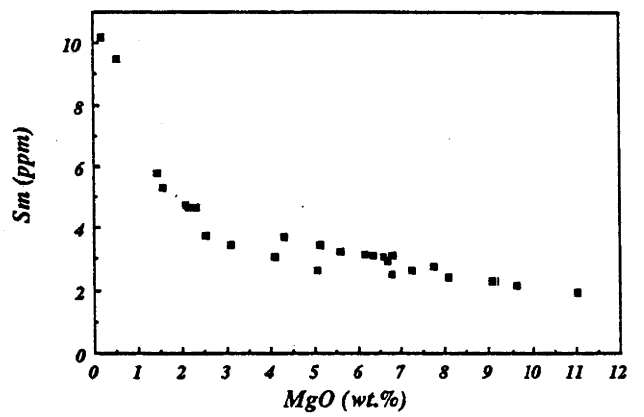
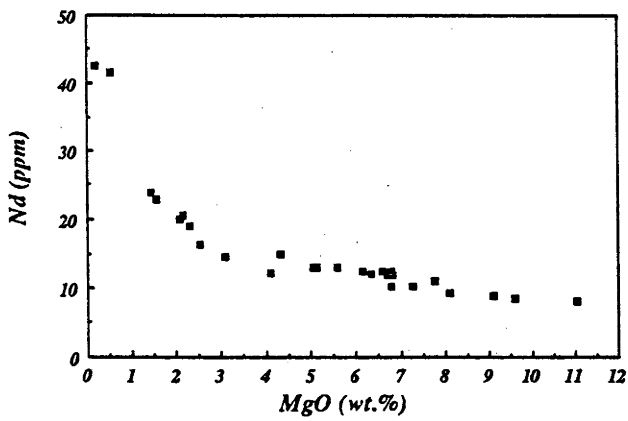
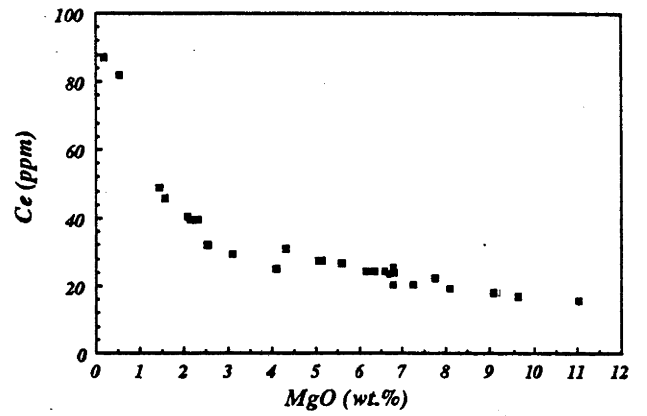
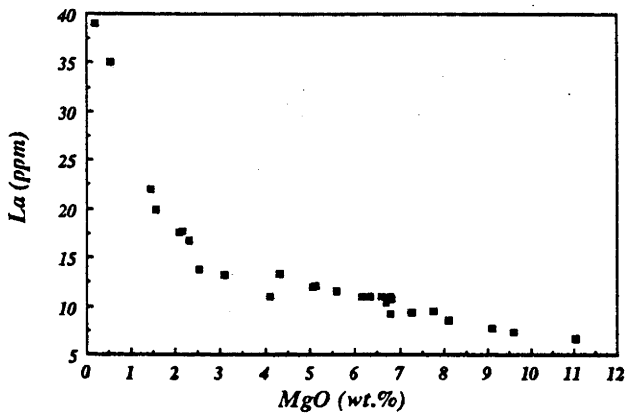
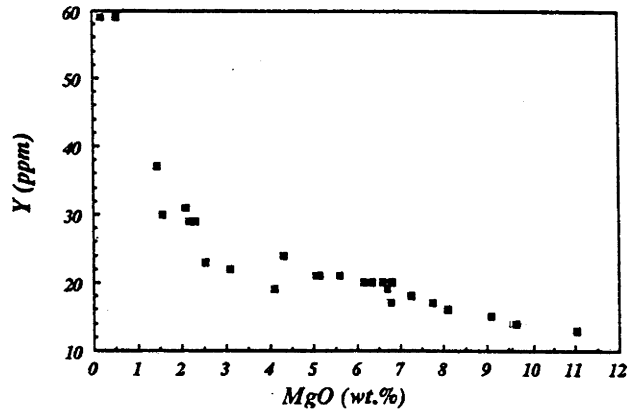
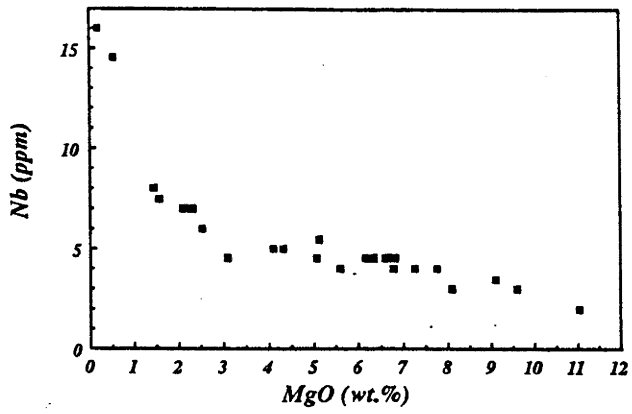


Fig. 3.7 Group 1: continued

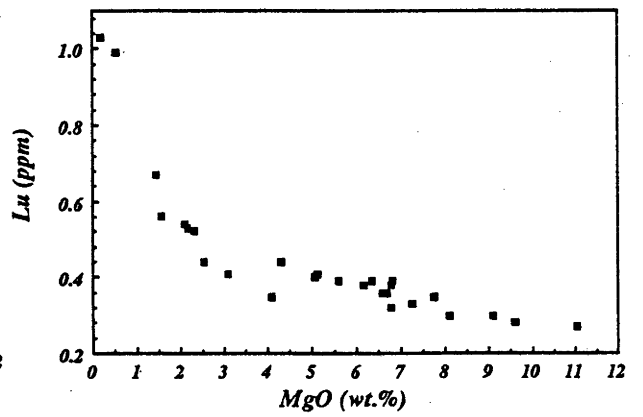
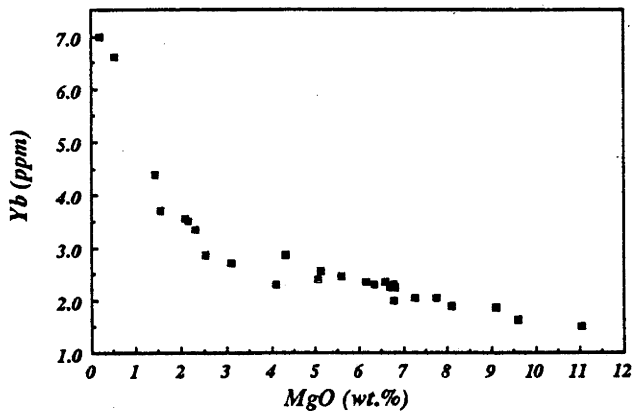
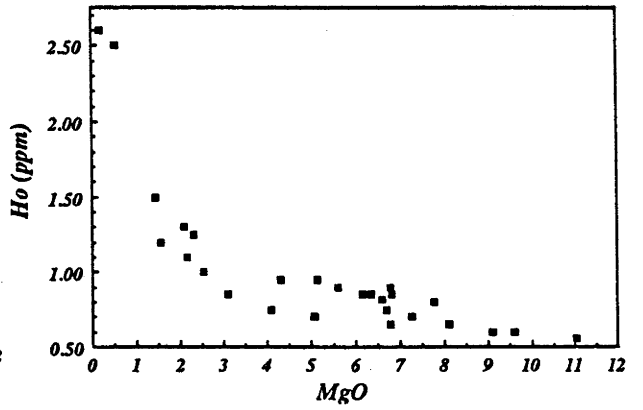
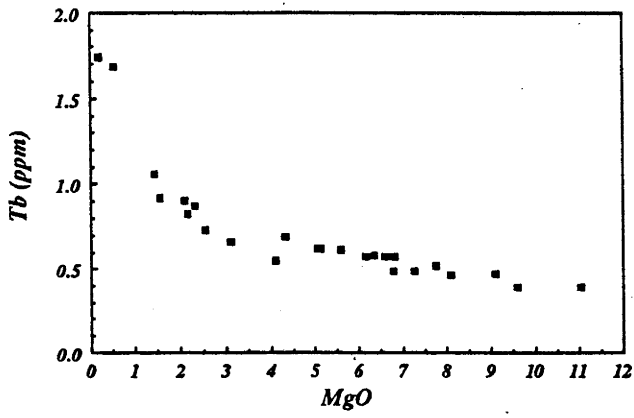
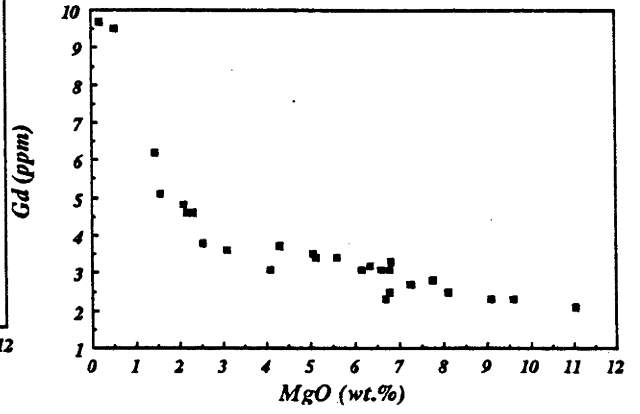
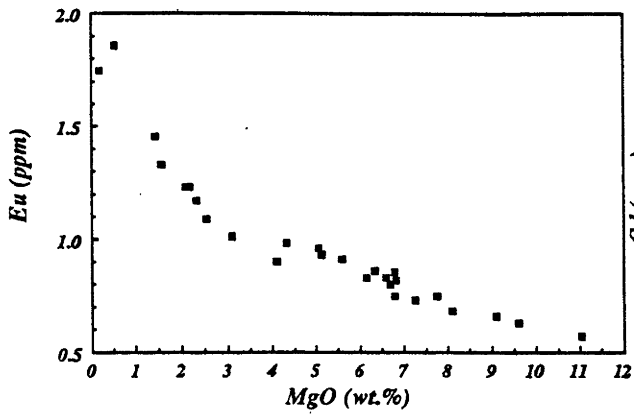


Fig. 3.7 Group 1: continued

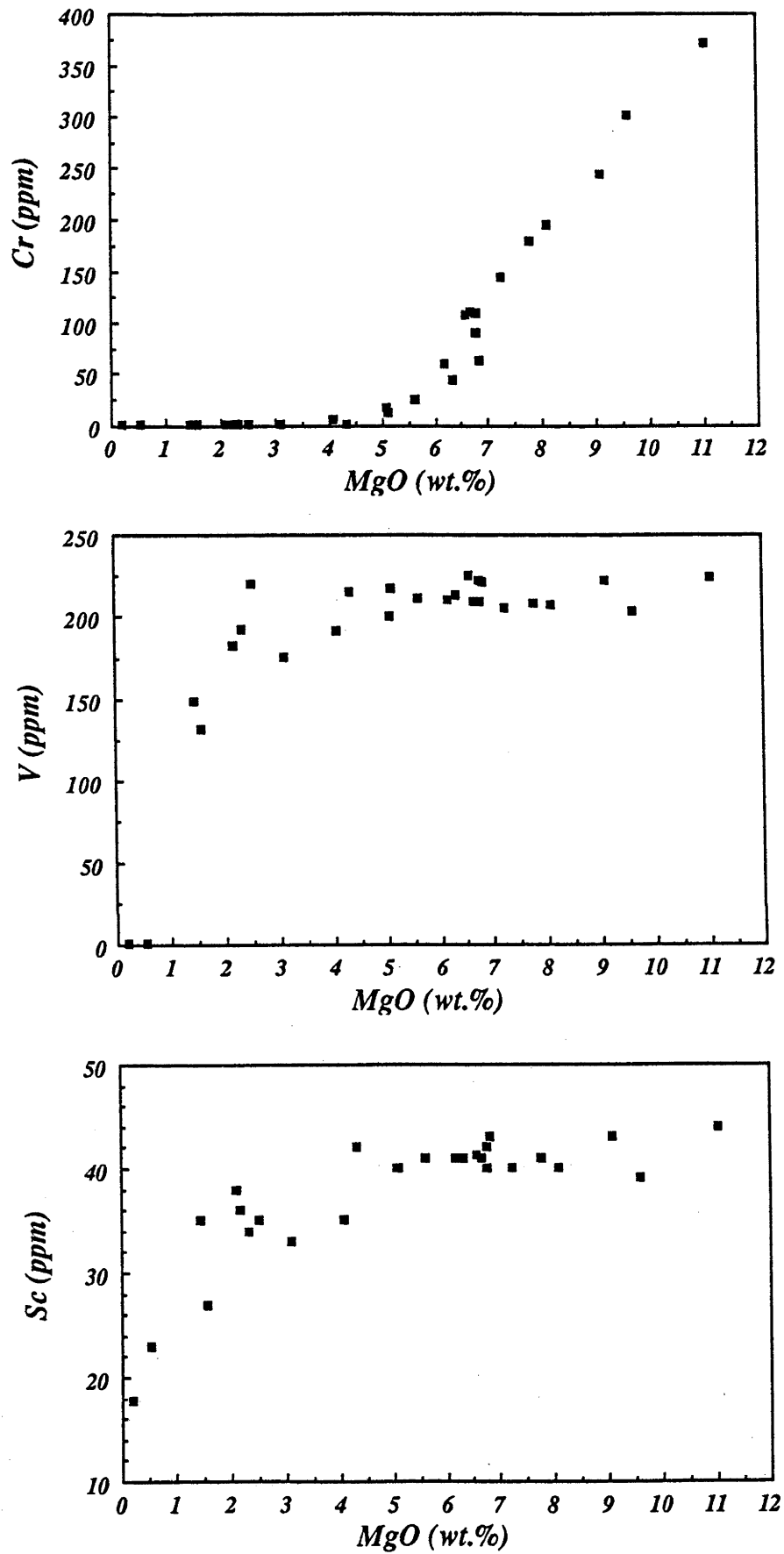


Fig. 3.8 Group 2: Elements which show a progressive decrease in concentration with decreasing MgO content.

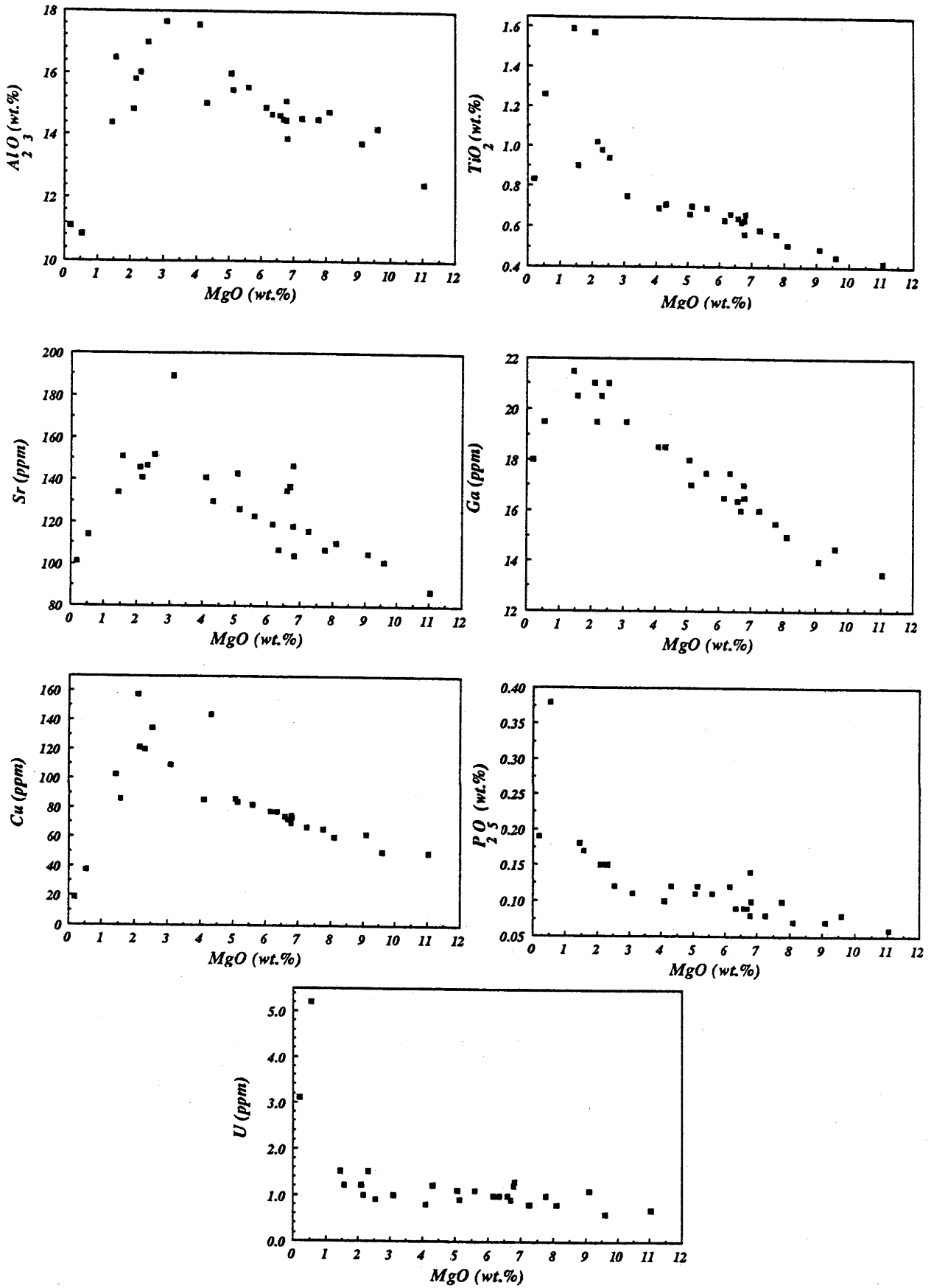


Fig. 3.9 Group 3: Elements and oxides which appear to show an increase in concentration down to low MgO values, followed by a decrease at lower MgO contents.

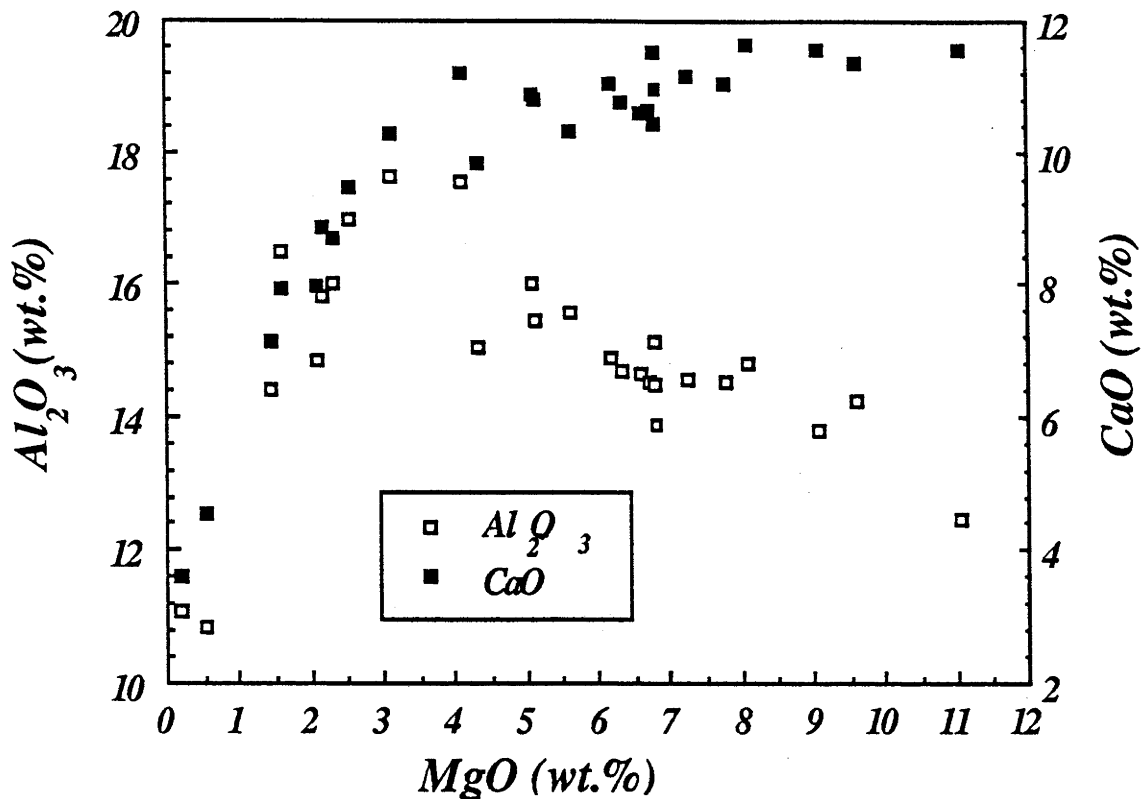


Fig. 3.10 Variation diagram illustrating the change in the relationship between CaO and Al_2O_3 with differentiation. Above ~3 wt.% MgO these oxides show opposing trends with MgO; at MgO contents less than this, the concentrations of both CaO and Al_2O_3 decrease.

The importance of accessory phases at lower MgO contents is demonstrated by the sharp decline in elements such as U and P in the most differentiated rocks.

3.3 FRACTIONATION MODELS

3.3.1 The important phases and their compositions

In order to model the relationship between rocks which are produced by fractionation processes, all phases likely to be involved in the evolution of the magma must be identified. It has been noted that the microprobe analyses of plagioclases varies considerably within a single polished section (section 3.1.2). The average plagioclase composition for each rock has been approximated from the bulk-rock CIPW norm, and representative analyses of this An-content were chosen from the probe results for the same sample.

Using the probe analyses of representative pyroxenes, the estimated plagioclase compositions, and additional components to permit calculation of oxides and mesostasis (i.e. SiO_2 , pure ilmenite and magnetite), a least-squares mixing program (based on Le Maitre, 1968) was used to determine the modal proportions (in wt.%) of phases present in selected differentiated rocks. The results were generally very good, with low residuals between the true analysis and that calculated by combining the different phases. Three of the samples used in the following discussion were collected from localities close to those of previously analysed rocks for which modal analyses (in volume %) are available (McDougall, 1962). Therefore, it was possible to make a more direct comparison between the modal analyses calculated by the

least-squares program (wt.%) and those obtained by point-counting (vol.%). One such comparison is outlined in Table 3.1, together with the calculated and analysed bulk rock compositions from the least-squares calculation.

Table 3.1 Comparison between modal mineral compositions obtained using a least-squares mixing program (wt.%) and the Rosiwal analysis (vol.%) obtained for a similar rock M210 by McDougall (1962). The whole-rock analysis is compared with that calculated, and the differences (Δ) are given. [Note: "Rest" in the Rosiwal analysis of M210 refers to amphibole, zeolite, and alteration products]. Major element oxides are given in wt.%.

	M210	84-127		84-127 (bulk)	84-127 (calc.)	Δ
Quartz+K-feldspar	14.6	14.83	SiO ₂	55.23	55.24	-0.01
Plagioclase	59.5	54.00	TiO ₂	0.76	0.77	-0.01
Pyroxene	21.3	28.69	Al ₂ O ₃	17.98	17.99	-0.01
Iron ore	1.9	2.49	FeO*	8.77	8.78	-0.01
Rest	2.7		MnO	0.14	0.09	0.05
			MgO	3.16	3.17	-0.01
			CaO	10.45	10.46	-0.01
			Na ₂ O	2.33	2.34	-0.01
			K ₂ O	1.07	1.08	-0.01
Residual sum of the squares = 0.015						

3.3.2 Least-squares mixing calculations

Having accounted for the compositions of all likely phases involved in the differentiation process, least-squares mixing calculations for the range of rock-types were attempted. In the case of a series of aphyric volcanics which have been quenched during eruption (e.g. Wood, 1978), the bulk-rock compositions may be used as a reasonable approximation to that of liquids; in this case mixing models can be calculated with some success. In contrast, slow cooling in magma chambers permits time for the relative movement of phases during solidification. It has been demonstrated that the rocks with higher MgO contents than the chilled margins are cumulates (section 3.1.1). However, there is no reason to assume that the rocks with lower MgO concentrations are liquids (residual to the magnesian cumulates) as they may just as easily represent cumulates derived from more fractionated liquids. Of course, if the last residual melts formed during fractionation were removed from the system, or, if the separation of solids and liquids was incomplete, then all of the differentiates could represent cumulates, the only liquid available being that preserved at the chilled margins.

In assuming liquid compositions for some of the Red Hill differentiates, McDougall (1962) calculated the volume of fayalite granophyre which could be generated by the removal of plagioclase and pyroxene from a parent liquid of chilled margin composition. He calculated that the mafic cumulate removed from the parent would be similar in composition to the rocks in the

Mg-rich zone observed in the Mt. Wellington sheet. Fractionation of a more mafic fayalite granophyre from the residual melt could then generate the more fractionated granophyres. McDougall (1962) believed that the chemistry was consistent with this model, but noted that the volume of granophyre present in the Red Hill intrusion exceeded that permitted by the calculation. He concluded that silicic residuum produced in the associated sheet during fractionation, migrated into the dyke-like cupola and increased the volume of granophyric differentiate observed.

In the present study, the use of a combination of sections from three different intrusions (i.e. Red Hill, Fingal and Mt. Wellington) permits a closer examination of the magmatic differentiation. Removal of mafic cumulates from the original liquid would drive the liquid (colinearly) towards a less magnesian composition. Using high MgO cumulates obtained from the Fingal sheet, the resulting fractionated liquid would be driven towards a composition similar to the rocks with MgO between approximately 5 and 6.5 wt.% (depending on the proportions of cumulate:liquid produced from the parent magma). Least-squares mixing calculations of the general form:

$$x\% \text{ minerals} + (100 - x)\% \text{ residual liquid} = 100\% \text{ parent liquid}$$

were performed using the average chilled margin composition (6.7 wt.% MgO) as "parent liquid", the most primitive pyroxene and plagioclase compositions as "minerals", and a derivative with lower MgO content, 84-267 (5.43 wt.% MgO) as "residual liquid". To generate 84-267 from the chilled margin liquid, ~12% (by mass) fractionation is calculated to have occurred (Table 3.2), and the fit between the true parent liquid and the calculated composition is reasonably close. The fractionated assemblage has a considerably higher magnesium compared with the known cumulates from this intrusion (Fingal; 16.57 cf. 11.04 wt.% MgO); however, adding the equivalent proportion (~12%) of this same assemblage to the parent liquid, a composition very similar to the cumulate 84-295 is calculated (Table 3.2). This is not entirely justified as the parent liquid is unlikely to be the same composition as the trapped liquid in the cumulate rock; however, as a first approximation it may be reasonable.

The percentage of fractionation calculated can be evaluated independently from incompatible trace element abundances. Although the mineral-melt partition coefficients for incompatible elements such as La and Ce are not zero during fractionation of pyroxene and plagioclase, the amount of fractionation can be estimated by examining the increase in concentration of these elements in the fractionated rocks analysed. For sample 84-267 (La = 14 ppm, Ce = 28 ppm) the percentage (by mass) of fractionation estimated from the original chilled margin composition (La = 11 ppm, Ce = 24 ppm) is ~10% (cf. ~12% obtained by the least-squares mixing calculations). Clearly, these calculations are consistent with the composition of sample 84-267 representing that of a derivative liquid formed by ~12% fractionation of the parent chilled margin composition.

Table 3.2 Results of the least-squares mixing calculation in which an attempt is made to reconstruct the parent magma (chilled margin average) from the addition of the most primitive minerals to a possible derivative liquid (84-267). The composition of the fractionating assemblage (comprising 4.43% plagioclase (An_{85}), 4.00% orthopyroxene (En_{83}) and 2.84% clinopyroxene ($Wo_{37}En_{55}$)) is given. This has also been added to the parent liquid (in the same proportion) to calculate a possible "cumulate" composition. This "cumulate" compares reasonably well with the composition of a true cumulate analysed from this same intrusion (84-295).

	Fractionating Assemblage (11.28%)	84-267 (88.72%)	Parent liquid	Calculated Parent	Δ	"Cumulate"	84-295
SiO ₂	53.77	55.29	55.05	55.12	-0.07	54.91	54.58
TiO ₂	0.08	0.72	0.65	0.64	0.01	0.59	0.57
Al ₂ O ₃	14.22	14.99	14.89	14.90	-0.01	14.81	14.68
FeO*	2.22	9.74	8.90	8.90	0.00	8.15	8.40
MnO	0.14	0.18	0.18	0.18	0.00	0.18	0.16
MgO	16.57	5.43	6.69	6.68	0.01	7.80	7.84
CaO	12.29	10.60	10.76	10.79	-0.03	10.93	11.15
Na ₂ O	0.71	1.96	1.89	1.82	0.07	1.76	1.76
K ₂ O	0.00	0.99	0.90	0.88	0.02	0.80	0.76
P ₂ O ₅	0.00	0.11	0.09	0.10	-0.01	0.08	0.10
Residual sum of squares = 0.1068							

This type of mixing calculation fails at greater degrees of fractionation, and attempts at fitting less magnesian bulk sample analyses to liquids, (by removing phases of appropriate composition from more mafic samples) have met with little success. This is not simply the result of attempting to use samples from different intrusions as representative of the unexposed rocks from individual bodies, because poor fit is also obtained for samples from the same intrusion. It appears that at least some of the low MgO rocks are cumulates rather than liquids, and it is this that produces the errors in mixing calculations.

A suggestion that the samples less magnesian than the chilled margins are a mixture of both liquids and cumulates is supported by two further pieces of evidence.

1. Some samples from Mt. Wellington may be fitted as cumulates and liquids (see hypothetical construction in Fig. 3.11). This figure illustrates graphically a possible model for the differentiation of the Tasmanian Dolerites. The composition of the liquid entering the chamber (L0) is well known and is represented by the chilled margins. From it may be produced an almost pure cumulate assemblage (C1), consisting of the liquidus pyroxenes and plagioclase, or, in most cases, rocks comprised of variable proportions of liquid and cumulate (i.e. compositions falling between L0 and C1, such as 84-295 estimated in the calculation presented in Table 3.2), and a fractionated liquid L1. This fractionated liquid may mix back into the evolving magma pool giving a bulk reservoir which evolves slowly from L0 to L1, at which

stage the fractionating assemblage changes dramatically (C2), and subsequent liquids progress towards L2. In exceptional cases such as at Red Hill (a cupola-like protrusion), the liquid L1 may separate from the rest of the magma column, pool at the top of the chamber, and itself fractionate to give a cumulate assemblage C2 and a residual granophyric liquid L2. Fractionation of L0 involves three phases which have slowly and consistently changing chemistry (i.e. the parent liquid, the cumulate assemblage removed, and the residual liquid); evolution of both liquids and cumulates is thus approximately colinear. Fractionation of L1 however, apparently involves varying assemblages of phases with changing compositions, hence the fractionation trend obtained may be strongly curvilinear (although this has been represented by a straight line in Fig. 3.11). The hypothetical construction using the Mt. Wellington samples can be applied to most of the variation diagrams which combine the data from the three intrusions (Figs. 3.6-3.9).

2. Examination of the rare-earth element (REE) patterns for samples from Red Hill indicates that the large Eu depletion observed in the parent liquid (chilled margins) is reduced in some less magnesian samples by the accumulation of plagioclase (84-132, MgO = 2.56 wt.%) but is enhanced in other lower magnesium rocks (84-104, MgO = 0.20 wt.%). This suggests that at least some of the rocks with low MgO are plagioclase cumulates, whereas other rocks with lower MgO concentrations may represent the residual liquids from fractionation (Fig. 3.12). The overall increase in all REE concentrations in the proposed plagioclase cumulate 84-132, requires that residual fractionated liquid (i.e. with a high total REE content) is trapped during accumulation of plagioclase.

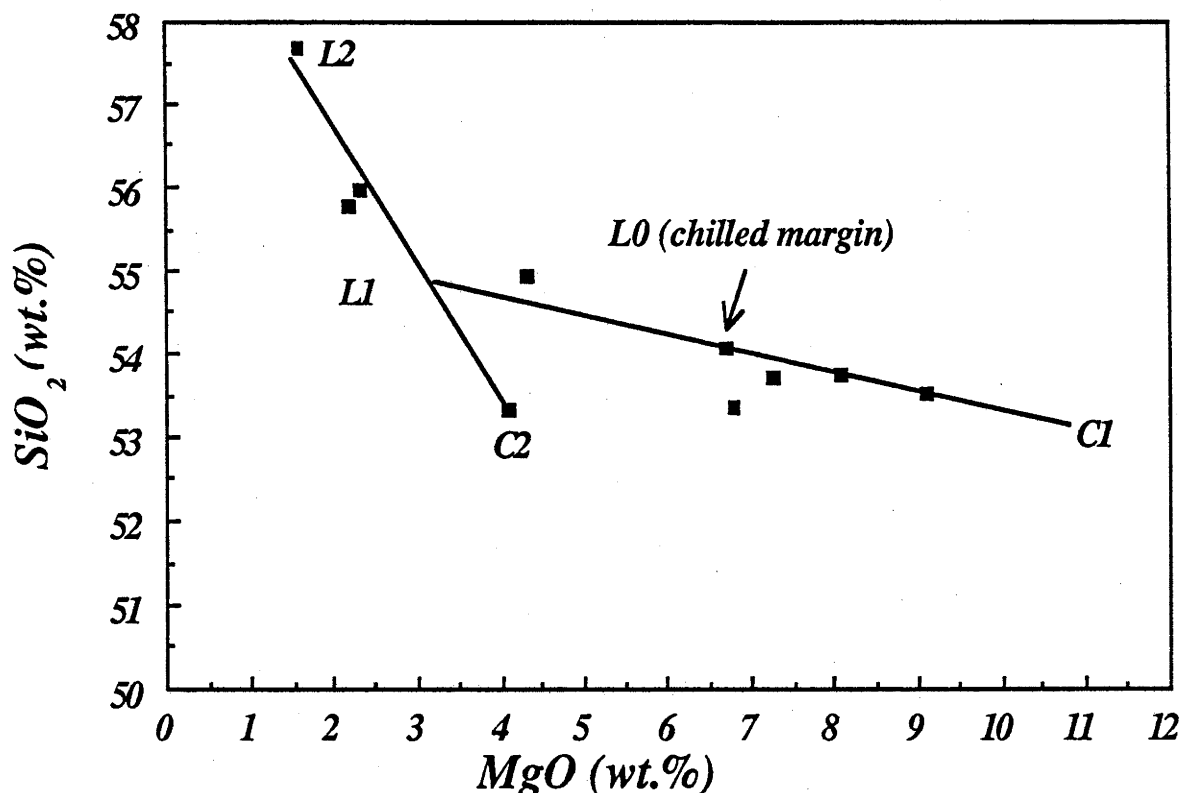


Fig. 3.11 Construction of possible relationships between cumulates (C) and derivative liquids (L) using analysed samples from the Mt. Wellington sheet. It is possible that the least magnesian rocks may be close to liquid compositions, and some samples less magnesian than the chilled margins are cumulates.

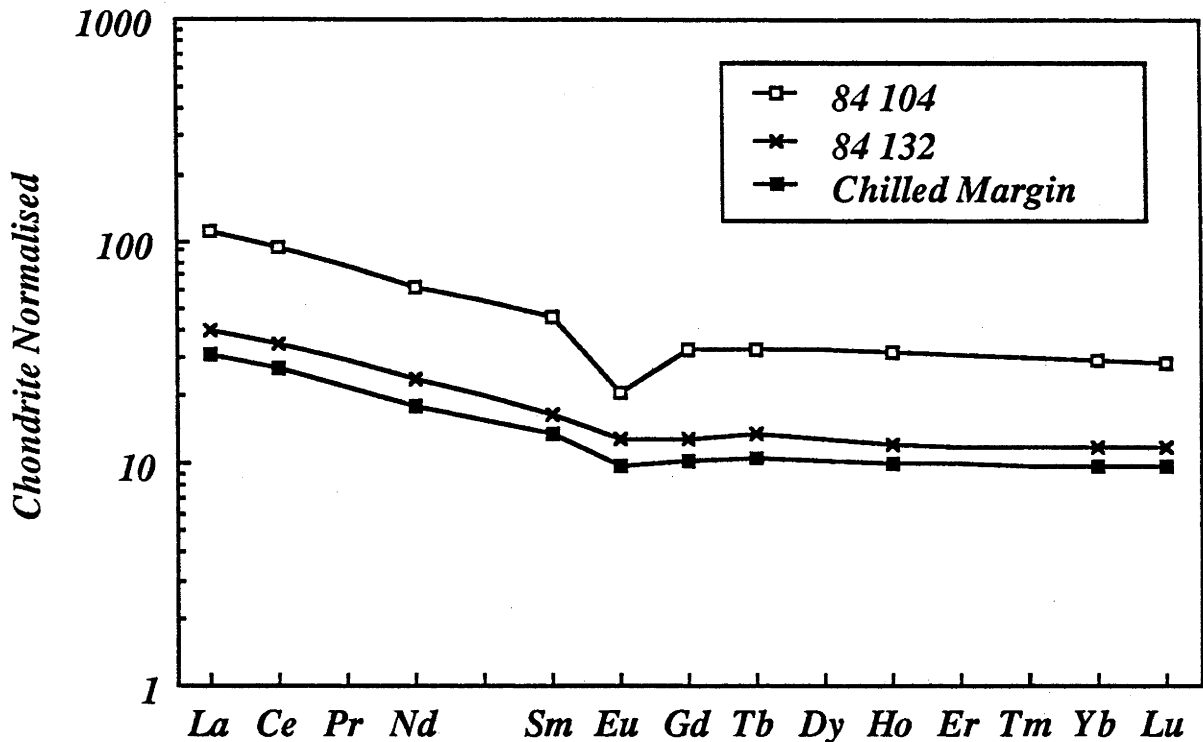


Fig. 3.12 Chondrite normalised rare-earth element (REE) diagram illustrating the change in abundances of REE and the size of the Eu depletion with differentiation. (Normalising values are taken from the unfractionated C1 estimate of Anders and Ebihara (1982) multiplied by 1.5 to allow for volatile loss).

3.4 MECHANISMS OF DIFFERENTIATION

3.4.1 Some aspects of settling versus *in situ* crystallization models

As some of the samples used in the least-squares mixing models probably represent cumulates rather than liquids, it not surprising that simple mixing calculations failed. It is useful to examine the possible differentiation mechanisms operating during fractionation to assess if the more hypothetical model described above is feasible.

Although the production of cumulates via mechanisms involving crystal settling have been favoured in the past (e.g. Edwards, 1942; Joplin, 1957; Wager and Brown, 1968), this perception has changed over the last decade with convincing evidence for the production of cumulates via *in situ* crystallization at the floor and walls of magma chambers (e.g. Campbell, 1978; Campbell *et al.*, 1978; McBirney and Noyes, 1979; Irvine, 1980). In the case of *in situ* crystallization, fractionation is achieved by the removal of residual liquid (or at least part of it) from the crystallizing liquidus assemblage. The removal of melt is principally achieved by convection (diffusion being comparatively slow), and contrasts with the settling hypothesis in which the crystals are removed from the melt and transported to the floor. Before examining the mechanism of *in situ* crystallization further, it is worth noting some of the main arguments proposed against crystal settling as a viable mechanism of fractionation.

The simple logic of fractionation being caused by crystals growing in a body of magma

and falling through the liquid to produce a crystalline "sediment" on the floor of the magma chamber is based on intuition rather than physics. It has been argued that although large, dense olivine crystals may sink in hot magmas of low viscosity, the increase in viscosity caused by cooling, changing composition, and an increase in crystal content (particularly once pyroxene and plagioclase become liquidus phases) is sufficient to increase the yield strength of the magma to the point where crystals will be unable to exert enough stress on the melt to sink (McBirney and Noyes, 1979). Sparks *et al.* (1984) argued that even if the crystals could sink through the magma, the settling velocities would normally be orders of magnitude lower than convective velocities. The dominance of convection over settling velocities means that any crystals formed during cooling would be maintained in suspension.

An important argument against crystal settling as a viable mechanism of fractionation relates to the behaviour of plagioclase in layered intrusions. It has been argued that if settling were an important cause of cumulate production, then the lower density of plagioclase relative to the basaltic magma should cause it to float (e.g. Campbell, 1978; Campbell *et al.*, 1978; McBirney and Noyes, 1979). Anorthosite cumulates should form only at the roof and gabbroic cumulates may not be expected, as pyroxene should settle and plagioclase should float, unless clots or blocks of intergrown pyroxene and plagioclase formed prior to sinking (e.g. Joplin, 1957). The objection to crystal settling based on the behaviour of plagioclase is possibly one of the most important, and remains the subject of some dispute (Irvine, 1986). Irvine argues that the presence of anorthositic blocks in the Skaergaard intrusion is problematic in both settling and *in situ* crystallization models; if an important argument against crystal settling is that plagioclase should float, then plagioclase would also be expected to rise after crystallization at the floor, unless the crystals grow against the floor and remain attached to it. There are clearly some difficulties in completely eliminating crystal settling as a means of fractionation. Therefore, although the following discussion is focussed on the mechanism of *in situ* crystallization, the possibility of crystal settling is not completely discounted.

The details of residual fluid migration during *in situ* crystallization have been examined from experimental studies (e.g. Turner and Gustafson, 1978; Chen and Turner, 1980; Sparks *et al.*, 1984). It has been demonstrated that cooling of a saturated liquid, resulting in nucleation of crystals on existing surfaces, causes a local depletion of the dense components in the residual liquid (in the case where the crystallizing phase is dense relative to the original bulk liquid). The less dense residual fluid will be buoyant and convect away from the crystal surface. The original magma therefore fractionates by the movement of liquid away from the cumulate as it forms. The effect of this process on the composition of the remaining magma depends on the geometry of the chamber. In the case of a sill, the residual buoyant melt will convectively mix with the overlying magma; in a walled intrusion however, the buoyant melt is likely to migrate along the wall in a boundary layer and collect at the top. It has been shown experimentally that the case of a walled intrusion is similar for wedge or funnel shaped intrusions in which the "walls" are replaced by a sloping floor (Huppert *et al.*, 1986; Turner and Campbell, 1986).

Essential to the efficiency of this mechanism is the density of the residual melt produced during crystallization, relative to the liquidus assemblage and overlying magma. The change in

liquid density during the fractional crystallization of basaltic magmas has been addressed by Sparks *et al.* (1984) and Sparks and Huppert (1984). These authors introduced the term *fractionation density* defined as "...the density of those components in the fluid which are being selectively removed by crystallization", and calculated that in basaltic magmas, where olivine is often the liquidus phase, the residual melt produced during crystallization would be less dense than the overlying magma and would be inclined to convect away from the site of crystallization. As this liquid is produced by removal of the most dense components from the original magma, it will have the most fractionated composition with the lowest density of the system, (unless a denser phase enters the liquidus assemblage at a later stage, e.g. magnetite). With an increase in cooling and crystallization, the remaining magma would gradually evolve towards this density minimum (Sparks and Huppert, 1984; Fig. 3.13).

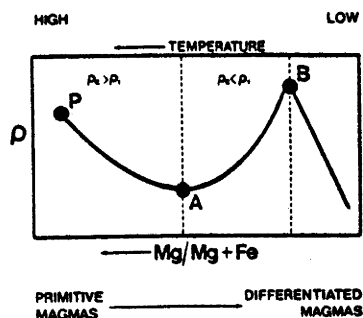


Fig. 3.13 Schematic diagram illustrating the general relationship between magma density (ρ), temperature and Mg/Mg+Fe for fractionating basaltic magmas. P is the density of the primitive olivine-bearing melt, A gives the density minimum, B is another maximum in density prior to magnetite fractionation (at which point the density of the magma decreases again). ρ_c and ρ_i are the calculated fractionation density, and the density of the magma respectively. (From Sparks and Huppert, 1984)

After reaching its density minimum (and before magnetite becomes a liquidus phase), further fractionation will cause the residual melt to become denser again (Fig. 3.13). This is because plagioclase typically has a fractionation density less than basaltic liquid; therefore, crystallization of an assemblage containing a significant amount of plagioclase may produce a residual melt denser than basaltic liquid, particularly as this is likely to be accompanied by Fe-enrichment (Sparks and Huppert, 1984). If crystallization is occurring at the floor, the denser liquid may not convect away from the cumulate, and will stagnate unless the thermal convection produced by cooling at the roof is sufficient to overcome the stabilizing effect of the compositional change. In the absence of sufficiently strong thermal convection, the dense fluid released does not convect away from the crystallizing assemblage and fractionation does not succeed (i.e the bulk composition remains the same). For these liquids to convect away from the cumulate and facilitate fractionation, a small amount of water concentrated into the Fe-rich melt during crystallization may be required. The decrease in density caused by a small increase in the amount of water may be sufficient to oppose the increase in density caused by Fe-enrichment (Hunter and Sparks, 1987).

After a peak in Fe-enrichment, magnetite (\pm ilmenite) is likely to become a liquidus phase. This will result in a dramatic reduction in iron, and increase in silica in the remaining magma, and will be accompanied by significant reduction in density of the melt (Sparks and

Huppert, 1984; Fig. 3.13). This behaviour has been suggested in a reappraisal of the differentiation of the Skaergaard intrusion (Hunter and Sparks, 1987). These authors argue that the Fe-enrichment trend in the Skaergaard intrusion has been misinterpreted as an absolute change in the iron concentration in the liquids rather than a relative change in FeO/MgO. Although the silica content in the liquid is buffered throughout the initial stages of differentiation by the fractionating assemblage, the saturation of magnetite results in a significant increase in silica, and decrease in Fe in the residual liquids. With the more efficient removal of MgO compared with FeO, the FeO/MgO in the liquid will increase, and the ferromagnesian minerals removed from the liquid will progress towards the Fe-rich endmembers. Cumulates which concentrate these minerals will show an absolute enrichment in iron, despite the progressive decrease in the Fe-content of the liquid.

An important feature of the interpretation of Hunter and Sparks (1987) is that the absolute concentration of iron in the liquids becomes progressively lower. They stress that this is not the case for the whole of the differentiation history, but becomes important when magnetite is included in the cumulate assemblage. The fact that there is an absolute depletion in iron and increase in silica in the fractionating liquids with "iron enrichment" rather than an increase results in a decrease in liquid density. In the case of *in situ* crystallization, the liquids released will be buoyant and will convect away from the cumulate.

3.4.2 Application to the Tasmanian tholeiites

Access to large sections of drill core (from the Tasmanian Hydro-Electric Commission and Tasmanian Department of Mines) has enabled a study of the spatial variation in chemistry and petrography within a vertical section. It has been shown previously that there is no smooth progressive variation in the elemental abundances above the chilled margins in differentiated sheets (Edwards, 1942). This is exemplified by the sharp increase in MgO near the base of the Mt Wellington sheet termed a "Mg-ledge" by Edwards. A similar result has been obtained in the present study and is well displayed in the basal 380 m of a sheet near Fingal in NE Tasmania (Fig. 3.14). In this section the magnesium ledge occurs about 70 m above the bottom contact.

The distribution of the elements in this vertical profile corresponds with the relationships previously described in section 3.1. The MgO, CaO, Ni and Cr abundances correlate closely, with mirrored behaviour in the more incompatible elements. The section shown in Figure 3.14 does not include the strongly differentiated rocks such as the granophyric rocks observed towards the top of the Red Hill Dyke.

Importantly, the Tasmanian dolerite magma intruded with pyroxene and plagioclase on the liquidus; as mentioned previously, Mg-olivine is absent (section 2.3.2). The densities of mid-ocean ridge basalts (MORB) have been studied by Sparks *et al.* (1980) and these authors suggest that generally, the most primitive magmas to erupt occupy a density minimum; the eruption of more picritic or evolved basalts being less favoured owing to their higher densities. In the case of MORB tholeiites, the density minimum of the magma occurs at approximately the same time as plagioclase and/or pyroxene become significant in the liquidus assemblage. In the case of the Tasmanian Dolerites, olivine has left the liquidus (possibly only a short time prior to

emplacement) and plagioclase and pyroxene exclusively control the fractionation. This possibly indicates that the dolerite magma may have been required to evolve to its minimum density before it could be emplaced, and may explain the apparent homogeneity in the major element composition of chilled margins from widely separated localities (e.g. Edwards, 1942; McDougall, 1962; and Chapter 4).

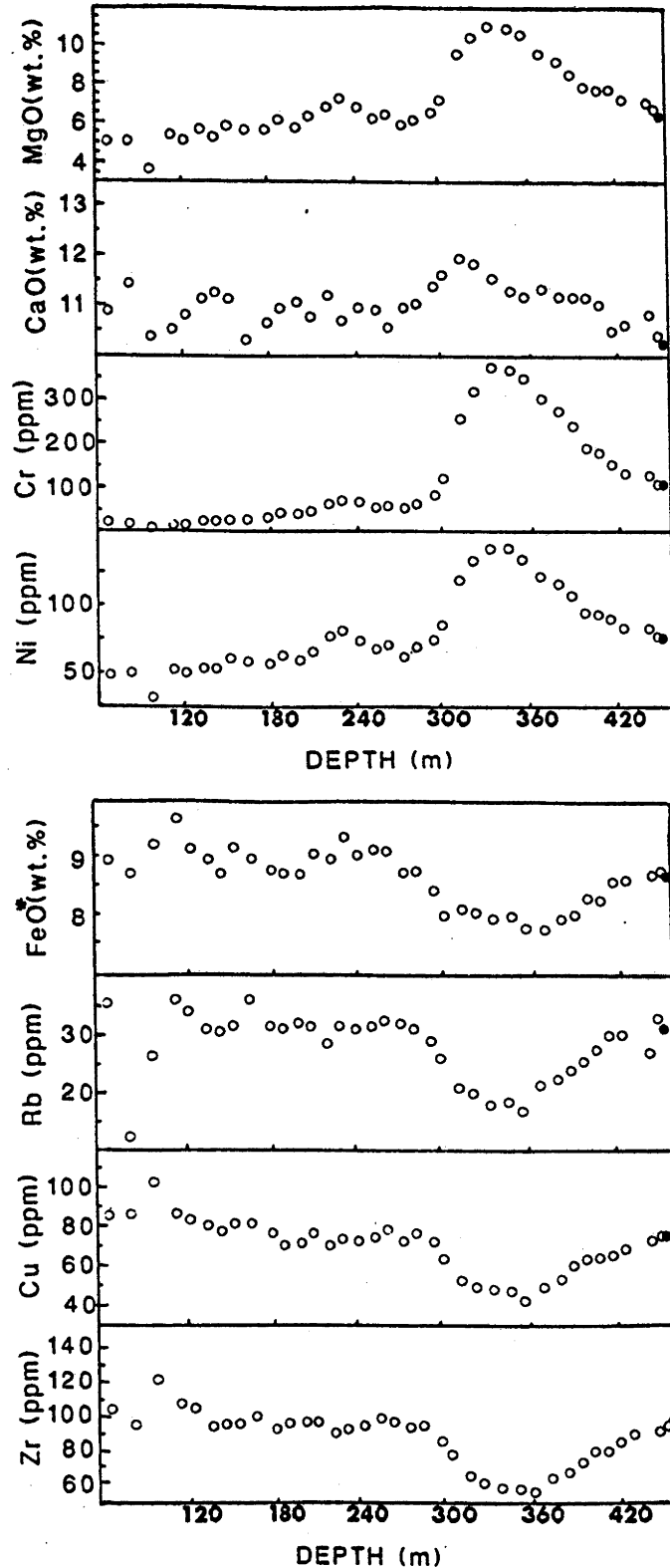


Fig. 3.14 Element (or oxide) versus depth diagrams for the basal section of the Fingal differentiated sheet. Filled circle represents the chilled margin at the bottom contact, open circles represent samples obtained from within the sheet. Note the similar behaviour within the two groups of elements (i.e. MgO, CaO, Cr and Ni; FeO*, Rb, Cu and Zr), and the mirrored distribution between the two groups.

If *in situ* mechanisms controlled the differentiation in the Tasmanian intrusions, it appears to have occurred with crystallization predominantly at the floor. This is because, away from the chilled margins, the most primitive pyroxenes (i.e. most magnesian) occur in the Mg-rich zones towards the base of the sections. According to the evolution in magma density proposed by Sparks and Huppert (1984), initial crystallization of the Tasmanian Dolerite magma should have resulted in an increase in the density, and absolute iron enrichment of the residual melt. Because fractionation persisted, the dense residual melt must have been swept away from the cumulate by strong thermal convection, possibly accompanied by the concentration of a small amount of water into the residual melt (which would serve to counteract the density effects of iron enrichment). Most of the intrusions in Tasmania approximate sills rather than the funnel- or rectangular box-shaped chambers frequently used in laboratory simulations. The residual melt produced during differentiation is most likely to have been convectively mixed back into the overlying magma rather than transported in a boundary layer to some level closer to the chamber roof. Exceptions to this may include the cupula-like protrusions from sheets (such as that observed at Red Hill), for which a walled chamber may better approximate the differentiation history.

In this case, migration of buoyant residual liquids up the walls may occur, producing a pool of silicic liquid near the roof. This liquid may continue to fractionate during cooling and crystallization, producing cumulates with low MgO content.

From the above discussion it appears that a model involving *in situ* crystallization in sill-like intrusions would favour most samples within intrusions to be cumulates. Liquid compositions would include the chilled margin rocks, and possibly the most differentiated compositions in any one intrusion (unless the residual melts were removed and erupted). This is entirely consistent with the hypothetical trends constructed from the geochemical data, (Fig. 3.11); however, it is worth noting, that such a mechanism cannot conclusively be distinguished from the process of crystal settling.

With crystal settling, the liquidus minerals are required to settle to the floor of the chamber leaving a bulk magma composition which becomes progressively less magnesian with differentiation. The major proportion of rock-types would be cumulates, with only the residual melt (if separation of solids and liquids is complete), and chilled margins preserving liquid compositions. A settling model for the origin of the Tasmanian differentiates was proposed by Edwards (1942). He envisaged that because cooling was greatest at the top and bottom of the Mt. Wellington sheet, crystallization occurred close to these margins. The pyroxenes that formed near the roof sank more readily than plagioclases, explaining the change from pyroxene-rich to plagioclase-rich cumulates with height.

Jaeger and Joplin (1955) and Joplin (1957) proposed that rather than settling of individual crystals, it was more likely that block-settling occurred in which crystalline mush formed near the roof, detached and sank to the floor. This would explain the enigma of ophitic or sub-ophitic textures, which indicate crystallization *in situ* of magnesium rich phases, found towards the floor of intrusions (Joplin, 1957). As evidence for blocks was not generally

apparent, Joplin (1957) suggested that either the blocks were large (and therefore would only be noted if they could be traced over a wider distance than exposed), or the blocks of crystalline mush shattered on reaching the floor.

Recent laboratory simulations would suggest that *in situ* crystallization models are more likely to have caused the compositional variation in differentiated intrusions. The geochemical data obtained in the present study indicate that although settling processes involving plagioclase flotation do not apply to the Tasmanian dolerites (i.e. Fig. 3.12), there is no definitive evidence to completely rule out crystal settling as a possible mechanism of differentiation.

CHAPTER 4

THE MAGMA COMPOSITION OF THE TASMANIAN DOLERITES AND ITS PETROGENESIS

Chilled margin samples were chosen to study the petrogenetic history of the dolerites. The chilled margin rocks are believed to be quenched liquids of the most primitive composition available in Tasmania, judging from their glassy texture and the low abundance and composition of microphenocrysts (Chapter 3.1). Therefore, these rocks are most likely to represent the magma composition at the time of intrusion, prior to post-emplacement differentiation. The assumption that chilled margins represent the quenched products of intruding magmas has been questioned (e.g. Cox *et al.*, 1979, 283-286); however, it will become clear in following discussions that in the case of the Tasmanian Dolerites this is a reasonable premise.

The sample localities of the 37 chilled margin rocks analysed are illustrated in Figure 1.1. Most of the samples were obtained from sills and discordant sheets, although chilled margins from the Red Hill Dyke were also sampled. The specimens collected were either in direct contact with the sedimentary host, or within 1 m or so from this contact. Both bottom and top contacts of intrusions are represented in the database, and in one case these are from the same sheet. Widely separated outcrops (and drill-core) in contact with a range of country-rock compositions were chosen in an effort to both maximize the chances of detecting variation in the magma composition, and investigate the extent of the homogeneity documented by previous studies (Edwards, 1942; McDougall, 1962; Allègre *et al.*, 1982). The purpose of attempting to characterise the composition of (and variation in) the intruding magma is to explore possible petrogenetic models for the generation of these continental tholeiites.

Detailed geochemical and isotopic results are contained in the accompanying appendices. The major and trace element data are compiled in Appendix 4.2 and the isotopic data in Appendix 5.

Because previous reports remarked on the homogeneity in the chilled margin compositions (Edwards, 1942; McDougall, 1962; Allègre *et al.*, 1982), it was necessary to make a detailed study of the precision of all analytical measurements in order to evaluate the variation genuinely caused by geological processes. To accomplish this, multiple analyses of the chilled margin sample 84-152 and the international standard W-2 have been performed (for the geochemical data), and three separate preparations of another international standard, BHVO-1, were analysed for Sr and Nd isotopic compositions. The results are presented in Appendix 3 and the estimates of the precision for each element are included in Table 3.1. Also presented in Appendix 3 are comparisons between the results obtained by different analytical techniques. For instance, the XRF measurements for Rb and Sr are compared with those obtained by isotope dilution for the same samples.

4.1 GEOCHEMISTRY

4.1.1 *Chemical variability of the chilled margin tholeiites*

The most striking feature of the geochemical data is the similarity between the chilled margin compositions for samples from widely separated localities. This includes a wide range of trace elements previously undocumented for the Tasmanian Dolerites and is entirely consistent with earlier reports (Edwards, 1942; McDougall, 1962). The lack of substantial geochemical variation is impressively displayed in Table 4.1. In this table, a comparison between the variation observed for each element (represented by the standard deviation expressed as a percentage relative to the mean) and the analytical precision estimates (Appendix 3) are listed. For many elements (e.g. rare-earth elements) the geochemical variation approaches the analytical precision of the measurement, implying that for these elements almost no measurable differences exist. In contrast, the standard deviation for most of the major elements is ~3 times as great as the precision, increasing to ~15 times the analytical uncertainty in the case of K_2O . Some of the trace elements (e.g. Cs, Ba, Rb, Sr, Cr) also vary significantly beyond uncertainties.

A single sample (84-168) is believed to be contaminated by carbonate veining resulting in its high CaO, CO_2 , H_2O and low SiO_2 contents. Assuming the carbonate is pure calcite, the amount calculated is ~1.5%. However, because of the high values of MnO, Ba and other elements in this sample, it is clear that this is an over-simplification and elements in addition to Ca and C have been involved. Care was taken in removing the rare carbonate veins from samples (as well as any surface alteration) during crushing. Because this sample was obtained from drill core it was of limited size and it appears that a small amount of carbonate left undetected during crushing has dominated the chemical analysis.

Two other samples from less than 1 m away from 84-168 in the same core (84-169 and 84-170) clearly have anomalously high Ba (785 and 1400 ppm respectively). The country-rock in contact with the dolerite in this locality is part of the Triassic sedimentary sequence typical of many other localities sampled; therefore, the unusual Ba contents in these chilled margin samples are not readily explained by local contamination. Similar enrichments in Ba have been observed in basaltic rocks from the Hawaiian island of Kahoolawe and have been attributed to some form of hydrothermal activity (Fodor *et al.*, 1987). As the high Ba contents in the Tasmanian samples appear to be the result of a process specific to this locality, these two Ba compositions and the carbonate-bearing sample 84-168 have been excluded from the calculated average chilled margin composition of Table 4.1.

In addition to the significant variation observed in some of the major and trace element abundances, comparison of the precision and variation columns in Table 4.1 also helps identify some of the fine-scale variation observed in the chilled margin dolerites that may otherwise have been thought absent. For example, the measurement of Sc by a technique less precise than INAA may not have detected the small amount of variation in this element!

Both the large- and small-scale variations in the contact dolerites are discussed in the following sections. The range in elemental compositions that has been identified may be the result of differences in fractionation prior to emplacement and/or alteration effects superimposed at some later stage. It will be argued in the following discussions that there is sufficient

evidence supporting the operation of a combination of these two processes, but that most elements are sufficiently unaffected to allow the characterisation of the intruding magma composition.

Table 4.1 Average composition of the Tasmanian Dolerite chilled margins (recalculated anhydrous) based on 36 samples (except for Ba where n=34). The standard deviations are expressed as percentages relative to the mean, as are the estimates of the analytical precision for each element. The oxides are expressed in weight percent and the trace elements in ppm. FeO* is the total iron expressed as FeO.

Element	Average	Standard Deviation (in %)	Analytical Precision (in %)
SiO ₂	54.98	0.9	0.3
TiO ₂	0.65	2.4	0.8
Al ₂ O ₃	14.84	0.8	0.3
FeO*	8.91	1.5	0.5
MnO	0.18	3.7	1.1
MgO	6.72	3.3	0.6
CaO	10.69	3.9	0.3
Na ₂ O	2.00	9.7	1.3
K ₂ O	0.89	13.6	0.9
P ₂ O ₅	0.09	6.1	1.9
S	0.05	37.2	16.5
Cs	1.5	59.3	4.8
Ba	217	15.1	
Rb	33	15.5	
Sr	135	15.5	
Pb	6	10.9	
La	10.9	2.5	1.2
Ce	24.4	3.9	2.0
Nd	12.4	4.8	2.4
Sm	3.07	2.9	1.1
Eu	0.83	3.3	0.8
Gd	3.1	5.7	4.5
Tb	0.57	4.8	5.4
Ho	0.82	7.9	4.0
Yb	2.36	3.5	3.9
Lu	0.36	3.1	1.1
Y	20	2.4	
Th	3.5	4.6	4.5
U	1.1	16.4	4.5
Zr	95	3.3	
Hf	1.9	5.7	4.3
Nb	4.5	8.6	
Sc	41.3	2.1	0.5
V	225	2.9	
Cr	108	12.4	
Mn	1351	4.0	
Co	49	2.5	
Ni	78	4.9	
Cu	74	6.2	
Zn	79	4.7	
Ga	16.4	3.5	

4.1.2 Major element composition

The chilled margin dolerites are quartz tholeiitic in composition (according to the classification of Wilkinson, 1986) with an average of 6.5 wt.% quartz in their norm and a mean MgO content of 6.7 wt.%. The Mg-numbers (Mg#) vary between 58-62 (Mg# = $\text{Mg}/\text{Mg} + \text{Fe}^{2+}$ (atomic), setting atomic $\text{Fe}^{3+}/\text{Fe}^{2+} = 0.15$). In addition to the high SiO_2 and relatively low MgO, the major element composition is characterised by low FeO^* , Na_2O , and particularly low TiO_2 and P_2O_5 contents compared with other tholeiitic rocks; these features are discussed later.

It has been noted that a small amount of variation has been detected in the major elements. Some of the data are plotted in Figures 4.1 and 4.2 and indicate that there is likely to be more than one process responsible for this small range. Correlated patterns with MgO content strongly support fractionation as the cause of some of the variation. [Although mixing different endmembers may also result in correlations with MgO, the isotopic data (presented in section 4.2) indicate that this is unlikely]. In contrast, variation not correlated with MgO implies that another process is responsible, and in the case of the mobile components such as K_2O this is most likely to involve alteration.

Major element oxides which correlate with MgO are SiO_2 and TiO_2 , and are shown in Figure 4.1.

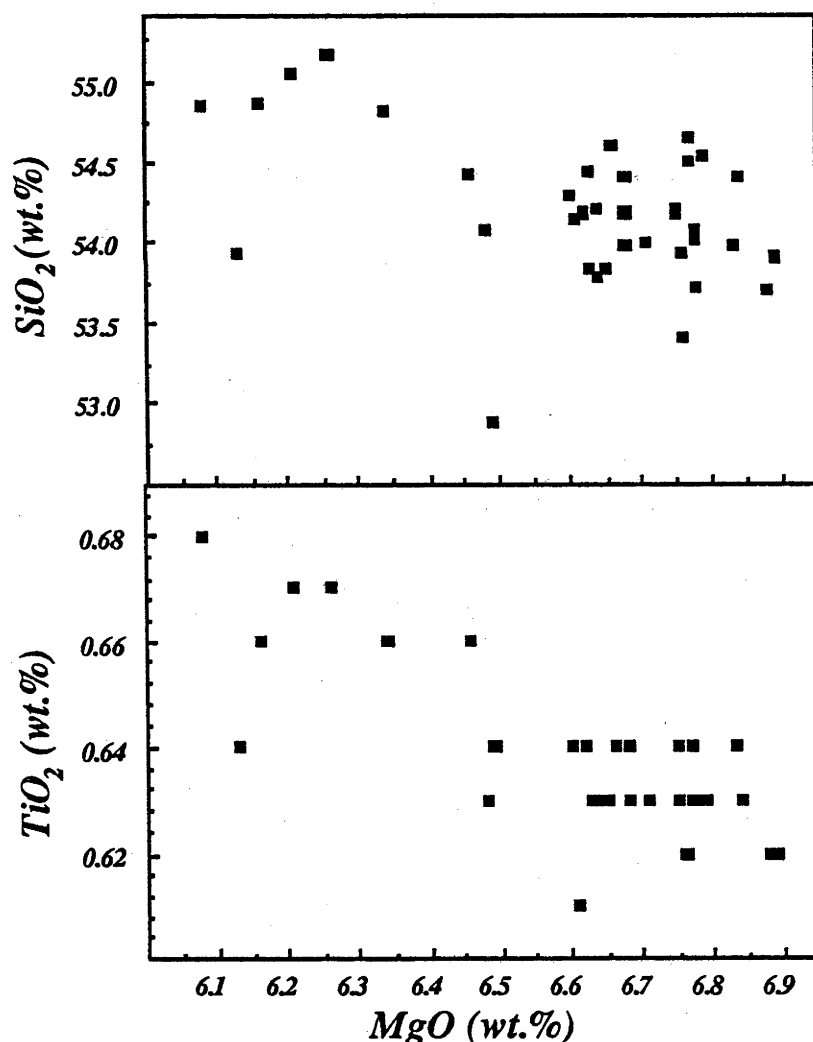


Fig. 4.1 Major-element oxide vs MgO diagrams for SiO_2 and TiO_2 . These plots show correlation which is interpreted as being the result of fractionation.

Although the total spread in the data is rather small, the SiO_2 content appears to be weakly correlated with MgO. The TiO_2 content is also reasonably well correlated with MgO, and implies that a more primitive parent (i.e. higher MgO) would have a TiO_2 content of less than 0.6 wt.%. Thus, no titaniferous phase could have been on the liquidus at the time of emplacement, indicating that the low TiO_2 cannot be attributed to fractionation.

It appears that the variation in SiO_2 and TiO_2 observed in the chilled margin rocks can be explained by some difference in the degree of fractionation of the magmas prior to emplacement. The phases involved in this process will be examined after the discussion of some of the trace element data.

In contrast, other major element oxides which show variation do not correlate with MgO. These include relatively mobile elements such as K, Ca, Na, and Fe, and some of the oxide-MgO plots are illustrated in Figure 4.2.

Trace element contents which have been disturbed by alteration are discussed in the following section. The fractionation effects are also explored further, and the compatible trace element contents are examined to assess the involvement of particular phases.

4.1.3 *Ba, Rb, Sr, Cs,*

Reference to Table 4.1 indicates that the range in these trace elements significantly exceeds the precision of the analyses. In Figure 4.3 a-c these elements are plotted against MgO and no obvious correlations are observed. In contrast, the incompatible elements Ba and Sr show weak positive correlation and increased scatter with K_2O suggesting that these elements have been mobilised during an alteration process, and do not owe their variation to crystal fractionation (Fig. 4.3d,f). Rubidium shows good correlation with K_2O indicating a strong similarity in the behaviour of these elements (Fig. 4.3e). It is also important to note the similar behaviour of Rb and Sr. It may be expected that these two elements would show an opposite sense of variation in fractionation processes because plagioclase partitions Sr into its structure whereas Rb remains in the residual melt. The similar trends displayed in these diagrams, and the lack of correlation with MgO argue against fractionation as the cause of the variation.

The effects of alteration on Ba, Rb and Sr have been documented previously together with a note of caution in using these elements to constrain petrogenetic models (e.g. Clague and Frey, 1982). Cs appears to have suffered a great deal of mobilisation and varies by more than an order of magnitude beyond analytical uncertainty (Table 4.1). There is no correlation between Cs and MgO or K_2O .

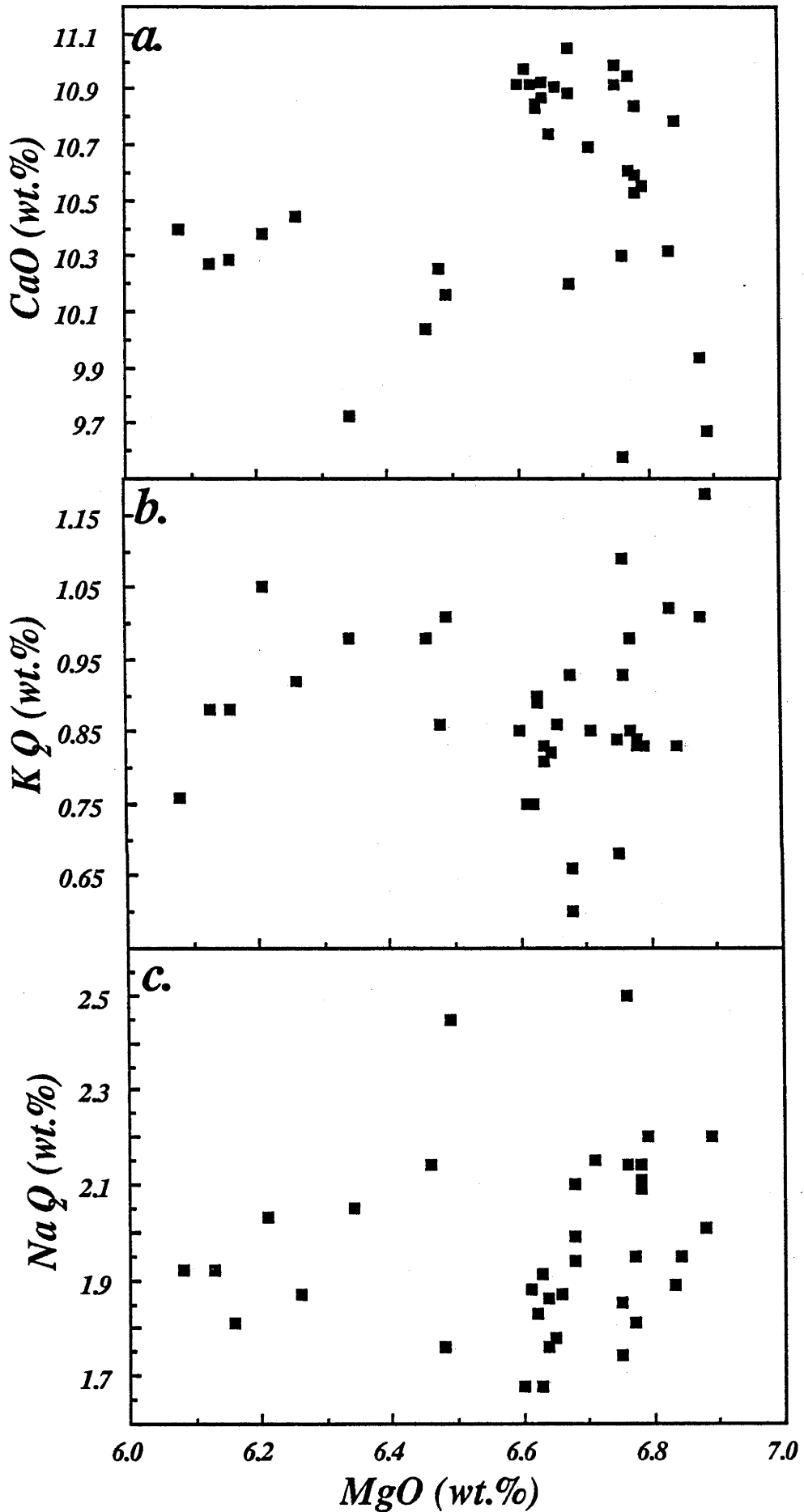


Fig. 4.2 Variation diagrams showing the lack of correlation between MgO and components which have been mobilised during alteration. a. CaO b. K₂O c. Na₂O

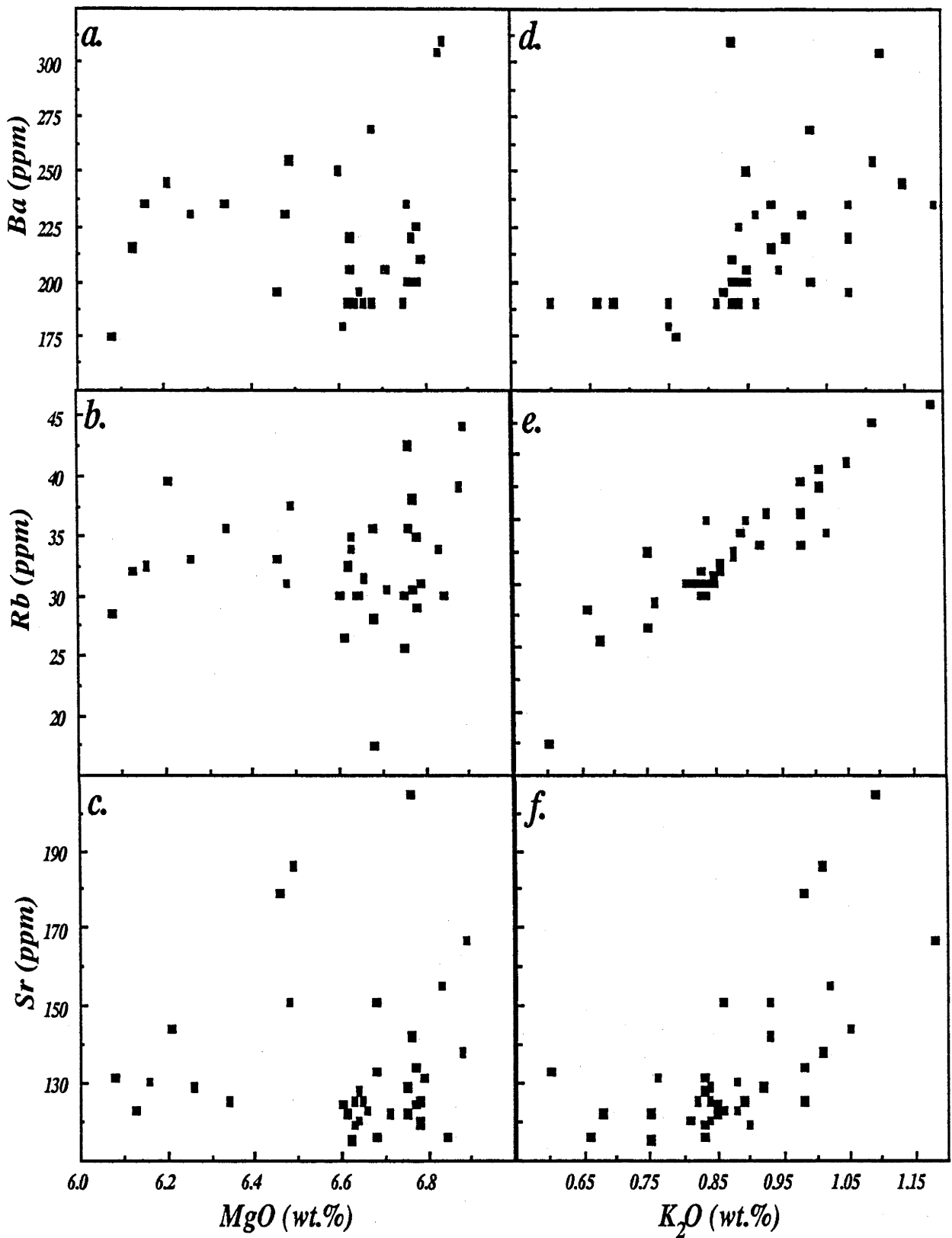


Fig. 4.3 a-c Plots of Ba, Rb and Sr against MgO illustrating the lack of correlation between these parameters. In figures d-f K₂O has been chosen as the abscissa as this element is strongly effected by alteration. d. Ba shows a general increase from ~200 to ~300ppm and an increase in scatter with higher K₂O contents (the 3 samples discussed in the text with high Ba have been excluded) b. Rb vs K₂O is well correlated illustrating the similarity in behaviour of these elements during alteration. c. A general increase in Sr with K₂O accompanied by a higher degree of scatter indicates that this element is also effected during mobilisation.

4.1.4 Sc, Co, Mn, V, Zn, Cu, Ga

The concentrations of these more compatible elements appear remarkably constant in the chilled margins although precision estimates have only been determined for Sc. These elements are important as they may partition into the phases likely to be on the liquidus at low pressure (i.e. pyroxenes, oxides and in the case of Ga, plagioclase). The homogeneity in concentration of Co, Cu, Mn and Zn suggests that any process of fractionation involving their removal was either very reproducible or was made effectively uniform by later efficient mixing (Fig 4.4). In addition to their uniformity, the abundance of these elements is also important to the fractionation history. The concentrations of this group of elements ranges from normal to high for basaltic magmas. For example, ocean-floor tholeiites have an average of Co ~47 ppm, Cu ~86 ppm and Zn ~85 ppm (BVSP, 1981; p 148).

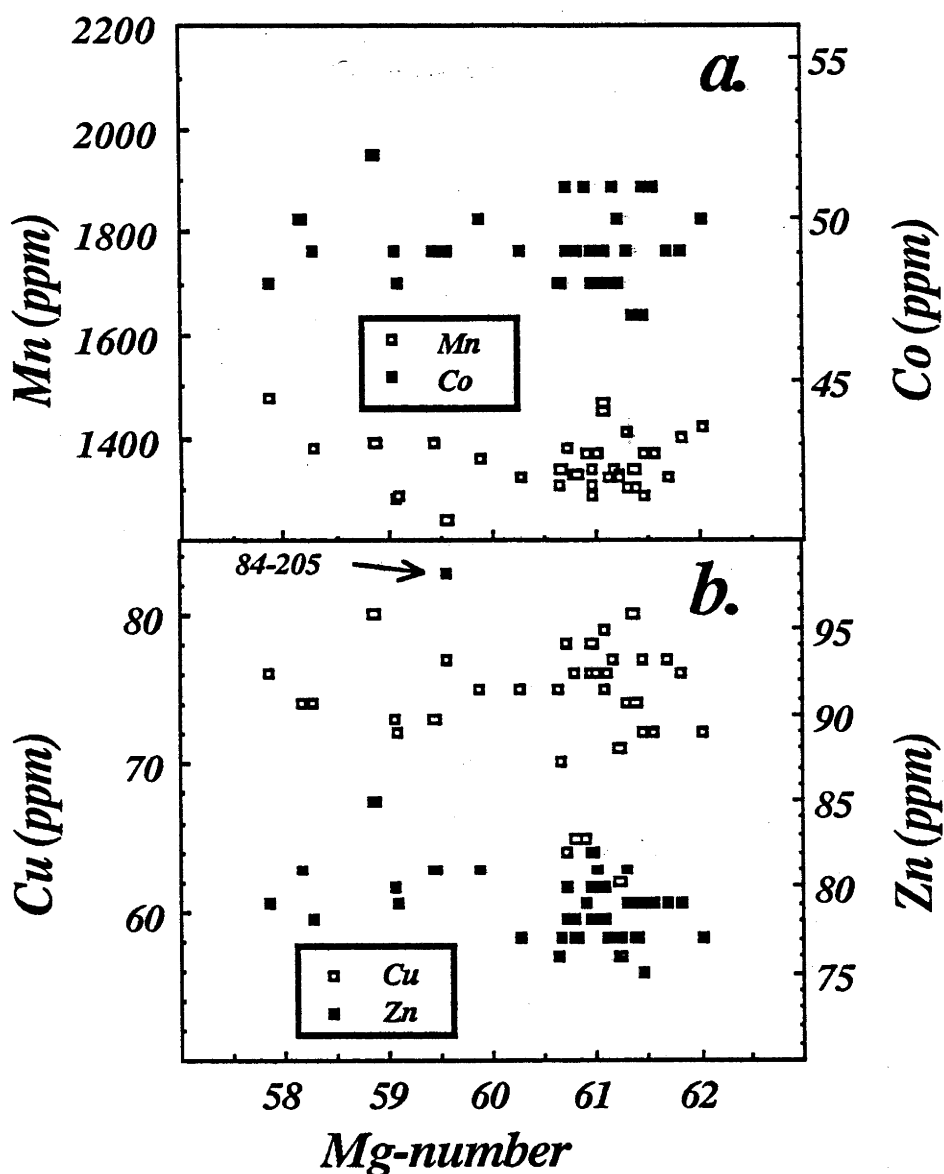


Fig. 4.4 Element vs Mg# diagrams illustrating the lack of variation in the elements Mn, Co (diagram a.), Cu and Zn (diagram b.). The reason for the high Zn content in 84-205 is unknown.

In contrast to Mn, Co, Cu and Zn, the Sc and V concentrations show a good inverse correlation with Mg# (Fig. 4.5), similar to the variation observed between MgO and TiO₂ previously. This relationship indicates that the phase(s) removed during fractionation caused an increase in these elements in the magma (i.e. excluded TiO₂, Sc and V) but did not significantly alter the Co, Mn, Cu and Zn contents (i.e. neither preferentially included or excluded these elements). Although there is no variation in Ga, the Ga concentrations were only measured to the nearest 0.5 ppm by XRF spectrometry, therefore small differences in the abundance of this element (resulting from the fractionation of plagioclase) may not be observed. [Note: If the Sc data obtained by INAA were unavailable and the results from XRF spectrometry were examined, then the variation in Sc would not be distinguishable either. The importance in acquiring precise elemental concentrations is highlighted by this example.]

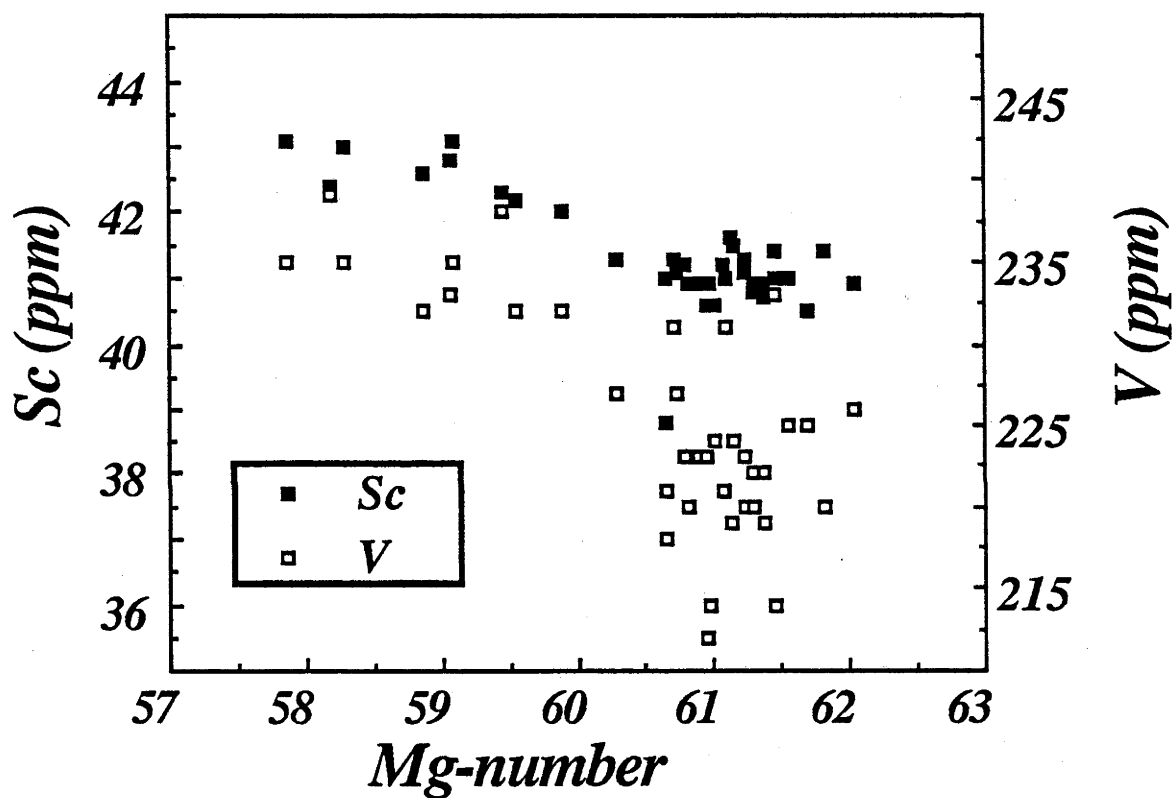


Fig. 4.5 Diagram illustrating the progressive increase in Sc and V with decreasing Mg#. The similarity in the behaviour of the two trace elements is also demonstrated in this figure.

4.1.5 Ni and Cr

Nickel and Cr have considerably higher distribution coefficients for phases such as pyroxene, and are therefore more sensitive to a small degree of evolution only weakly detected by analysis of other transition-metal elements. The variation in Ni and Cr, relative to Mg#, is illustrated in Figure 4.6. Most of the chilled margins have Ni and Cr contents of ~80 and ~115 ppm respectively. At an Mg# of ~59.5 this drops to ~70 and ~80 ppm implying that with a slightly higher degree of evolution, a phase (or phases) selectively removed these elements.

The cause of this variation is explored in the following section. It is important to note that the higher Ni and Cr contents of the more primitive members are still very low for basaltic rocks and also require explanation.

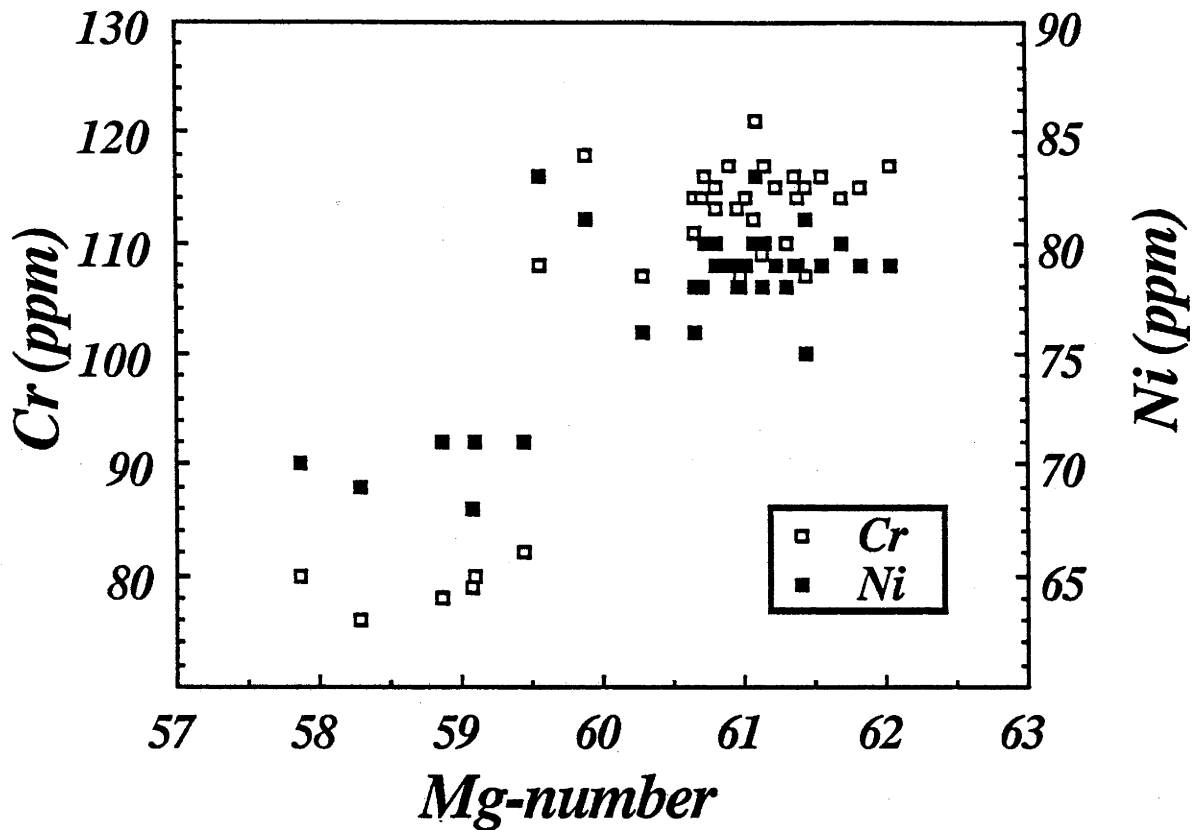


Fig. 4.6 Diagram illustrating the similarity in behaviour of Ni and Cr with decreasing Mg#. At an Mg# of around 59.5 the Ni and Cr contents both decrease sharply.

4.1.6 The pre-intrusion evolution of the melt.

"Few geologists would disagree with the statement that most basalts are derived from liquids produced by partial melting of peridotites in the Earth's upper mantle. This is the main premise of this chapter, indeed, of this book, and the primary ingredient of the foundation on which most current research on basaltic igneous rocks is built."

BVSP (1981, p. 495)

It is widely accepted that basalts are produced by melting a source in which olivine (as magnesian as Fo_{90-94}) and orthopyroxene are major constituents. It is not unreasonable to expect these basaltic melts to be in equilibrium with the residual olivine and orthopyroxene in the source, and primary basalts are therefore required to be high in magnesium. Although this is supported by experimental petrology, controversy exists as to whether primary melts are necessarily picritic, or may have lower MgO contents providing that the Mg# of the basalt is consistent with equilibrium between the melt and magnesian olivine. Frey *et al.* (1978) used the relationship of Roeder and Emslie (1970; i.e. the distribution coefficient relating the partitioning of Fe between olivine and liquid, divided by that for Mg between olivine and liquid is constant at ~ 0.30), and calculated the Mg#s required for primary basaltic melts. Frey *et al.* (1978) estimated that primary magmas should have Mg#s $\sim 68-75$ for up to approximately 30% partial melting in the source.

The Mg#s of the Tasmanian chilled margin dolerites vary between 57.9 and 61.7 (ignoring the value of 62.0 from one of the high-Ba samples, 84-169). These comparatively low values indicate that the tholeiite magmas were not in equilibrium with magnesian mantle olivine at the time of emplacement. The possible explanations for this are that the magmas:

1. Underwent fractionation (and contamination?) after leaving a typical mantle source
2. Were derived from an unusually Fe-rich mantle source
3. Were derived from a crustal source with a lower Mg# than typical mantle sources

The temperature of the tholeiitic magmas at the time of intrusion is estimated as $\sim 1200^{\circ}\text{C}$ from melting experiments, pyroxene thermometry, and phase equilibria calculations (Appendix 8). The high temperature, together with the large quantity of magma emplaced in Tasmania, appear sufficient to rule out purely crustal melting as a viable option for the origin of the magma. This is because the geothermal gradient in Tasmania would need to have been unusually high in the Jurassic. Even using the rather high geothermal gradients estimated for southeastern Australia (elevated by the Cenozoic volcanism, Sass and Lachenbruch, 1979) and measured surface heat flow in Tasmania (also from Sass and Lachenbruch), the temperature would not be estimated at more than 1000°C at a depth of 50 km. This is also consistent with more recent models for the geothermal regime in southeastern Australia (O'Reilly and Griffin, 1985).

Low pressure, anhydrous melting paths defined by magmas derived from both primitive and depleted mantle sources have been documented by Jaques and Green (1980). These authors demonstrated that although mantle-derived melts may approach quartz tholeiitic compositions at low degrees of partial melting ($< 10\%$; or conversely, high degrees of crystallization in equilibrium with mantle assemblages), this occurs at very low pressures 2-5 kbar (i.e. ~ 7 -17 km) and therefore necessarily in the oceanic environment where the crust is thin. Other workers have suggested that it is possible to produce quartz tholeiitic melts within the mantle at pressures of up to ~ 10 kbar if the source is water-saturated (e.g. Kushiro, 1972; Green, 1973, 1976; Nicholls, 1974).

Even if it is assumed that the crust in Tasmania may be as thin as ~ 22 -27 km (Richardson, 1980), this still exceeds the thickness allowed for the production of quartz tholeiites directly from typical (i.e. essentially anhydrous) mantle sources. It has been noted that although primary melts may not be picritic, the Mg# of a primary melt must be high and probably in the range ~ 68 -75. The experimental results, therefore, indicate that if derived from anhydrous or water-saturated peridotite source, the dolerite magma evolved in the crust prior to emplacement owing to its low Mg#.

It is possible to estimate which minerals are likely to be on the liquidus using phase equilibria models. Calculations using the models of Nielsen and Dungan (1983) and Glazner (1984), assuming the average chilled margin composition approximates that of a liquid, indicate that plagioclase would be expected on the liquidus. Similar calculations indicate that although olivine is not a liquidus phase for this melt composition, orthopyroxene would be expected on the liquidus with plagioclase. This is consistent with the microphenocryst phases observed in some of the quenched margin rocks noted in the previous chapter.

The results of these calculations can be used to determine whether the variation caused by

fractionation documented in the chilled margin samples (e.g. Mg#, Ni, Cr, Sc, V and TiO₂) is explained by the fractionation of orthopyroxene and plagioclase. Mineral-melt distribution coefficients (K_D s) of Ni and Cr for orthopyroxene in tholeiitic basalts (Sun *et al.*, 1979) are of similar magnitude (~2.5-3), and it may be expected that by removing an assemblage containing appreciable orthopyroxene, the Ni and Cr contents will be reduced. In contrast, Sc and V have K_D s of less than ~0.5 in orthopyroxene and these elements would be expected to increase in the melt with loss of both orthopyroxene and plagioclase. Between these two extremes are elements such as Co and Mn that possess K_D s of approximately 1 for orthopyroxene (although the bulk fractionating assemblage is likely to have a K_D of less than 1 owing to the low K_D for these elements in plagioclase). These general relationships are similar to those displayed in Figures 4.4-4.6 and are consistent with the fractionation of a bulk assemblage containing significant orthopyroxene.

Removal of plagioclase will have a considerable effect on the trace elements partitioned into its structure. Europium and Sr are likely candidates for examination; however, the use of the Sr contents is meaningless as they are believed to have been disrupted during alteration. In the 2+ valence state, Eu partitions into the plagioclase structure and removal of this phase should result in its depletion relative to the other rare-earth elements. Using K_D s for Eu in tholeiitic compositions (e.g. Elthon, 1984) it is calculated that a difference of ~5% plagioclase results in a change in the size of the Eu depletion relative to Sm and Gd (i.e. the Eu/Eu* value where Eu* is the value calculated for the chondrite normalised europium if there were no anomaly) of between 0 and 2%. That is, an unfractionated magma with Eu/Eu* of 1 would have a value of Eu/Eu* = 0.98-1 after the loss of ~5% plagioclase. Clearly, unless the proportion of plagioclase removed is greater than ~5% (by mass), the variation in Eu/Eu* will be within the analytical precision and therefore undetectable.

To examine the change in the magma composition during fractionation more closely, the proportions of orthopyroxene and plagioclase removed must be calculated. This calculation has been performed using a least-squares mixing program (as used in the previous chapter). For these calculations the most primitive (84-111) and evolved (84-213) chilled margin samples have been chosen (on the basis of their Mg#) together with representative compositions of orthopyroxene and plagioclase phenocrysts determined by electron probe. The closest fit between the more primitive sample 84-111 and a recalculated composition for 84-213 prior to fractionation, is obtained by adding 9.05% (by mass) of a 48.7 : 51.3 mixture of orthopyroxene and plagioclase (i.e. 4.41% opx: 4.64% plag). The recalculated composition of 84-213 is listed in Table 4.2 and compares well with 84-111 for most elements. Poor fit is obtained for K₂O; however, the mobility demonstrated for this component during alteration may explain the discrepancy in concentration.

In a more detailed treatment of this type of modelling, Cox (1980) demonstrated that the apparent homogeneity of continental flood basalts may simply be the result of effective buffering of the magma composition by the fractionating assemblage. The remarkable similarity in the compositions of 84-111 and 84-213 indicates that despite the small variation in composition, this range may be the result of significant differences in fractionation.

Table 4.2 This table shows the composition of the most evolved chilled dolerite (84-213) recalculated to the most primitive chilled dolerite composition using 9.05% of a 48.7 : 51.3 mixture of orthopyroxene and plagioclase. Analyses quoted as anhydrous compositions recalculated to 100%, with iron expressed as total iron in the form of FeO. The difference between the recalculated primitive composition, and 84-111 are given in the last column (84-111 minus the recalculated composition of 84-213) and the results are discussed in the text.

	84-111	84-213	Opx	Plag	84-213+9.05% Opx+ Plag	Δ
SiO ₂	54.92	55.60	54.91	48.59	55.24	-0.32
TiO ₂	0.65	0.69	0.08		0.63	0.02
Al ₂ O ₃	14.90	14.78	0.92	32.46	15.05	-0.14
FeO*	8.83	9.19	12.43	0.66	8.81	0.03
MnO	0.17	0.19	0.28		0.19	-0.02
MgO	6.94	6.16	28.99		6.98	-0.04
CaO	10.49	10.53	2.34	15.34	10.40	0.10
Na ₂ O	1.92	1.94	0.03	2.33	1.88	0.04
K ₂ O	1.04	0.77		0.13	0.71	0.33
P ₂ O ₅	0.09	0.11			0.10	-0.01
NiO ₂	0.01	0.009	0.04		0.010	0.00
Cr ₂ O ₇	0.017	0.012	0.14		0.017	0.00
Mg#	61.7	57.9	(80.6)	(An ₇₇)		61.9

Although the small range in composition between chilled margin samples may be modelled by the loss of orthopyroxene and feldspar, the most "primitive" samples (i.e. similar to 84-111) could not have been in equilibrium with mantle olivine and must also represent fractionated products, if derived from a typical peridotite or pyrolite source. Some authors have determined the original composition of basalts, prior to fractionation in the crust for samples in which olivine is a dominant phenocryst phase, by assuming that the fractionation of olivine has been the major cause of the evolution of the magma (e.g. Frey *et al.*, 1978). In these calculations, olivine (the composition of which may be calculated using the relationship between Fe and Mg in olivine and the magma of Roeder and Emslie, 1970) is added to the bulk composition of the evolved magma in a proportion required to raise its Mg content to that of a melt capable of being in equilibrium with mantle olivine. In the study mentioned, this was defined as the point at which olivine of composition Fo₈₈₋₉₀ would be calculated as a liquidus phase.

It is possible that although olivine has not been observed in the Tasmanian chilled margin samples, it may only just have become unstable prior to emplacement judging from the high magnesian composition of some of the orthopyroxene microphenocrysts (~En₈₃). However, as olivine is not observed, it is necessary to calculate the least fractionated composition that would have olivine on the liquidus before olivine addition calculations can be performed.

It has been suggested that the loss of orthopyroxene and plagioclase has resulted in the small compositional variation in the chilled margin dolerites. Assuming that this fractionation is representative of the evolution occurring prior to emplacement, the same pyroxene-plagioclase mix has been added to the most primitive sample (84-111) until olivine is calculated as a liquidus

phase (using the equations of Nielsen and Dungan, 1983). After 25% (by mass) addition, olivine ($\sim\text{Fo}_{87}$) is theoretically present on the liquidus. The composition of the olivine is determined both by the calculation of the phase equilibria (Fo_{86}), and using the relationship of Roeder and Emslie (1970) mentioned previously (Fo_{87}).

The resulting composition calculated for the magma is very similar to an olivine-bearing Jurassic tholeiite from Antarctica (Ortiz, unpublished data) and the chemistries are compared in Table 4.3. The fit is remarkably good although the SiO_2 is high and Al_2O_3 and FeO^* are low in the calculated Tasmanian magma when compared with the Antarctic sample. The reconstruction of an olivine-bearing tholeiitic magma (as the precursor to the quenched liquids now present at the chilled margins in Tasmania) using the model suggested, produces a feasible composition which can actually be sampled in the field in other continental tholeiitic provinces. The fact that the match is so close to the sample shown from the Ferrar province of Antarctica is particularly relevant to the discussion in Chapter 5.

Table 4.3 Comparison between the composition of the Tasmanian magma calculated to have olivine on the liquidus and an olivine-bearing chilled margin dolerite from the Ferrar Group in Antarctica (analysis provided courtesy of Prof. D.H. Green, Univ. Tas.). Also shown is the calculated primary magma composition obtained by adding 5% olivine to the "olivine-bearing" magma of column 1. Mg# and olivine compositions (calculated using the relationship of Roeder and Emslie, 1970) are also given.

	Tasmanian Dolerite 84-111 + 25% mix opx+plag	Ferrar Olivine Dolerite Darwin Glacier; DG 49	Calculated primary Tasmanian tholeiite (column 1 + 5% ol)
SiO_2	54.09	52.96	53.40
TiO_2	0.50	0.50	0.48
Al_2O_3	15.62	16.41	14.84
FeO^*	7.84	8.41	8.08
MnO	0.16	0.17	0.15
MgO	9.05	8.67	10.95
CaO	10.11	10.63	9.60
Na_2O	1.75	1.64	1.66
K_2O	0.80	0.47	0.76
P_2O_5	0.07	0.06	0.07
Mg#	70.3	67.9	73.5
Olivine (Fo)	~ 86	86	89

Using the estimate of the Tasmanian olivine-bearing tholeiite composition, it is possible to calculate a primary melt composition for the Tasmanian Dolerite magma employing olivine addition calculations similar to Frey *et al.* (1978). The addition of 5% olivine with the composition Fo_{87} is required to bring olivine of Fo_{89} onto the liquidus. The "primary" melt composition determined for the Tasmanian Dolerites is shown in Table 4.3. It is notable that the calculated magma is high in SiO_2 , and very low in TiO_2 , FeO^* , Na_2O and P_2O_5 . These features are similar to characteristics displayed by tholeiites associated with island arc and interarc basins, which have been derived from a very depleted mantle source (Sun and Nesbit, 1978). The unusually low TiO_2 and P_2O_5 contents in the Tasmanian chilled margins will be

explored further in sections 4.1.8, 4.1.9 and 4.2.

The generally low Ni and Cr contents of the Tasmanian chilled dolerites may now be considered in the light of the calculations performed in this section. Addition of ~12% orthopyroxene (i.e. ~48% of the total assemblage of plagioclase and orthopyroxene added to 84-111), increases the Ni and Cr contents to at least 100 and 210 ppm respectively. This is based on the Ni and Cr abundances in the orthopyroxene composition shown in Table 4.2. The concentration of Ni will also be increased by the addition of 4% olivine; using the mineral-melt K_D of Sun *et al.* (1979) for olivine in MORB, the Ni may be raised to ~140 ppm. These Ni and Cr values are still rather low compared with concentrations observed in many other tholeiitic rocks, and the fractionation of a small amount of Cr-spinel may also be involved in the evolution of the primary magma.

The general results of all of these calculations suggest that evolution of a mantle-derived tholeiite, possibly derived from a somewhat depleted source, can explain much of the major element chemistry of the Tasmanian Dolerites. Although this solution is non-unique, it appears unnecessary to appeal to an unusually iron-rich mantle source for the production of the Tasmanian Dolerite magma.

4.1.7 Rare earth elements, (REE)

As mentioned previously, the REE in the chilled margin dolerites show limited variation beyond the precision of analytical measurement. The average composition has been plotted normalised to chondrites (Fig. 4.7a). The chilled margins are LREE enriched ($La_N/Sm_N = 2.2$) with a relatively flat HREE pattern at approximately 10 x Chondrite ($Gd_N/Lu_N = 1.1$); where the subscript N refers to concentrations normalised to chondrites. The depletion in Eu is significant with $Eu/Eu^* = 0.83$. Although this is consistent with the results of the last section, in which plagioclase was found to be a liquidus phase during the fractionation of the magma prior to emplacement, the magnitude of the depletion is far too great. The estimate for the amount of fractionation of plagioclase (~13%) would produce a depletion in Eu of ~2% (i.e. $Eu/Eu^* \approx 0.98$) in a magma having no prior Eu anomaly. It is clear that this is much smaller than the depletion observed in the dolerites and necessitates that the magma already possessed a depletion in Eu.

The existence of a prior depletion in Eu is considered even more likely when the Gd results from different techniques are compared. The value of Eu/Eu^* depends critically on the precise and accurate measurement of Sm, Eu and Gd because the equation for the calculation of this parameter is: $Eu/Eu^* = Eu_N / \sqrt{(Sm_N \times Gd_N)}$. The REE data obtained for sample 84-152 from both INAA and SSMS are shown in Figure 4.7b. Although the Sm and Eu values agree closely from the two techniques (so much so that they overlap completely in the case of Eu), the difference of 0.44 ppm (or 12%) in the Gd numbers results in a difference in Eu/Eu^* values of 0.80 (for INAA) compared with 0.73 (for SSMS). It is conceded that Gd is one of the least precise elements measured by INAA (Appendix 3), and a smooth REE pattern would suggest a Gd concentration similar to that obtained by SSMS. If the SSMS analysis is closer to the true Gd concentration, it emphasises that the amount of plagioclase removed during fractionation cannot explain the depletion in Eu, and that it is necessary for the magma to have possessed a

negative Eu anomaly prior to this event. This may be the result of mixing a component already bearing a depletion in Eu into the magma, or represent the signature of the original mantle source.

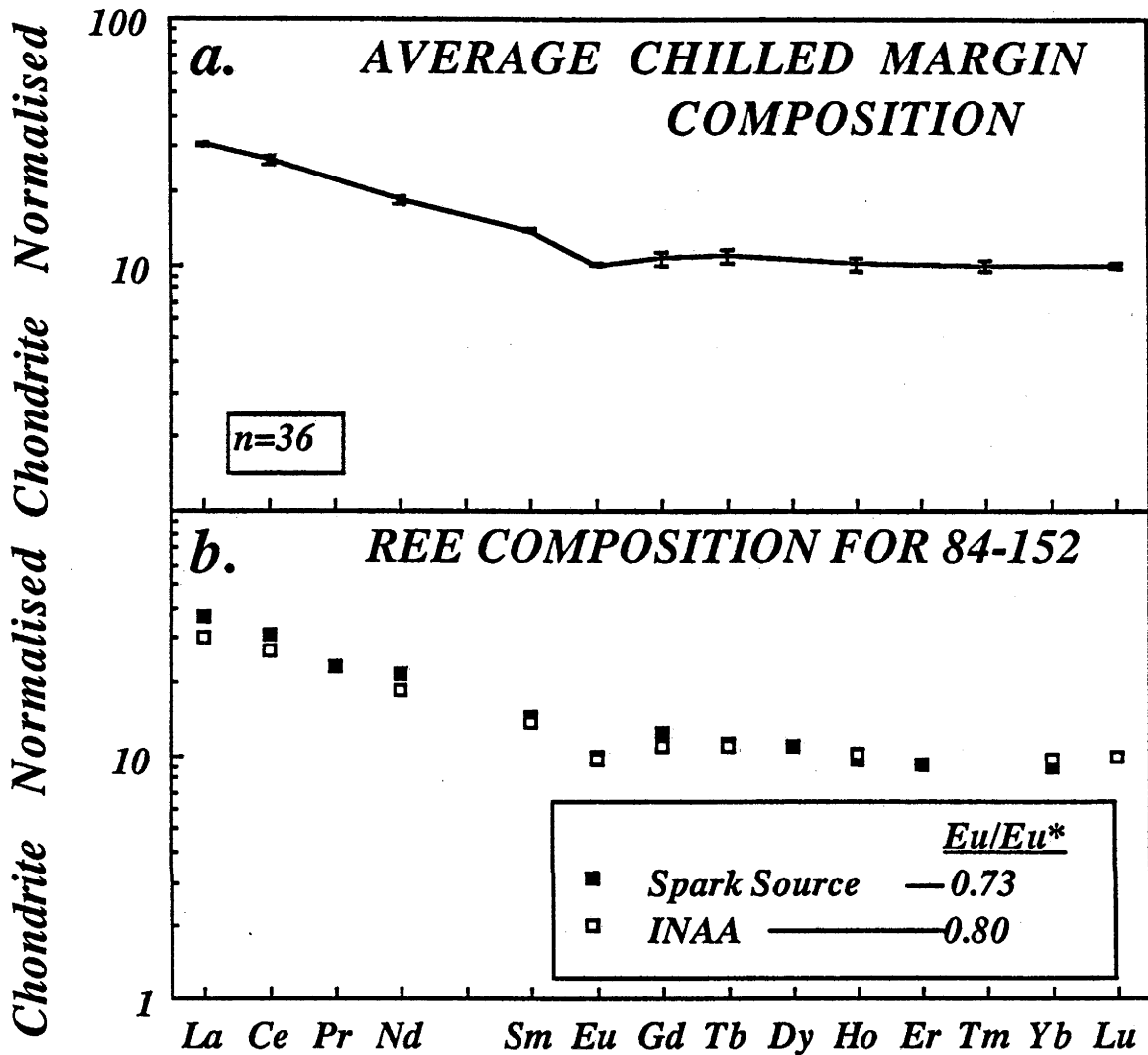


Fig. 4.7 Chondrite normalised diagrams illustrating the REE signature of the chilled margin dolerites. a. The total range in the chilled margin compositions is shown, and the data have been plotted as error-bars because the use of symbols otherwise obscures the variation observed. b. A comparison between the results of two different analytical techniques (i.e. instrumental neutron activation analysis and spark-source mass spectrometry) illustrates the difficulty in using the Eu/Eu^* values in the discussion of the petrogenetic history of the chilled dolerites. [Normalising values are taken from the unfractionated C1 estimate of Anders and Ebihara (1982) multiplied by 1.5 to allow for volatile loss.]

4.1.8 Primitive mantle normalised (PMN) pattern

The chondrite normalised REE pattern is an effective method of characterising the trace element signature of a sample. Another illustration of the trace element signature is given by the Primitive Mantle Normalised (PMN) diagram of Figure 4.8a. The elements are plotted with essentially increasing incompatibility towards the left, and the range in the data (excluding the Ba from the three drill-core samples mentioned previously) is given. The pattern is similar to many continental flood basalts, i.e. enriched in incompatible elements and Pb, accompanied by characteristic depletions in Nb, Sr, P and Ti (e.g. Thompson *et al.*, 1983; Dupuy and Dostal,

1984). This general pattern in turn resembles that observed in island arc basalts (IAB) except that IABs do not possess a depletion in Sr relative to Pb and Nd (e.g. Nakamura *et al.*, 1985).

The log-scale used in this diagram tends to disguise the increased spread in the more incompatible elements. To illustrate this variation the standard deviations of the data have been normalised to the estimated precision (data from Table 4.1) and the results are given in Figure 4.8b. It is evident that Cs, Rb, Ba, K and Sr vary significantly outside the limits of analytical precision as discussed above (section 4.1.3).

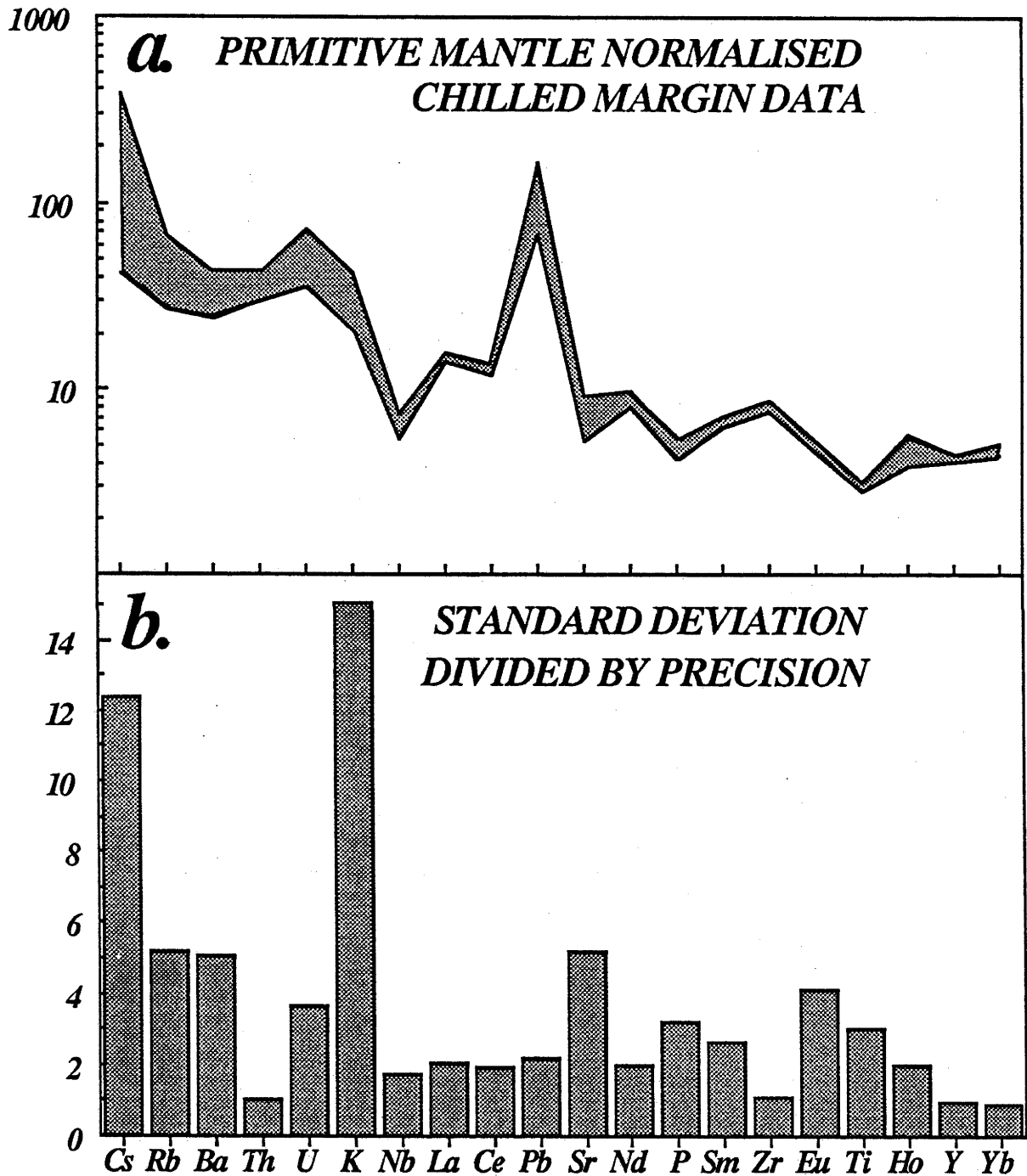


Fig. 4.8 Trace element diagrams illustrating the signature of the Tasmanian chilled dolerites. a. Primitive mantle normalised diagram with the elements in order with increasing incompatibility towards the left-hand side (normalising values and order of listing from Sun and McDonough (1987)). b. Histogram illustrating the variation of the more incompatible (or mobile) elements beyond the precision of the analytical measurements. The standard deviation of the chilled margin data (from Table 4.1) is divided by the analytical precision. [Note: in the absence of a more reliable estimate, errors of 3% were assigned to Rb, Ba and Sr; this is considered a maximum.]

4.1.9 Elemental ratios: a comparison with mantle and crustal reservoirs

The observation by earlier workers that the Tasmanian Dolerites possess crustal-like ratios for some elements (Heier *et al.*, 1965) prompts a more detailed comparison utilising the new data available. Several recent contributions allow comparison between primitive mantle, ocean island (OIB), island arc (IAB), and mid-ocean ridge (N-type MORB and E-type MORB) basalts and crustal environments (Sun, 1980-82; Hofmann *et al.*, 1986; Sun and McDonough, 1987; Taylor and McLennan, 1985 and others). For simplicity, the data are given in Table 4.4.

It is evident that for many of the elemental ratios listed, the Tasmanian chilled margin dolerites show greater affinities with crustal rather than mantle signatures (e.g. compare the relatively uniform Nb/U and Ce/Pb ratios of modern mantle basalts (originally documented by Hofmann *et al.*, 1986; and Newsom *et al.*, 1986) with those of the crustal and Tasmanian values). One exception is the average arc tholeiite in which these ratios are very similar to the Tasmanian chilled margin values. Note however, that the other ratios (e.g. K/U, Rb/Sr, Rb/Cs, P/Nd, Ti/Zr, and La_N/Sm_N) compare more favourably with the crustal values than the arc tholeiite. The Tasmanian samples clearly have strong crustal signatures in agreement with the earlier observations. The crustal reservoirs listed possess ratios similar to those of many granitic rocks. This is consistent with the earlier suggestion that the crustal signature of these dolerites is reminiscent of granitic compositions (Compston *et al.*, 1968) and is discussed in more detail in section 4.3.

Table 4.4 Selected elemental ratios for mantle and crustal environments compared with the Tasmanian chilled margin average. Estimates of primitive mantle and MORB compositions used are from Sun and McDonough (1987); the OIB tholeiite is the Kilauean sample KL2 of Newsom *et al.* (1987) with additional data (e.g. Ti and Th) from Leeman *et al.* (1980) and P from BVSP (p. 166); the IAB tholeiite is the average from Sun (1980). The average crust and shale used are those of Taylor and McLennan (1985), the shale composition being that of their Post-Archaean Terrestrial Shale average.

Ratio	Primitive Mantle	N-MORB Average	E-MORB Average	OIB Tholeiite	IAB Tholeiite	Average Crust	Shale Average	Tasmanian Dolerite
K/U	10455	12500	11667	12455	32400	10000	9908	7305
Th/U	4.2	2.5	3.3	3.3	2.5	3.8	4.7	3.4
Nb/U	33.5	50.0	46.1	51.5	7	12	6	4
Ce/Pb	9.46	25	25	33	2	4	4	4
Rb/Sr	0.03	0.006	0.03	0.03	0.023	0.12	0.80	0.24
Rb/Cs	20	80	80	110	21	32	11	31
P/Nd	65	72	69	53	-	-	22	32
Ti/Zr	112	103	82	97.8	136	54	29	40
La_N/Sm_N	1.00	0.59	1.51	1.50	0.7	2.9	4.3	2.2
Eu/Eu*	1.00	1.01	1.01	1.02	-	0.99	0.66	0.74 ?

4.2 ISOTOPE GEOCHEMISTRY

4.2.1 Sr isotopic composition

The unusually radiogenic composition of the initial $^{87}\text{Sr}/^{86}\text{Sr}$ of the Tasmanian Dolerites was first documented by Heier *et al.* (1965). These authors measured a range in this ratio of approximately 0.711 ± 0.001 ; however, the poor precision available at that time did not permit the discussion of the variation, and statistical treatment of the data suggested that almost all of the variation could be attributed to experimental error. Several explanations for the radiogenic character of the Sr from these rocks were discussed. Although continental crustal contamination was considered a possibility, it was thought to be unlikely owing to the geochemical homogeneity of the dolerites. The low K/Rb ratios observed were also thought to be difficult to generate in a process involving contamination. It was concluded that the radiogenic initial Sr-isotopic composition could have been produced by one of three processes; a) contamination by a process of selective diffusion, b) generation within the crust if the geothermal gradient in Tasmania was substantially higher than at present, or c) production from a mantle of unusual composition.

Subsequent work has confirmed the unusual character of the Sr isotopic system in the Tasmanian Dolerites (Allègre *et al.*, 1982). These authors suggested that the results were consistent with a model whereby a depleted mantle melt similar to MORB had mixed with a crustal component (having variable regional characteristics) to produce the variation in the highly radiogenic $^{87}\text{Sr}/^{86}\text{Sr}$ compositions determined. Despite the admission of problems involved in mixing large quantities of crust into the melt required to satisfy the strontium isotopic system (e.g. in a ratio of around 1:1), it was considered that processes such as zone refining, assimilation with simultaneous fractionation, wall rock alteration, or diffusion may facilitate transfer of the isotopic character of the crustal contaminant to the magma without developing a melt composition much more silicic than a basalt.

The isotopic results of the present study are presented in Appendix 5 and show a range in initial $^{87}\text{Sr}/^{86}\text{Sr}$ of 0.70940 to 0.71284, consistent with the earlier reports. The high values compared with typical mantle source compositions (~ 0.703 - 0.705) imply derivation from a source (or incorporation of a component) with an extended history of high Rb/Sr ratio.

The variation of initial $^{87}\text{Sr}/^{86}\text{Sr}$ ratios is of the order of 60-70 times greater than the error associated with their measurement and requires explanation. The components showing marked variation in concentration (e.g. Cr, Mg#, TiO_2) were plotted against these initial ratios to evaluate the possibility of contamination processes. Two of the plots are presented in Figure 4.9 and illustrate that no obvious correlation exists between these parameters.

In section 4.1.3, it was noted that the Sr concentrations in the chilled margin dolerites appear to have been changed during some form of alteration process. If the mobilisation of Sr was also accompanied by exchange or addition of Sr involving source of different isotopic compositions, the scatter in initial $^{87}\text{Sr}/^{86}\text{Sr}$ ratios may be at least partially attributed to this process.

The strong coupling between the Sr and Nd isotopic systems has also been employed to

investigate the cause of the range in initial $^{87}\text{Sr}/^{86}\text{Sr}$ ratios. The combined use of these two radiogenic systems was expected to reveal processes such as contamination or magma-mixing, which may have operated to produce the variation observed in the initial Sr isotopic compositions.

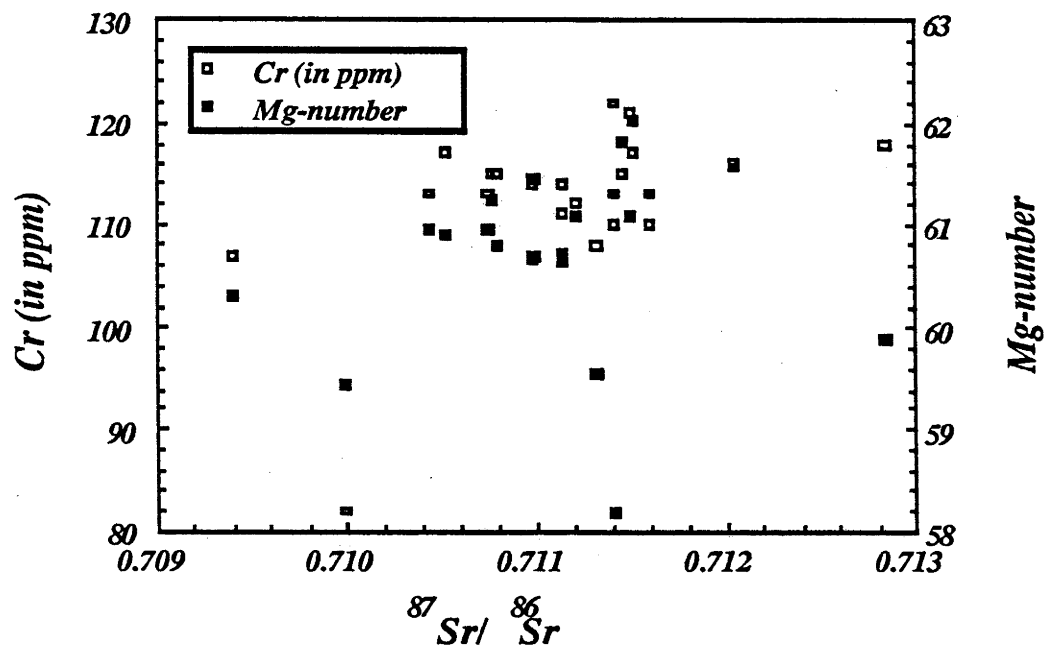


Fig. 4.9 Plot of two of the parameters believed to owe their variation to fractionation prior to intrusion against the range of Sr-isotope initial ratios. The lack of correlation between these parameters suggests that the variations observed were not the result of a single process (e.g. assimilation accompanied by simultaneous fractional crystallization).

4.2.2 Nd isotopic composition

The first set of Nd isotopic data obtained for 21 of the chilled margin samples are given in the first table of Appendix 5 and show a total variation in initial ϵ_{Nd} of -6.4 to -4.9. Although the average error associated with these measurements is approximately ± 0.5 of an epsilon unit, the range obtained is close to the analytical uncertainty and suggests that the Nd isotopic composition for these samples is approximately -5.6 ± 0.5 . This composition is unusually unradiogenic for mantle-derived magmas and implies derivation from a source with a time-integrated history of LREE enrichment.

The initial compositions for Sr and Nd isotopes are plotted together in Figure 4.10 along with data for oceanic basalts for comparison. It is clear that the Tasmanian Dolerites possess an isotopic signature quite different from modern oceanic basalts. This is a function of both the highly radiogenic Sr composition and the distinctly unradiogenic Nd composition compared with basalts from a range of oceanic environments.

Although the spread in Sr compositions is well illustrated in this diagram, the Nd data concentrate at an ϵ_{Nd} of ~ -5.6 . The 2σ error-bars associated with these data generally overlap, although one or two points appear to vary beyond these limits by a small amount. To detect any fine-scale variation in the Nd compositions, 12 samples that encompassed the total range of ϵ_{Nd} were chosen and re-analysed using the recently acquired Finnigan-Mat 261 multiple collector mass spectrometer. The precision of the measurements improved from approximately ± 0.5 of

an epsilon unit to ± 0.1 - 0.2 of an epsilon unit. Despite this, no variation was observed outside the analytical precision! The range in the data obtained is -5.04 to -5.36 with an average of -5.17 ± 0.2 (2σ , Fig. 4.10 inset). The ~ 0.5 epsilon unit machine bias has been removed from the data by normalising the results to the value obtained for BCR-1 obtained from each instrument (see Appendix 3 for further discussion).

It is apparent that the process(es?) which caused the variation in the Sr-isotopic composition did not cause a change in the Nd isotopic signature. It is possible that

1. Mixing occurred between components with very similar Nd signature but different Sr-isotopic compositions.
2. Mixing occurred between components with different Sr and Nd isotopic signatures; however, the Nd signature is dominated by one member as a result of a large difference in their relative contribution of Nd.
3. The magmas intruded with uniform Sr and Nd compositions, but the Sr system was later disturbed by a mobilization event which did not effect the Nd isotopic composition.

To evaluate the likelihood of each of these alternatives, additional isotopic analyses were performed. The Pb-isotopic system may be sensitive to processes involving the mixing of mantle and crustal components owing to the relatively high Pb content of crustal rocks compared with mantle-derived basalts. Oxygen isotopes were also used to examine the three possibilities. This element is useful because it is a major element and therefore not easily dominated by one component during mixing (unless trivial amounts of one component are added or the endmembers have similar $\delta^{18}\text{O}$ compositions). It is also likely that this system would record any post-emplacement alteration processes operating on the samples.

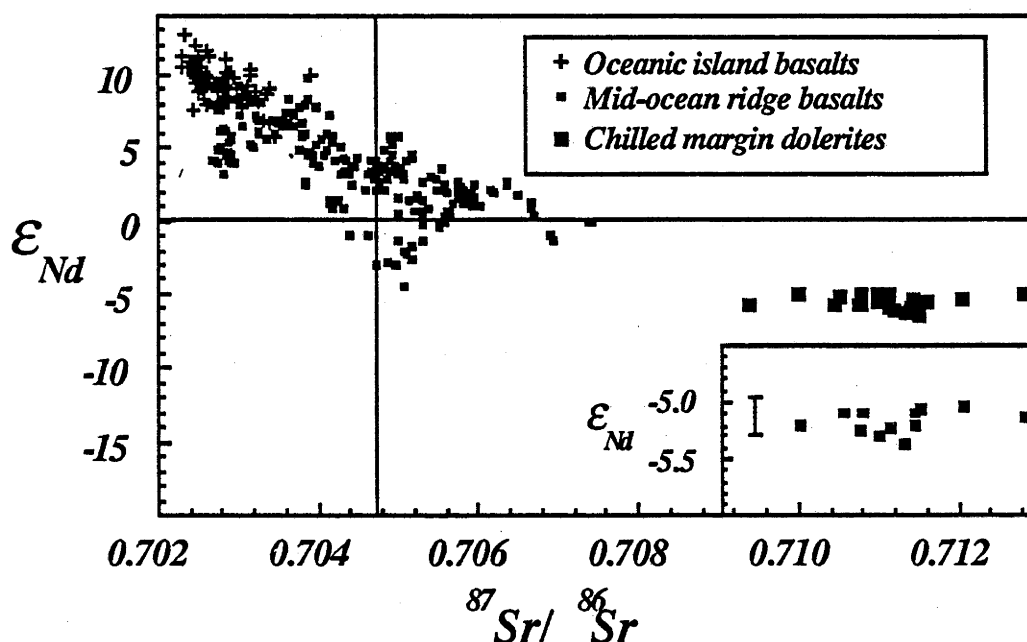


Fig. 4.10 Diagram illustrating the initial Nd and Sr isotopic compositions of the Tasmanian chilled margin dolerites. The insert shows the Nd data obtained from the MAT 261 spectrometer. Fields for mid-ocean ridge and ocean island basalts are included for comparison (data from Cohen and O'Nions (1982a,b), Richardson *et al.* (1982), White and Hofmann (1982), Vidal *et al.* (1984), Palacz and Saunders (1986), Wright and White, (1986/87), Dupuy *et al.* (1987) and Ito *et al.* (1987)).

4.2.3 Pb isotopic composition

The Pb-isotopic compositions were obtained for four samples spanning a large range in initial $^{87}\text{Sr}/^{86}\text{Sr}$ compositions. These samples were chosen to maximize the chance of detecting a mixing trend if this were the cause of the spread in initial $^{87}\text{Sr}/^{86}\text{Sr}$.

The data are presented in Table 4.5 and demonstrate the uniformity of the compositions obtained. Each analysis was performed in duplicate to safeguard against errors resulting from the correction for mass fractionation during data collection. It is clear that the variation between duplicate analyses is close to the total variation observed between samples.

These Pb data are consistent with the results of Allègre *et al.* (1982) and both sets of data have been plotted in Figure 4.11. Compared with oceanic basalts, the present-day and age corrected data plot close to the interface between the main clusters of the MORB and OIB-IAB data for $^{208}\text{Pb}/^{204}\text{Pb}$. In contrast, the dolerites are enriched in $^{207}\text{Pb}/^{204}\text{Pb}$ and plot amongst the oceanic island data. The high values for $^{207}\text{Pb}/^{204}\text{Pb}$ suggest an old origin for the lead because ^{207}Pb is produced by the radioactive decay of ^{235}U which is now only a minor constituent of "modern-day uranium" owing to its short half-life. These results imply that the Pb in the Tasmanian Dolerites was derived from an old source enriched in U, either a crustal component mixed into a basalt magma, or a mantle source bearing an unusual but old signature. Because the results are so uniform it is impossible to distinguish between these alternatives; however, if a crustal component is involved it is clear that it must totally dominate the signature. This is quite feasible owing to the low Pb contents of typical mantle-derived basalts.

Table 4.5 Lead isotopic data for selected Tasmanian chilled margin samples. Duplicate runs are shown and age (175 Ma) corrected data (using the average of the duplicate analyses, Th/U ratios obtained from INAA, and the U data given) are included in parentheses. The high ratios obtained for the duplicate analyses of 84-101 are probably the result of mass fractionation (values shown with an asterix).

Sample	U ppm	Pb ppm	$^{238}\text{U}/^{204}\text{Pb}$	$^{206}\text{Pb}/^{204}\text{Pb}$	$^{207}\text{Pb}/^{204}\text{Pb}$	$^{208}\text{Pb}/^{204}\text{Pb}$
84-101	0.84	5.10	12.21	18.904	15.648	38.787
				18.939*	15.681*	38.874*
				(18.57)	(15.63)	(38.49)
84-106	0.76	4.42	12.63	18.901	15.639	38.733
				18.917	15.657	38.767
				(18.56)	(15.63)	(38.40)
84-129	0.82	4.50	13.45	18.924	15.643	38.780
				18.915	15.638	38.750
				(18.55)	(15.62)	(38.39)
84-221	0.86	4.95	12.81	18.900	15.637	38.743
				18.910	15.644	38.758
				(18.55)	(15.62)	(38.47)

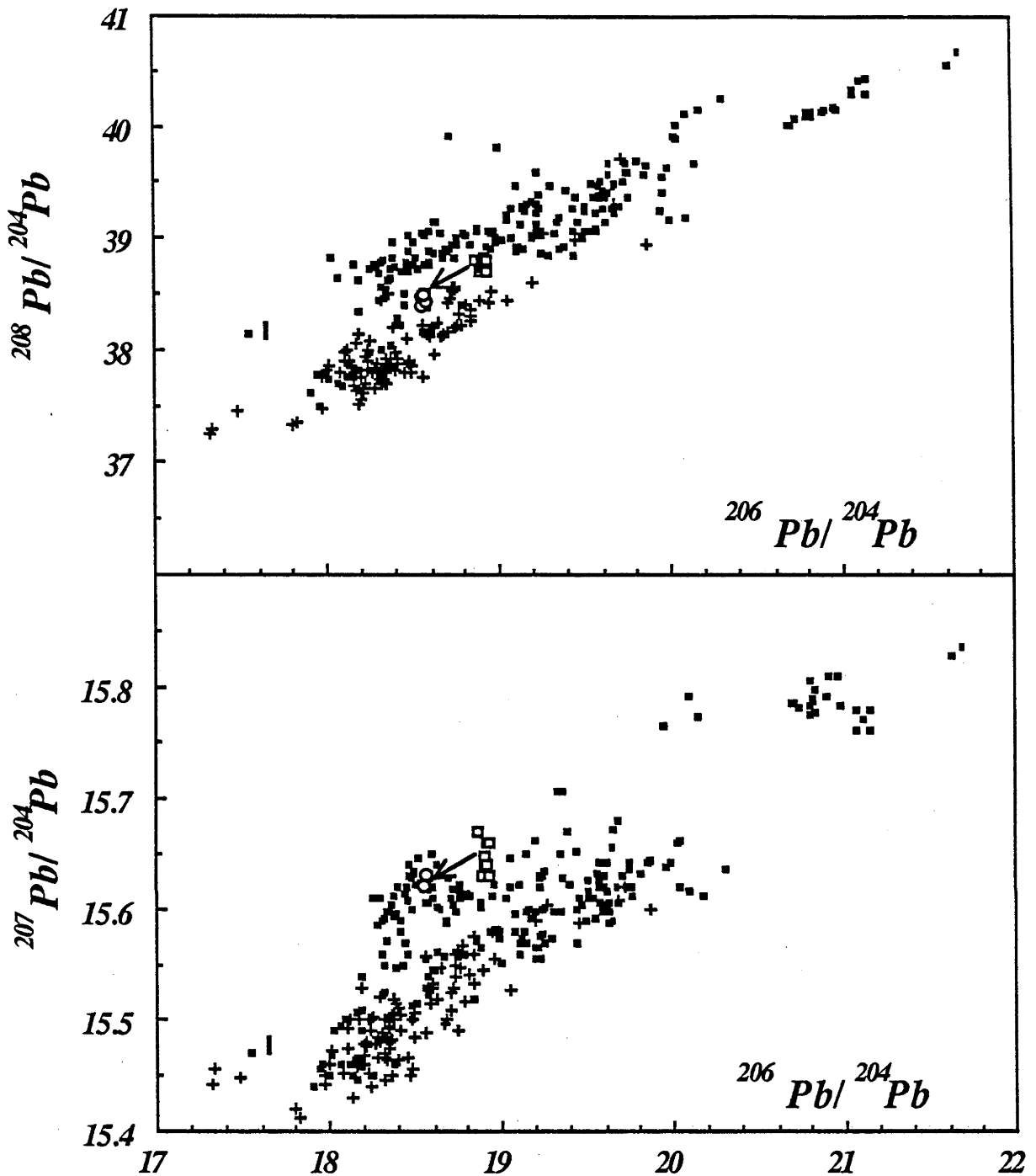


Fig. 4.11 Pb-isotope compositions of the Tasmanian Dolerites (open squares) compared with oceanic basaltic rocks (MORB data are represented by the crosses, and OIB-IAB data by small closed squares). Arrows from the Tasmanian data to open circles indicate age corrected compositions obtained from this study. Additional data from Tasmania are from Allègre *et al.* (1982); data for the oceanic basalts are from Dupré and Allègre (1980), Sun (1980), Cohen and O'Nions (1982a,b), Richardson *et al.* (1982), Vidal *et al.* (1984), Palacz and Saunders (1986), Wright and White (1986/87) and Ito *et al.* (1987).

4.2.4 O isotopic composition

The uniformity of Nd and Pb isotopic compositions and variation in $^{87}\text{Sr}/^{86}\text{Sr}$ initial ratios suggests that the Sr owes its variation to a process which did not involve these other radiogenic systems. Oxygen isotopic analyses were performed on a number of chilled margins already analysed for their Sr and Nd compositions (Appendix 5). A significant range in the $\delta^{18}\text{O}$ (relative to standard mean ocean water, SMOW) was obtained from the very low value of

+1.9‰ to a composition more typical of mantle derived melts, +6.1‰ (values are ± 0.3 , 2σ). This range is illustrated in Figure 4.12 together with the Sr-isotopic data.

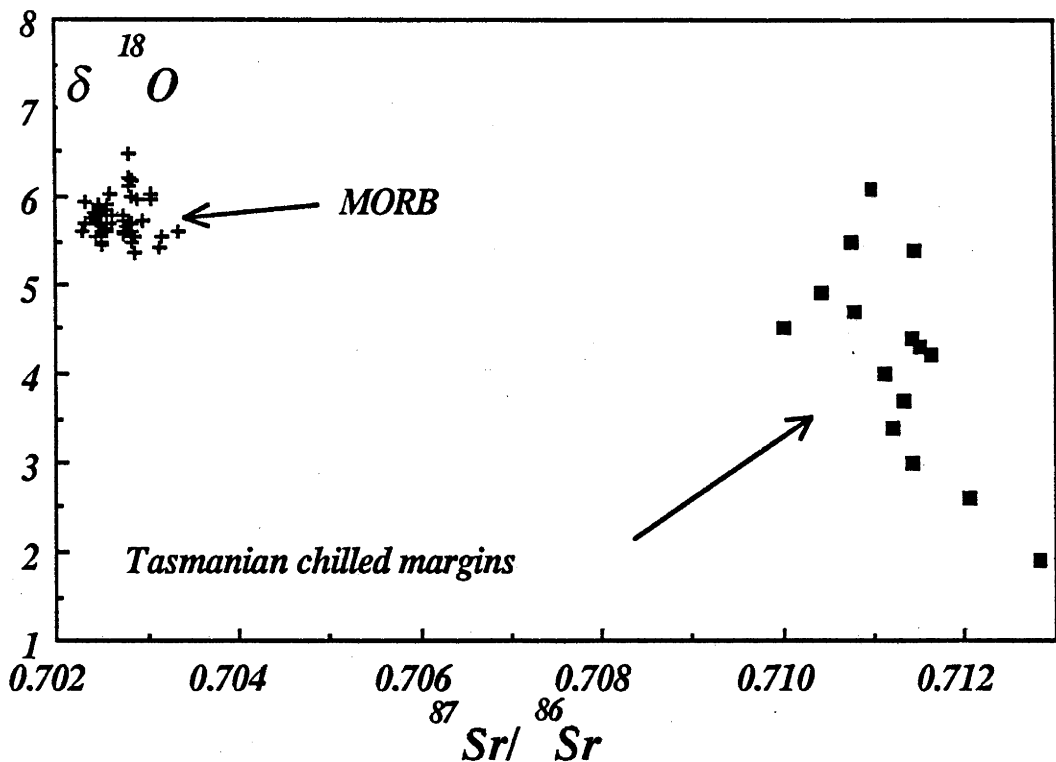


Fig. 4.12 Plot of the isotopic compositions of oxygen (in ‰ relative to SMOW) and strontium for the Tasmanian chilled margin dolerites compared with mid-ocean ridge basalts. MORB data are from Ito *et al.* (1987).

The weak negative correlation observed may be the result of the following processes: 1) mixing between a mantle derived melt ($\delta^{18}\text{O} = \sim +5.7\text{‰}$) and a lithology with low $\delta^{18}\text{O}$ but high $^{87}\text{Sr}/^{86}\text{Sr}$ composition prior to emplacement, 2) dolerite interaction with sea-water, or 3) dolerite interaction with meteoric water

To produce the low $\delta^{18}\text{O}$ value of +1.9‰ and the high initial $^{87}\text{Sr}/^{86}\text{Sr}$ composition (0.7128) of sample 84-222 by mixing a typical mantle melt with a crustal component, it would be necessary to appeal to a crustal material with values more extreme than this (i.e. $\delta^{18}\text{O} < +1.9\text{‰}$ and $^{87}\text{Sr}/^{86}\text{Sr} > 0.7128$). Lithologies with $\delta^{18}\text{O} \ll +1.9\text{‰}$ are exceedingly rare and include materials such as ophiolites and serpentinites, or some potassic mafic volcanics (Graham and Harmon, 1983). Even if these components were available contaminants, it is unlikely that the requirement of a very radiogenic Sr-isotopic composition could be fulfilled by these rocks.

In contrast, seawater by definition has a $\delta^{18}\text{O}$ of zero and has been shown to have a variable radiogenic Sr-isotopic composition in the past (e.g. Burke *et al.*, 1982). Using the compilation of $^{87}\text{Sr}/^{86}\text{Sr}$ versus time of these authors for the Middle Jurassic, it is evident that the $^{87}\text{Sr}/^{86}\text{Sr}$ composition of sea-water has not exceeded 0.70805 in this period and is best estimated as ~ 0.7075 . Clearly, if sea-water interaction had been responsible for the decrease in the $\delta^{18}\text{O}$ compositions of the chilled dolerites, it should have been accompanied by a decrease in the initial $^{87}\text{Sr}/^{86}\text{Sr}$ signature rather than the increase observed.

The isotopic composition of meteoric water is well documented and has been shown to

define a strict correlation with the isotopic signature of hydrogen (Craig, 1961). The variation of $\delta^{18}\text{O}$ with δD was shown to be very systematic and correlated with the latitude or elevation of the location sampled (i.e. the greater the elevation or the closer to the polar regions, the lower the $\delta^{18}\text{O}$ composition of the groundwaters). A compilation of $\delta^{18}\text{O}$ and δD data for groundwaters by Taylor (1974) showed that meteoric waters span an enormous range in $\delta^{18}\text{O}$ from $\sim+5\text{‰}$ to less than -50‰ . It was also shown that heated groundwaters have $\delta^{18}\text{O}$ signatures between ~ 2 and $\sim 5\text{‰}$ higher than those of unheated groundwaters from the same vicinity.

Taylor also reviewed the evidence for the exchange of meteoric oxygen with igneous intrusions and demonstrated that it is very common, especially when the country-rocks are permeable to groundwater movement. He pointed out that in some cases there is no petrographic evidence of interaction (e.g. partial alteration of primary pyroxenes or olivines to secondary phases such as amphiboles, chlorites or epidote) implying that the exchange probably occurred at high temperature.

It is possible, and probably likely, that emplacement of $\sim 15,000 \text{ km}^3$ of magma into the Permo-Triassic sediments of the Tasmanian crust resulted in an increase in the temperature of the surrounding groundwaters. Exchange of oxygen between the chilled margin dolerites and meteoric water occurred producing the low $\delta^{18}\text{O}$ values observed in some samples. Because the incompatible elements (e.g. Ba, Rb Cs etc...) can be mobile in alteration processes (e.g. Clague and Frey, 1982), these elements may also be affected. A weak correlation between the $\delta^{18}\text{O}$ and initial $^{87}\text{Sr}/^{86}\text{Sr}$ signatures of the chilled margins suggests that radiogenic Sr has also been transported to the contacts in this process. It is stressed however, that the correlation is weak and the open-system nature of the exchange mechanism envisaged should not be expected to produce a correlation between the initial $^{87}\text{Sr}/^{86}\text{Sr}$ signature of the dolerites and other effected parameters (e.g. mobile elements).

The favoured mechanism for producing the correlation between the Sr and O isotopic compositions is that of meteoric water interaction with the dolerites at the time of emplacement. The distance from the chilled margins penetrated by this type of alteration will be discussed further in Chapter 5. Interestingly, the Pb-isotopic system, which may be expected to show scatter during interaction with meteoric water, does not appear to have been disrupted (e.g. Slawson, 1983). Therefore, it must be assumed that the meteoric water did not contain appreciable Pb which was available for exchange.

4.3 MAGMA GENESIS

It has been demonstrated that the chemical and isotopic compositions of the magmas which gave rise to the Tasmanian Dolerites were changed by at least two processes. Prior to emplacement, the crystallization of olivine, pyroxene and plagioclase produced a residual liquid of quartz tholeiitic composition (now represented by the chilled margin rocks). This evolution appears to have been buffered by the fractionating assemblage because significant differences in the amount of fractionation ($\sim 11\%$ in the most extreme case), resulted in quenched dolerites with essentially the same compositions. Shortly after emplacement, the dolerites underwent variable degrees of exchange with meteoric water. Not only did this alter the oxygen isotope

composition of these rocks, but radiogenic strontium carried in the water was added to the dolerites, and some of the more incompatible elements were mobilised (e.g. Ba, Cs, Rb, K). This process of exchange was the cause of much of the variation observed in the Tasmanian chilled dolerites.

Despite the variation caused by the fractionation prior to emplacement and the alteration shortly afterwards, the signatures preserved in the Tasmanian Dolerites have distinctly crustal characteristics. For example, although the alteration process produced a degree of spread in the initial $^{87}\text{Sr}/^{86}\text{Sr}$ ratios, these nevertheless are uncommonly high for basaltic rocks, requiring production from an old environment enriched in Rb relative to Sr. The Nd radiogenic system also requires a long-lived incompatible element enriched history (i.e. LREE enriched with high Nd/Sm retarding the effect of radiogenic growth). Also, as mentioned previously, the high $^{207}\text{Pb}/^{204}\text{Pb}$ supports an old origin for the Pb.

Given that the geochemical and isotopic data strongly support the addition of a crustal component in the petrogenesis of these tholeiites, the question of the mechanism involved must be addressed. Essentially two options are available when considering the introduction of a crustal component into a basaltic melt; either magmas were derived from the mantle and introduced into a level in the crust where they suffered contamination (probably accompanied by fractionation), or a crustal component was introduced into the mantle source during a process of subduction either contemporaneous with, or prior to, the magmatism in the Mesozoic. It should be noted that the high temperature of the magma at the time of emplacement ($\sim 1200^\circ\text{C}$ or thereabouts) means that processes involving the exchange of isotopic and/or trace element signatures by equilibration with the lower crust are not possible. This is because heat is transferred faster than elemental components; therefore, to have the elemental signatures in the basalts produced during equilibration with the lower crust would require the lower crust to be at $\sim 1200^\circ\text{C}$. Even using the unusually high geothermal gradients calculated for southeastern Australia (e.g. Sass and Lachenbruch, 1979; Griffin and O'Reilly, 1987) temperatures in the lower crust do not reach 1200°C .

Because of the mobilisation of some of the most incompatible elements, these will not be used in constraining petrogenetic models; however, their generally high abundances must be consistent with any petrogenetic model proposed. Also it is assumed that the lowest initial $^{87}\text{Sr}/^{86}\text{Sr}$ ratios and highest $\delta^{18}\text{O}$ values approximate the general composition of the magmas prior to exchange with meteoric water, although it is conceded that a small amount of variation produced during the magma petrogenesis may be obscured by the mobilisation and can be accommodated. Both crustal level contamination, and models involving a contaminated mantle source will be addressed in the following discussion. As crustal-level fractionation has been demonstrated for the dolerites, the magma may have had the opportunity of interacting with crustal rocks, and the possibility of contamination during ascent will be addressed first.

4.3.1 Crustal-level contamination

In this section, the likelihood of contaminating a typical mantle-derived melt with crust to produce the composition observed in the Tasmanian chilled margins is discussed. To begin with the constraints provided by the isotopic data are evaluated. Using the trace element signatures, the component of the crust most likely to be involved is then chosen, and the possible mantle endmembers available are explored.

Little crustal material is required to dominate the Pb-isotopic composition because of the low abundance of Pb in mantle-derived melts compared to crustal reservoirs. For example, the Pb concentration in magmas formed by contaminating MORBs (~0.3-0.6 ppm Pb) with 10% of a sediment (~20 ppm Pb) will be between 2.3-2.5 ppm Pb. Of this, 79-88% of the Pb is derived from the sediment. In contrast, the Sr content is typically around 90 and 155 ppm for normal and enriched MORB respectively (Sun and McDonough, 1987) and commonly exceeds 300 ppm in ocean island tholeiites (e.g. Leeman et al., 1980; Newsom *et al.*, 1986) and young tholeiitic basalts in the continental environment (e.g. Frey *et al.*, 1978; McDonough *et al.*, 1985). As the average Sr content in the Tasmanian chilled margin dolerites is around 135 ppm (with an original value of ~100 ppm if the plagioclase, orthopyroxene and olivine fractionation is compensated for) then it is clear that at least half (and probably much more) of this may be expected to be derived from the mantle-derived melt. Clearly, in order for the crustal component to dominate the initial Sr-isotopic composition, it is required to have a very radiogenic signature. In contrast to the Pb-isotopic system, the Sr composition may be expected to be more sensitive to any variation in the amount of crust added during contamination. Unfortunately, the superimposed effects of post-emplacment alteration also caused scatter in the Sr-isotopic system; therefore, although the unusually radiogenic signature can be used as a guide, evaluation of the amount of variation in $^{87}\text{Sr}/^{86}\text{Sr}$ caused by differences in contamination is impossible.

The unradiogenic ϵ_{Nd} signature of the chilled margin dolerites has been contrasted with more typical mantle values and implies a significant effect from the crustal component. In addition, the uniformity of this signature requires that the composition of the crustal endmember and extent of assimilation were either uniform for the various batches of dolerite magma, or that the signature produced in the dolerites was insensitive to the amount of crustal assimilation. It is unlikely that either the crustal components available for assimilation or the extent of contamination could fortuitously be identical across Tasmania, and therefore the first alternative requires a large magma chamber at depth in which the dolerite magma was well mixed. The second option requires that the Nd-isotopic composition of the crustal component be close to that of the dolerite and therefore with continued assimilation this signature is not altered. In this case, the mixing hyperbola connecting a basalt from the mantle array, and a crustal contaminant, must be very shallow, so that with increased contamination, the $^{87}\text{Sr}/^{86}\text{Sr}$ composition may change without a variation in the ϵ_{Nd} signature. DePaolo and Wasserberg (1979) showed that for a shallow mixing hyperbola, the parameter K must be high (i.e. possibly higher than 10) where $K = (\text{Sr}/\text{Nd})_1 / (\text{Sr}/\text{Nd})_2$ for a basalt (1) and contaminant (2). This means that for a typical Sr/Nd ratio of ~12-18 in MORB and OIB tholeiites, the contaminant must have Sr/Nd ~1-2 (i.e. either a very low Sr or high Nd component).

As well as keeping the Nd-isotopic signature balanced, the concentration of Nd in the tholeiites also places constraints on the composition of the crustal component. Tholeiitic basalts from oceanic and continental environments typically have Nd contents of ~7-10 ppm and ~30 ppm respectively. Therefore, it appears most unlikely that the dolerite liquid (with around 13 ppm Nd) could be produced by swamping the mantle melt with crustal Nd. In fact, if it is considered that the value of ~13 ppm Nd for the dolerite may be the result of concentration during the loss of approximately 5% olivine, 12% orthopyroxene and 13% plagioclase, then the original Nd content of the magma may have been only about 8-9 ppm. (As the bulk distribution coefficient for Nd is less than 1, Nd will not be removed during crystallization and therefore fractionation cannot be held responsible for keeping the Nd content low). The importance of this, is that in order to keep the concentration of the Nd balanced, any crustal component added must either have a Nd content close to that of the mantle melt, or be added in such a small quantity that it does not increase the Nd concentration.

There are a number of consequences of this argument. First, if the Nd concentration in the crustal component is high (relative to the dolerite magma) and, therefore, only a small amount of contamination can be accommodated, then the Nd-isotopic composition must be very unradiogenic so that the dolerite magma signature is produced. In this case the Nd-isotopic system will be sensitive to any variation in the amount of contamination and implies that the magma was well mixed at depth. Second, if the concentration of Nd in the crustal endmember is similar to that of the magma, then although considerable contamination may theoretically be accommodated, the amount of contamination required to produce the ϵ_{Nd} of the dolerites would be unrealistically high, resulting in a bulk magma composition far removed from a basalt. In either case, the ϵ_{Nd} composition of the contaminant is required to be significantly less radiogenic than -5.2 and, therefore, to maintain the homogeneity in ϵ_{Nd} observed, the magmas must have been drawn from a single well-mixed magma chamber.

Finally, although affected by alteration, the oxygen-isotope compositions preserved in the dolerites do not exceed $\delta^{18}O = 6.1\text{‰}$. The original values may have been higher prior to alteration; however, assuming that the original magma had a composition similar to 6.1‰ (further discussed in Chapter 5), it would mean that the contaminant was either added in very small quantities, or it possessed an oxygen composition more typical of mantle reservoirs. It has been argued that although most crustal reservoirs have high $\delta^{18}O$ values (e.g. Graham and Harmon, 1983), lithologies exist in the lower crust which possess values of $\delta^{18}O$ similar to the mantle, and therefore care must be used in employing oxygen compositions to derive the petrogenetic history of magmas (Rudnick *et al.*, 1986). The $\delta^{18}O$ of the dolerites, therefore, constrains the contaminant to the lower crust if it is involved in appreciable quantities, or other crustal reservoirs if only a few percent is added.

To summarize, the isotopic data require an old crustal component with high $^{87}Sr/^{86}Sr$ (>0.713), and radiogenic Pb isotopic ratios (probably similar to the dolerite composition) but low ϵ_{Nd} signatures (< -5.2). The uniformity of the Nd composition also suggests that the magmas were homogenised in a single magma chamber. The $\delta^{18}O$ of the assimilant is either similar to mantle values or else the amount added is less than a few percent.

Although the uniformity of many of the isotopic characteristics indicate that contamination occurred prior to the emplacement of the dolerites, different country-rocks were sampled from the contacts to evaluate possible local contamination effects. The Nd and Sr isotopic data obtained are given in Appendix 5 and indicate that at ~175 Ma, the $^{87}\text{Sr}/^{86}\text{Sr}$ ratios were either similar or lower, and the ϵ_{Nd} similar or higher, relative to the compositions of the dolerites. Clearly, if local contamination had any effect at all, it would have reduced the $^{87}\text{Sr}/^{86}\text{Sr}$ ratios and increased the ϵ_{Nd} values in the dolerites.

With this rather general view in mind, the trace element data may be used to examine the possible crustal components involved in the contamination. In section 4.1.9, a comparison was made between the ratios of some trace elements in crustal and mantle compositions. As many of the trace element ratios of the dolerites are similar to crustal reservoirs, this signature can be used to determine the identity of the contaminant. Here, the model compositions for upper, and lower crust, as well as Post-Archaean Terrestrial Shale or PATS (Taylor and McLennan, 1985) are compared with the chilled margin dolerites. Using the primitive mantle normalised (PMN) patterns of these compositions to simplify the comparison, it can be shown that the average PATS of Taylor and McLennan (1985) shows a remarkable similarity to the signature of the dolerites although it has more elevated abundances of the elements (Fig. 4.13). The upper crust composition is also very similar to the dolerite signature; however, the lower abundances of the less-incompatible elements does not compare as well with the chilled margin signature.

In contrast, the bulk average lower crustal trace element signature does not share the same pattern as the dolerites, except for the groups between Nb-Sr and Ho-Yb. In these cases, however, the concentrations of the elements are similar to those observed in the dolerite. A crustal assimilant with the trace element signature of PATS may be a reasonable choice for modelling the contamination of the dolerite magma during ascent.

The above comparison employs model compositions to constrain the signature of the contaminant and it may be argued that such "bulk" compositions are not available in the crust. For instance, although there is a similarity between the upper-crustal and dolerite PMN patterns, the upper-crustal estimate is necessarily an average of a number of lithologies and it is not obvious that a single component should exist with this composition. It is, therefore, important to demonstrate that the use of the PATS signature does represent a feasible component available to a mantle derived magma during ascent.

In addition to the various shales measured by Taylor and McLennan (1985), the PATS pattern describes the trace element composition of many granitic rocks. A comparison between the patterns for Proterozoic granites, average Palaeozoic S-type and I-type granites of southeastern Australia, and PATS is illustrated in Figure 4.14. Clearly, shales, granites and probably granite source-rocks possess the characteristics required by the crustal assimilant. A possible exception is the lower Ti in the granitic rocks (by around a factor of 4-5). It is important to note that this PMN signature is similar in both S and I-type granites and, therefore, only provides a constraint on the elements illustrated in these plots.

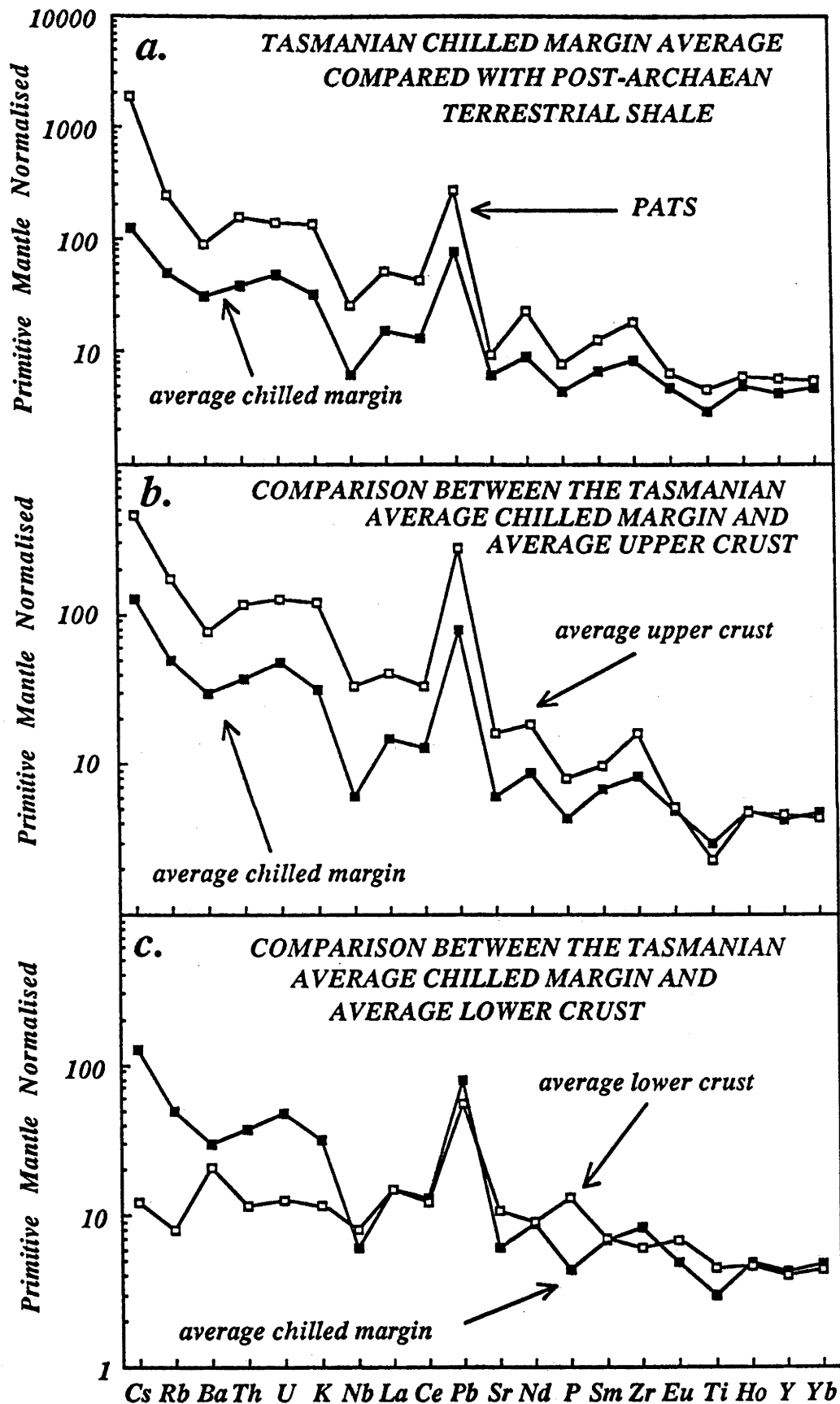


Fig. 4.13 Primitive Mantle Normalised abundance patterns of the Tasmanian chilled margin average compared with various model crust compositions. a. Post-Archaeon Terrestrial Shale (PATS). b. Average upper crust and c. Average lower crust. (Crustal compositions are from Taylor and McLennan, 1985; values for P have been estimated from the crustal compositions of Weaver and Tarney, 1984).

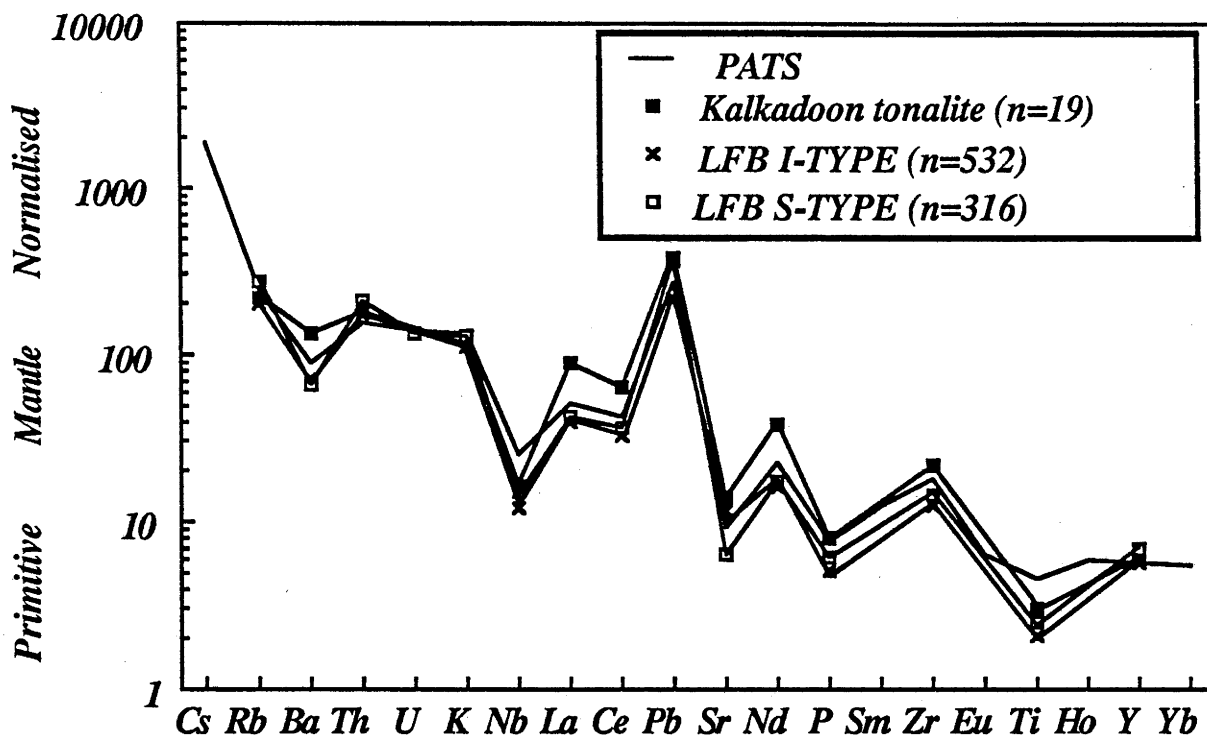


Fig. 4.14 Illustration of the similarities between the primitive mantle normalised abundance patterns for Post-Archaean Terrestrial Shales (Taylor and McLennan, 1985), Proterozoic granitic rocks (Wyborn and Page, 1983) and Palaeozoic granitic rocks from the Lachlan Fold Belt (LFB) of southeastern Australia (White and Chappell, 1983). Much of the discrepancy between these patterns stems from the incomplete data set for the granites e.g. the lack of Ho data produces a straight-line extrapolation between Ti and Y.

The possible mantle endmember is far more difficult to constrain because of the dominance of the crustal component on the trace element chemistry. In previous modelling, MORB has been used as the mantle melt which subsequently underwent contamination (Allègre et al., 1982). The low concentrations of several of the major elements in the dolerites is consistent with derivation of the primary magma from a depleted mantle source. Although a few of these signatures (including some trace element ratios), are similar to arc-tholeiites, the PMN patterns of the dolerites are more akin to crustal rocks. Therefore, in the following calculations, the depleted signature is approximated by N-MORB rocks. Despite their scarcity, E-MORB and OIB tholeiites have also been used to explore possible contamination models. In addition, because picritic rocks are sometimes observed in continental tholeiitic provinces, these are also considered as a possible mantle component.

An illustration of tholeiites from the oceanic environment is shown in Figure 4.15a together with the PATS pattern. It has been argued that bulk assimilation is more likely than the addition of a partial melt; this is because, even if partial melting occurs, the rheology of the silicate melt will not favour the separation of the solid phases, and it is likely that both the melt and its residue will be swept into the basaltic magma (Campbell, 1985; Huppert and Sparks, 1985). For this reason, simple mixing calculations combining the MORB endmembers with PATS have been performed and some of the results are illustrated in Figure 4.15b,c. (To simplify the calculations, the assumption was made that no crystallization occurred during contamination. This is unlikely, and the elemental abundances determined in these mixing

calculations must be considered to be minimum estimates).

As might be expected, the lower the relative abundance of the elements in the basalt (compared with the contaminant), the more easily they become dominated by the crustal component. This is well displayed in Figure 4.15. Addition of only 5% PATS to N-MORB (in which the highly incompatible elements are strongly depleted) produces the characteristic PATS signature from Cs to Pb. In contrast, the higher abundance of these elements in E-MORB necessitates that ~30% addition of PATS is required to produce this signature. In both types of MORB, development of the crustal pattern from Sr to Yb requires high degrees of crustal addition (>30%) because the abundances of many of these elements are similar in the two endmembers. Clearly, the OIB tholeiite requires a greater proportion of crustal addition than either of these two MORB compositions because of the higher concentration of the trace elements in this basalt.

These calculations show that the amount of the PATS component required to generate a crustal trace element signature in typical mantle-derived tholeiites is in the order of ~30%, and even then the depletions in Ti and P are not very well defined. With this proportion of crust however (and in fact even 5% for some elements), the abundances of these elements is far greater than found in the Tasmanian chilled margin composition. It is, therefore, necessary to add less crust in order to reduce the level of these trace elements in the mixtures but in doing this the crustal signature is lost. The balance between the signature required and the trace element abundances permitted has been taken into consideration, and the best results of the mixing calculations are shown in Figure 4.16.

These simple calculations have assumed that no fractionation has accompanied the assimilation process. This is considered unrealistic as the heat released during fractional crystallization is believed to be the engine that provides the energy required for assimilation (e.g. Bowen, 1928, p 175-223; DePaolo, 1981; Campbell, 1985; Turner and Campbell, 1986). Because all of the trace elements used in these calculations will be enriched into the melt during crystallization (except for Sr and Eu in the case of plagioclase precipitation, and Ti to a lesser degree in pyroxene fractionation), the problem of the balance in trace element concentrations in the contaminated oceanic basalts is further aggravated.

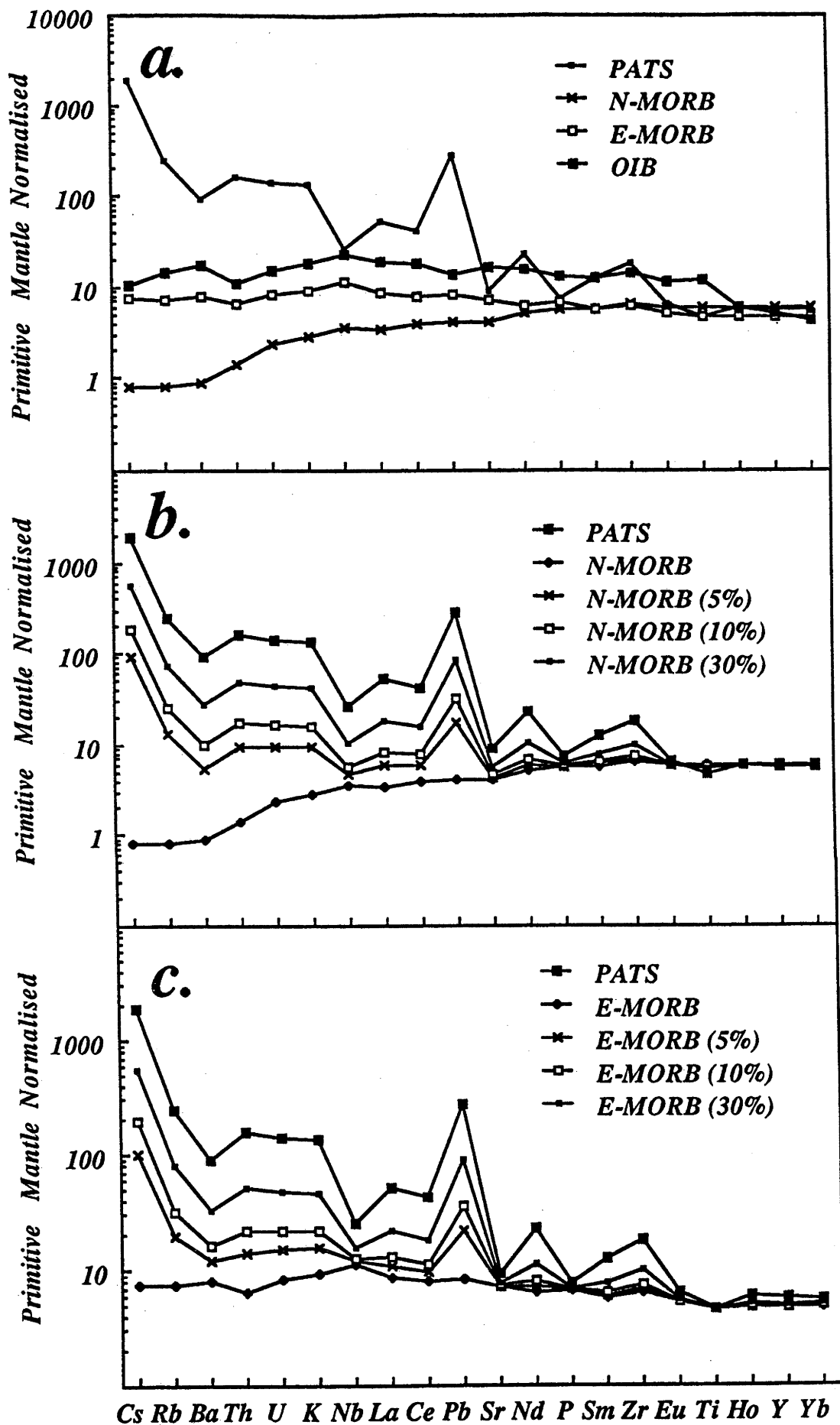


Fig. 4.15 Primitive Mantle Normalised abundance patterns a. Comparison between oceanic basalts and PATS compositions b. Calculated abundance patterns for the addition of between 5 and 30% PATS to average N-MORB. c. Calculated abundance patterns for the addition of between 5 and 30% PATS to average E-MORB. The compositions of MORB are from Sun and McDonough (1987), the OIB tholeiite is the Kilauean sample KL2 of Newsom *et al.* (1987) with additional data from Leeman *et al.* (1980) and BVSP (1981, p. 166).

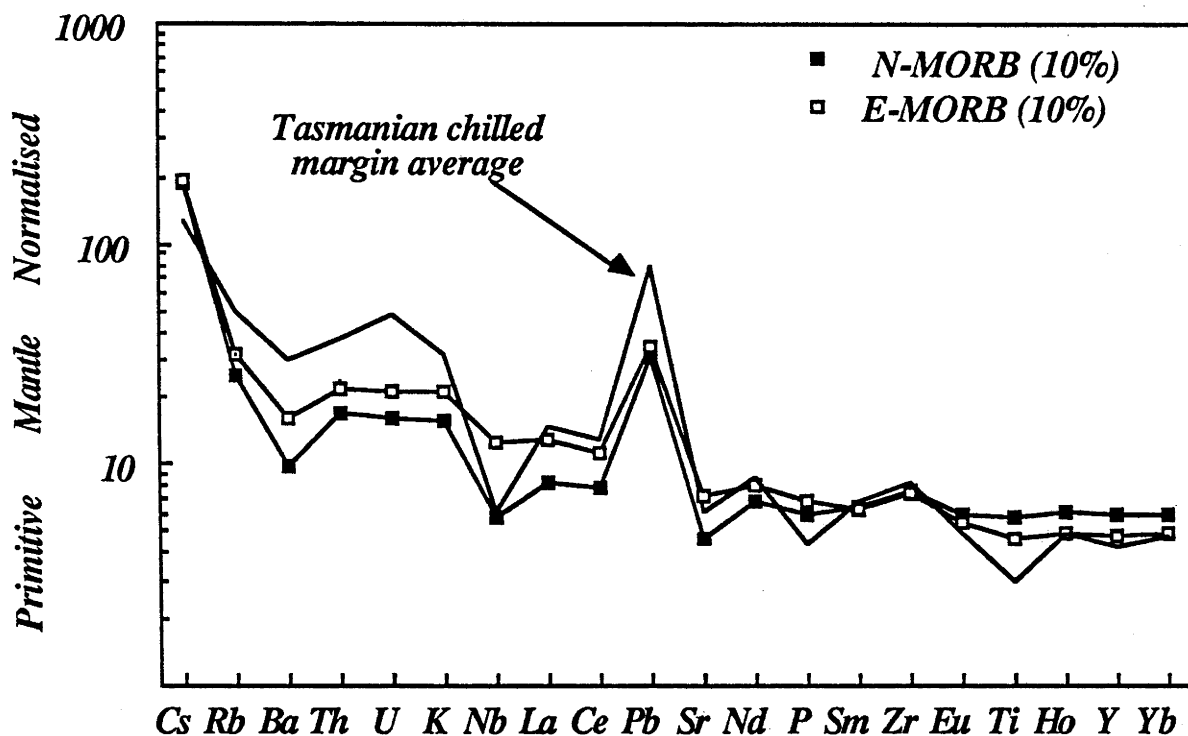


Fig. 4.16 Primitive Mantle Normalised diagram illustrating the discrepancies between "contaminated" MORB tholeiitic melts and the Tasmanian Dolerite chilled margins. Although some of the "crustal" trace element signatures are developed in the basalts after the addition of 10% PATS, the fit for the trace element abundances is poor (particularly when it is recalled that this contamination has not accounted for any fractionation of the basalts).

It appears that simple contamination cannot explain the production of the Tasmanian dolerite signatures using oceanic basaltic or continental tholeiitic endmembers as the mantle component. This is not changed by appealing to crustal partial melts of contaminants rather than bulk assimilation. In addition, any fractionation accompanying the contamination only increases the difficulty of balancing the abundances of the trace elements.

Picritic melts may have low abundances of many trace elements (e.g. Langmuir *et al.*, 1977) and their PMN signatures may therefore be more easily swamped by a small addition of the PATS component. The fractionation of phases such as olivine from this type of magma during contamination would also serve to concentrate the trace elements to the abundances calculated for the "primitive" dolerite melt. The difficulty with this scenario is that not all trace elements are necessarily low in picritic melts (e.g. Cox *et al.*, 1984). Little detailed trace element data for picrites are available from the literature and the following discussion is based on data from MORB picrites from the FAMOUS region of the mid-Atlantic ridge (Langmuir *et al.*, 1977).

Figure 4.17 illustrates the normalised pattern of a picrite sample (plotted as discrete points rather than a connected series owing to the lack of data). Although Nd, P, Sm, Zr, Eu and Ti are lower in abundance in this picrite compared with other mantle products (N-MORB shown as an example), other elements are of similar or higher concentration (e.g. Ba, Th, U, K, Nb, La, Ce, Y and Yb). In addition, Ti, Y and Yb are very similar to (or greater than) the abundances in the average Tasmanian Dolerite magma. Clearly, the addition of any PATS component, as well

as fractionation from a picritic composition to quartz tholeiite, will result in abundances of Ti, Y and Yb higher than that observed in the dolerites.

The use of picritic melts (at least judging from the small amount of published data available) does not appear to provide any major advantages over other mantle-derived melt compositions in modelling the production of the dolerite magma by contamination.

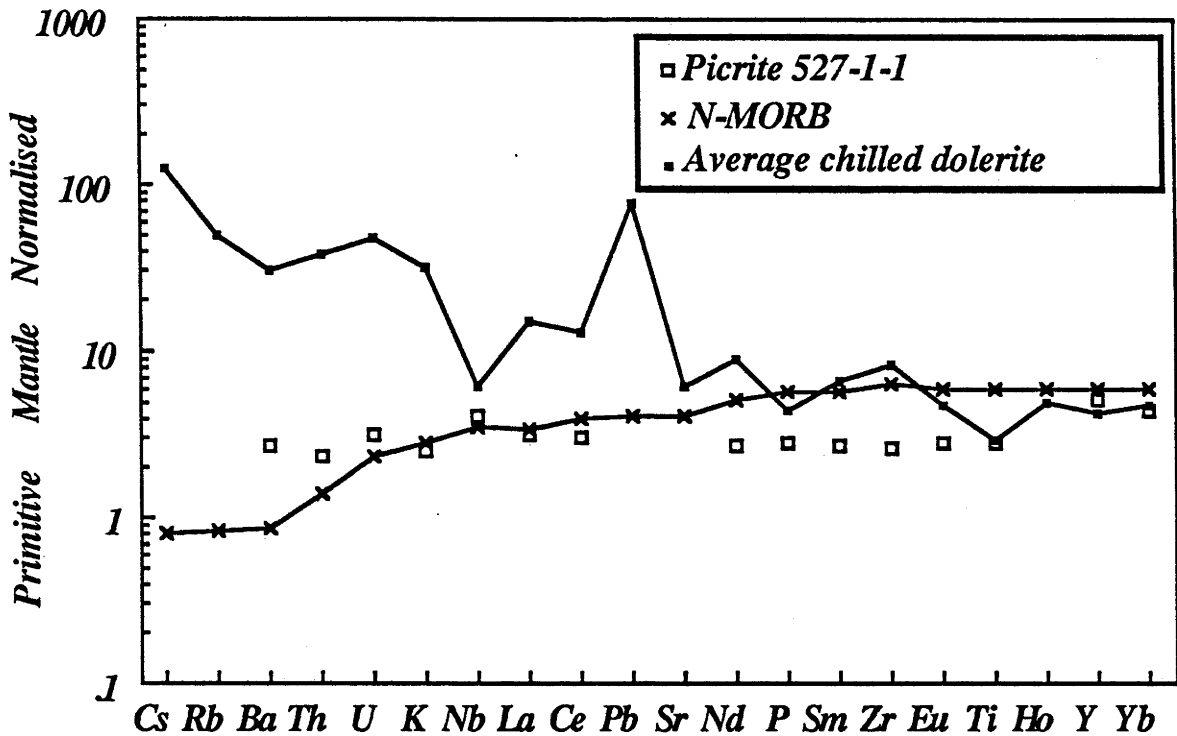


Fig. 4.17 Primitive Mantle Normalised diagram illustrating the signature of a picritic composition (527-1-1 from the FAMOUS area; Langmuir *et al.*, 1977) with N-MORB and the average Tasmanian chilled margin composition. Note that the abundances of many of the elements in the picrite are similar to those in the other basalts.

Simple calculations performed for bulk mixing of various proportions of PATS into mantle-derived melts have been presented. There appears to be a very real trade-off between the trace element signature required in the resultant magma, and the abundances of the trace elements in the chilled margin dolerites. The best results obtained (although still violating the abundances permitted in the contaminated magma) are for ~10% addition of PATS into the MORB melts (Fig. 4.16). It is important to recall however, that this does not account for any fractionation during contamination, and 10% addition must be considered to be an upper estimate. The isotopic constraints are re-examined in the light of this possible model.

Although it has been noted that samples from the lower crust have mantle-like $\delta^{18}\text{O}$ values (e.g. Rudnick *et al.*, 1986), the PATS component used to satisfy the trace element signatures is more typical of shales and granitic rocks. The $\delta^{18}\text{O}$ of these components ranges from approximately +5‰ (for granites) to greater than +20‰ (in the case of sediments). Addition of ~10% of the crustal component requires that its $\delta^{18}\text{O}$ value was below ~10‰, and therefore favours a granitic source for the assimilate.

The requirements of the PATS component can also be evaluated from the radiogenic isotopic systems. Using the concentrations of Pb, Sr and Nd in the E-MORB, N-MORB and PATS endmembers, the proportion of these elements supplied by each component have been calculated (Table 4.6). As noted previously, the Pb composition of a contaminated basalt is easily dominated by the crustal assimilant. In contrast, the contribution of Sr and Nd from the contaminant is considerably lower (Table 4.6). Estimates of the Sr and Nd isotopic signatures required by the PATS endmember have been calculated using the chilled margin data (i.e. $\epsilon_{Nd} = -5.2$, and assuming 0.7095 is a lower limit for the $^{87}Sr/^{86}Sr$ initial ratio) and average values for the mantle melts (see Table 3.8 legend for details). The results are presented in Table 4.6, and similar calculations have been performed for the OIB tholeiite composition for comparison. Although the Sr composition required by the contaminant is not unreasonable, the calculated values for ϵ_{Nd} are unrealistically low.

Table 4.6 Estimates of the Sr and Nd isotopic compositions required by the crustal component for a model involving 10% bulk assimilation into a mantle-derived melt. The concentration of the elements Pb, Sr, and Nd (in ppm) as well as the contribution derived from the contaminant in the final mix are also given. $^{87}Sr/^{86}Sr$ values used for the MORB and OIB endmembers are 0.7025 and 0.7030 respectively; ϵ_{Nd} values used are +10 and +5 for MORB and OIB respectively.

	N-MORB		E-MORB		OIB	
	total ppm	% from PATS	total ppm	% from PATS	total ppm	% from PATS
Pb	2.27	88%	2.54	79%	2.92	69%
Sr	101.0	20%	159.5	13%	346.7	6%
Nd	9.77	33%	11.30	28%	23.27	23%
Isotopic compositions required by PATS						
$^{87}Sr/^{86}Sr$	0.7379		0.7585		0.8151	
ϵ_{Nd}	-36		-44		-69	

It has already been noted that the country-rock lithologies in contact with the dolerites do not possess the isotopic signatures required of the assimilant. A widespread basement lithology in eastern Tasmania consists of turbidite and mudstone sequences (Mathinna Beds, see Chapter 2.1). Although isotopic analyses of these rocks are scarce, two samples analysed for their Nd isotopic compositions (Sun, unpublished data) give ϵ_{Nd} values of approximately -13 at 175 Ma. Clearly, if this is typical of the Mathinna Beds, these rocks are not viable as contaminants either.

4.3.2 Mantle source contamination

In the preceding discussion, it has been suggested that although there is strong evidence of crustal trace element and isotopic signatures in the Tasmanian Dolerites, contamination of typical mantle-derived basalts occurring during ascent through the crust appears difficult to model successfully. McLennan and Taylor (1981) showed that the REE signature of a crustal component is much more efficiently imparted to a basalt if it is introduced into the source where

the abundance of these trace elements is about an order of magnitude lower. They calculated the proportion of contaminant required for the development of detectable Eu depletions ($\text{Eu}/\text{Eu}^* < 0.95$) in island arc basalts and found that incorporation of only 0.1 wt.% sediment into a typical depleted source was required. A melt produced from this "contaminated" source would retain a depletion in Eu (relative to the other REE) but with only a comparatively trivial addition of the crustal component.

If the crustal signature observed in the Tasmanian Dolerites is actually a mantle source feature, then sediment introduced into the mantle by subduction may be a feasible mechanism of producing the correct source composition. In other words, partial melting of a mantle source contaminated by a small percentage of crustal material would produce a composition in which the major elements are dominated by the mantle component (and therefore basaltic) whereas the minor and trace element components may be dominated by the crustal component. The isotopic signatures in the resultant magma will necessarily be a function of the relative contribution from each reservoir.

Weaver and Tarney (1981) have also suggested that granitic segregations produced in the mantle during crustal generation may generate a similar signature. This type of model was proposed to explain the crustal signatures observed in the Proterozoic Scourie Dyke suite of NW Scotland. If this process occurred early in the production of the crust in Tasmania, and the "contaminated mantle source" was preserved until the Jurassic, the crustal isotopic compositions in the dolerites may also be explained by this model.

In the following discussion, the constraints on the amount of the crustal component which may be introduced into the source region, and its likely composition will be evaluated. It will be assumed that the type of mantle source region available to produce the dolerites is a typical MORB depleted mantle source (the effects of using a more primitive composition will be discussed later). In the previous section, mantle derived magmas were contaminated with a component bearing a trace element signature of PATS. This same composition will be used in the following discussion; in the case of the "subducted component" model, PATS will be a sediment, whereas in the Weaver and Tarney process PATS will be a granitic segregation.

Unlike the lower crustal reservoirs which may be available to an intruding magma, subducted sediments are likely to have high values for $\delta^{18}\text{O}$ (e.g. Graham and Harmon, 1983). In this type of model, the mantle-like oxygen-isotopic signature of the least altered dolerite should provide a strict constraint on the amount of sediment involved in the source contamination. The usefulness of this parameter is partially offset by the effects of meteoric interaction disrupting the oxygen-isotope system. It may be argued that the original $\delta^{18}\text{O}$ value of the dolerite magma was considerably higher than is now preserved and, therefore, a higher proportion of subducted sediment can be accommodated. It will become clear that the trace elements themselves place considerable constraints on the percentage of sediment introduced into the source region.

The composition of a normal depleted MORB source calculated by Wood (1979) has been used for the trace element modelling. Both the source and the average melt composition derived from this type of composition (Sun and McDonough, 1987) are illustrated in Figure 4.18a. This

diagram shows that the general signature of the source is maintained, and no major decoupling of this group of elements occurs during partial melting. [Note: The source composition of Wood has a small depletion in Sm relative to P and Zr which may possibly BE an artifact of the model?].

Using the mantle source composition of Wood (1979) and the PATS composition of Taylor and McLennan (1985), the source composition obtained by adding a few percent of the sediment has a trace element signature dominated by the crustal component for many elements (Fig. 4.18b). The amount of PATS required to produce this type of signature in melts of N-MORB source was an order of magnitude greater.

From the relationship between the N-MORB source and N-MORB melts it has been assumed that in melting a source region with 2-3% PATS added, the trace elements do not become decoupled from each other. In contrast, the mathematical addition of one component to another tells us nothing of the physical relationships between the two. For this reason it is not clear whether during partial melting the source should behave as a single entity, or whether the sedimentary component (in whatever form it is preserved) will prefer to melt completely.

During melting of the types of source illustrated in Figure 4.18, the trace elements will be concentrated relative to the source abundances. Obviously the smaller the degree of partial melting, the higher the abundances of these trace elements. Production of tholeiitic magmas is likely to involve a relatively large degree of partial melting and may be expected to approach 20-30% (e.g. Frey *et al.*, 1978; Jaques and Green, 1980). The large degree of partial melting expected for the "contaminated source" is sufficiently high that it has been assumed that essentially the entire budget of incompatible trace elements are partitioned into the melt.

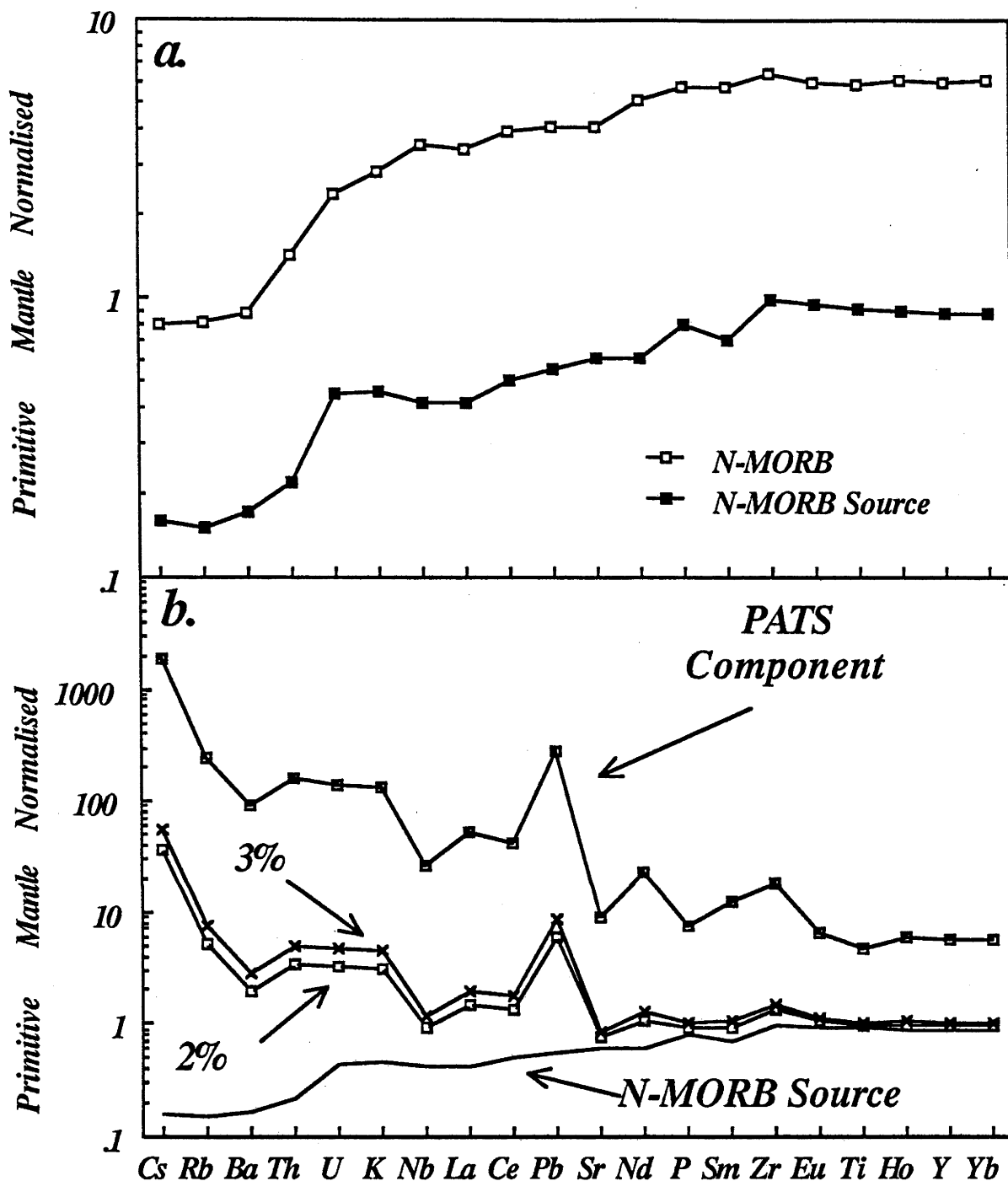


Fig. 4.18 a. Primitive Mantle Normalised abundance patterns for average N-MORB (Sun and McDonough, 1987) and the calculated composition of N-MORB source (Wood, 1979). Note the similarity in the general signatures of these two compositions indicating the preservation of the source signature during partial melting. b. Plot of the model abundance patterns calculated for the source produced by addition of 2 and 3% of the PATS component into an N-MORB source. Clearly a crustal signature is produced after only a small addition of the contaminant.

Many calculations have been performed using a variety of different proportions of contaminant and different degrees of partial melting. The results obtained which best approximate the composition of the "primitive" Tasmanian dolerite magma is displayed in Figure 4.19. The primitive dolerite composition (calculated in section 4.1.6) is used because in this model the major elements are controlled by the basaltic endmember; the criteria for primary mantle-derived magmas, and the fractionation modelled in section 4.1.6 therefore apply in this case. The fractionation is believed to be superimposed on a tholeiitic melt which already has a

case. The fractionation is believed to be superimposed on a tholeiitic melt which already has a crustal signature.

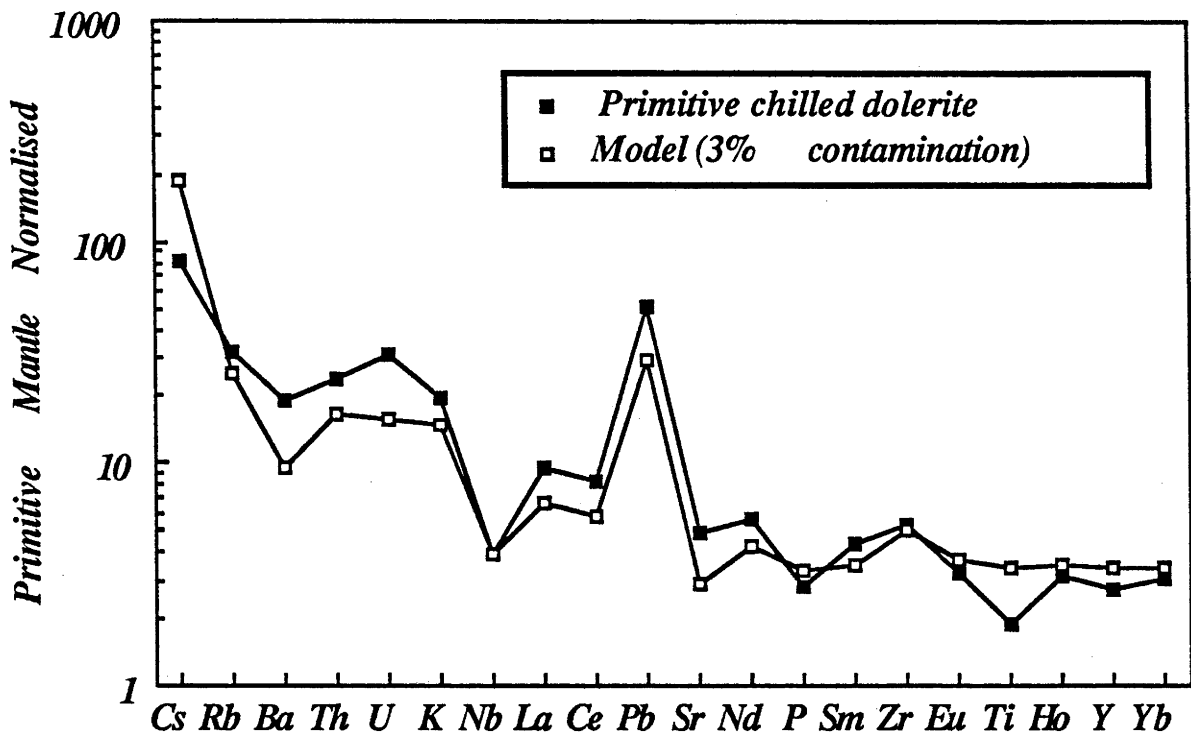


Fig. 4.19 Normalised compositions of the "primitive" Tasmanian Dolerite magma compared with the best-fit model composition calculated. A source contaminated with 3% PATS best approximates the primitive dolerite magma if the degree of melting is approximately 30%.

The best fit between a melt derived from a source contaminated by crust, and the primitive Tasmanian Dolerite is for 3% addition of PATS and approximately 30% partial melting. It is important to note that the high degree of partial melting is required to dilute the trace element abundances of the magma produced from the source. Of course less contaminant could be used but the size of the depletions and enrichments are also reduced and do not correspond to the magnitudes observed in the calculated primary dolerite. An upper limit is also placed on the percentage of PATS which may be introduced into the source. If more than 3% is added then the abundances of the trace elements become so high that the degree of partial melting required to dilute them to level of the dolerites is greater than ~40%.

One of the largest discrepancies between the calculated partial melt composition and the primitive dolerite signature is the lower abundance of Ti in the latter. This cannot be the result of fractionation of a titaniferous phase (e.g. ilmenite) as it has been demonstrated that TiO_2 was increasing with fractionation at the time of emplacement (Fig. 4.1). It may be recalled that the granitic averages (Fig. 4.14) have a greater depletion in Ti relative to PATS. However, even if the crustal component added to the mantle source were more granitic in character, this discrepancy is not resolved. It is possible that the uncontaminated mantle source was more depleted than a MORB source, and similar to the composition proposed for the wedge above a subducting slab (e.g. Green, 1976; Sun and Nesbitt, 1978). If this is the case, the low Ti

content would be an original source feature which was retained during the incorporation of sediment owing to the low concentration of TiO_2 in the proposed contaminant (particularly if Ti was stabilised in the slab in a phase such as rutile and was not added to the source at all). This would also be consistent with the derivation of siliceous primary magmas which may have been parental to the dolerite magma (Table 4.4). If this is the case, then the lower abundances of trace elements in the source would require less contamination to produce the crustal trace element and isotopic signatures, and consequently a lower degree of partial melting (i.e. less dilution of the trace element abundances would be required).

It was noted in a previous discussion that if the highest value of $\delta^{18}\text{O}$ measured in the dolerites is considered approximately primary, then constraints can be placed on the amount of PATS introduced into the source. If the sediment subducted is a shale, then its $\delta^{18}\text{O}$ composition will be high and lie somewhere in the range $\sim +15\text{-}20\text{‰}$ (e.g. Graham and Harmon, 1983). Using a value of 5.7‰ for the $\delta^{18}\text{O}$ composition of the mantle (5.71‰ recently reported as the average value of 46 MORB basalts from all oceans; Ito *et al.*, 1987), then the maximum proportion of sediment allowed in order to maintain the $\delta^{18}\text{O}$ of the dolerite at $\sim 6\text{‰}$ is 2-4%. This is consistent with the value of $\sim 3\%$ calculated in the previous model.

It is necessary to reconsider the radiogenic isotopic systems and evaluate whether the source contamination models are consistent with these signatures. In the same way in which the proportions of Pb, Sr and Nd, and isotopic compositions of the contaminant required were calculated in Table 4.6, the same parameters have been calculated for this model. The results indicate that of the Pb, Sr and Nd in the partial melt generated from the contaminated source, approximately 94%, 32% and 54% respectively are contributed by the PATS component. Clearly, the Pb composition measured in this material will essentially be a measure of the PATS isotopic signature. Using typical MORB values of ϵ_{Nd} (+8 to +12) and $^{87}\text{Sr}/^{86}\text{Sr}$ (0.7022 to 0.7028), and the values -5.2 and 0.7095 for the dolerite, the PATS contaminant in this model is required to have Nd and Sr compositions of between -16.5 to -20 and 0.7250 to 0.7237 respectively.

4.4 SUMMARY

The Jurassic dolerites from Tasmania are quartz tholeiitic magmas which may have been generated from the partial melting ($\sim 20\text{-}30\%$) of a peridotite mantle source with a major element composition similar to, or more depleted than that of typical olivine tholeiites. The primary magmas probably fractionated olivine, orthopyroxene and plagioclase to generate the compositions now observed in the chilled dolerites. The fractionating assemblage effectively buffered the magma composition, and the small variation in compatible trace elements and major elements such as MgO are probably the result of significant differences in magma evolution (up to $\sim 9\%$). Additional variation in the chilled margin dolerites may be attributed to interaction with meteoric water. In this category are included the more mobile elements such as Cs, Ba, Rb, K, Sr and the isotopic compositions of Sr and O. Other incompatible trace elements appear to be unaffected by either fractionation or alteration (e.g. REE).

Although features of the major element composition of the chilled dolerites is not unlike

that observed in other fractionated tholeiites, the minor, trace element, and isotopic signatures are more typical of crustal rocks. Contamination of the tholeiite by a crustal component is believed to be a necessary requirement, and an attempt has been made to model the introduction of the crustal component into the dolerite melt. Both the isotopic and trace element signatures place constraints on the amount and type of crust involved in the contamination process.

The abundances of trace elements in the dolerite magma have been particularly useful in constraining the process of contamination. When combined with the isotopic results the trace element data imply that crustal-level assimilation is unlikely to be the dominant cause of the crustal signatures in the dolerites. This is because of the similar levels of many trace elements in basaltic melts compared with the Tasmanian average chilled margin composition. For the trace element signature of basaltic magma to become swamped by the contaminant, a large amount of assimilation is required; conversely, the similar levels of many elements in the basalt and dolerite compositions means that little addition of a more trace element enriched component can be accommodated. Even if a poor fit in trace element signatures is accepted and ~10% of crustal component is added to a basaltic magma, the isotopic composition of Nd required in the crustal endmember is unrealistically low.

A process whereby a small percentage of a granitic or shale-like contaminant is introduced into a typical mantle source poses fewer difficulties. The trace element signatures compare well with that required in the unfractionated dolerite magma, and the isotopic compositions are more realistic. This model is favoured for the petrogenesis of the Tasmanian Dolerites.

Although the similarity in shale and granite compositions from different localities has been demonstrated (e.g. Taylor and McLennan, 1985; and Figure 4.14), it is necessary to examine the sensitivity of the isotopes to variations in the composition or amount of contaminant introduced into the mantle source. The Pb system will be very sensitive to changes in the isotopic composition of the contaminant since essentially all of the Pb in the magma is derived from this source. The uncertainty in the most precise Nd isotopic measurements is ± 0.2 of an epsilon unit. Using the same Nd compositions for the endmembers, and allowing variation only in the quantity of contaminant added to the source, a difference of less than 0.2 of an epsilon unit in the dolerite magma is equivalent to a variation of <0.16% in the amount of contaminant in the mantle source. Alternatively, if the Nd composition of the mantle endmember and the quantity of contaminant added to it are fixed, the difference of less than 0.2 of an epsilon unit is equivalent to a change of less than 0.5 of an epsilon unit in the Nd composition of the contaminant. Like the Pb system, the Nd composition is also very sensitive to small differences in the composition and quantity of the crust and mantle endmembers. The Sr and O isotopic systems are less well constrained owing to the effects of post-emplacement alteration.

The sensitivity of the isotopic signatures to small changes in the source contamination requires that the mantle source was either uniform beneath Tasmania, or that the large degree of partial melting required to produce the tholeiites effectively homogenised any small-scale variations. This is further addressed in the following chapter.

Reference to the mechanism by which the PATS component is added to the mantle source has been carefully avoided in the preceding discussion. Although the subduction of sediments

into the mantle is preferred, there is no conclusive geochemical or isotopic parameter which excludes the alternative of the production of granitic segregations in the upper mantle during crust formation (Weaver and Tarney, 1981). One argument against the latter is the probability that the crust to the east and west of the Tamar Fracture System experienced different histories prior to juxtaposition (Chapter 2.1). It would appear unlikely that the upper mantle formed during an early stage of crust formation in two separate microplates should be identical.

CHAPTER 5

RELATED THOLEIITES FROM ANTARCTICA AND SOUTHERN AUSTRALIA

Reference to the similarities between Jurassic tholeiites from Antarctica and the Tasmanian Dolerites has been made in the preceding text (e.g. Chapter 2). In this chapter previous research on the tholeiites of Antarctica is reviewed. In order to make a closer comparison between these two provinces, detailed geochemical and isotopic analyses have been performed on a suite of samples from Portal Peak near the Beardmore Glacier in Antarctica. These data are combined with the results of studies on other samples from Antarctica wherever possible. Finally, data from Jurassic basalts from Kangaroo Island (South Australia) and western Victoria are also presented. It will be demonstrated that the similarity in isotopic and geochemical compositions for these three areas indicates that a "clan" of magmatism with the same unusual signature occurred over a distance of many thousands of kilometres.

5.1 A REVIEW OF PREVIOUS WORK ON ANTARCTIC THOLEIITES

5.1.1 *Distribution and age*

Mesozoic tholeiites occur from Horn Bluff in George V Land to Queen Maud Land, a distance of around 4,500 km (Fig. 5.1). The width of this belt is ~20 km (Gunn, 1966); however, this may be an underestimate if the tholeiites continue beneath the extensive ice cover. The volume of Mesozoic tholeiite preserved in Antarctica is ~500,000 km³ (Elliot, 1987). This figure is largely dependent on the estimated volume of the enormous Dufek layered intrusion (~400,000 km³) which is questionable because of the poor exposure (Ford and Himmelberg, 1987).

Although basalts are represented in this province (e.g. the Kirkpatrick Basalts of Grindley, 1963; Fig. 5.1), the tholeiites are dominated by intrusive dolerites in the form of large sills, sheets and dykes. The intrusive bodies were emplaced into the deformed basement of granites and metamorphics, the overlying sedimentary sequences of the Beacon Supergroup, and the unconformity between the two (McKelvey and Webb, 1959; Gunn, 1962, 1966; Harrington and Speden, 1962; Grindley, 1963; and many others). The intrusive relationships between large sheets and the flat-lying sediments have been described in detail in some accounts (e.g. McKelvey and Webb, 1959). These authors commented that despite the enormous extent of intrusion in the Upper Taylor Glacier region of South Victoria Land, the sediments appear almost "unmoved" and have suffered limited contact metamorphism. The dolerite is described as having intruded along bedding planes and then "stepping" upwards along vertical fractures. The triangular cross-section defined by the dolerite (Harrington and Speden, 1962) is consistent with the mechanism of intrusion proposed by Carey (1961a, 1961b) for the dolerites of Tasmania (see Chapter 2).

The first potassium-argon ages for dolerites and basalts were obtained on samples collected between South Victoria Land and George V Land (Starik *et al.*, 1959; Evernden and

Richards, 1962; Webb, 1962; McDougall, 1963). The ages obtained span a range from approximately 150 to 200 Ma (recalculated using the revised decay constants of Steiger and Jager, 1977), which exceeds the range attributable to experimental error. Recently, the analysis of samples by the $^{40}\text{Ar}/^{39}\text{Ar}$ step-heating method, and compilation of other new data has reduced this spread to an average of 179 ± 7 Ma with the possibility of a later event at around 165 ± 2 Ma (Kyle *et al.*, 1980a). This is consistent with the results of Rex (1972) on more remote samples from the Theron Mountains and Queen Maud Land. These age determinations place the magmatism in the Middle Jurassic according to the timescale of Harland *et al.* (1982).

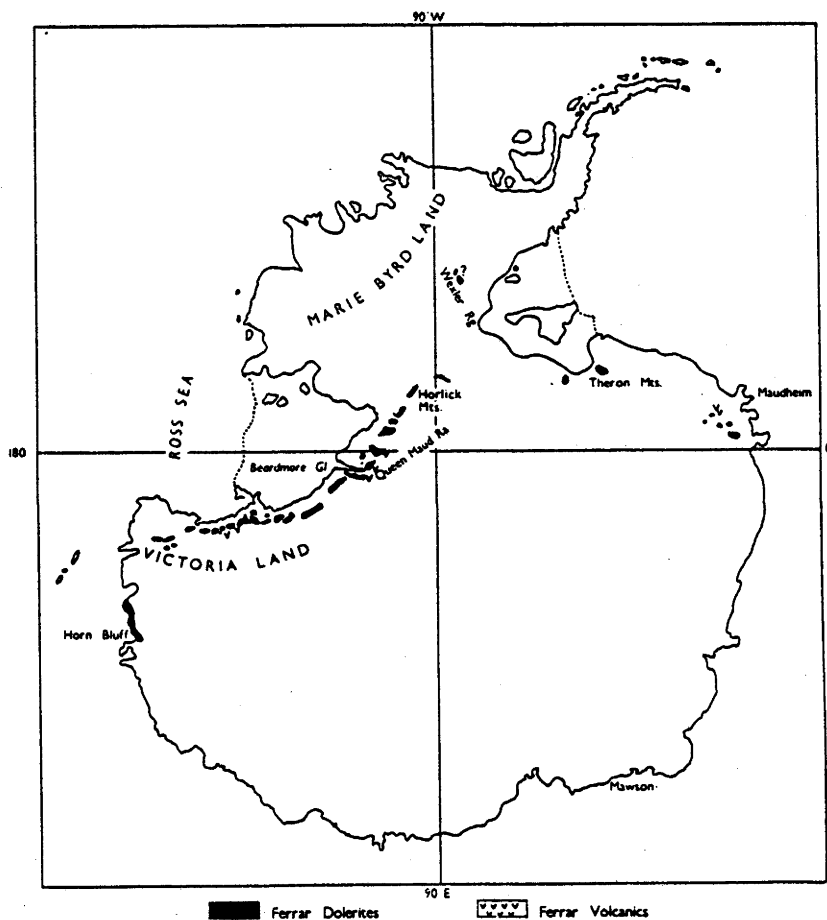


Fig. 5.1 Sketch map illustrating the widespread distribution of Jurassic tholeiites in Antarctica (After Gunn, 1962).

5.1.2 Petrological work

The general characteristics of dolerite sills in the Upper Taylor Glacier region were described by Ferrar (1907), McKelvey and Webb (1959) and Harrington and Speden (1962), and two petrographic types of dolerite were described.

A more detailed study of five intrusions and one flow near McMurdo Sound, extended the

range of rock-types observed from hypersthene cumulates (MgO=22 wt.%) to granophyric tholeiites (MgO<1 wt.%); however, the interpretation of mineralogical and geochemical data was that the tholeiites belong to a single differentiation series (Gunn, 1962). Petrographic observations identified a complex history of zoning in the pyroxene and plagioclase crystals. It was shown that although the magmas crystallized in place, differentiation (controlled largely by pyroxene) had produced marked chemical variation. Gunn compared the geochemistry of the Ferrar tholeiites with compositions of tholeiites from other continents and showed that the general characteristics were similar, especially in the case of the Tasmanian Dolerites.

In 1966 Gunn combined data from fourteen sections in Victoria Land and produced the most detailed geochemical and mineralogical description of the Ferrar Dolerites. Gunn was able to divide the dolerites into three groups on the basis of their mineral assemblages (although he used chemical compositions to place some samples into the hypersthene group in the absence of phenocrysts). The first group is comparatively rare and contains the olivine-bearing tholeiites with no normative quartz. These display mineralogical banding interpreted as the result of post-emplacement differentiation. The second is the hypersthene group, which display strong chemical variation in both major and trace elements, as well as significant modal and mineralogical variation resulting from differentiation. The third group is the most abundant and consists of the pigeonite tholeiites. These do not appear to preserve any differentiation in their major element compositions, however trace element variation is observed.

In a study of K/Rb and K/Ba ratios in 41 Antarctic tholeiites (Gunn, 1965), it was shown that the differentiated tholeiites had constant but low K/Rb ratios (240), whereas the K/Ba ratios increased with differentiation from 26 in the olivine tholeiites to 36 in the pigeonite tholeiites. The low values for K/Rb were ratified in a later study and it was further shown that a similar ratio could be found in the tholeiites from Queen Maud Land, although one anomalously high value was obtained (Erlank and Hofmeyr, 1968).

The first rare-earth element (REE) data for the Ferrar Dolerites consisted of the analysis of a single chilled margin sample of unknown petrographic affinity (Philpotts and Schnetzler, 1968). This sample is enriched in the light REE (and Ba), with a flat heavy REE pattern and a depletion in europium. Comparison with other continental tholeiites indicated that although the REE patterns for samples from four separate continents are very similar, the Ferrar and Tasmanian samples are almost identical and differ only in the depth of their europium anomaly; the Tasmanian sample having a greater depletion in this element.

In addition to the intrusive tholeiites, the petrography and/or geochemistry of the Kirkpatrick Basalts has been described in a number of articles (e.g. Gunn and Warren, 1962; Gunn, 1962; Grindley, 1963) and more recently by Elliot (1972) and Siders and Elliot (1985). Petrographically the basalts are typical tholeiites with plagioclase, augite and pigeonite as the major phases and opaques, glass (sometimes devitrified) and quartzo-feldspathic mesostasis. The basalts appear to have erupted subaerially, and some of the thicker flows are ponded basalts with a coarse-grained zone giving them an appearance similar to dolerite sills.

These flood basalts are the remnants of an originally more extensive field (Elliot, 1972) and consist of numerous separate flows. They have been described as the extrusive equivalents of the

Ferrar Dolerites (e.g. Faure *et al.*; 1979); however, Elliot (1972) indicated that many of the basalts appear to be more evolved than most of the dolerites. Elliot suggested that the magmas were more fractionated (and possibly contaminated) compared with most of the Ferrar Dolerites and may have originated from the same magma chamber, but after a more prolonged period of evolution.

5.1.3 Magma genesis

A significant contribution to the study of the Ferrar Dolerites was made with the first publication of their initial $^{87}\text{Sr}/^{86}\text{Sr}$ ratios (Compston *et al.*, 1968). The compositions obtained ranging between 0.7090 and 0.7143 are exceptionally high for basaltic rocks but almost identical to the data previously reported for the Tasmanian Dolerites (Heier *et al.*, 1965). Although more akin to ratios observed in rocks from continental crust, these authors considered the production of tholeiitic magma from within the crust unlikely. In addition, ratios between the elements K, Th, Rb and U were used to argue against bulk crustal contamination of a mantle derived magma unless the crustal assimilate was of granitic composition. Selective diffusion of elements or incorporation of partial melts were other mechanisms suggested for adding crustal material to a basaltic melt. Another alternative acknowledged by these authors is that the dolerites may have been derived from a mantle source with an unusual chemical and isotopic signature.

The distinctive signature in the Tasmanian and Ferrar dolerites was reinforced with the comparison of data obtained from other Mesozoic tholeiites (Compston *et al.*, 1968). The lower initial $^{87}\text{Sr}/^{86}\text{Sr}$ ratios obtained for samples from the Karoo and Paraná Basin (Serra Geral) was presented as evidence for two large, distinct magmatic provinces; the Antarctic-Tasmanian province and the African-South American province.

Interest in the petrogenetic history of the Ferrar tholeiites initiated by Heier *et al.* (1965) and Compston *et al.* (1968) was later developed by Faure and Elliot (1971) and Faure *et al.* (1972). In the latter study a limited number of major and trace element data were combined with initial $^{87}\text{Sr}/^{86}\text{Sr}$ data for dolerites and basalts from the Transantarctic Mountains, as well as tholeiites from Vestfjella, Mannefalknaussane and Heimefrontfjella in Dronning Maud Land. It was shown that although the results obtained for the Transantarctic Mountain samples were consistent with the work of Compston *et al.* (1968), the Dronning Maud Land samples could be divided into two groups with much lower initial $^{87}\text{Sr}/^{86}\text{Sr}$ ratios, one with 0.7037 ± 0.0004 and the other 0.7072 ± 0.0003 . This study highlighted the existence of two different suites of tholeiites in Antarctica; however, it was initially suggested that they represented a single petrogenetic group preserved at different stages of geochemical and isotopic evolution. Correlations between initial $^{87}\text{Sr}/^{86}\text{Sr}$ ratios and geochemical parameters (although weak in many cases) were interpreted as evidence for mixing between a normal unradiogenic mantle melt and a silica-rich high $^{87}\text{Sr}/^{86}\text{Sr}$ crustal component. In a more detailed investigation, Faure *et al.* (1979) confirmed the existence of two distinct suites of tholeiites in Antarctica and suggested that the significant differences in chemical and isotopic compositions were related to differences in tectonism and magma formation during the fragmentation of Gondwanaland. Recent research in the vicinity of the Weddell Sea has further documented the characteristics of the two tholeiite groups (Brewer *et al.*, 1987). A large number of samples (124), showing a range in composition from SiO_2 ~47-62 wt.%, were divided

into two groups by these authors. The first group is characterised by high TiO_2 contents (1.9-3.4 wt.%) compared with the lower values in the second group (0.6-1.4 wt.%). Selected samples have been analysed for Sr and Nd isotopic compositions by Brewer *et al.* (1987). Although the high Ti tholeiites generally have lower initial $^{87}\text{Sr}/^{86}\text{Sr}$ ratios, some have radiogenic Sr compositions more typical of the low Ti tholeiites.

Although the geochemical vs Sr-isotopic "trends" combining the Queen Maud Land and Ferrar tholeiites have been re-interpreted, the SiO_2 vs $^{87}\text{Sr}/^{86}\text{Sr}$ correlation for the Kirkpatrick Basalts was regarded as convincing evidence for crustal assimilation (Faure *et al.*, 1974, 1979). Further research was carried out on a larger number of samples by these authors, and correlations between geochemical parameters and the Sr-isotopic signatures were interpreted as evidence for crustal assimilation during ascent by these basalts. Oxygen-isotope data of Hoefs *et al.* (1980) reinforced this interpretation when it was shown that a positive correlation existed between the oxygen data and the initial $^{87}\text{Sr}/^{86}\text{Sr}$ ratios. Kyle *et al.* (1983) noted that although the correlation between the initial $^{87}\text{Sr}/^{86}\text{Sr}$ composition and $\delta^{18}\text{O}$ of samples is convincing, tholeiites with mantle-like $\delta^{18}\text{O}$ values have initial $^{87}\text{Sr}/^{86}\text{Sr}$ ratios which are still unusually high for basalts (~0.709).

Mensing *et al.* (1984) explained the Sr and O isotopic signatures of the Kirkpatrick Basalts as the result of a basaltic magma undergoing variable assimilation (of a crustal partial melt) with simultaneous fractional crystallization (AFC). Although successful in modelling the Sr and O variation caused by crustal-level processes, the elemental abundances are not entirely consistent with the AFC model proposed. For example, the sample considered to have experienced the highest amount of AFC (I-1-1) has a similar MgO content to the least contaminated/fractionated basalt (I-21-1); whereas, a "middle of the range" AFC sample (I-2-1, judging from its initial $^{87}\text{Sr}/^{86}\text{Sr}$ ratio) has a significantly lower MgO content compared to both the least and most evolved endmember basalts. Also, these calculations did not explain the origin of the very radiogenic Sr composition of the basaltic endmember (taken as 0.710 prior to AFC).

In addition to the crustal initial $^{87}\text{Sr}/^{86}\text{Sr}$ ratios, Kyle *et al.* (1983), Thompson *et al.* (1983) and Siders and Elliot (1985) showed that the trace element signatures of Ferrar tholeiites are also very similar to those of continental crust. Siders and Elliot showed that a significant range in major and trace element composition exists in the Kirkpatrick Basalts, with the more typical low TiO_2 and P_2O_5 tholeiites dominating a less abundant group with higher SiO_2 , TiO_2 , P_2O_5 and lower MgO (i.e. ~2.3 wt.% MgO; Siders and Elliot, 1983). The variation was explained in terms of variable evolution (involving fractionation, possibly accompanied by assimilation) within a single magma chamber; however, others have argued that such simple processes cannot explain the data, and more complicated (but as yet unspecified) processes may have operated (Fleming and Elliot, 1987). Thompson *et al.* (1983) suggested that the Ferrar Dolerite GFBS3 from Basement Sill was contaminated by upper crust during shallow-level fractionation. In contrast, Kyle *et al.* (1983) interpreted the crustal trace element signature of the Kirkpatrick Basalt Group as a mantle source feature, possibly related to largescale recycling of crust into the mantle by subduction.

Much effort has been invested in explaining the variation in isotopic compositions in the

Ferrar Group tholeiites. Assimilation, and combined AFC models have been proposed with varying degrees of success. Although explaining some of the variation (much of which is attributed to alteration by Kyle, 1980), the origin of most of the crustal characteristics remains the subject of dispute. Cox (1978) speculated on the role of subduction in generating the Gondwana tholeiites, and recently, Kyle *et al.* (1987) argued that the consistently "crustal" radiogenic isotopic signatures, coupled with the limited extent of crustal assimilation permitted by element-isotope plots and oxygen isotopic signatures, requires that the crustal signatures are derived from the mantle source region. These authors proposed that the rough parallelism between the Ferrar Group tholeiites, and the active Pacific margin of Gondwanaland during the Jurassic, support a subduction related origin for the mantle signature. In their model, enrichment of the mantle above the subducting slab resulted from the dehydration of the slab and/or the recycling of subducted sediments, giving rise to the upper-crustal signatures observed in the dolerites. It was further suggested, that the delamination of this enriched mantle during the fragmentation of Gondwanaland, followed by mixing with other mantle sources, was responsible for the development of the DUPAL anomalous mantle in regions of the southern hemisphere documented by Hart (1984). This type of explanation for the development of the DUPAL signature is also favoured by Sun and McDonough (1987).

5.2 ANALYTICAL RESULTS FROM THE DOLERITES OF PORTAL PEAK

In order to make direct comparisons between the tholeiites of Tasmania and Antarctica a detailed database was obtained for samples from the Ferrar Group. Samples from Portal Peak were generously provided by Prof. G. Faure, and have been analysed for isotopic (Sr and Nd) and geochemical compositions.

Portal Peak is situated near the Beardmore Glacier in the Transantarctic Mountains. A sill approximately 130 m thick intrudes sediments of the Beacon Supergroup, and a measured section was sampled at intervals of 3 m in the interior of the intrusion and more closely at the contacts by Faure and Mensing. The 44 samples analysed include 4 sediments sampled from the contact zones, chilled margins from both the upper and lower contacts, and numerous samples from the interior.

The tholeiites from Portal Peak are fine-grained to glassy near the chilled contacts, and grade rapidly into coarser dolerites towards the interior of the sheet. The principle phases are augite, plagioclase and pigeonite, with interstitial mesostasis (often consisting of a graphic intergrowth of quartz and feldspar). Almost all samples show evidence of alteration in the form of rusty discoloration and break-down of mafic minerals, and sericitization of plagioclases.

5.2.1 Geochemical composition

The geochemical data are located in Appendix 4.2. These include XRF major and trace element results and wet-chemical data for all samples. Additional data (e.g. REE) were also obtained by INAA for six selected samples.

The sill is relatively thin and shows only minor differentiation (Fig. 5.2). It would appear from Figure 5.2 that mass-balance is not preserved in the sheet, and the overall composition of the

interior dolerite is more mafic relative to the chilled margins. In contrast, sample 87-117 contains far less MgO (3.12 wt.%) and related elements compared with most other samples. This sample is not a silicic differentiate as the silica and incompatible element concentrations are also low. The high Al_2O_3 and CaO contents in 87-117 indicate that this rock is likely to represent a plagioclase-dominated cumulate, which is strongly supported by the high Sr (206 ppm) and Ga (19 ppm) contents and Eu/Eu* of ~ 1.1 (cf. ~ 0.84 in the chilled margins!).

The occurrence of mafic and more felsic cumulates implies that residual silicic liquids were produced during crystallization of this sill. It is possible that the silicic differentiates may have been overlooked during sampling (if they are concentrated in isolated pods?), or that they escaped from the sill prior to its solidification.

Regardless of whether mass-balance is maintained in the Portal Peak sheet, the geochemical variation is very limited. Table 5.1 lists two average chemical compositions of the Portal Peak samples; the average of the 40 dolerite samples analysed, and the average of the two chilled margin samples. The Tasmanian chilled margin average (believed to represent quenched magma, Chapter 4), is also included for comparison and demonstrates the remarkable similarity between their chemical compositions. Like the Tasmanian Dolerites, the Portal Peak rocks are quartz tholeiites with relatively low MgO contents and are likely to have evolved from a more primitive composition prior to emplacement.

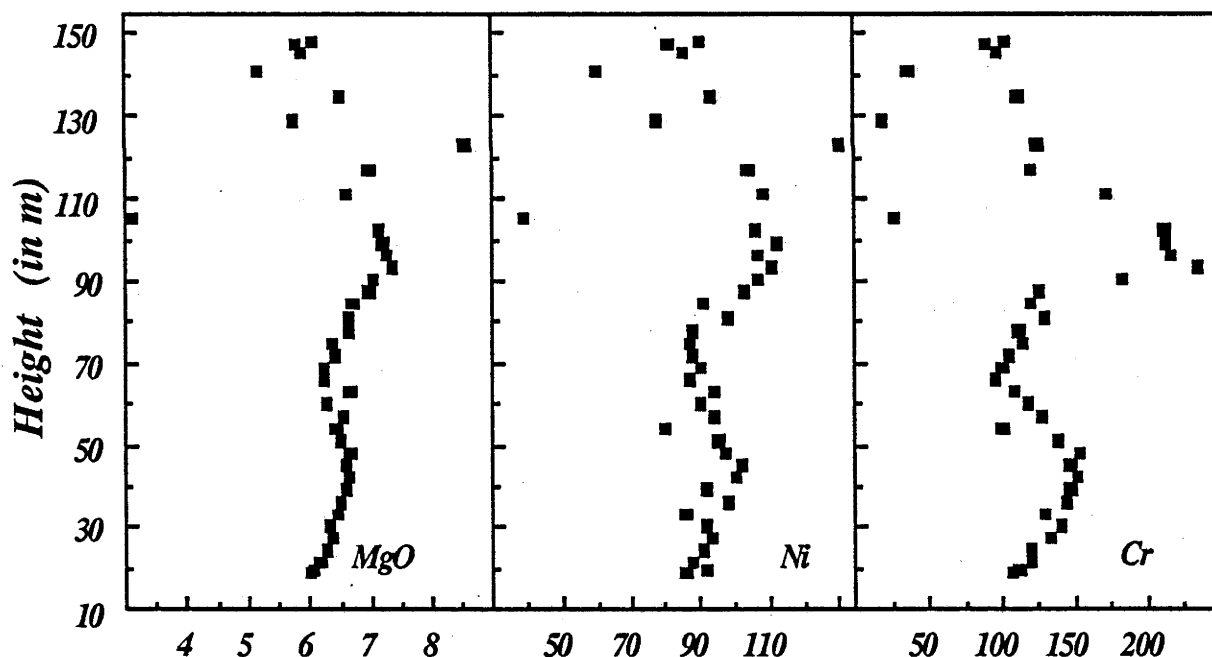


Fig. 5.2 Height versus element profiles for the Portal Peak sheet. Height is measured in metres above the base of a section measured by Faure and Mensing. Their section includes contact sedimentary rocks (0-19 m and >148 m above the measured base); MgO is in wt.%, Ni and Cr are in ppm.

The data obtained in this study are consistent with previous reports that the Tasmanian and Ferrar tholeiites are closely related (e.g. Edwards, 1942; Gunn, 1962; Compston *et al.*, 1968). One of the unusual characteristics of the Tasmanian Dolerites discussed previously (Chapter 4) is the striking similarity of their minor and trace element signatures to those of crustal rocks. From their compositions (Table 5.1) it is clear that these are also shared by the Portal Peak samples,

although the concentrations of many incompatible elements (particularly TiO_2 and P_2O_5) are higher in the Antarctic tholeiites.

Table 5.1 Average compositions of Jurassic tholeiites from Portal Peak and Tasmania. Column 1 gives the average of 40 tholeiites analysed from Portal Peak in Antarctica. This is compared with the average of the 2 chilled margin samples chosen for more detailed analysis and the average Tasmanian chilled margin composition.

	Portal Peak Sheet (n=40)	Portal Peak Sheet (n=2)	Tasmanian Chilled Margins (n=34)
SiO_2	53.48	53.85	54.12
TiO_2	0.69	0.78	0.64
Al_2O_3	14.86	14.36	14.64
Fe_2O_3	1.97	1.93	1.20
FeO	7.27	7.70	7.67
MnO	0.15	0.15	0.18
MgO	6.44	6.04	6.58
CaO	10.95	10.49	10.58
Na_2O	2.05	2.11	1.86
K_2O	0.76	0.78	0.88
P_2O_5	0.11	0.13	0.09
S	0.01	0.02	0.05
H_2O^+	1.06	1.41	0.92
H_2O^-	0.37	0.48	0.44
CO_2	0.13	0.13	0.24
Cs		0.55	1.49
Ba	201	210	220
Rb	23.6	19.5	32.3
Sr	148	151	135
Pb	4	5	6
La	10.3	11.4	10.9
Ce	23.5	26.5	24.4
Nd		13.1	12.4
Sm		3.35	3.07
Eu		0.96	0.93
Gd		3.65	3.09
Tb		0.62	0.57
Ho		0.85	0.82
Yb		2.60	2.36
Lu		0.42	0.36
Y	19	22	20
Th		3.40	3.47
U		1.2	1.1
Zr	88	103	95
Hf		2.1	1.91
Nb	4.4	5.0	4.5
Sc		39.6	41.3
V	210	234	225
Cr	126	105	108
Mn	1188	1180	1371
Ni	93	88	78
Cu	82	93	74
Zn	64	72	79
Ga	16.4	16.8	16.4

The PMN patterns of the Portal Peak and Tasmanian averages are illustrated in Figure 5.3a. The Ferrar average shows the same crustal signature as the Tasmanian Dolerites but with less severe depletions in P and Ti, and lower Rb. Although there is a strong similarity in the Ni, Cr and Sr contents of the Portal Peak and Tasmanian chilled margin compositions, the MgO content of the Portal Peak average is considerably lower ($Mg\# = 56.8$) indicating a higher degree of fractionation of the magma at the time of intrusion. If this is the cause of the higher abundances of incompatible elements, then plagioclase was not involved as the Sr and Eu contents are also higher relative to the Tasmanian composition.

The signatures of the Portal Peak samples are consistent with data published for tholeiites from other areas in Antarctica (Basement Sill, Wright Valley, Thompson *et al.*, 1983; Kirkpatrick basalts, Mesa Range area, Siders and Elliot, 1985). These are shown in Figure 5.3b and indicate that the Ferrar tholeiites share remarkable similarities in their PMN patterns.

Figure 5.3b is plotted without Cs as this element is not available in the data obtained from the literature. The analysis of GFBS3 is the most complete trace element data set available and the only interpolation required is for U (assumed to be colinear with the normalised values for Th and K). In contrast, the data from the Kirkpatrick Basalts lacks the important elements Pb, Nd, and Ho in addition to U, and interpolation cannot be made objectively.

The data from Portal Peak, and the low-Ti Kirkpatrick Basalts lie close to the line plotted for GFBS3 (Fig. 5.3b). The major discrepancies are higher La and lower Rb of these two groups relative to GFBS3, and lower Pb in Portal Peak relative to GFBS3. The unusually high Pb content in the Basement Sill sample may be the result of contamination (during transport or crushing?) or analytical problems.

Although interpolation of the Kirkpatrick Basalt data is not strictly possible, the data from 81-2-56 have been connected (assuming U, Pb, Nd and Ho compositions) to indicate the general parallelism between these evolved basalts, and their more primitive precursors. The Sr content of 81-2-56 is conspicuously low and indicates that plagioclase has been involved in the evolution of this basalt. Further support is given by the more severe depletion of Eu in this sample; estimates of the Eu/Eu^* values are 0.83 for the more primitive compositions compared with 0.74 for 81-2-56. Another estimate of the increased magnitude of the Eu depletion in the evolved basalt is given by the Sm_N/Eu_N ratio of the two groups (1.36 cf. 1.52 for the least and most fractionated basalts respectively).

Trace elements in tholeiites more primitive than GFBS3 ($MgO = 6.97$ wt.%) from the Ferrar Group have not been analysed in detail. A limited amount of data from an olivine-bearing chilled margin from Painted Cliffs Sill ($MgO = 10.60$ wt.%) is reported by Gunn (1966) and has been plotted relative to GFBS3 (Fig. 5.3c). Also plotted are data from an olivine-bearing chilled margin in the Darwin Glacier region which has an MgO content of 8.67 wt.% (Ortez, unpublished data). Although the data are limited to a few of the elements of interest, it is apparent that a similar pattern of "crustal" enrichments and depletions may be expected given more information.

Clearly, the presence of the same trace element character in olivine tholeiites with high MgO contents, implies that the crustal signature was imposed prior to the fractionation which produced the more common, evolved compositions. This argument has been proposed by Kyle (1980) on

the basis of both the chemistry of the Painted Cliffs Sill of Gunn (1966) and its initial Sr-isotopic composition (0.7111, Compston *et al.*, 1968).

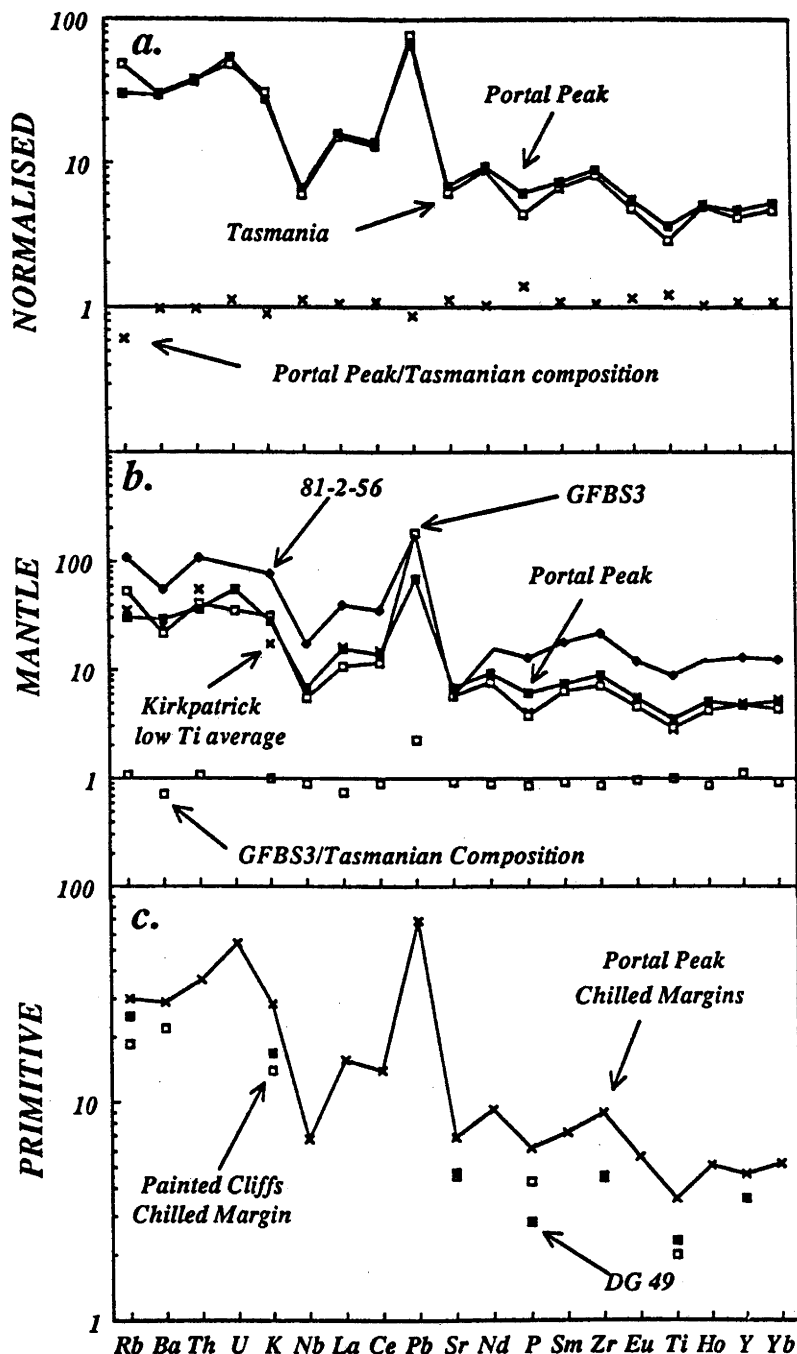


Fig. 5.3 Primitive Mantle Normalised Diagrams a. Illustration of the similarity between the Portal Peak and Tasmanian average chilled margin compositions. Noteable discrepancies include the lower Rb and higher P and Ti in the Portal Peak samples. This is more clearly indicated by normalising the Portal Peak data to the average Tasmanian composition (indicated by the open squares). b. Comparison between the Portal Peak data and other Ferrar Group data from the literature. GFBS3 is a sample 3.0 m above the lower contact of the Basement Sill in Wright Valley (data from Thompson *et al.*, 1983); the low Ti average for the Kirkpatrick Basalts is based on data from Siders and Elliot (1985); and 81-2-56 is a representative sample of the high Ti and P Kirkpatrick Basalts (Siders and Elliot, 1985). c. Trace element signatures of GFBS3 and the Portal Peak chilled margins compared with the available data from olivine-bearing tholeiites from the Ferrar Group. The Painted Cliffs data are from Gunn (1966) and DG 49 is a sample analysed at the University of Tasmania (Ortez, unpublished data).

5.2.2 Isotopic composition

It may be expected on the basis of the geochemical data, that the isotopic compositions of the Portal Peak and Tasmanian samples would also be similar, particularly as it has already been demonstrated that the two provinces share almost the same range in initial $^{87}\text{Sr}/^{86}\text{Sr}$ ratios (e.g. Compston *et al.*, 1968). In contrast, Nd isotopic data are scarce and the results of the six samples presented here (Appendix 5) provide the basis for comparison in Figure 5.4. Kyle *et al.* (1987) give a narrow range in tholeiites from Gorgon Peak from ϵ_{Nd} -4.6 to -6.1, corresponding to a range in initial $^{87}\text{Sr}/^{86}\text{Sr}$ ratios of 0.709 to 0.712. Like the Tasmanian data, the variation in Sr is beyond the analytical uncertainties; however, the precision of the Nd analyses is not reported for the Gorgon Peak data, and it is not clear whether the small range reported by Kyle *et al.* (1987) is significant. A narrow range in Pb compositions is also given by these authors. The characteristically high $^{207}\text{Pb}/^{204}\text{Pb}$ ratios observed in the Tasmanian samples are also shown by the Gorgon Peak tholeiites; the other ratios also compare remarkably well. Lead isotopic ratios from Gorgon Peak and Tasmanian chilled margins are; $^{206}\text{Pb}/^{204}\text{Pb}$, 18.89-18.95 and 18.90-18.94, $^{207}\text{Pb}/^{204}\text{Pb}$, 15.63-15.66 and 15.64-15.68, and $^{208}\text{Pb}/^{204}\text{Pb}$, 38.69-38.80 and 38.73-38.87 respectively (Kyle *et al.*, 1987; and Table 4.7, Chapter 4.2.3).

The Sr and Nd isotopic results obtained from the Tasmanian and Portal Peak samples in this study are illustrated in Figure 5.4. The compositions of both Sr and Nd for the two data sets are very similar, although the Antarctic samples have consistently lower initial $^{87}\text{Sr}/^{86}\text{Sr}$ ratios and higher ϵ_{Nd} compositions.

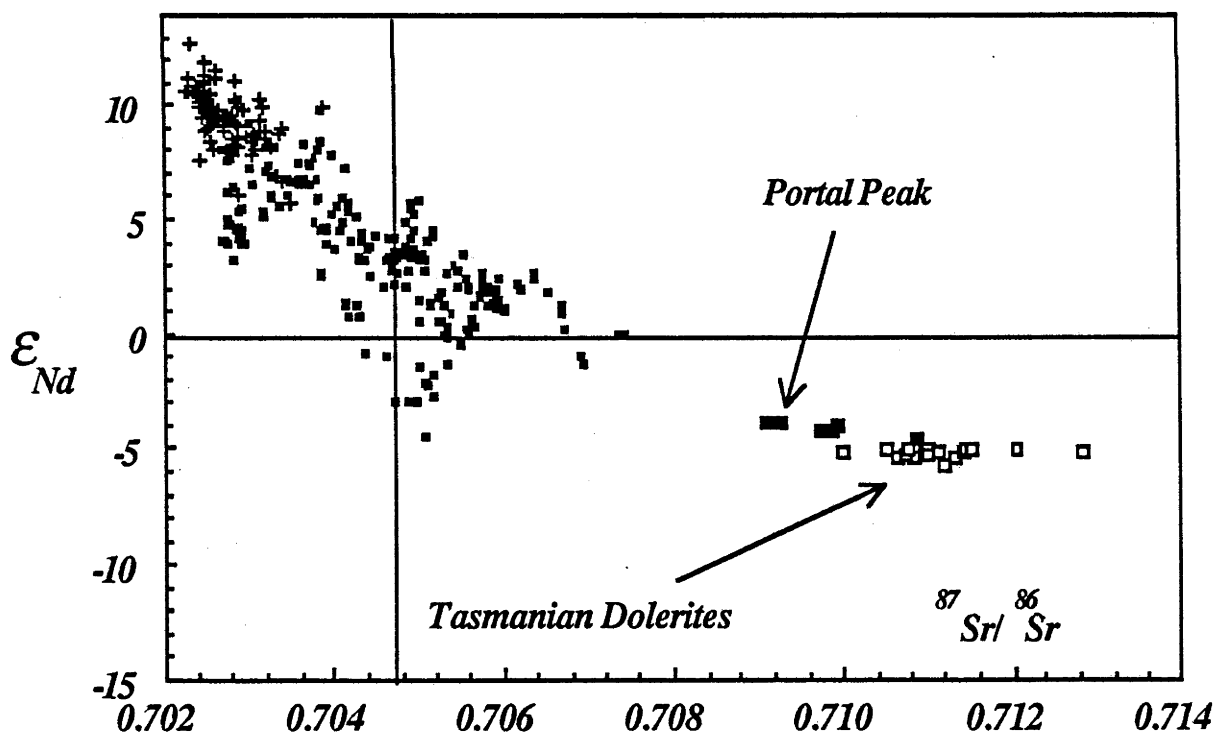


Fig. 5.4 ϵ_{Nd} versus $^{87}\text{Sr}/^{86}\text{Sr}$ initial ratio (calculated at 175 Ma) for the Portal Peak tholeiites (large filled squares) compared with the Tasmanian Dolerites (large open squares). MORB (crosses) and OIB-IAB (small filled squares) are shown for comparison. Sources of the oceanic basalt data are given in the caption to Figure 4.10.

It is interesting to note that the two chilled margin samples from Portal Peak (87-126 in particular) have more radiogenic initial $^{87}\text{Sr}/^{86}\text{Sr}$ compositions compared with dolerites from within the sill. Figure 5.5 illustrates the progressive decrease in the initial $^{87}\text{Sr}/^{86}\text{Sr}$ ratios of the dolerites towards the interior of the intrusion. This is consistent with the results for the Tasmanian chilled margin dolerites, where it is argued that alteration involving meteoric water has resulted in the addition of radiogenic strontium to dolerites at the contact (Chapter 4). This effect has been noted in other Ferrar tholeiites, and Sr-isotopic disequilibrium in altered samples is documented (e.g. Kyle, 1980).

Although no oxygen isotopic data have been obtained for the Portal Peak samples in this study, analyses on the same rocks by Hoefs indicate that interaction with meteoric water has occurred in this sill (Gunter Faure, written comm. 1987). It would be interesting to compare the oxygen and Sr compositions and properly document the interaction between these parameters during alteration. The prediction based on the Tasmanian chilled dolerites is that radiogenic Sr carried in the meteoric water is added to the altered rocks during exchange of the oxygen. It would be anticipated that the Sr and O isotopic compositions should therefore show an anti-correlation for the Portal Peak dolerites.

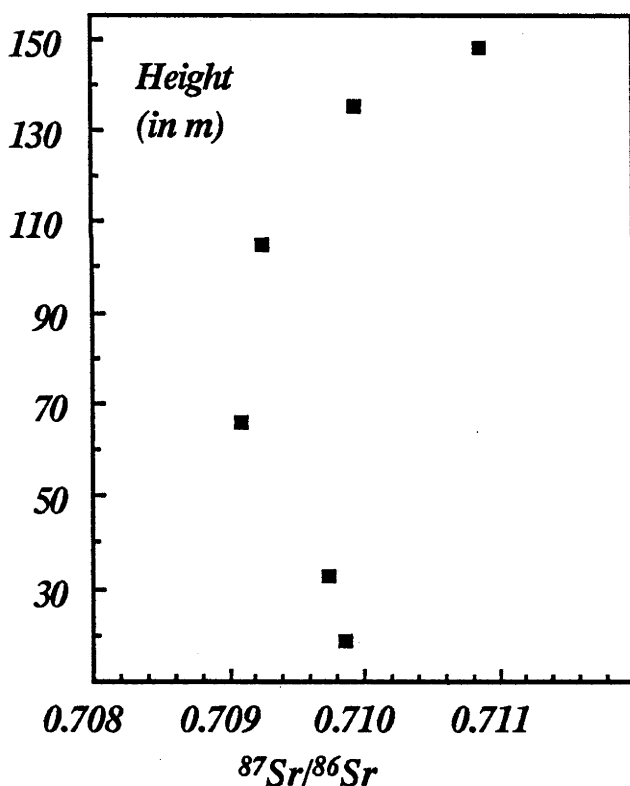


Fig. 5.5 Profile of initial Sr-isotopic composition versus height for the Portal Peak sill. Note the increase in radiogenic Sr character of the dolerites towards the chilled contacts.

The combination of O and Sr isotopic compositions has been used to explain at least some of the variation in initial $^{87}\text{Sr}/^{86}\text{Sr}$ ratios in dolerites from Tasmania (Chapter 4) and the Kirkpatrick Basalts from Antarctica (Hoefs *et al.*, 1980; Kyle *et al.*, 1983; Mensing *et al.*, 1984). It is instructive to compare the negative relationship between the isotopic compositions of Sr and O observed in the Tasmanian chilled margins, with published data available on the Ferrar tholeiites (Hoefs *et al.*, 1980; Mensing *et al.*, 1984). These data have been plotted together and show opposing trends (Fig. 5.6). The two Antarctic groups display an increase in initial $^{87}\text{Sr}/^{86}\text{Sr}$ with

increasing $\delta^{18}\text{O}$ and have been interpreted as mixing trends between the original magma and a crustal component. In contrast, the Tasmanian data show a negative (albeit weak) variation between these parameters, which is interpreted as the result of alteration during interaction with meteoric water at the time of emplacement.

It is important to note that the "uncontaminated" endmembers of the Ferrar tholeiites plot in a similar position to the most "unaltered" samples analysed from Tasmania. This probably indicates that the processes of contamination and alteration which may have operated, have only introduced a small degree of scatter into the data and do not obscure the dominant signature of these rocks.

Clearly, the close similarity between the Tasmanian Dolerites and tholeiites of the Ferrar Group extending over thousands of kilometres supports the existence of a major province of distinctive and remarkably uniform composition.

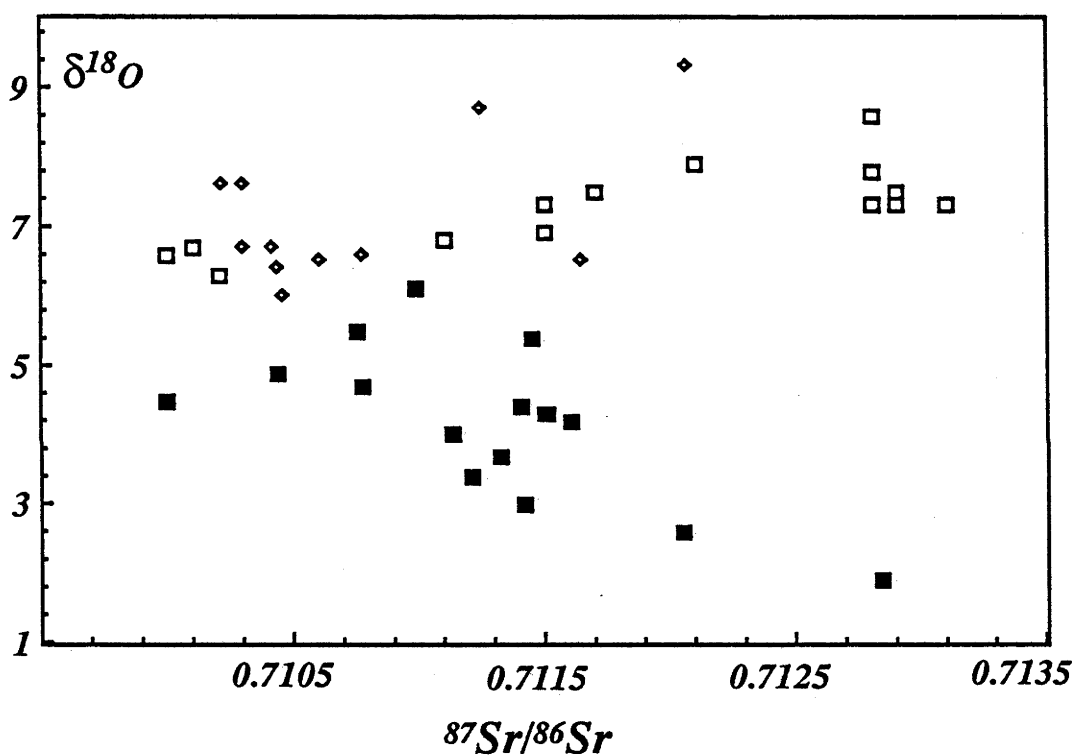


Fig. 5.6 Plot of initial $^{87}\text{Sr}/^{86}\text{Sr}$ ratio versus $\delta^{18}\text{O}$ for three groups of Jurassic tholeiites. The open symbols represent Ferrar Group tholeiites (squares are data from Hoefs *et al.*, 1980; diamonds are data from Mensing *et al.*, 1984); the weak negative trend (filled squares) is defined by the data for the chilled margin dolerites of Tasmania presented in Chapter 4.

5.3 ANALYTICAL RESULTS FOR BASALTS FROM KANGAROO ISLAND AND WESTERN VICTORIA

Basalts of Jurassic age have been documented in both Kangaroo Island ($\sim 170 \pm 5$ Ma) and western Victoria ($\sim 190 \pm 10$ Ma; McDougall and Wellman, 1976). The basalts near Coleraine in Victoria include both alkalic and tholeiitic members which occur together in outcrop, and the major element, Ba, Sr, Rb and Y contents of tholeiites from Kangaroo Island and western Victoria are similar to the Tasmanian chilled margin dolerites (Ortez, unpublished data). Sr-isotopic data for samples from Kangaroo Island (initial $^{87}\text{Sr}/^{86}\text{Sr}$ from 0.711 to 0.712; Milnes *et al.*, 1982) are also similar to the unusual character of the Tasmanian Dolerites.

Seven samples of these basalts (including two alkali basalts) were provided by Prof. D.H. Green for detailed geochemical and isotopic analysis. The purpose of measuring the compositions of these samples was to assess the similarity between Tasmanian Dolerites and the tholeiites of these localities, and examine the role of the alkali basalts in the Victorian magmatism.

5.3.1 Geochemical composition

Major element (XRF) and wet-chemical analyses have been performed on the samples provided and the trace element data were obtained using SSMS (Appendix 4.3). A comparison between the same elements analysed in these tholeiites and the Tasmanian chilled margin average is presented in Table 5.2.

Table 5.2 Comparison between the geochemical compositions of Jurassic tholeiites from southern Australia, and the average Tasmanian chilled margin. Columns 1 and 2 list the data for the western Victorian basalts and columns 3-5 are the tholeiites from Kangaroo Island (Pr, Gd, Dy, Er, Sn and Mo for the 5 basalts are given in Appendix 4.3)

	87 130	87 131	87 133	87 134	87 135	Tas. Dolerite
SiO ₂	52.04	54.37	55.46	54.89	55.55	54.12
TiO ₂	0.59	0.64	0.63	0.75	0.65	0.64
Al ₂ O ₃	14.49	14.91	15.13	15.06	14.84	14.64
Fe ₂ O ₃	1.48	1.48	1.29	1.14	1.19	1.20
FeO	8.80	6.64	6.27	7.90	7.36	7.67
MnO	0.32	0.16	0.15	0.23	0.17	0.18
MgO	6.03	6.58	7.21	4.97	7.36	6.58
CaO	10.01	10.59	11.01	9.84	10.98	10.58
Na ₂ O	1.94	2.00	1.96	2.13	1.87	1.86
K ₂ O	0.75	0.46	0.76	0.79	0.71	0.88
P ₂ O ₅	0.08	0.09	0.09	0.11	0.09	0.09
S	0.02	0.04	0.02	0.05	0.04	0.05
H ₂ O+	0.73	1.36	0.55	0.71	0.50	0.92
H ₂ O-	0.67	1.24	0.54	0.77	0.22	0.44
CO ₂	3.29	0.45	0.10	1.01	0.16	0.24
Cs	1.00	1.20	0.66	1.00	1.10	1.49
Ba	250	640	450	230	195	220
Rb	23.6	26.0	25.1	29.9	26.0	32.3
Sr	130.3	162.1	131.8	133.0	155.4	135.0
Pb	5.4	4.4	6.1	6.9	7.2	6
La	10.6	13.1	11.5	17.0	12.6	10.9
Ce	24.2	27.5	25.7	36.9	28.6	24.4
Nd	12.6	13.6	12.5	19.0	13.7	12.4
Sm	3.10	2.93	2.93	3.71	2.85	3.07
Eu	0.83	0.83	0.73	0.94	0.74	0.83
Gd	3.12	3.34	2.56	3.96	2.74	3.07
Tb	0.65	0.56	0.55	0.71	0.49	0.57
Ho	0.85	0.74	0.95	1.03	0.73	0.82
Yb	2.48	2.11	2.52	2.89	2.17	2.36
Y	24	19	23	26	18	20.0
Th	3.04	2.78	3.00	4.21	3.11	3.47
U	0.86	0.68	0.77	0.89	0.81	1.1
Zr	122	70	73	105	70	95
Hf	3.20	2.10	2.46	2.95	2.46	1.91
Nb	5.9	3.6	5.0	5.1	5.0	4.5

The tholeiites from Kangaroo Island and western Victoria show strong similarities to the Tasmanian chilled margin dolerites. This is most convincingly displayed in their PMN patterns which indicate that all share the same characteristic signature of high incompatible element contents, depletions in Nb, Sr, P and Ti, and significant enrichment in Pb relative to Ce and Sr (Fig. 5.7).

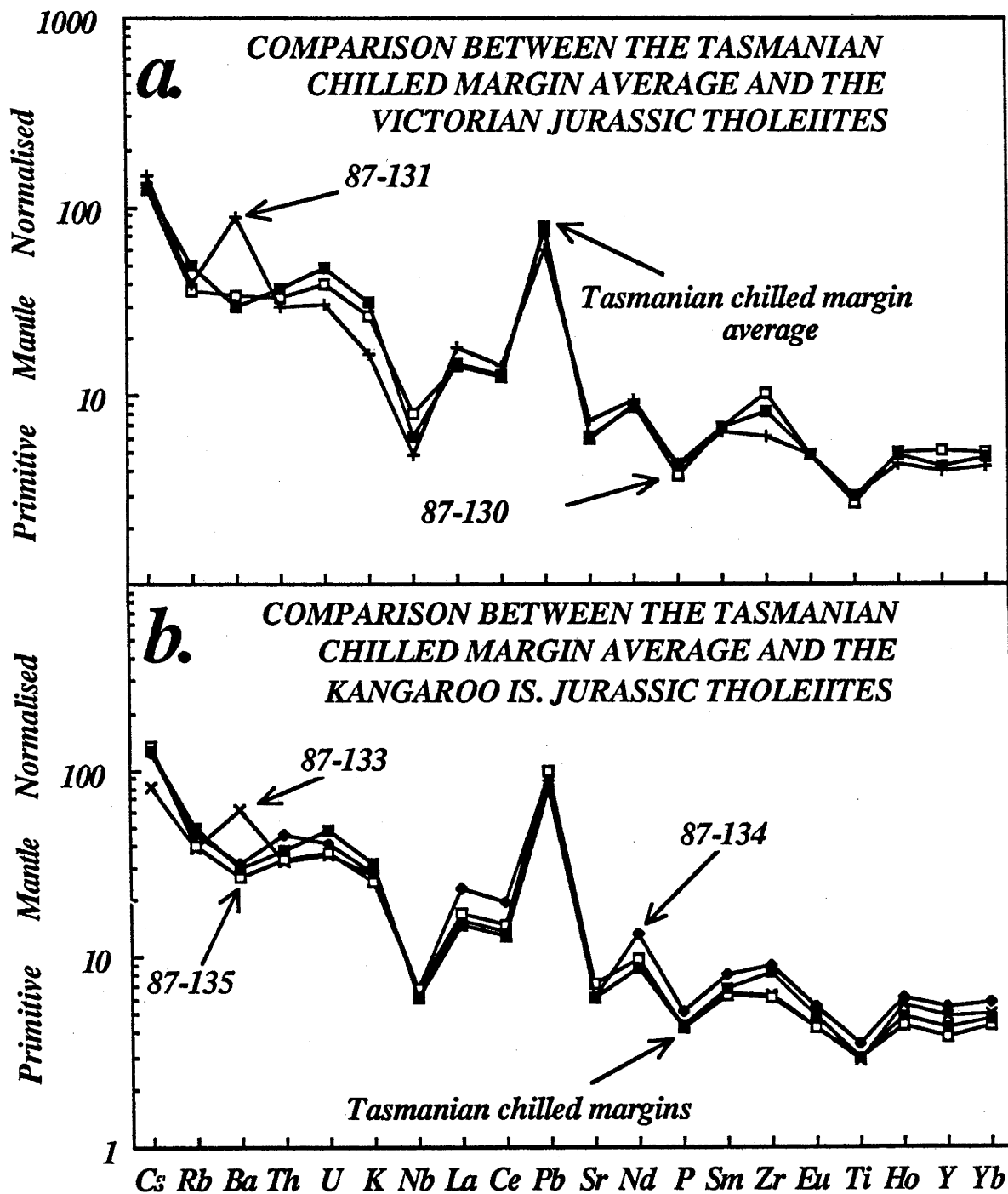


Fig. 5.7 Primitive Mantle Normalised (PMN) diagrams illustrating the remarkable similarity between the western Victorian (a.), Kangaroo Island (b.), and Tasmanian chilled margin tholeiite compositions.

The alkali basalts related closely in both space and time to the Victorian tholeiites show patterns typical of oceanic and continental alkali basalts (Table 5.3, Fig. 5.8). This requires that the tholeiites were either produced from the same source as the alkalic basalts and later contaminated by crust, or that the two basalt types derive from quite unrelated sources. In modelling the petrogenesis of the Tasmanian Dolerites (Chapter 4), it was shown that crustal-level contamination was difficult to achieve, despite evidence for stagnation and fractionation of the magma within the crust. From the petrogenetic history favoured for the Tasmanian Dolerites, and the similarities in composition of the 3 groups of tholeiites, derivation of the tholeiitic and alkalic basalts of western Victoria from two unrelated sources would appear most likely.

Table 5.3 Comparison between the geochemical compositions of alkali basalts from western Victoria (columns 1 and 2 recalculated volatile free) and typical alkalic basalts from intraplate settings. OIB is an average ocean island alkali basalt (trace element data from Sun and McDonough, 1987), 69-1036 is from the Tertiary-Recent volcanic province of Victoria (data from Frey *et al.*, 1978; McDonough *et al.*, 1985).

	87 129	87 132	OIB	69-1036
SiO ₂	46.73	47.89	45.50	48.00
TiO ₂	2.69	2.91	3.70	2.14
Al ₂ O ₃	16.15	15.40	13.50	13.91
Fe ₂ O ₃	4.91	3.51	2.95	1.85
FeO	6.87	7.61	7.50	9.27
MnO	0.15	0.15	0.17	0.16
MgO	6.99	7.31	10.50	11.39
CaO	8.85	8.17	11.00	8.35
Na ₂ O	2.50	3.53	2.75	3.23
K ₂ O	1.77	2.55	1.45	1.18
P ₂ O ₅	0.63	0.96	0.62	0.51
Cs	0.74	0.31	0.36	0.43
Ba	785	1420	350	309
Rb	38	48	29	24
Sr	784	1029	660	543
Pb	4.5	4.4	3.2	2.27
La	61.1	65.5	37.0	22.3
Ce	123	132	80	47
Pr	12.9	15.7	9.7	5.7
Nd	47.7	59.5	38.5	24.6
Sm	8.43	9.70	10.0	5.83
Eu	2.51	3.08	3.0	1.9
Gd	6.30	6.56	7.6	5.3
Tb	0.97	0.96	0.97	0.89
Dy	5.33	5.57	5.55	5.20
Ho	1.01	1.04	1.02	0.84
Er	2.62	2.49	2.64	2.18
Yb	1.90	1.78	2.16	1.61
Y	27	27	29	23
Th	6.57	4.47	4.0	2.63
U	1.15	0.94	1.02	0.63
Zr	220	223	280	173
Hf	5.60	6.12	7.8	3.63
Nb	66	61	48	38

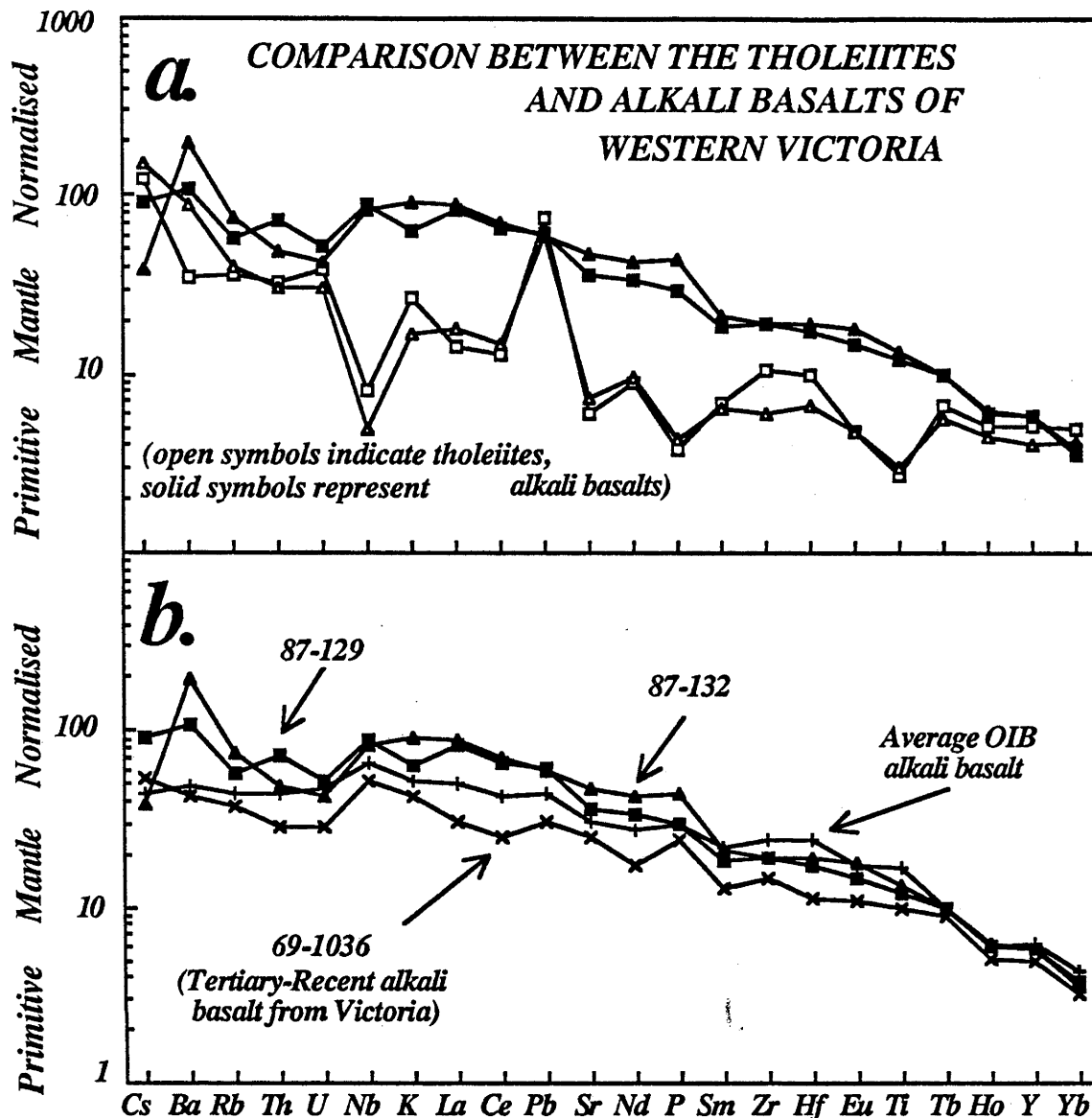


Fig. 5.8 Primitive Mantle Normalised diagrams illustrating a. the differences in trace element signature between the alkali basalts and tholeiites from western Victoria and b. the similarities in trace element characteristics of alkali basalts from different environments.

5.3.2 Isotopic composition

The Sr and Nd isotopic results for the tholeiitic and alkalic basalts are presented in Appendix 5 and illustrated in Figure 5.9. The alkali basalts have compositions typical of OIB and plot in the oceanic island field. The tholeiites have similar Nd and Sr isotopic compositions to the Tasmanian-Ferrar tholeiites, although one sample from Kangaroo Island (87-134) has a significantly lower ϵ_{Nd} (-7.9). The higher Nd content in 87-134 (19.0 ppm) may indicate that this unusually low Nd-isotopic composition is a superimposed effect resulting from the incorporation of crustal material. If this is the case, the contribution of Nd (and other REE) from a crustal source was not accompanied by a significant shift in the $^{87}Sr/^{86}Sr$ composition (possibly because the ratios are already high and therefore relatively insensitive), and the contamination was specific to this example. This rock also has a lower MgO content compared with the other tholeiites which may reflect contemporaneous fractionation.

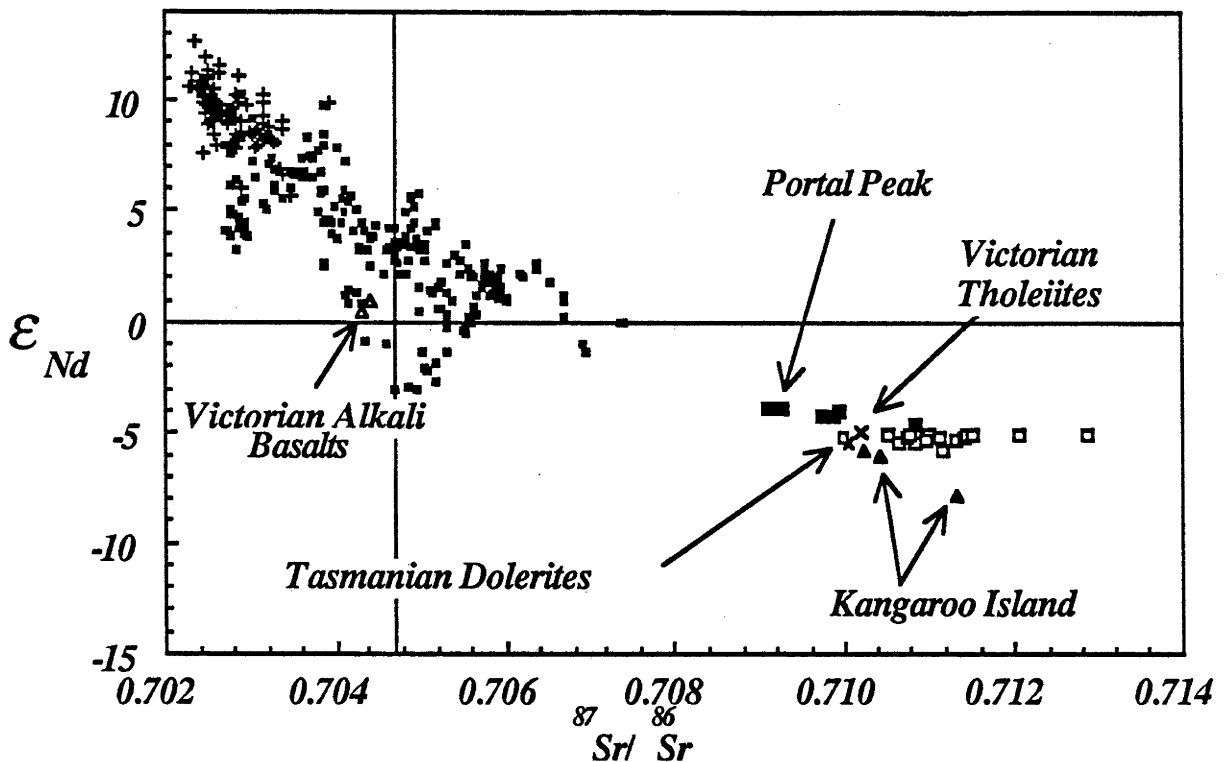


Fig. 5.9 ϵ_{Nd} versus $^{87}Sr/^{86}Sr$ initial ratio (calculated at 175 Ma) for the Jurassic tholeiites from Kangaroo Island (filled triangles) western Victoria (diagonal crosses), Tasmania (open squares) and Portal Peak Antarctica (large filled squares). The western Victorian alkali basalts (open triangles), MORB (vertical crosses) and OIB-IAB (small filled squares) are shown for comparison. References for the oceanic basalt data are given in the caption to Figure 4.11.

5.4 DISTRIBUTION OF MAGMATIC CLAN

The results presented in this chapter support the existence of a large, single magmatic province comprising the Ferrar Group of Antarctica and the Tasmanian, Kangaroo Island and western Victorian tholeiites of southern Australia, prior to the fragmentation of Gondwanaland (Fig. 5.10). It has been argued that the tholeiites produced over a distance of thousands of kilometres were remarkably uniform in elemental and isotopic composition, despite the variation superimposed by possible contamination, alteration and fractionation processes.

Importantly, the characteristic trace element and isotopic signatures are present in the most primitive olivine-bearing dolerites from Antarctica, as well as the more common evolved tholeiites. This indicates that the "crustal" characteristics were imposed prior to much of the magma fractionation. Contamination must have occurred either in the early stages of interaction between the basalt magma and the crustal environment (i.e. in the lower crust prior to more shallow level fractionation), or within the mantle source prior to magma generation.

In order to derive the crustal signature of these tholeiites by assimilation of crustal material, an isotopically and geochemically uniform assimilant is required over a considerable distance. As it is believed that in Tasmania, the dolerites have migrated through two distinct basement lithologies of different geological history (Chapter 2), it would appear unlikely that a uniform assimilant exists in the deeper crust throughout this province. This argument is particularly strong in the light of the relatively uniform isotopic compositions of the tholeiites. Although contamination by granitic melts from various crustal source rocks may yield very similar trace

element signatures, the isotopic compositions would remain different depending on the original parent-daughter element ratios and age of the source from which the melts were derived.

The alternative, that the heterogeneous mixture of crust and basalt was homogenised in a magma chamber of enormous proportions is also considered unlikely. Although large magma chambers exist (e.g. the Dufek intrusion contains most of the known tholeiite of the Ferrar Group), these large bodies are compositionally stratified rather than uniformly well-mixed. In addition, the effects of contamination in large intrusions by assimilation of roof-rocks during fractionation has been recently reviewed by Turner and Campbell (1986). These authors showed that unless the contaminant breaks away from the roof of the chamber in large blocks and falls through the basalt, the contaminated magma will be confined to a narrow zone ponded at the top of the chamber.

Rather than appealing to an enormous magma chamber, derivation of the tholeiites from a complex system of sill and sheet-like chambers emplaced at or around the crust-mantle boundary may be more likely (e.g. Cox, 1980; Thompson *et al.*, 1983). Given the unlikelihood that a system of sills and dykes could communicate geochemically, it must be concluded that the "contamination" occurred prior to the formation of these magma chambers.

In Chapter 4 it was argued that even if a uniform crustal component were available to the intruding magma, the trace element abundances in any typical basalt (e.g. OIB or MORB) makes modelling of assimilation difficult. It was shown that the trace element and isotopic characteristics of the Tasmanian Dolerites could be more easily explained by introducing a shale or granitic component into a typical mantle source region, and melting this contaminated source to produce the tholeiites. If a similar explanation is proposed for the entire Ferrar-Australia clan of tholeiites, then clearly, the homogeneity of the magmas poses an equally difficult problem for this mechanism as it does for crustal assimilation models.

The tectonic setting of the Jurassic magmatism is relevant when considering the magma production and its possible homogenisation. Elliot (1976) noted that the Ferrar Group magmatism occurred at a time when the Pacific margin of Gondwanaland was in a state of compression caused by subduction (although the rate and extent of underthrusting are uncertain). This contrasts with the opinion that continental flood volcanism is related to extensional tectonics, and lead Elliot to postulate that the Ferrar Group were generated in a back-arc spreading regime within a continental plate. This hypothesis is consistent with geophysical evidence which indicates that the crust in eastern Antarctica is considerably thicker than in the adjacent Ross embayment, the latter representing an area in which thinning would occur in Elliot's model (e.g. Evison *et al.*, 1960; Robinson and Splettstoesser, 1984 and references therein). Kyle *et al.* (1987) have also appealed to this type of tectonic setting for the production of the Ferrar tholeiites.

Assuming that magma generation in Antarctica occurred in a region of extension during the Jurassic, and that (following the arguments of Chapter 4) the basalt was derived from a contaminated mantle source, then there are two major processes which may contribute to the uniformity of the mantle source region. The first possibility concerns the sediments introduced into the mantle source by the postulated subduction. Taylor and McLennan (1985) showed that post-Archaeon terrestrial shales from different localities have essentially the same geochemical

composition. Thus it is possible that shales produced along the Pacific margin of Gondwanaland were similar in composition, particularly as the geological history along this margin shortly prior to the magmatism produced uniform lithologies over wide areas (e.g. Late Carboniferous-Triassic sedimentation). It has also been shown that the isotopic composition of sediments derived from landmasses can also be of remarkably uniform composition. Goldstein *et al.* (1984) analysed atmospheric dusts and river sediments presently being deposited in several localities around the world and noted that most of the $^{143}\text{Nd}/^{144}\text{Nd}$ and $^{147}\text{Sm}/^{144}\text{Nd}$ ratios lie in a very restricted range. Homogenisation during transport appears to be an effective mechanism of producing uniform elemental and isotopic signatures in sediments.

In a subduction setting, uniformity in the isotopic signatures of basaltic magmas may also result from mixing caused by rapid extension as suggested by Oversby and Ewart (1972) for the Pb-isotopic signatures of the Tongan volcanics. Another aspect to be considered in the "source contamination" hypothesis is that variable amounts of the subducted component may have been added to the mantle source in different areas. The widespread, and probably high degree of partial melting which took place in the Jurassic may have subsequently eliminated any differences caused by this effect.

If the component in the mantle source is a granitic residue remaining from crustal growth in the Proterozoic rather than a subducted sedimentary component (see Chapter 4.4), it is likely that the trace element signature will be relatively homogeneous (see Fig. 4.14), and therefore it is possible that the isotopic systems will have evolved to produce a compositionally uniform source region. Any heterogeneities produced by the development of variable proportions of this component in the source, would then need to be destroyed by large-scale melting and/or rapid extension as suggested above for the subducted sediment model.

It is evident that just as crustal-level contamination models have difficulty in explaining the remarkable uniformity of the Ferrar-Australian clan of Jurassic magmatism, so too does a model involving a contaminated source region. Although the mechanisms suggested here require a degree of special pleading, this may be justified by the unique occurrence of tholeiites with such extreme compositions.

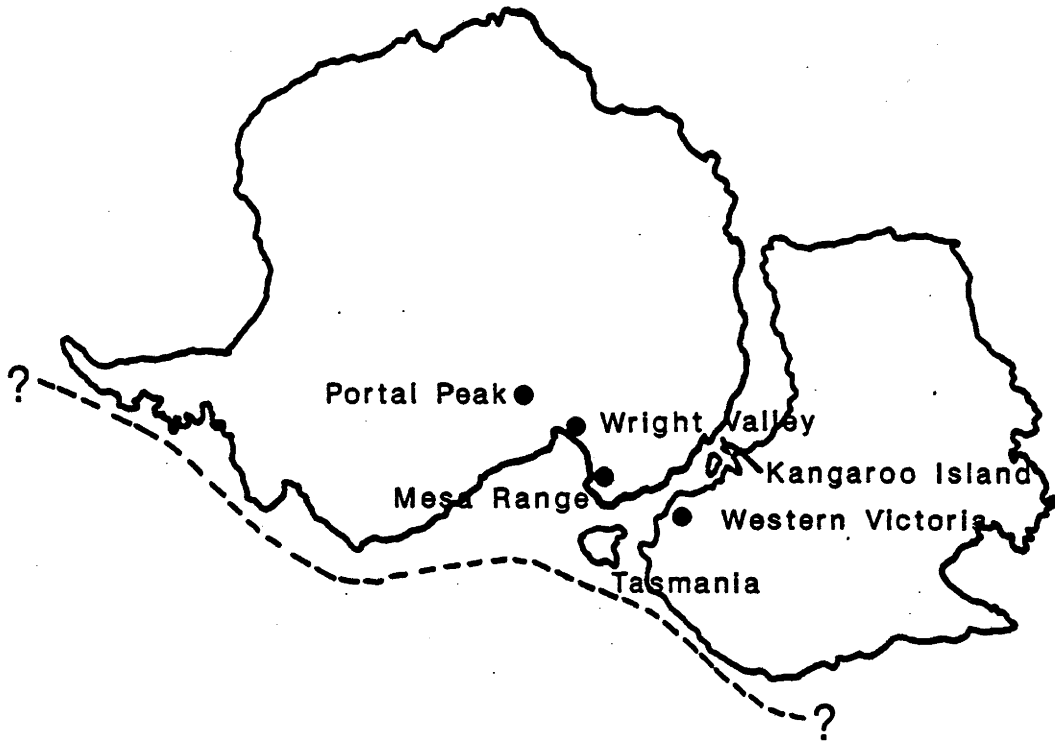


Fig. 5.10 Sketch map showing the reconstruction of Antarctica and Australia (Craddock, 1975). Indicated are the locations referred to in the text for which trace element data have been obtained (either in this study or in the literature), and the possible location of the proposed subduction zone.

CHAPTER 6

CONTINENTAL THOLEIITES- A COMPARISON

It has long been recognized that continental tholeiites throughout the world exhibit remarkable similarities. Whether represented by flood basalts or their intrusive equivalents, these provinces constitute a significant proportion of the continental landmass. Some of the larger examples include the Karoo (southern Africa), Paraná (South America), Ferrar (Antarctica), Deccan Traps (India) and Columbia River Basalts (North America).

It is well beyond the scope of this thesis to review all research carried out on the many continental tholeiitic provinces of the earth. In this chapter some broad comparisons are made between the Ferrar-Tasmania-southern Australia "clan" (hereafter referred to as the Ferrar-Tasmania province) and some of the large, well documented provinces associated with the disintegration of Gondwanaland (i.e. the Karoo, Paraná and Deccan tholeiites).

After a brief summary of the size, locality and lithologies present in the three major provinces studied, a review of the present consensus regarding the petrogenesis of the tholeiites in each continent is given. Following this, a closer comparison is made between the tholeiites from the Karoo, Paraná and Deccan provinces, and those of the Ferrar Group. It has been demonstrated in Chapter 4 that the features distinguishing the Ferrar Group from other tholeiites (i.e. MORB and OIB tholeiites) are their unusual trace/minor element characteristics and isotopic compositions. Thus, it is these areas in which comparisons between the provinces are made. The discussion is necessarily limited to the more detailed geochemical and isotopic studies, and it is fortunate that recent research on the Karoo, Paraná and Deccan provinces has been focussed in these areas.

6.1 THE MAJOR PROVINCES

6.1.1 *The Karoo, southern Africa*

The results of several years research, by many scientists, on rocks from the Karoo volcanic province have recently been published in a special volume of the Geological Society of South Africa. This section is not intended to be a review of all such work; rather, a generalised account of some of the results more relevant to the present study are given. Much of the information regarding the general geology has been derived from the excellent reviews of Bristow & Saggerson (1983) and Eales *et al.* (1984), and more specific reference is made to additional publications where necessary.

The Karoo igneous event spanned approximately 75 million years beginning at ~205 Ma and persisting until ~130 Ma. Volcanism began in SE Zimbabwe with the emplacement of carbonatites; however, the presence of glass shards and tuffaceous fragments in earlier sediments indicates a less abrupt beginning. Activity spread to the Nuanetsi-Tuli areas, and south through the Lebombo belt (Fig.6.1). The volcanicity culminated in these regions between about 190 and 177 Ma, and was also extensive in the Central area at that time. In its waning stages, the volcanism shifted towards the NW (Namibia) and NE (NE Mozambique, Lupata and

Malawi), and terminated in the early Cretaceous.

Cox *et al.* (1967) carried out regional work and subdivided the Karoo tholeiites into two geochemical provinces. Tholeiites in the northern part of the Karoo province were described as being characterised by high incompatible element contents compared with the tholeiites further south (i.e. Ti, P, K, Ba, Sr and Zr). Later work shows that although the 140,000 km² of exposed tholeiite has been divided into four main sub-provinces on the basis of both chemical variation and geographical distribution, the northern/southern distinction remains. This is particularly evident in the Sabie River Basalt Formation, where the change from one type to the other occurs within a distance of ~30 km (Cox and Bristow, 1984).

The four major subdivisions of the Karoo province are:

1. The Central area- Stormberg, Drakensberg (or the Lesotho Plateau), Springbok Flats, SWA/Namibia volcanics and widespread dolerites.
2. Southern Lebombo- includes the Swaziland and Zululand volcanics and the Rooi Rand Dyke Swarm.
3. Northern Lebombo- includes Zimbabwe (i.e. Nuanetsi, Tuli and Sabi rocks).
4. The Etendeka area- includes the Kaokoveld lavas, Etendeka and Cape Cross.

1. CENTRAL: The rocks in this area are predominantly quartz normative tholeiites, including intrusive dolerites and basalt flows. These generally contain plagioclase, augite and pigeonite; and although present, orthopyroxene is not usually a major phase. Olivine-bearing flows are present but are restricted to the base of the succession. In these flows, Cr-spinel appears to have crystallized first, and often is enclosed in the olivines. Small amounts of silicic differentiate occur (containing considerable quartz and alkali feldspar, with ferroaugite, fayalite and apatite as additional phases) but felsic rocks (e.g. rhyolites) are notably absent (Marsh and Eales, 1984).

The Central area is normally divided into two major regions, the Lesotho Plateau and Stormberg. Lesotho has been widely studied and is the larger, and geochemically simpler of the two; in contrast, Stormberg shows more variation than indicated by the description in the preceding paragraph. In this area basal flows include andesites and high and low K-basalts. It is suggested that these are the result of a small degree of partial melting of heterogeneous mantle compared with the rest of the Central rocks (originating from a picritic precursor).

The chemistry of the Lesotho-type rocks has strong affinities with "normal" tholeiites. They are only slightly LREE enriched and although high in SiO₂ (50-55 wt.%) and low in MgO (6-8 wt.%), are consistent with evolution from a picritic parent. The initial ⁸⁷Sr/⁸⁶Sr ratios range between 0.70462 ± 0.00005 and 0.70681 ± 0.00010 for the dolerites and 0.70458 ± 0.00005 and 0.70686 ± 0.00006 for the flows (Marsh and Eales, 1984). Tholeiites with affinities to the Lesotho magmas have been noted hundreds of kilometres from the Lesotho Plateau (e.g. Botswana, Duncan *et al.*, 1984), so that the geographical distribution of this magma type is considerable.

Overall, the Central sub-province is chemically simple compared with the marginal areas. A number of magma types occur (i.e. Vaalkop, Moshesh's Ford, Kraai River, Pronksberg),

however these are subordinate to the Lesotho magmas.

2. SOUTHERN LEBOMBO: Both Southern and Northern Lebombo display an approximately 10 km thick pile of mafic and rhyolitic flows which occur in similar abundance. In each case the uppermost flows are of early Cretaceous age. The Southern Lebombo area is also known for its areas of well developed dykes, particularly the Rooi Rand Dyke Swarm. This swarm is situated in Swaziland and South Lebombo and is depleted in incompatible elements relative to the more evolved rocks. The initial $^{87}\text{Sr}/^{86}\text{Sr}$ ratios are close to typical tholeiitic values and average 0.7039 ± 0.0002 .

Granophyre dykes occur in Swaziland and Central Lebombo and rhyolitic dykes have been found in southern Lebombo. These dykes, and the lavas of the Southern Lebombo sub-province, have initial $^{87}\text{Sr}/^{86}\text{Sr}$ ratios of 0.70795 ± 0.00026 .

The Karoo volcanic rocks (for which Sr and Nd isotopic compositions are available) have been plotted on an ϵ_{Nd} versus ϵ_{Sr} diagram, and the Sm/Nd ratios have been plotted against Rb/Sr ratios for the same samples (Hawkesworth *et al.*, 1983). These authors argued that because the positions of the Southern Lebombo samples relative to the fields for the other subprovinces varied between the two diagrams, the trace element signatures were decoupled from the isotopic signatures. The interpretation of Hawkesworth *et al.* (1983) was that the Southern Lebombo group may have been contaminated by continental crust.

3. NORTHERN LEBOMBO: Carbonatites mark the beginning of the main period of volcanism in this area, and the base of the thick lava pile is chemically diverse. Rock-types at the base of the sequence include nephelinites, glassy olivine basalts or "limburgites" and picritic basalts (abnormally enriched in incompatible elements) overlain by olivine-poor basalts, tholeiitic andesites and rare shonkinites.

Initial $^{87}\text{Sr}/^{86}\text{Sr}$ ratios for Northern Lebombo rocks range between ~ 0.705 and 0.707 with a range in ϵ_{Nd} from approximately -3 to -10 ; the variation in these signatures is interpreted as the result of heterogeneity in the enriched mantle source from which the magmas were derived.

4. ETENDEKA: This area is located on the western margin of the continent and like its eastern equivalent (the Lebombo Belt) contains thick flows of both felsic and mafic extrusives. In addition, a 900 m section of interbedded latites and quartz latites is exposed at Tafelberg. A large range in Sr-isotope ratios (~ 0.708 - 0.714) contrasts with the comparatively narrow spread in ϵ_{Nd} values (-3 to -7) for the rocks of this sub-province. Although originally interpreted as a purely mantle derived suite (Erlank *et al.*, 1984), recently acquired oxygen isotope data have been interpreted as evidence for the incorporation of mafic lower crustal material (Duncan *et al.*, 1987).

Volcanics in this sub-province can be correlated with basalts from the Paraná Basin of South America, and the youngest rocks in the Etendeka area are thought to be contemporaneous with the opening of the South Atlantic.

SUMMARY: The marginal sub-provinces contain both the oldest and youngest members of the Karoo igneous province. These are far more chemically diverse compared with the rocks of the Central area, implying a more complex, and possibly tectonically controlled petrogenetic

history. A broad division has been made between more incompatible element enriched volcanics towards the north compared with those in the south; however, further subdivision into four main chemical groups (each of which may contain different magma types) has been possible.

Apart from rare exceptions such as the Rooi Rand Dyke Swarm, the Karoo basalts are generally enriched in incompatible elements, including the rare picrites. Chondrite normalized REE plots show LREE enrichment, relatively flat HREE patterns and slight negative Eu anomalies in many cases. This unusual chemistry, coupled with the early exotic rock-types (e.g. carbonatites and nephelinites) in some areas, has been interpreted as evidence supporting the derivation of the magmas from an inhomogeneous, metasomatised mantle source.

It is suggested that the variation in initial isotopic ratios and trace element signatures is related to heterogeneity in the source regions which the tholeiites mimic. This is particularly noted in the abrupt change in composition of the Sabie River Basalt Formation in the eastern part of the Karoo Province. The strongest evidence for crustal contamination is the decoupling of the Rb/Sr and Sm/Nd ratios from their respective isotopic signatures in rocks in the Southern Lebombo area, and the correlation of Sr and O isotopic signatures in the Etendeka tholeiites.

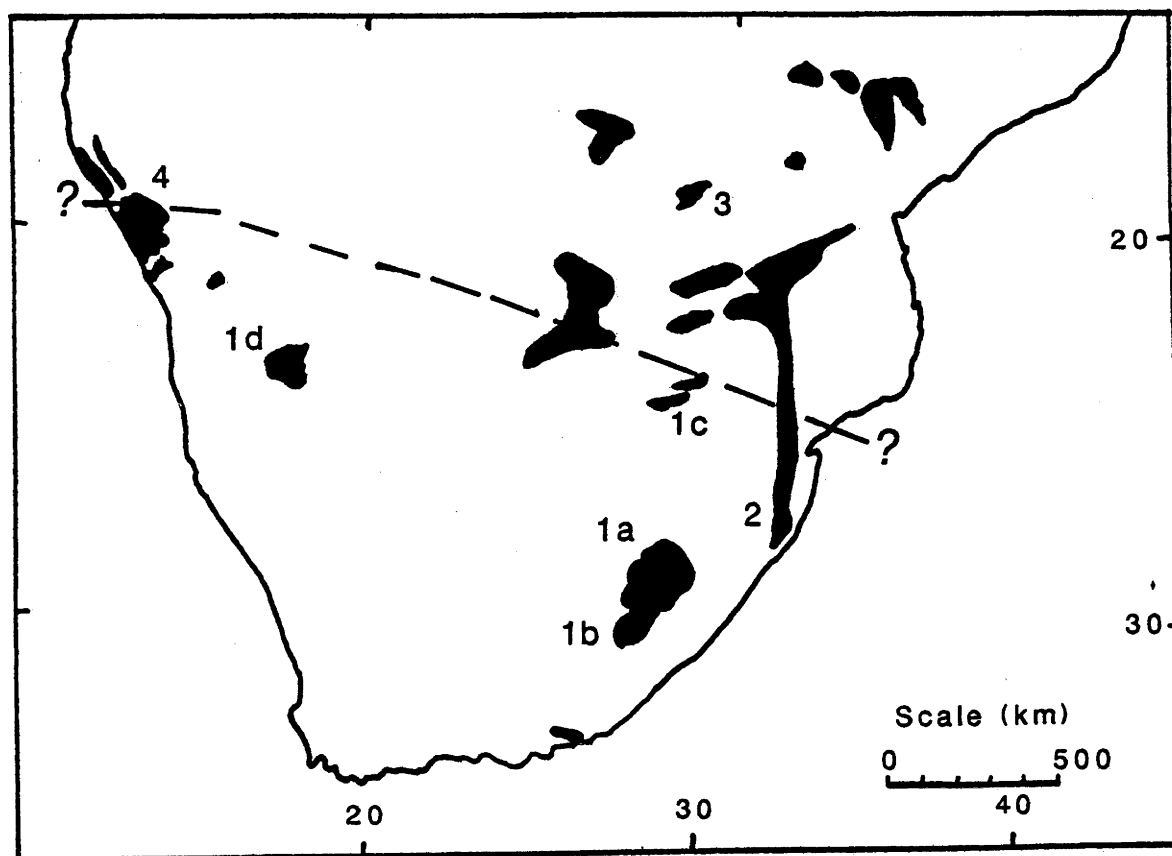


Fig. 6.1 Sketch map of southern Africa illustrating the location and extent of the major Jurassic magmatism. (Modified from Duncan *et al.*, 1984). 1. Central Area: a. Lesotho, b. Stormberg, c. Springbok Flats, d. SWA/Namibia. 2. Southern Lebombo. 3. Northern Lebombo. 4. Etendeka Area. The broader division into a high incompatible element sub-province in the north, and a lower incompatible element sub-province in the south is also shown (based on Erlank *et al.*, 1984 p. 236, Cox and Bristow, 1984, and Duncan *et al.*, 1984 fig. 4)

6.1.2 The Paraná, South America

The Paraná Basin of South America is elongate, trending NE-SW, and contains sediments of Devonian to Permian age (Fig. 6.2). Volcanism in the Paraná Basin occurred between ~140 and 120 Ma ago and extended over an area of approximately 1.2×10^6 km² (estimated volume, ~790,000 km³). Of these volcanic products, approximately 90% (by volume) are basalts of quartz tholeiitic composition, with intermediate and acidic volcanics representing only 7% and 3% respectively (Bellieni *et al.*, 1986).

Bellieni *et al.* (1986) divided the volcanics in the basin into three areas, comprising northern, southern and central zones. This has been noted in other research (e.g. Mantovani *et al.*, 1985; Hawkesworth *et al.*, 1987) and a brief outline of the characteristics of each zone is given below.

The southern Paraná Basin is typified by volcanics bearing chemical signatures depleted in Ti and P and having high ⁸⁷Sr/⁸⁶Sr initial ratios (termed the low phosphorus-titanium, or LPT group by Mantovani *et al.*, 1985). This geochemical group includes lithologies ranging from basalts to rhyolites and signifies a close petrogenetic link between these magmas. Acid volcanics are most prevalent in this zone (~13 vol.%) and are concentrated towards the eastern and southern margins of the basin suggesting a possible tectonic control for this type of magmatism (Bellieni *et al.*, 1986).

In contrast, the northern Paraná Basin contains only minor rhyolitic material (~0.3 vol.%) and intermediate rocks are virtually absent. The volcanics in this zone are characterised by higher Ti and P contents (HPT group) compared with the southern zone demonstrating that essentially two clans of magmatism exist in this province. The initial ⁸⁷Sr/⁸⁶Sr ratios in the northern area are also considerably lower than in the LPT rocks (e.g. Mantovani *et al.*, 1985). Again, these general chemical signatures occur both in the basaltic (quartz tholeiitic) and rhyolitic members (Bellieni *et al.*, 1986).

The central zone contains lithologies from each of the LPT and HPT groups. These may be closely related in both time and space, being intercalated in some sections (e.g. Hawkesworth *et al.*, 1987).

Recently, detailed geochemical and isotopic data have been published for samples from the Paraná basin tholeiites. The HPT tholeiites are generally thought to be mantle derived magmas which have evolved without being contaminated by crust (Mantovani *et al.*, 1985; Bellieni *et al.* 1984; Hawkesworth *et al.*, 1986). Therefore, the signatures preserved in the HPT basalts are expected to preserve the character of the mantle source.

In contrast, it is generally accepted that at least some of the LPT tholeiites were contaminated with crustal material (e.g. Fodor *et al.*, 1985a,b; Mantovani *et al.*, 1985; Hughes *et al.*, 1986). The contaminated basalts may be confined to those in the silica range ~52-58 wt.%, with the "uncontaminated" basalts still having high initial ⁸⁷Sr/⁸⁶Sr ratios (~0.707; Mantovani *et al.*, 1985).

Although petrogenesis of the LPT group is complicated by assimilation of crust, the results of trace element and isotopic modelling based on the more primitive members suggests that the LPT and HPT magma types were originally derived from different mantle source regions

(e.g. Mantovani *et al.*, 1985; Hawkesworth *et al.*, 1986). A detailed isotopic study on the transition area between LPT and HPT fields has been carried out by Hawkesworth *et al.* (1986). These authors presented Sr, Nd and Pb data for samples from each petrogenetic clan and demonstrated that strong similarities exist between the HPT group and oceanic basalts from Kerguelen, Walvis Ridge and Bouvet. The derivation of the signatures in the oceanic basalts were related to the possible destabilisation of an enriched upper mantle source (originally underlying the Paraná and Etendeka fields) during the break-up of Gondwanaland. The mechanism envisaged by these authors is that the unusual mantle beneath the continental volcanic fields was thinned during rifting and continental separation, and reincorporated into the mantle underlying the new oceanic crust being formed. Therefore, in addition to proposing an enriched mantle as the source for the Paraná (and Etendeka) tholeiites, these authors also suggest an origin for the unusual oceanic signature termed the DUPAL anomaly (Hart, 1984). Interestingly, this would place the DUPAL anomaly at a relatively shallow level in the mantle, compared with a more stable deep-seated region proposed by Hart (1984).

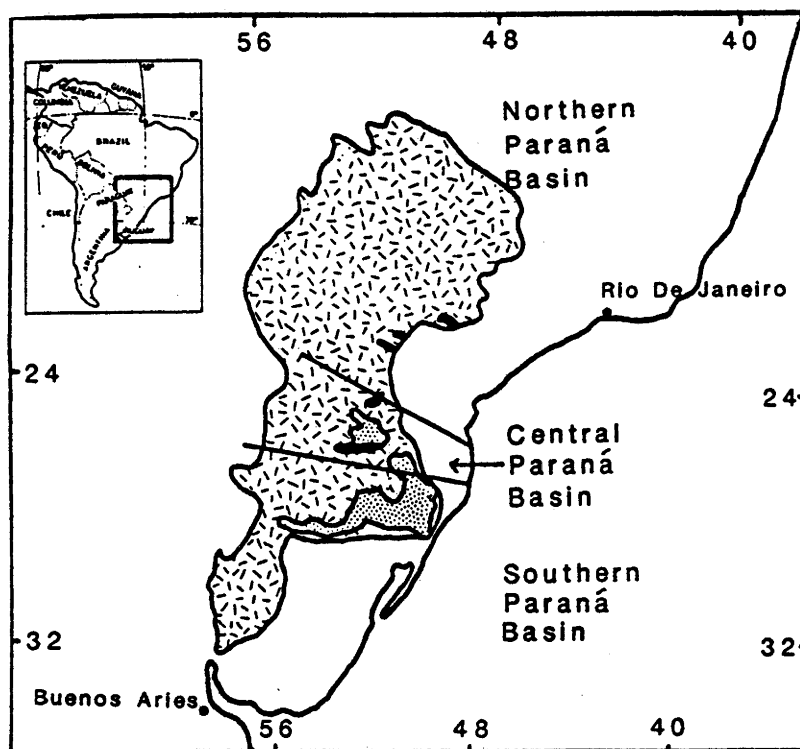


Fig. 6.2 Sketch map showing the general extent of Mesozoic tholeiites (random-line pattern), and rhyolites (HPT or Chapecó type shaded in black, LPT or Palmas type is shown by the stipple pattern) in the Paraná basin of South America (Modified from Bellieni *et al.*, 1986).

6.1.3 The Deccan Traps, India

An area of approximately 500,000 km² is presently covered by tholeiitic basalt in central and NW India (Fig. 6.3). The thickness of the succession varies from only 100-200 m in the east, to approximately 2000 m along the west coast (Ghose, 1976).

The volcanism occurred between 65 and 50 Ma ago with the older members confined to the west; however, carbonatites and other undersaturated rocks appear to have persisted until ~35 Ma. The Deccan basalts generally are quartz-normative, however some olivine tholeiites

occur. Both fissure and vent systems are present, and are responsible for mainly tholeiitic and undersaturated eruptives respectively. Rare picrites (confined to the base of the volcanic sequences) are believed to represent samples of the parent magma, however some of the phenocrysts could be of cumulate origin (Krishnamurthy & Cox, 1977).

The undersaturated rocks occur in the western areas, and are absent in the eastern and southeastern regions (Ghose, 1977; Krishnamurthy and Udas, 1981). Where they occur, the alkali basalts may have some tholeiitic affinities and gradations between alkalic and tholeiitic rock-types have been noted (Alexander and Gibson, 1977; Krishnamurthy and Cox, 1981; Paul *et al.*, 1984).

Although Ghose (1976) suggested there was evidence supporting a gradual change in chemical composition of the tholeiites from the east towards the west, Paul *et al.* (1984) maintained that when basalts exclusively are examined, no systematic variation is obvious either from east to west or throughout a vertical section. The studies of a number of areas by Alexander and Paul (1977) and Paul *et al.* (1984) indicated that the geochemical compositions in the tholeiites compared from several areas (Fig. 6.3) were rather uniform. Small variations were attributed to the fractionation of olivine and plagioclase (pyroxene was not favoured owing to the high and uniform Sc contents), differences between the degree of partial melting in the source region, and restricted selective contamination. The $^{87}\text{Sr}/^{86}\text{Sr}$ initial ratios measured in tholeiites from Sagar, range between 0.7039 and 0.7084 (Alexander and Paul, 1977), and were interpreted as the result of selective introduction of ^{87}Sr into the basalts from the granitic basement. Bulk assimilation and alteration models were not favoured owing to the lack of correlation between the $^{87}\text{Sr}/^{86}\text{Sr}$ initial ratios, and parameters such as the $\delta^{18}\text{O}$.

Although there were few detailed major, trace element, and isotopic studies of the Deccan basalts until relatively recently (Bose, 1983), the early 1980s saw a resurgence of interest in the Deccan province, and numerous new data became available. In 1982, Allègre *et al.* presented Sr, Nd and Pb isotopic data for tholeiites from the Mahabaleshwar area. Based on the ranges observed [$^{87}\text{Sr}/^{86}\text{Sr} = 0.70410$ to 0.71305 ; $^{206}\text{Pb}/^{204}\text{Pb} = 17.4$ to 22.7 , $^{207}\text{Pb}/^{204}\text{Pb} = 15.3$ to 15.7 , $^{208}\text{Pb}/^{204}\text{Pb} = 38.04$ to 43.78 ; $\epsilon_{\text{Nd}} = +5.1$ to -5.6] these authors proposed that the basalts were derived from a fossil depleted mantle source in the subcontinental lithosphere, and were subsequently contaminated by crustal rocks. At approximately the same time, Mahoney *et al.* (1982) presented Sr, Nd isotopic results, and trace element data for Mahabaleshwar basalts. The range in values from Allègre *et al.* (1982) was extended considerably by Mahoney *et al.* (1982) with initial $^{87}\text{Sr}/^{86}\text{Sr} = 0.7039$ - 0.7179 , and $\epsilon_{\text{Nd}} = +7.8$ to -16.2 . In addition, the new isotopic data defined two correlations which were interpreted as mixing trends. Mahoney *et al.* (1982) suggested that the high ϵ_{Nd} , low $^{87}\text{Sr}/^{86}\text{Sr}$ mantle endmember was the same for each trend; however, the two "contaminants" were isotopically distinct, one being in the continental crust, and the other either a different crustal component or an enriched mantle component.

Additional research on basalt sections from Mahabaleshwar performed by Cox and Hawkesworth (1984), enabled division of the section into 3 formations using trace element signatures. The lowermost member (Poladpur) was characterised by high Ba, Rb, K, Si, Zr/Nb and low Sr, with high and variable $^{87}\text{Sr}/^{86}\text{Sr}$ (0.7043 to 0.7196) and low and variable ϵ_{Nd} (+2.6

to -17.4). It was proposed that these basalts were formed by an AFC process in which the contaminant was an ancient granitic crustal component, and the mantle endmember was similar to the overlying Ambenali basalt type.

The middle formation in the section studied by Cox and Hawkesworth (1984) was termed the Ambenali type. In contrast with the Poladpur Formation, the Ambenali basalts were characterised by low Ba, Rb, Sr, and Zr/Nb, with low and uniform $^{87}\text{Sr}/^{86}\text{Sr}$ (0.7038 to 0.7043) and high and uniform ϵ_{Nd} (+4.7 to +6.4). It was suggested that the basalts from this formation were derived from a slightly enriched MORB source without crustal contamination.

The third and uppermost group assigned by these authors, was termed the Mahabaleshwar Formation. These basalts are similar to the Poladpur rocks, but with lower Zr/Nb and higher Sr contents. The range in isotopic compositions for the Mahabaleshwar Formation basalts is $(^{87}\text{Sr}/^{86}\text{Sr})_i = 0.7040$ to 0.7056 and $\epsilon_{\text{Nd}} = +7.1$ to -3.0 . Unlike the Poladpur basalts, the Sr contents correlate positively with other incompatible elements and $^{87}\text{Sr}/^{86}\text{Sr}$ in the Mahabaleshwar rocks. It was proposed that this correlation was evidence in favour of a mantle enrichment process, rather than assimilation of crust, in the petrogenesis of the Mahabaleshwar basalts.

Cox and Hawkesworth (1984) concluded that crustal contamination in the Deccan basalts was very limited (~2-3%) and only evident in the Poladpur Formation where the contamination was ~6-12% (mass). It was considered that the Ambenali basalts were derived from a slightly enriched mantle source, and the Mahabaleshwar rocks originated from a variably enriched mantle source. This was developed in a subsequent paper by these authors (Cox and Hawkesworth, 1985), where additional sections were included, and further subdivisions were made; however, the general models proposed were essentially unchanged.

In a study of the relationship between the alkalic and tholeiitic basalts in the NW of the Deccan province, Mahoney *et al.* (1985), obtained the same two isotopic trends as noted previously for the tholeiitic basalts in Mahabaleshwar (Mahoney *et al.*, 1982; Cox and Hawkesworth, 1984, 1985). It was noted that almost complete overlap existed between the isotopic compositions of the tholeiitic and alkalic rocks, indicating a convincing link between the petrogenesis of the two magma types. Although the two isotopic arrays showed considerable spread, there was no correlation between fractionation and isotopic signatures. Mahoney *et al.* (1985) proposed that the alkalic and tholeiitic basalts were derived by different degrees of partial melting of the same mantle source. The two isotopic arrays were then developed by mixing the mantle melts with one of two homogeneous evolved endmembers; both of which were crustal components, or one was a crustal component and the second was an enriched mantle endmember.

MacDougall (1986) recently compared the Deccan tholeiites with those in the ocean ridge environment, and suggested that the Deccan rocks may have been produced during the opening of the Arabian Sea. He agreed with the suggestion of Mahoney *et al.* (1985) that the high ϵ_{Nd} mantle endmember was the same for the two isotopic arrays. Based on $\delta^{18}\text{O}$ values, MacDougall argued that the mantle endmember was contaminated by crust in both cases because there was a progressive increase in $\delta^{18}\text{O}$ (up to ~8‰) with increasing $^{87}\text{Sr}/^{86}\text{Sr}$ for the samples

from each array. MacDougall (1986) preferred a MORB endmember (rather than an OIB endmember) for the uncontaminated tholeiite; however, like Allègre *et al.* (1982), MacDougall noted that most MORB tholeiites have higher ϵ_{Nd} ($> +8$) and lower $^{87}Sr/^{86}Sr$ (< 0.7039) than the apparent Deccan mantle endmember. MacDougall (1986) suggested that, owing to the "mantle-like" $\delta^{18}O$ of the least contaminated Deccan tholeiites from Mahabaleshwar ($\sim 5.6\text{‰}$), the displacement from MORB Sr and Nd isotopic compositions could be explained if the rising mantle diapirs first interacted with a kimberlitic component at the base of the lithosphere, prior to contamination by crustal rocks. [It should be noted, however, that the $\delta^{18}O$ compositions of some lower crustal materials may not be too far removed from mantle values, (e.g. Rudnick *et al.*, 1986) and displacement by crustal contamination need not necessarily be ruled out].

Devey and Cox (1987) suggested that the evidence for contamination in many of the tholeiites is convincing. They noted a general relationship whereby the more mafic basalts are the most contaminated. This was related to contamination processes operating during magma ascent, caused by the higher temperature of the magmas (giving them a greater capability of assimilating country-rocks from the walls of the conduits), as well as the increased availability of crustal contaminants in the early stages of eruption (when the conduits are less likely to be lined with chilled liquids and/or cumulates). Devey and Cox (1987) explained the lack of correlation between assimilation and fractional crystallisation (observed in other provinces where contamination is believed to have occurred, e.g. the Etendeka rocks in the Karoo) as resulting from the retention of crystallized phases owing to turbulent flow during magma ascent. Therefore, the generally high proportion of phenocrysts in the Deccan basalts is considered to relate to the cooling of the magma during ascent and assimilation, although there is no strict correlation between the proportion of phenocrysts and the degree of assimilation. These authors noted that although this model may explain some of the characteristics of basalts considered to have experienced contamination, the petrogenesis of basalts previously attributed to derivation from an enriched mantle source (Mahabaleshwar Formation) remains the subject of some dispute.

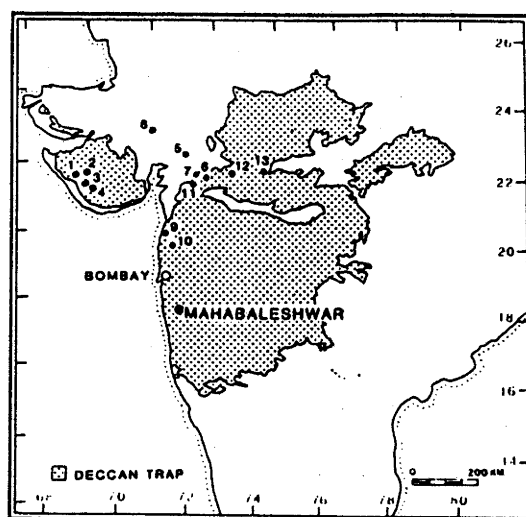


Fig. 6.3 Sketch map showing the extent of the Deccan magmatism. The area most extensively researched is Mahabaleshwar, which is indicated. In addition, the numbered circles represent areas in which acidic and alkaline rocks occur (From Sen, 1986).

6.2 GENERAL CHARACTERISTICS

The Gondwanide continental tholeiitic provinces may be viewed in chronological perspective. Analogues of the Tasmanian and Karoo tholeiites are found in eastern (Ferrar) and western (Queen Maud Land) Antarctica respectively. All are early Jurassic in age and represent the first large-scale outpouring of continental tholeiite in Gondwanaland. The Etendeka sub-province in NW Namibia was formed in the early Cretaceous with equivalent tholeiites in South America (Paraná tholeiites); and is understood to coincide with the opening of the South Atlantic (e.g. Eales *et al.*, 1984). Tertiary activity began in India with the formation of the Deccan Traps and represented the close of magmatism resulting from the breakup of this supercontinent.

General similarities in the Ferrar, Karoo, Paraná and Deccan provinces can be summarised from the previous discussion. The provinces are volumetrically enormous with the dominant rock-type being quartz tholeiite. The petrography is simple and phenocrysts generally are limited to olivine, clinopyroxene, orthopyroxene and plagioclase. Variation within a province is often only revealed by more detailed chemical analyses. Both picrites (or primary basalts) and xenoliths are rare, and this complicates the investigation of magma genesis because the starting material and its possible contaminant are largely unknown. Chondrite-normalised REE patterns are generally LREE enriched. Negative Eu anomalies are not uncommon, but are absent in many cases. Large ranges in isotopic signatures are generally characteristic, especially in the case of initial Sr (in the Ferrar-Tasmania province, only the Sr and O isotopes appear to show significant variation). Geochemical and isotopic signatures support the involvement of enriched mantle, crustal contamination, and alteration, in the petrogenesis of continental tholeiites from different localities. In most provinces, the evidence for geochemically unusual mantle sources for the tholeiites is convincing. In many cases where crustal contamination is favoured, the mantle source is still required to be enriched relative to most modern oceanic mantle source regions (for the Deccan, the mantle source may be only slightly modified from a MORB-type composition).

It would be very useful if it were possible to divide the various tholeiitic provinces into groups on the basis of their mantle source signatures. Illustrated in Figure 6.4 are many of the Sr and Nd isotopic data available for the tholeiites from the provinces described above. For the Deccan Traps, the evidence for a single mantle endmember is widely accepted, and the data closest in composition to this endmember have been plotted. However, if the model of Cox and Hawkesworth (1984, 1985) is correct, and a variably enriched mantle component is also involved, then additional "mantle" data would extend to ϵ_{Nd} values of -3.0 and $^{87}Sr/^{86}Sr$ of 0.7056. Distinction between uncontaminated (or unaltered) tholeiites from the Parana LPT, S. Lebombo, Etendeka and Ferrar regions is more difficult. The vertical line labelled "B" in Figure 6.4 has been included as an arbitrary cut-off for the samples likely to have undergone a change in isotopic signature subsequent to derivation from a mantle source; data plotting to the right of this line (i.e. more radiogenic Sr compositions) are likely to have been effected by alteration and/or contamination processes. This line is intended as a guide, and the data which plot to the left of line "B" may also be contaminated.

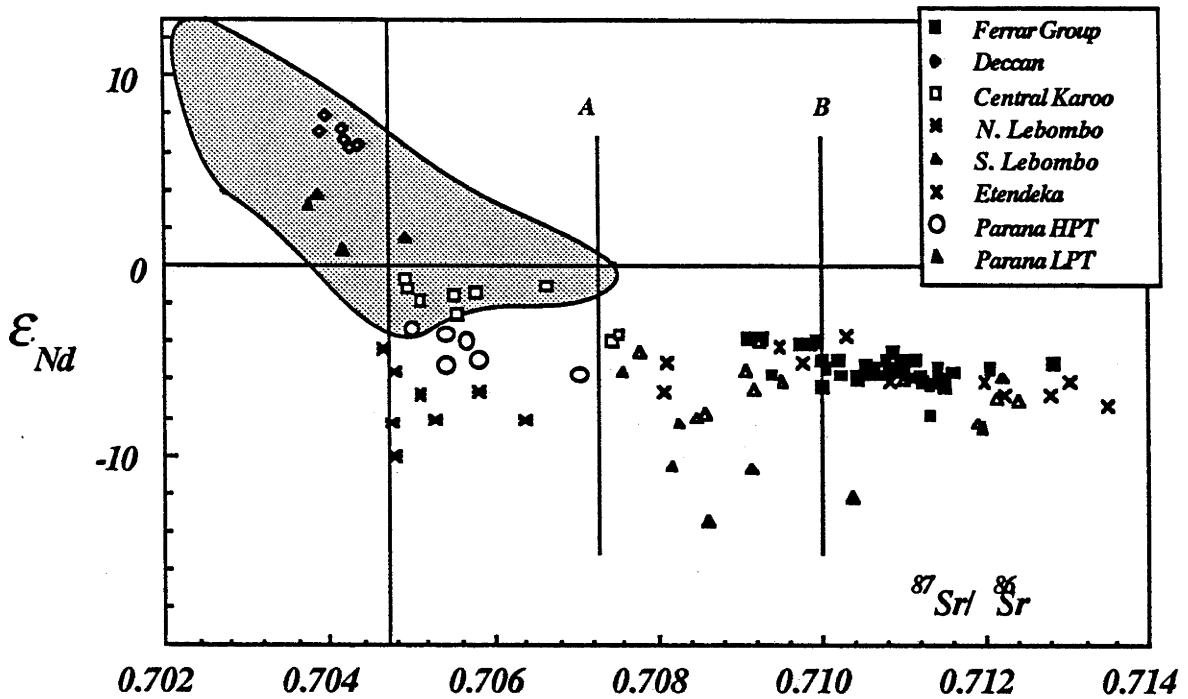


Fig. 6.4 Compilation diagram of Sr and Nd isotopic data available for the Deccan, Paraná, Karoo and Ferrar-Tasmania provinces. The Deccan data have been limited to the uncontaminated mantle endmember; an arbitrary line at $^{87}\text{Sr}/^{86}\text{Sr} \sim 0.71$ ("B") is suggested as marking the upper limit of mantle-derived Sr compositions (i.e. uncontaminated or altered since leaving the mantle source). The field of data between lines "A" and "B" is tentatively suggested as appropriate for true LPT tholeiites. To the left of "A" are the HPT and more transitional magma-types. The shaded region represents the mantle array, and includes the fields of MORB, OIB and IAB for comparison. Data sources for the oceanic field (shaded) are given in the caption to Fig. 4.10. The continental tholeiitic data are from Hawkesworth *et al.* (1984, 1986), Mahoney *et al.* (1982), and this study.

A second line ("A") is based on the isotopic data from the Paraná Basin tholeiites, and attempts to divide the rocks with HPT affinities (left) from those with LPT affinities (right). The line is an over-simplification, as HPT-like rocks may also have high $^{87}\text{Sr}/^{86}\text{Sr}$ compositions (e.g. Brewer *et al.*, 1987); although, this may be the result of superimposed processes rather than source features. The difficulties in compensating for crustal processes are obvious. Clearly, contamination may translate an oceanic-isotopic signature towards more crustal compositions. Based on the results for the Paraná, Karoo, and limited data on Antarctic samples from near the Weddell Sea, the LPT-type rocks are considered generally as having more "crustal" isotopic signatures compared with the HPT rocks. In addition to the isotopic compositions, the trace element signatures must also be used in the distinction between the different magma-types (and therefore, mantle source compositions).

Comparisons between tholeiitic provinces have been made using the REE contents of the tholeiites (e.g. Philpotts and Schnetzler, 1968), and more recently utilizing PMN patterns (e.g. Dupuy and Dostal, 1984; Thompson *et al.*, 1983). The trace element signatures are capable of revealing subtle variations related to the petrogenetic history of the magmas, and the large database now available in the literature permits greater scope for comparison.

The data are best represented in diagrammatic form and have been combined in Figure 6.5 [Note: The limited data available has reduced the number of elements possible for comparison. Unless otherwise stated, reference to the "content" of a particular element in the following

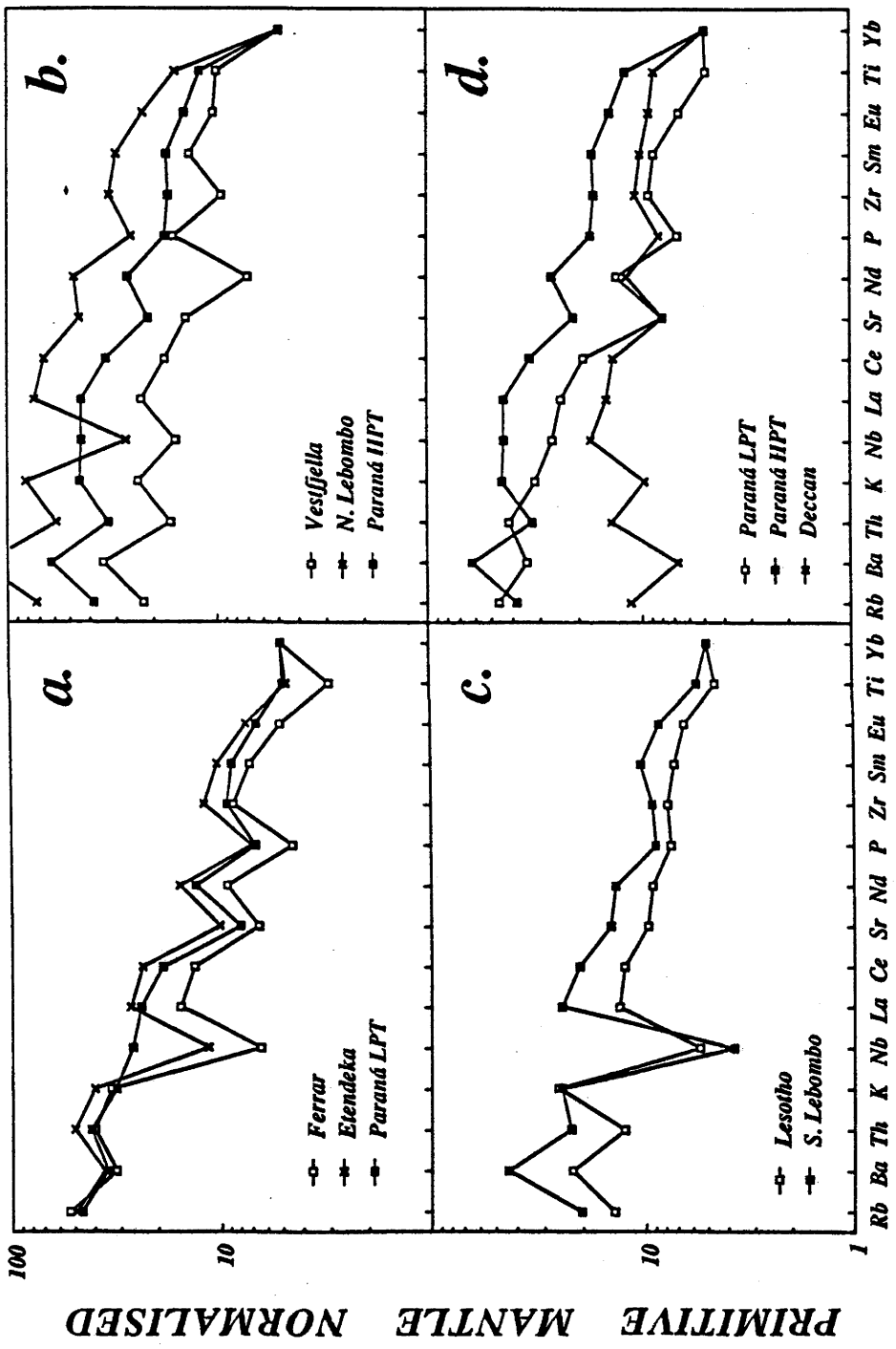


Fig. 6.5 Possible distinction between Mesozoic continental tholeiitic rocks from different provinces, on the basis of their PMN patterns

a. Indicates the similarity between the Ferrar-Tasmania province (labelled "Ferrar"), the average Etendeka signature, and the Paraná LPT signature. These rocks have been collectively termed the LPT group.

b. Compares the Vestfjella rocks from Dronning Maud Land (Antarctica) with tholeiites from N. Lebombo (Karoo) and the Paraná HPT rocks. These have been collectively termed the HPT group.

c. This figure illustrates two magma types from southern Karoo which appear to show characteristics in common with both LPT and HPT groups, but are probably most like the former.

d. The Deccan tholeiites are quite different from both LPT and HPT types, having a depletion in the more incompatible elements, more typical of MORB or OIB tholeiites. The strong depletion in Yb relative to Ti is most comparable with the HPT group.

Note: all analyses have been adjusted to give a PMN Yb of 5

discussion relates to its calculated value from the PMN diagrams, not the absolute concentration in ppm]. It was intended to compare tholeiites of similar MgO content to avoid differences resulting from fractionation, however this has not always been possible. In order to reduce the complication in the patterns caused by variable fractionation, the data have been renormalised by a factor which yields $(Yb)_N = 5$ (similar to Thompson *et al.*, 1983). This recalculation does not change the positions of the patterns by too much; most of the primitive mantle normalised Yb values are ~4 to 5.5 for the samples chosen.

The normalised patterns for the 4 regions of the Karoo, the Parana HPT and LPT, the Ferrar-Tasmania province, and the Antarctic area of Vestfjella, have been divided into two main groups; the LPT and HPT-type magmas. The LPT Group comprises the Parana LPT, Ferrar and Etendeka tholeiites (Fig. 6.5a). These three members are characterised by steep patterns (incompatible element enriched) with notable depletions in P, Ti and Sr. Significant depletions in Nb relative to K and La are noted in the Ferrar and Etendeka tholeiites; however, the Nb value for the Paraná LPT group is not similarly low.

It may be argued that the comparison between average Paraná LPT and Etendeka tholeiites is not valid, as these are thought to have undergone extensive AFC since leaving the mantle source (e.g. Mantovani *et al.*, 1985; Duncan *et al.*, 1987). Worth noting, however, is that in the case of the Ferrar-Tasmania province, superimposed fractionation, contamination, and alteration effects have not disguised the mantle source signature (Chapters 4 and 5). This has been tested for the Paraná LPT and Etendeka tholeiites by plotting the PMN patterns for the samples with the lowest $^{87}\text{Sr}/^{86}\text{Sr}$ compositions (Fig. 6.6). The results indicate that the compositions of the least contaminated-fractionated tholeiites possess the same signatures shown by the more evolved magmas, and it is concluded that the comparison made in Figure 6.5a is reasonable.

The HPT group (Fig. 6.5b), comprising the Paraná HPT, N. Lebombo, and Vestfjella, have flatter PMN patterns, and most elements are higher in abundance compared with the LPT rocks (i.e. the elements from Rb to Ti are all greater than 10 times PM, remembering that Yb_N has been fixed at 5 times PM). Although the P signature varies from depleted to enriched for this group (relative to Zr and Nd), Ti is always high relative to Yb. As with the LPT group, Nb varies from values similar to K and La, to less than K and La (although the low Nb in the N. Lebombo tholeiites does not approach the depletion observed in some of the LPT Group rocks).

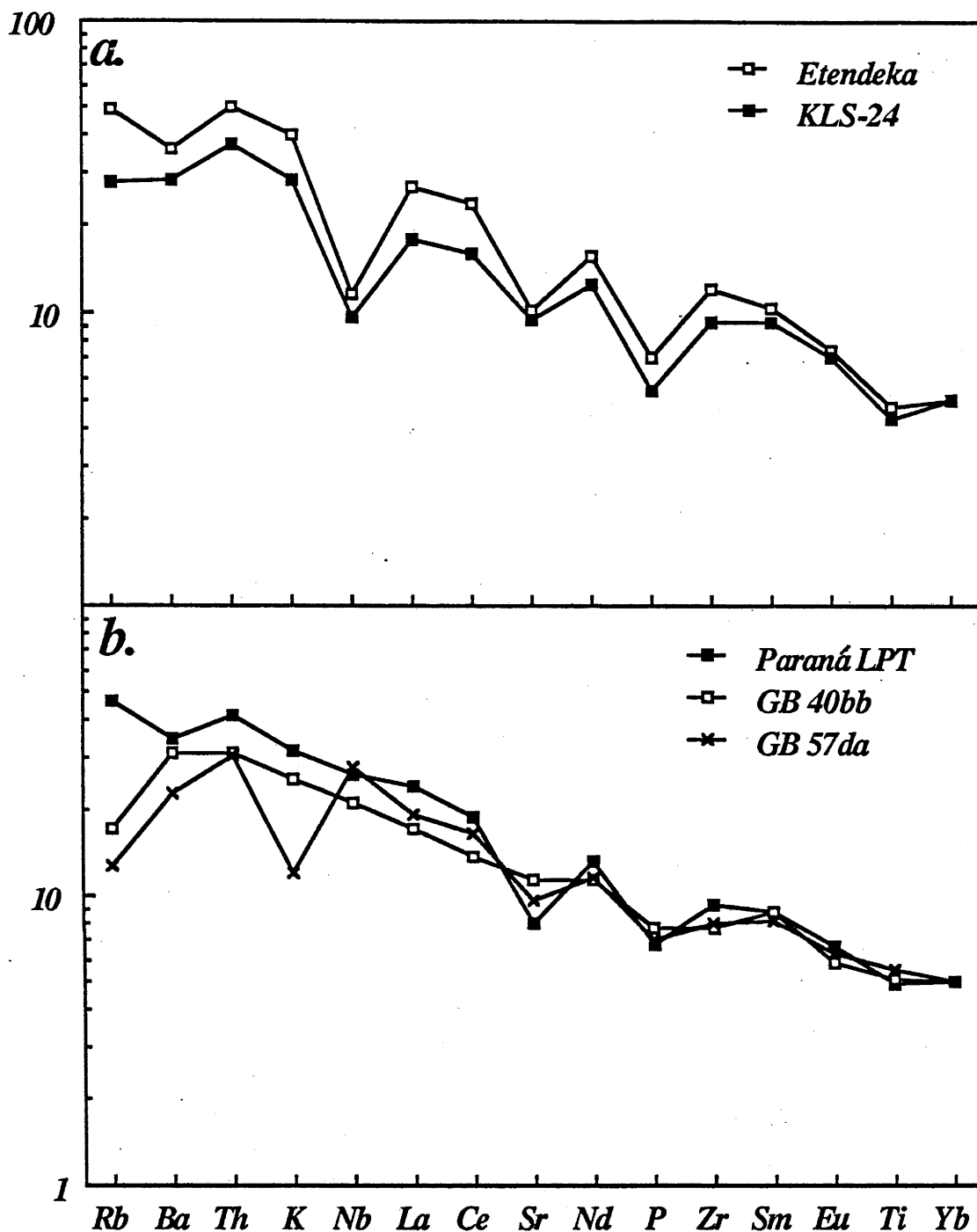


Fig. 6.6 Comparison between the primitive mantle normalised patterns (adjusted for $Yb_N = 5$) of the average compositions used in Figure 6.5, and the least contaminated tholeiites from a. the Etendeka subprovince of the Karoo, and b. the LPT group of the Paraná. Although particular depletions may not be as well developed in the lesser evolved tholeiites, the general pattern is still evident, indicating that much of the signature was developed early in the genesis of these basalts. The unusually low K in the Paraná tholeiite, GB 57da is possibly the result of alteration (?).

The tholeiites from three areas do not fit well into either the HPT or LPT subdivision. These include tholeiites from the Central area of the Karoo (represented by the most abundant magma-type, Lesotho), S. Lebombo, and the Deccan Traps. Although the two Karoo magma types have different abundances of trace elements, they have very similar PMN signatures (Fig. 6.5c). This is despite a large difference in the initial isotopic compositions of the samples used (Lesotho: $\epsilon_{Nd} \sim -2$, $^{87}Sr/^{86}Sr \sim 0.705$ cf. S. Lebombo: $\epsilon_{Nd} \sim -13$, $^{87}Sr/^{86}Sr \sim 0.7085$), and

implies that the sources of these two southern Karoo magma types were probably very similar (the difference in isotopic signature possibly resulting from the contamination suspected for the S. Lebombo rocks). In other words, if the S. Lebombo samples were contaminated with crust after leaving their mantle source (e.g. Hawkesworth *et al.*, 1983), then this has not destroyed the original PMN signature of these rocks (as noted above for the LPT group tholeiites). The two southern Karoo subprovinces are characterised by incompatible element enrichment and large depletions in Nb which are more typical of the LPT group; however, the small or negligible depletions in Sr and P are similar to the HPT tholeiites. A marked difference between the tholeiites from the two southern Karoo subprovinces and the HPT group, is the relationship between Ti and Yb; the HPT groups have high Ti/Yb which is not observed in the Lesotho and S. Lebombo tholeiites. The southern Karoo tholeiites therefore appear to have characteristics of the two groups, although their similarity with the LPT group is closer. Interestingly, two Central Karoo samples from Kraai River (KF-2 and KF-11) which plot just inside the LPT field defined in the Sr-Nd isotope diagram (Fig. 6.4), have PMN patterns between the LPT and southern Karoo types (Fig. 6.7). It appears that the source for the Kraai River tholeiites may have been a blend of the LPT and southern Karoo mantle compositions.

The Deccan tholeiites also have characteristics in their PMN signature which are not readily explained by either the HPT or LPT patterns. The limited availability of detailed trace element data for Deccan basalts has meant that the "mantle" endmember tholeiites (Nd and Sr signatures closest to MORB) could not be used in the comparison. The most complete data for a number of tholeiites is given in Paul *et al.* (1984); however, no isotopic data for these samples is given. The pattern of the average Deccan tholeiite given in Figure 6.5d has been compared with the limited trace element data from Mahoney *et al.* (1982) using the samples with the highest ϵ_{Nd} compositions, and in most respects, the average pattern used in figure 6.5d appears to be representative of the isotopically MORB-like endmember (not shown). One exception is the relationship between Rb and Ba; in the pattern shown Ba is depleted relative to Rb, whereas the reverse is true based on data from Mahoney *et al.* (1982). The depletions in Sr and P appear similar to the Paraná LPT tholeiites; however, these depletions are greater than those of the uncontaminated component of Mahoney *et al.* (1982). The high Ti relative to Yb in the Deccan pattern is only observed in the HPT tholeiites, and as small depletions in Sr and P are also frequently observed in the HPT Group, the Deccan basalts, if categorised, are probably best placed in the HPT Group. The significantly lower abundances of the more incompatible elements in the Deccan tholeiites, implies that the source for these magmas is more typical of oceanic basaltic source compositions, a feature also indicated by the isotopic signatures, and suggested to be similar to MORB by numerous previous workers (e.g. Allègre *et al.*, 1982; Fodor *et al.*, 1982; Cox and Hawkesworth, 1984, 1985; MacDougall, 1987).

It is conceded that the treatment of the trace element and isotopic data in the above discussions is grossly simplistic, and the consideration of contamination and alteration effects has been minimal. As a first order evaluation however, the broad subdivision above appears reasonable.

6.3 POSSIBLE PETROGENETIC IMPLICATIONS

Brooks and Hart (1978) noted two regional zones of different average Sr isotopic composition in the Mesozoic tholeiites of Gondwanaland, one comprising the Paraná, Karoo, Deccan, and Queen Maud Land areas, and the other comprising the Ferrar and Tasmanian tholeiites. They discounted crustal contamination as the main cause for their unusual signatures, and proposed that enriched lithospheric components were the source regions for the tholeiites. In the case of the Ferrar-Tasmanian zone, the lithospheric source was homogeneous; however, the sources involved in the production of the tholeiites in the second zone were considered to be heterogeneously enriched. Cox (1978) speculated on the role of subduction in the production of continental tholeiitic provinces of Gondwanaland, and suggested that it was important to discover if geochemical zonation occurred throughout Gondwanaland in keeping with his subduction hypothesis.

In Chapters 4 and 5, it was proposed that the Ferrar Group was derived from a mantle which had been contaminated by a crustal component during subduction; probably involving a well-mixed shale transported from the continental landmass. The zonation of chemical and isotopic signatures shown in Figure 6.8 may be related to the same subduction processes. It is speculated here, that the change from the extreme compositions noted in the Ferrar Group, through less extreme LPT-HPT hybrids (southern Karoo, and possibly Queen Maud Land), to HPT, and finally HPT-"MORB" (Deccan) tholeiites, can be interpreted as a progressive decrease in the contribution of the subducted components to the mantle source regions of the provinces more distant from the Pacific margin. This may be the result of a decrease in the amount of sediment transported to these areas; more likely however, is the possibility that fluids generated during subduction, may have pervaded the mantle region more effectively than the subducted sediment. The change in tholeiitic signatures (reflecting a change in their mantle source regions) may be related to the composition of fluids released from the subducting slab and sediments, and the distance to which the fluid fronts extended. The HPT tholeiites, being more distant from the Pacific margin, would therefore represent the products of a fluid enriched rather than sediment (or more likely melt) enriched mantle source (i.e. Ferrar), and the Deccan tholeiites may be derived from an almost unaffected mantle source.

If this model is tenable, then the HPT, and "transitional HPT" rocks should have PMN signatures similar to those of metasomatised mantle nodules. Data from xenoliths brought to the surface in kimberlite pipes in southern Africa have recently been reviewed by Duncan *et al.* (1984). Four different xenolith types were recognised on the basis of mineralogy, these include garnet peridotites (with no primary phlogopite), garnet phlogopite peridotite, phlogopite peridotite, and phlogopite K-richterite peridotite (Erlank *et al.*, 1982). The two garnet bearing xenoliths have different trace element enrichment styles compared with the garnet free xenoliths, and Duncan *et al.* (1984) have compared these different signatures with the compositions of the Karoo tholeiites. These authors proposed that the enrichment style in the garnet peridotites may be consistent with a source area for the Etendeka and Kraai River tholeiites (or LPT-group), while the style preserved in the garnet-free xenoliths was more akin to the Central Area, Nuanetsi and Lebombo magmas (or HPT-transitional to HPT-Group). Duncan *et al.* (1984)

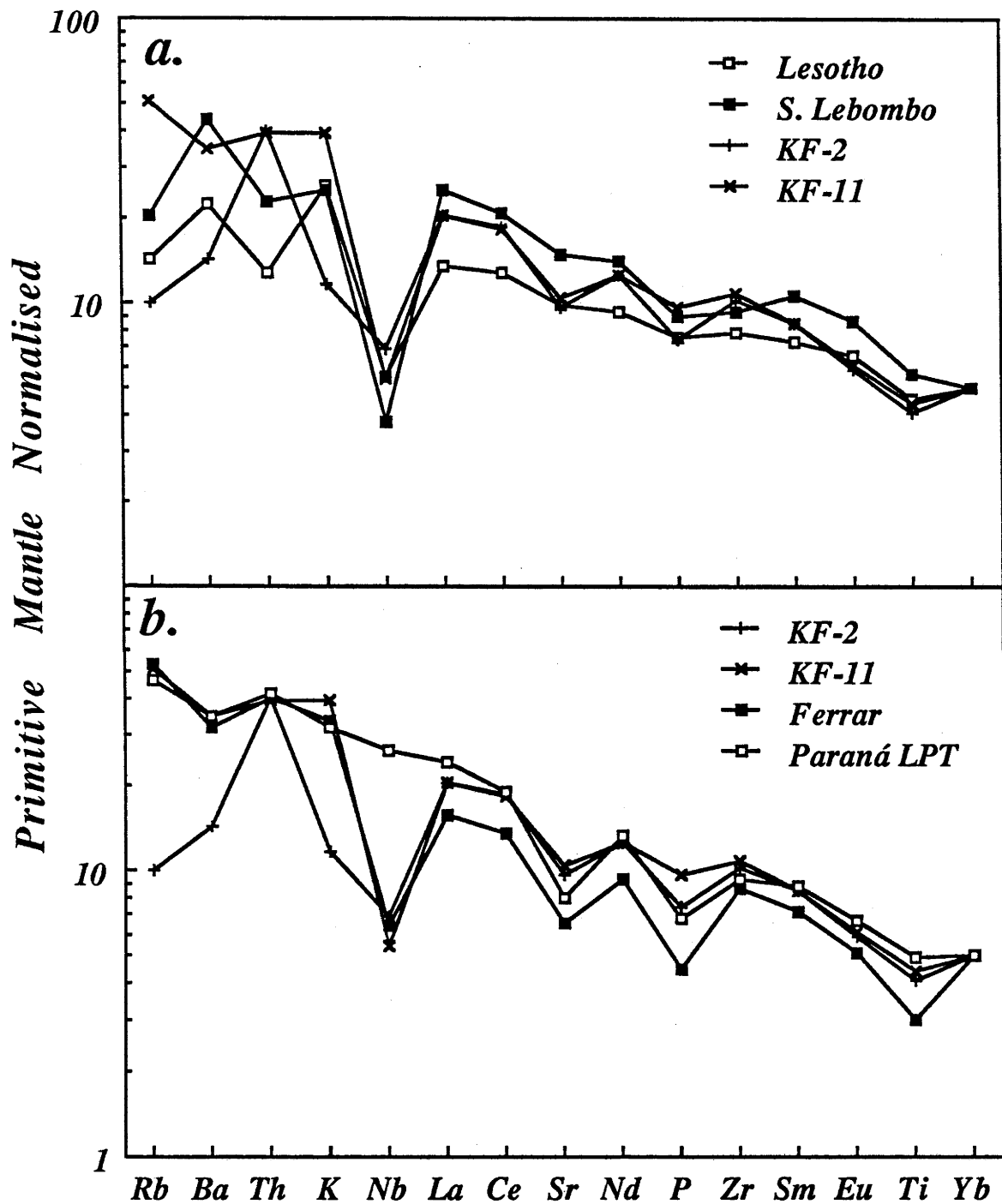


Fig. 6.7 Comparison between two Central Karoo samples from Kraai River and rocks more typical of the southern Karoo (a.) and LPT (b.) magma types.

concluded that the regional characteristics of the Karoo magmas were related to largescale differences in the styles of enrichment in the mantle source regions, whereas compositional differences within a particular subprovince were likely to be related to smaller scale mantle heterogeneities. It was emphasised that the particular xenoliths examined by Erlank *et al.* (1982) were too young to represent actual pieces of the Karoo magma source regions; however, similar enrichments at an earlier time would be consistent with the signatures observed in the Karoo rocks.

The proposed model involving subduction along the Pacific margin of Gondwanaland, would require the transport of materials derived from the slab (i.e. both fluids and sediments) over considerable distances (i.e. thousands of kilometers). Clearly, this is one of the most difficult aspects to account for in the proposed model. Similar models suggested for the source of the Columbia River Basalts (e.g. Carlson, 1984; Prestvik and Goles, 1985; Church, 1985) suggest that distances at least as great as 400 km may be involved (Church, 1985).

Much of the distance required may be achieved if the continent migrated over the area of enrichment. It is apparent that the Gondwana continents have traversed considerable distances over geological time. Although speculative, Donovan (1987) suggested that the continents may have been close to the equator during the Late Precambrian. At the time of emplacement of the dolerites, Tasmania and Antarctica were close to the southern pole (from the paleomagnetic data obtained by Irving, 1963 and Schmidt and McDougall, 1977). Therefore, there would have been considerable opportunity for Gondwanaland to override a contaminated mantle source produced by an earlier episode of subduction. This may be required for the source regions more distant from the Pacific margin of Gondwanaland (e.g. the Karoo), and the mechanics of the process by which such regional variation may occur remains unknown.

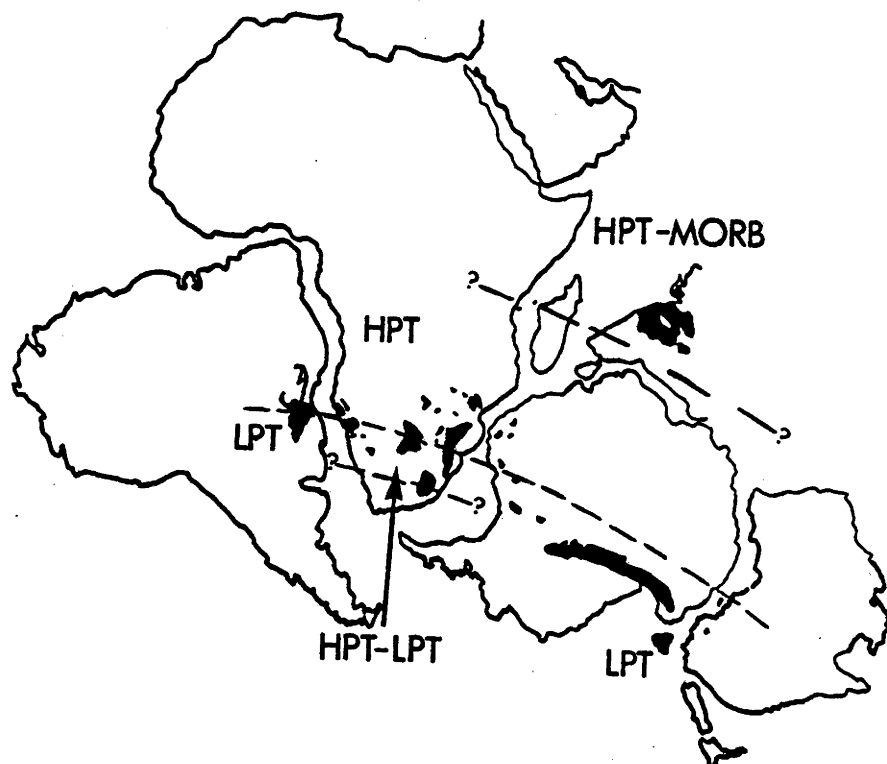


Fig. 6.8 Schematic representation of the geochemical zonation observed in the Mesozoic tholeiites of Gondwanaland. The major zones include the LPT and HPT provinces, with transitional LPT-HPT and possibly HPT-MORB areas.

CHAPTER 7

SYNTHESIS

During the Middle Jurassic, approximately 15,000 km³ of quartz tholeiitic liquid were emplaced into a sequence of essentially flat-lying Permo-Triassic sediments of Tasmania. In most cases, these magmas (~1200°C) quenched against their sedimentary hosts, preserving much of the original signature of the liquids. The uniformity of these chilled dolerites is remarkable, despite small differences in the fractionation history prior to emplacement (up to ~9 wt. %), and subsequent interaction with heated meteoric water.

During cooling, many of the thicker sheets (>~250-300 m) and dyke-like bodies (up to ~1 km or more wide) became differentiated, producing a large range in mineralogical and whole-rock compositions. The pyroxene compositions show progressive Fe-enrichment with increased differentiation, extending from very magnesium-rich orthopyroxenes in the chilled margins (up to En₈₃) to the ferroaugites in the most differentiated rocks (~Wo₄₅En₅). These ferroaugites are accompanied by exceptionally Fe-rich fayalites which have compositions of Fa₉₅.

Rocks with MgO contents greater than that observed in the chilled margins (~7 wt. %) are cumulates, dominated by early-formed pyroxenes and plagioclase. Rocks with MgO contents less than the chilled margins probably represent both liquids and cumulates. The difficulty in recognising true liquid compositions (away from chilled contacts) has made it impossible to obtain reasonable results for simple least-squares mixing calculations. A more hypothetical model has been presented, whereby the liquids produced during fractionation evolve to approximately 3 wt. % MgO, almost colinearly with the parent magma and cumulates. At MgO contents lower than this, a marked change in the fractionating assemblage occurs, and the subsequent liquids become enriched in SiO₂ and the more incompatible elements. The first part of the differentiation history is dominated by pyroxene fractionation, compared with plagioclase and minor phases towards the later stages.

The mechanism by which differentiation occurred remains debatable, and both crystal settling and *in situ* crystallization models can explain the chemical and mineralogical observations. If the arguments concerning the difficulties of crystal settling through a thermally convecting viscous fluid are proven correct, then it is more likely that *in situ* crystallization has been the dominant differentiation mechanism in the case of the Tasmanian Dolerites.

From their composition, the liquids emplaced in Tasmania during the Jurassic were not in equilibrium with typical mantle compositions. It is likely that at least some crustal-level fractionation had occurred prior to emplacement, judging from some aspects of the small range in composition observed between chilled contact rocks. Although calculation of more primitive magma compositions is non-unique, a possible primary magma has been calculated for the Tasmanian Dolerites (using the assemblage known to have caused some fractionation prior to emplacement, and a small amount of added olivine). Like the chilled margins, this composition has high SiO₂ and low concentrations of other major elements (e.g. FeO*, Na₂O, TiO₂ and

P_2O_5). If this calculated composition is reasonably representative of the true primary magma, it suggests that the mantle source may be somewhat depleted (i.e more depleted than an N-MORB composition); possibly a MORB source that has previously generated magma.

In addition to the remarkable geochemical uniformity of the emplaced magmas, the Nd and Pb isotopic compositions in the samples analysed show no detectable variation. In contrast, the Sr and O isotopic compositions display a wide range, at least part of which can be attributed to interaction with meteoric water.

The trace element and radiogenic isotopic compositions, show extraordinarily strong similarities to crustal rocks, and require the dominance of a crustal contaminant over any mantle signature. Difficulties arise in balancing the trace element abundances of the dolerite magma, for models in which the assimilation of crustal material is involved. Regardless of the type of tholeiitic endmember used, little incorporation of contaminant can be accommodated (particularly considering the likelihood of induced fractional crystallization). The results of reducing the amount of assimilation, are to 1. produce trace element signatures with less similarity to the chilled margin rocks, and 2. require the contaminant to possess unrealistic isotopic compositions. Unless a large volume of basaltic material can be generated with exceptionally low trace element abundances (for all elements used in the discussion), assimilation models appear unlikely.

Many of the difficulties experienced with crustal-level assimilation are avoided if a small percentage (3% or less) of crustal contaminant is introduced into a depleted mantle source (3% calculated using NMORB source, less for a more depleted composition). The isotopic signatures required of the contaminant are less extreme compared with assimilation models, and the crustal signature imposed on the mantle source would be inherited by magmas derived from it by partial melting.

The unusual trace element and isotopic signatures preserved in the Tasmanian tholeiites have been compared with Jurassic tholeiites from the Ferrar Province of Antarctica, and other localities in southern Australia. The results are conclusive, and demonstrate the enormity of a single, remarkably homogeneous tholeiitic province. The extraordinary uniformity of these tholeiites (Ferrar-Tasmania province), provides problems in both crustal-assimilation and source contamination models. In the case of source contamination, it is possible that materials derived from the Pacific margin of Gondwanaland were originally of uniform composition, and were further homogenised during subduction and partial melting. Apart from the difficulties in modelling crustal assimilation, the requirement for the contaminant to have a uniform composition, and be added in an exceptionally reproducible way, is considered less likely.

The enormity of this linear belt of unusual tholeiites, approximately parallel to the ancient Pacific margin of Gondwanaland, leads to speculation of the signatures observed in other continental tholeiites of this supercontinent. Although treated in a simplistic manner, it appears that several zones of broadly similar signature can be identified for Antarctic (Ferrar-Tasmania, and Dronning Maud Land), Africa, South America and possibly the Deccan traps of India. It has been suggested here, that these sub-parallel zones of different signature may be related to the same subduction processes which generated the Ferrar-Tasmania province. With an increase in

the distance from the Pacific margin, the tholeiites (and by inference, their sources), yield signatures which become less like crustal rocks, and more like that of metasomatised mantle xenoliths. It is possible that unlike the crustal component, fluids released from the slab and sediments during subduction, may pervade the mantle for considerable distances. Certainly, the mechanism by which transport of subduction-related components occurs over distances of thousands of kilometres requires further speculation. Finally, it will be most interesting to see the results of more detailed work in areas close to the boundaries between different magma types. These areas may provide additional clues to the causes of the change in the source regions which appear to be surprisingly abrupt, at least in some locations.

BIBLIOGRAPHY

- ABBEY, S. (1983) Studies in "standard samples" of silicate rocks and minerals 1969-1982. *Geol. Surv. Can. Pap.* 83-115
- AHRENS, L.H. (1965) Some observations on the uranium and thorium distributions in accessory zircon from granitic rocks. *Geochim. Cosmochim. Acta.* 29; 711-716.
- ALEXANDER, P.O. & GIBSON, I.L. (1977) Rare earth abundances in Deccan Trap basalts. *Lithos* 10; 143-147.
- ALEXANDER, P.O. & PAUL, D.K. (1977) Geochemistry and strontium isotopic composition of basalts from the eastern Deccan volcanic province, India. *Mineral. Mag.* 41; 165-172.
- ALLEGRE, C.J., DUPRE, B., RICHARD P., ROUSSEAU, D. & BROOKS, C. (1982) Subcontinental versus suboceanic mantle, II. Nd-Sr-Pb isotopic comparison of continental tholeiites with mid-ocean ridge tholeiites, and the structure of the continental lithosphere. *Earth Planet. Sci. Lett.* 57; 25-34.
- ATKINS, F.B. (1969) Pyroxenes of the Bushveld intrusion, South Africa. *J. Petrol.* 10; 222-249.
- BANKS M.R. (1962a) Silurian and Devonian systems. In: *Geology of Tasmania*. Spry, A. & Banks M. R. (eds). *J. Geol. Soc. Aust.* 9; 177-187.
- BANKS, M.R. (1962b) Ordovician System. In: *Geology of Tasmania*. Spry, A. & Banks, M. R. (eds). *J. Geol. Soc. Aust.* 9; 147-176.
- BANKS, M.R. (1962c) Cambrian System. In: *Geology of Tasmania*. Spry, A. & Banks, M. R. (eds). *J. Geol. Soc. Aust.* 9; 127-145.
- BANKS, M.R. (1973) General Geology. In: *The Lake Country of Tasmania*. Royal Society of Tasmania.; 25-34.
- BANKS, M.R., GREEN, D.H. MCDUGALL, I., HERGT, J.M. & STEVENS, S. (1987) Jurassic basalts from Tasmania.(Manuscript in preparation).
- BARNES, S.J. (1986) The effect of trapped liquid crystallization on cumulus mineral compositions in layered intrusions. *Contrib. Mineral. Petrol.* 93; 524-531.
- BASALTIC VOLCANISM STUDY PROJECT (1981) *Basaltic Volcanism on the Terrestrial Planets*. Pergamon Press, Inc, New York. pp 1286.
- BELLIENI, G., BROTZU, P., COMIN-CHIARAMONTI, P., ERNESTO, M., MELFI, A., PACCA, I. G. & PICCIRILLO, E M. (1984) Flood basalt to rhyolite suites in the Southern Paraná Plateau (Brazil): paleomagnetism, petrogenesis and geodynamic implications. *J. Petrol.* 25; 579-618.
- BELLIENI, G., COMIN-CHIARAMONTI, P., MARQUES, L. S., MELFI, A.J., NARDY, A.J.R., PAPTRECHAS, C., PICCIRILLO, E.M., ROISENBERG, A. & STOLFA, D. (1986) Petrogenetic aspects of acid and basaltic lavas from the Paraná Plateau (Brazil): geological, mineralogical and petrochemical relationships. *J. Petrol.* 27; 915-944.
- BOSE, M.K. (1983) The Deccan Volcanic Province. *Indian J. Earth Sci. Spec. Issue, The Solid Earth.*; 45-53.
- BOWEN, N.L. (1928) *The Evolution of the Igneous Rocks*. General Publishing Co. Ltd., Ontario, 334pp.
- BREWER, T.S., PALACZ, Z. & HAWKESWORTH, C.J. (1987) Mesozoic tholeiites from Coats

Land and Dronning Maud Land, Antarctica: further pieces in the Gondwanaland jigsaw. *Terra Cognita*. 7; 604.

- BRISTOW, J.W. & SAGGERSON, E.P. (1983) A general account of Karoo vulcanicity in southern Africa. *Geol. Rund.* 72; 1015-1060.
- BROOKS, C. & HART, S.R. (1978) Rb-Sr mantle isochrons and variations in the chemistry of Gondwanaland's lithosphere. *Nature* 271; 220-223.
- BROOKS, C. & JAMES, D.E. (1978) Strontium and oxygen isotopes and the case for heterogeneous mantle. *Geol. Soc. Am. Abs. Prog.* 10; 372.
- BROWN, G.M. (1957) Pyroxenes from the early and middle stages of fractionation of the Skaergaard intrusion, Eastern Greenland. *Mineral. Mag.* 31; 511-543.
- BROWN, G.M. & VINCENT, E.A. (1963) Pyroxenes from the late stages of fractionation of the Skaergaard intrusion, East Greenland. *J. Petrol.* 4; 175-197.
- BULLARD, E.C., EVERETT, J.E. & SMITH, A.G. (1965) The fit of the continents around the Atlantic. *Phil. Trans. Royal Soc. Lond.* 258A; 41-51.
- BURKE, W.H., DENISON, R.E., HETHERINGTON, E.A., KOEPNICK, R.B., NELSON, H.F. & OTTO, J.B. (1982) Variation of seawater $^{87}\text{Sr}/^{86}\text{Sr}$ throughout Phanerozoic time. *Geology* 10; 516-519.
- BUTTERMAN, W.C. & FOSTER, W.R. (1967) Zircon stability and the $\text{ZrO}_2\text{-SiO}_2$ phase diagram. *Am. Mineral.* 52; 880-885.
- CAMPBELL, I.H. (1978) Some problems with the cumulus theory. *Lithos* 11; 311-323.
- CAMPBELL, I.H. (1985) The difference between oceanic and continental tholeiites: a fluid dynamic explanation. *Contrib. Mineral. Petrol.* 91; 37-43
- CAMPBELL, I.H. & BORLEY, G.D. (1974) The geochemistry of pyroxenes from the lower layered series of the Jimberlana Intrusion, Western Australia. *Contrib. Mineral. Petrol.* 47; 281-297.
- CAMPBELL, I.H. & NOLAN, J. (1974) Factors affecting the stability field of Ca-poor pyroxene and the origin of the Ca-poor minimum in Ca-rich pyroxenes from tholeiitic intrusions. *Contrib. Mineral. Petrol.* 48; 205-219.
- CAMPBELL, I.H., ROEDER, P.L. & DIXON, J.M. (1978) Crystal buoyancy in basaltic liquids and other experiments with a centrifuge furnace. *Contrib. Mineral. Petrol.* 67; 269-377.
- CAREY, S.W. (1955) Wegener's South America-Africa assembly, fit or misfit? *Geol. Mag.* 92; 196-200.
- CAREY, S.W. (1961a) The isostrat, a new technique for the analysis of the structure of the Tasmanian dolerite. In: *Dolerite: a symposium*. Uni. Tas.; 130-164.
- CAREY, S.W. (1961b) Relation of basic intrusions to thickness of sediments. In: *Dolerite: a symposium*. Uni. Tas.; 165-169.
- CARLSON, R.W. (1984) Isotopic constraints on Columbia River flood basalt genesis and the nature of the subcontinental mantle. *Geochim. Cosmochim. Acta.* 48; 2357-2372.
- CARMICHAEL, I.S.E., NICHOLLS, J. & SMITH, A.L. (1970) Silica activity in igneous rocks. *Am. Mineral.* 55; 246-263.
- CATANZARO, E.J., MURPHY, T.J., SHIELDS, W.R. & GARNER, E.L. (1968) Absolute isotope abundance ratios of common, equal atom, and radiogenic lead isotopic standards. *J. Res.*

Nat. Bur. Stand. (US.) 72A; 261-267.

- CHAPPELL, B.W. (1979) Granites as images of their source rocks. *Geol. Soc. Am. Abs. Prog.* 11; 400.
- CHEN, C.F. & TURNER, J.S. (1980) Crystallization in a double-diffusive system. *J. Geophys. Res.* 85; 2537-2593.
- CHURCH, S.E. (1985) Genetic interpretation of lead-isotopic data from the Columbia River Basalt Group, Oregon, Washington and Idaho. *Geol. Soc. Am. Bull.* 96; 676-690.
- CLAGUE, D.A. & FREY, F.A. (1982) Petrology and trace element geochemistry of the Honolulu Volcanics, Oahu: implications for the oceanic mantle below Hawaii. *J. Petrol.* 23; 447-504.
- CLARKE, M.J. & BANKS, M.R. (1975) The stratigraphy of the lower (Permo-Carboniferous) parts of the Parmeener Super-Group, Tasmania. In: *Gondwana Geology*. A. N. U. Press; 453-467.
- CLAYTON, R.N. & MAYEDA, T.K. (1963) The use of bromine pentafluoride in the extraction of oxygen from oxides and silicates for isotopic analysis. *Geochim. Cosmochim. Acta.* 27; 43-52.
- CLEMENTS, S. & COMPSTON, W. (1972) The design and performance of a mass spectrometer using beam transport theory. *Int. J. Mass Spectrom. Ion Phys.* 10; 323-342.
- COCKER, J.D. (1982) Rb-Sr geochronology and Sr isotopic composition of Devonian granitoids, eastern Tasmania. *J. Geol. Soc. Aust.* 29; 139-158.
- COHEN, R.S. & O'NIONS, R.K. (1982a) The lead, neodymium and strontium isotopic structure of ocean ridge basalts. *J. Petrol.* 23; 299-324.
- COHEN, R.S. & O'NIONS, R.K. (1982b) Identification of recycled continental material in the mantle from Sr, Nd and Pb isotope investigations. *Earth Planet. Sci. Lett.* 61; 73-84.
- COMPSTON, W., KINNY, P.D., WILLIAMS, I.S. & FOSTER, J.J. (1986) The age and Pb loss behaviour of zircons from the Isua supracrustal belt as determined by ion microprobe. *Earth. Planet. Sci. Lett.* 80; 71-81.
- COMPSTON, W., MCDUGALL, I. & HEIER, K.S. (1968) Geochemical comparison of the Mesozoic basaltic rocks of Antarctica, South Africa, South America and Tasmania. *Geochim. Cosmochim. Acta.* 32; 129-149.
- COMPSTON, W., WILLIAMS, I.S. & MEYER, C. (1984) U-Pb geochronology of zircons from Lunar Breccia 73217 using a sensitive high mass-resolution ion microprobe. *Proc. XIV Lunar Planet. Sci. Conf; J. Geophys. Res.* 89 Supp.; B525-B534.
- COX, K.G. (1978) Flood basalts, subduction and the breakup of Gondwanaland. *Nature* 274; 47-49.
- COX, K.G. (1980) A model for flood basalt vulcanism. *J. Petrol.* 21; 629-650.
- COX, K.G., BELL, J.D. & PANKHURST, R.J. (1979) *The Interpretation of Igneous Rocks*. George Allen & Unwin, Ltd, London; 450pp.
- COX, K.G. & BRISTOW, J.W. (1984) The Sabie River basalt formation of the Lebombo Monocline and South-east Zimbabwe. *Spec. Publ. geol. Soc. S. Afr.* 13; 125-147.
- COX, K.G., DUNCAN, A.R., BRISTOW, J.W., TAYLOR, S.R. & ERLANK, A.J. (1984) Petrogenesis of the basic rocks of the Lebombo. *Spec. Publ. geol. Soc. S. Afr.* 13; 149-171.

- COX, K.G. & HAWKESWORTH C.J. (1984) Relative contribution of crust and mantle to flood basalt magmatism, Mahabaleshwar area, Deccan Traps. *Phil. Trans. Royal Soc. Lond.* **A310**; 627-641.
- COX, K.G. & HAWKESWORTH C.J. (1985) Geochemical stratigraphy of the Deccan Traps at Mahabaleshwar, Western Ghats, India, with implications for open system magmatic processes. *J. Petrol.* **26**; 355-377.
- COX, K.G., MACDONALD, R. & HORNING, G. (1967) Geochemical and petrographic provinces in the Karoo Basalts of southern Africa. *Am. Mineral.* **52**; 1451-1474.
- CRADDOCK, C. (1982) Antarctica and Gondwanaland - review paper. In: *Antarctic Geoscience*. Craddock, C. (ed). Univ. Wisconsin Press, ?.
- CRADDOCK, C. (1975) Tectonic evolution of the Pacific margin of Gondwanaland. *Gondwana Geology*. Campbell, K. S. W. (ed), A. N. U. Press; 609-618.
- CRAIG, H. (1961) Isotopic variations in meteoric waters. *Science* **133**; 1702-1703.
- DE PAOLO, D.J. (1981) Trace element and isotopic effects of combined wallrock assimilation and fractional crystallization. *Earth Planet. Sci. Lett.* **53**; 189-202.
- DE PAOLO, D.J. & WASSERBERG, G.J. (1979) Petrogenetic mixing models and Nd-Sr isotopic patterns. *Geochim. Cosmochim. Acta.* **43**; 615-627.
- DEVEY, C.W. & COX, K.G. (1987) Relationships between crustal contamination and crystallisation in continental flood basalt magmas with special reference to the Deccan Traps of the Western Ghats, India. *Earth Planet. Sci. Lett.* **84**; 59-68.
- DIVAKARARAO, V., SUBBARAO, M.V. & ASHALATHA, B. (1984) Major igneous episodes of the Indian sub-continent: geochemistry and significance. *Geoph. Res. Bull.* **22**; 89-104.
- DONOVAN, S.K. (1987) The fit of the continents in the late Precambrian. *Nature* **327**; 139-141.
- DUNCAN, A.R., ERLANK, A.J. & MARSH, J.S. (1984) Regional geochemistry of the Karoo Igneous Province. *Spec. Publ. Geol. Soc. S. Afr.* **13**; 355-388.
- DUNCAN, A.R., ERLANK, A.J. & SMITH, H.S. (1987) Crustal contamination in the petrogenesis of some Karoo basalts - implications for other continental basalt provinces. *Geol. Soc. Am. Abs. Prog.* **19**; 374.
- DUPRE, B. & ALLEGRE, C.J. (1980) Pb-Sr-Nd isotope correlation and the chemistry of the North Atlantic Mantle. *Nature* **286**; 17-22.
- DUPUY, C. & DOSTAL, J. (1984) Trace element geochemistry of some continental tholeiites. *Earth Planet. Sci. Lett.* **67**; 61-69.
- DUPUY, C., VIDAL, P., BARSCZUS, H. G. & CHAUVEL, C. (1987) Origin of basalts from the Marquesas Archipelago (south central Pacific Ocean): isotope and trace element constraints. *Earth. Planet. Sci. Lett.* **82**; 145-152.
- DU TOIT, A.L. (1937) *Our Wandering Continents; an hypothesis of continental drifting*. Oliver & Boyd Ltd., Edinburgh.
- EALLES, H.V., MARSH, J.S. & COX, K.G. (1984) The Karoo igneous province: an introduction. *Spec. Publ. Geol. Soc. S.Afr.* **13**; 1-26.
- EDWARDS, A.B. (1942) Differentiation of the dolerites of Tasmania. *J. Geol.* **50**; 451-480 and 579-610.

- ELLIOT, D.H. (1972) Major oxide chemistry of the Kirkpatrick Basalts, Central Transantarctic Mountains. In: *Antarctic Geology and Geophysics*. Adie, R. J. (ed). Universitetsforlaget, Oslo; 414-418.
- ELLIOT, D.H. (1976) The tectonic setting of the Jurassic Ferrar Group, Antarctica. In: *Proc. Symp. on "Andean and Antarctic Volcanology Problems"*. I.A.V.C.E.I.; 357-372.
- ELLIOT, D.H. (1987) Jurassic tholeiites of Antarctica: tectonic setting. *Geol. Soc. Am. Abs. Prog.* 19; 375.
- ELTHON, D. (1984) Plagioclase buoyancy in oceanic basalts: chemical effects. *Geochim. Cosmochim. Acta.* 48; 753-768.
- ERLANK, A. J., ALLSOP, H.L., HAWKESWORTH, C.J. & MENZIES, M.A. (1982) Chemical and isotopic characterization of upper mantle metasomatism in periodite nodules from the Bulfontein Kimberlite. *Terra Cognita* 2; 261-263.
- ERLANK, A.J. & HOFMEYR, P.K. (1968) K/Rb ratios in mesozoic tholeiites from Antarctica, Brazil and India. *Earth Planet. Sci. Lett.* 4; 33-38.
- ERLANK, A.J., MARSH, J.S., DUNCAN, A.R., MILLER, R.MCG., HAWKESWORTH, C.J., BETTON, P.J. & REX, D.C. (1984) Geochemistry and petrogenesis of the Etendeka volcanic rocks from SWA/Namibia. *Spec. Publ. geol. Soc. S. Afr.* 13; 195-245.
- EVERNDEN, J.F. & RICHARDS, J.R. (1962) Potassium-argon ages in eastern Australia. *J. Geol. Soc. Aust.* 9; 1-50.
- EVISON, F.F., INGHAM, C.E., ORR, R.H. & LE FORT, J.H. (1960) Thickness of the Earth's crust in Antarctica and the surrounding oceans. *Geophys. J.* 3; 289-306.
- FAURE, G., BOWMAN, J.R. & ELLIOT, D.H. (1979) The initial $^{87}\text{Sr}/^{86}\text{Sr}$ ratios of the Kirwan Volcanics of Dronning Maud Land: comparison with Kirkpatrick Basalt, Transantarctic mountains. *Chem. Geol.* 26; 77-90.
- FAURE, G., BOWMAN, J.R., ELLIOT, D.H. & JONES, L.M. (1974) Strontium isotope composition and petrogenesis of the Kirkpatrick Basalt, Queen Alexandra Range, Antarctica. *Contrib. Mineral. Petrol.* 48; 153-169.
- FAURE, G. & ELLIOT, D.H. (1971) Isotope composition of strontium in Mesozoic basalt and dolerite from Dronning Maud Land. *Br. Antarct. Surv. Bull.* 25; 23-27.
- FAURE, G., HILL, R.L., JONES, L.M. & ELLIOT, D.H. (1972) Isotope composition of strontium and silica content of Mesozoic basalt and dolerite from Antarctica. In: *Antarctic Geology and Geophysics*. Adie, R. J. (ed). Universitetsforlaget, Oslo; 617-624.
- FAURE, G., PACE, K.K. & ELLIOT, D.H. (1982) Systematic variations of $^{87}\text{Sr}/^{86}\text{Sr}$ ratios and major element concentrations in the Kirkpatrick Basalt of Mt. Fulla, Queen Alexandra Range, Transantarctic Mountains. In: *Antarctic Geoscience*. Craddock, C. (ed). University of Wisconsin, Madison, Wisc.; 715-723.
- FERRAR, H.T. (1907) Report on the field geology of the region explored during the "Discovery" Antarctic Expedition 1901-4. *Natl. Hist. Rep. Nat. Antarct. Exped. 1901-4.* 1; 1-100.
- FLANAGAN, F.J. (1984) Three USGS mafic rock reference samples, W-2, DNC-1, and BIR-1. *US Geol. Surv. Bull.* 1623.
- FLEMING, T.H. & ELLIOT, D.H. (1987) Jurassic tholeiites of Antarctica: geochemistry. *Geol. Soc. Am. Abs. Prog.* 19; 377.
- FODOR, R.V., BAUER, G.R., JACOBS, R.S. & BORNHORST, T.U. (1987) Kahoolawe Island,

Hawaii: tholeiitic, alkalic, and unusual hydrothermal (?) "enrichment" characteristics. *J. Volcanol. Geoth. Res.* 31; 171-176.

- FODOR, R.V., CORWIN, C. & ROISENBERG, A. (1985a) Petrology of the Serra Geral (Paraná) continental flood basalts, southern Brazil: crustal contamination, source material, and South Atlantic magmatism. *Contrib. Mineral. Petrol.* 91; 54-65.
- FODOR, R.V., CORWIN, C. & SIAL, A.N. (1985b) Crustal signatures in the Serra Geral flood-basalt province, southern Brazil: O- and Sr-isotope evidence. *Geology* 13; 763-765.
- FORD, A.B. & HIMMELBERG, G.R. (1987) Geology and crystallization of the Dufek intrusion. In: *Geology of Antarctica*. Tingey, R. J. (ed). Oxford Uni. Press, (in prep).
- FREY, F.A., GREEN, D.H. & ROY, S.D. (1978) Integrated models of basalt petrogenesis: a study of quartz tholeiites to olivine melilitites from south eastern Australia utilizing geochemical and experimental petrological data. *J. Petrol.* 19; 463-513.
- FURNES, H., NEUMANN, E.R. & SUNDVOLL, B. (1982) Petrology and geochemistry of Jurassic basalt dykes from Vestfjella, Dronning Maud Land, Antarctica. *Lithos* 15; 295-304.
- GHOSE, M.C. (1976) Composition and origin of Deccan basalts. *Lithos* 9; 65-73.
- GLAZNER, A.F. (1984) Activities of olivine and plagioclase components in silicate melts and their application to geothermometry. *Contrib. Mineral. Petrol.* 88; 260-268.
- GOLDSTEIN, S.L., O'NIONS, R.K. & HAMILTON, P.J. (1984) A Sm-Nd isotopic study of atmospheric dusts and particulates from major river systems. *Earth Planet. Sci. Lett.* 70; 221-236.
- GRAHAM, C.M. & HARMON, R.S. (1983) Stable isotope evidence on the nature of crust-mantle interactions. In: *Continental Basalts and Mantle Xenoliths*. Hawkesworth, C.J. & Norry, M.J. (eds). Shiva Ltd.; 20-45.
- GREEN, D.H. (1973) Experimental melting studies on a model upper mantle composition at high pressure under water-saturated and water-unsaturated conditions. *Earth Planet. Sci. Lett.* 19; 37-53.
- GREEN, D.H. (1976) Experimental testing of "equilibrium" partial melting of peridotite under water-saturated high pressure conditions. *Can. Mineral.* 14; 255-268.
- GRIFFIN, W.L. & O'REILLY, S.Y. (1987) Is the Moho the crust-mantle boundary? *Geology* 15; 241-244.
- GRINDLEY, G.W. (1963) The geology of the Queen Alexandra Range, Beardmore Glacier, Ross Dependency, Antarctica; with notes on the correlation of Gondwana Sequences. *N.Z. J. Geol. Geophys.* 6; 307-347.
- GUNN, B.M. (1962) Differentiation in Ferrar Dolerites, Antarctica. *N.Z. J. Geol. Geophys.* ?; 820-863.
- GUNN, B.M. (1965) K/Rb and K/Ba ratios in Antarctic and New Zealand tholeiitic and alkali basalts. *J. Geophys. Res.* 70; 6241-6247.
- GUNN, B.M. (1966) Modal and element variation in Antarctic tholeiites. *Geochim. Cosmochim. Acta.* 30; 881-920.
- GUNN, B.M. & WARREN, G. (1962) Geology of Victoria Land between the Mawson and Mulock Glaciers, Antarctica. *Bull. N.Z. Geol. Serv.* 71; 1-157.

- HALE, G.E. (1962) Triassic System. In: *Geology of Tasmania*. Spry, A. & Banks, M. R. (eds.); 217-231.
- HARLAND, W.B., COX, A.V., LLEWELLYN, P.G., PICKTON, C.A.G., SMITH, A.G. & WALTERS, R. (1982) *A Geological Time Scale*. Cambridge University Press.
- HARRINGTON, H.J. & SPEDEN, I.G. (1962) Section through the Beacon Sandstone at Beacon Heights West, Antarctica. *N.Z. J. Geol. Geophys.* 5; 707-717.
- HART, S.R. (1984) A large-scale isotope anomaly in the southern hemisphere mantle. *Nature* 309; 753-757.
- HAWKESWORTH, C.J., ERLANK, A.J., MARSH, J.S., MENZIES, M.A. & VAN CALSTEREN, P. (1983) Evolution of the continental lithosphere: evidence from volcanics and xenoliths in southern Africa. In: *Continental Basalts and Mantle Xenoliths*. Hawkesworth, C.J and Norry, M.J. (eds). Shiva Ltd.; 111-138.
- HAWKESWORTH, C.J., MANTOVANI, M.S.M., PEATE, D., WRIGHT, D.W., PALACZ, Z. & VAN CALSTEREN, P W. (1987) Magmatic processes in the Paraná. *Terra Cognita* 7; 611.
- HAWKESWORTH, C.J., MANTOVANI, M.S.M., TAYLOR, P.N. & PALACZ, Z. (1986) Evidence from the Paraná of south Brazil for a continental contribution to Dupal basalts. *Nature* 322; 356-359.
- HAWKESWORTH, C.J., MARSH, J.S., DUNCAN, A.R., ERLANK, A.J. & NORRY, M.J. (1984) The role of continental lithosphere in the generation of the Karoo volcanic rocks: evidence from combined Nd- and Sr-isotope studies. *Spec. Publ. geol. Soc. S. Afr.* 13; 341-354.
- HEIER, K.S., COMPSTON, W. & MCDUGALL, I. (1965) Thorium and uranium concentrations, and the isotopic composition of strontium in the differentiated Tasmanian dolerites. *Geochim. Cosmochim. Acta* 29; 643-659.
- HERMANTO, M.R. (1985) Unpublished MSc. Thesis. University of Tasmania.
- HESS, H.H. (1949) Chemical composition and optical properties of common clinopyroxenes, Part I. *Am. Mineral.* 34; 621-666
- HOEFS, J., FAURE, G. & ELLIOT, D.H. (1980) Correlation of $\delta^{18}\text{O}$ and initial $^{87}\text{Sr}/^{86}\text{Sr}$ ratios in Kirkpatrick Basalt on Mt. Falla, Transantarctic Mountains. *Contrib. Mineral. Petrol.* 75; 199-203.
- HOFMANN, A.W. & HART, S.R. (1978) An assessment of local and regional isotopic equilibrium in the mantle. *Earth Planet. Sci. Lett.* 38; 44-62.
- HOFMANN, A.W., JOCHUM, K.P., SEUFERT, M. & WHITE, W.M. (1986) Nb and Pb in oceanic basalts: new constraints on mantle evolution. *Earth Planet. Sci. Lett.* 79; 33-45.
- HUGHES, S.S., SCHMITT, R.A., WANG, Y.L. & WASSERBURG, G.J. (1986) Trace element and Sr-Nd isotopic constraints on the compositions of lithospheric primary sources of Serra Geral continental flood basalts, southern Brazil. *Geochem. J.* 20; 173-189.
- HUNTER, R.H. & SPARKS, R.S.J. (1987) The differentiation of the Skaergaard intrusion. *Contrib. Mineral. Petrol.* 95; 451-461.
- HUPPERT, H.E. & SPARKS, R.S.J. (1985) Cooling and contamination of mafic and ultramafic magmas during ascent through continental crust. *Earth Planet. Sci. Lett.* 74; 371-386.
- HUPPERT, H.E., SPARKS, R.S.J., WILSON, J.R. & HALLWORTH, M.A. (1986) Cooling and crystallization at an inclined plane. *Earth Planet. Sci. Lett.* 79; 319-328.
- IRVINE, T.N. (1980) Infiltration metasomatism, adcumulus growth, and double-diffusive

fractional crystallization in the Musk ox intrusion and other layered intrusions. In: *Physics of Magmatic Processes*. Hargraves, R. B. (ed). Princeton Univ. Press.; 325-383.

- IRVINE, T.N. (1986) Layering and related structures in the Duke Island and Skaergaard intrusions: similarities, differences and origins. In: *Origins of Igneous Layering*. Parsons, I. (ed), D. Reidel Pub. Co. Holland.; 185-245.
- IRVING, E. (1963) Palaeomagnetism of the Narrabeen. *J. Geophys. Res.* **68**; 2283-2287.
- ITO, E., WHITE, W.M. & GOPEL, C. (1987) The O, Sr, Nd and Pb isotope geochemistry of MORB. *Chem. Geol.* **62**; 157-176.
- JAEGER, J.C. & GREEN, R. (1961) A cross-section of a tholeiite sill. In: *Dolerite: a symposium*. Uni. Tas., 26-37.
- JAEGER, J.C. & JOPLIN, G.A. (1955) Rock magnetism and the differentiation of dolerite sill. *Geol. Soc. Aust.* **2**; 1-19.
- JAQUES, A.L. & GREEN, D.H. (1980) Anhydrous melting of periodite at 0-15 Kb pressure and the genesis of tholeiitic basalts. *Contrib. Mineral. Petrol.* **73**; 287-310.
- JOPLIN, G.A. (1961) The problem of the quartz dolerites: some significant facts concerning mineral volume, grain size and fabric. *Pap. Proc. Royal Soc. Tas.* **91**; 129-142.
- KISS, E. (1977) Rapid potentiometric determination of the iron oxidation state in silicates. *Anal. Chim. Acta.* **89**; 303-314.
- KRISHNAMURTHY, P. & COX, K.G. (1977) Picrite basalts and related lavas from the Deccan Traps of western India. *Contr. Mineral. Petrol.* **62**; 53-75.
- KRISHNAMURTHY, P. & UDAS, G.P. (1981) Regional geochemical characters of the Deccan Trap lavas and their genetic implications. *Geol. Soc. India Mem.* **3**; 394-418.
- KUSHIRO, I. (1960) Si-Al relations in clinopyroxenes from igneous rocks. *Am. J. Sci.* **258**; 548-554.
- KUSHIRO, I. (1972) Effect of water on the composition of magmas formed at high pressures. *J. Petrol.* **13**; 311-334.
- KYLE, P.R. (1980) Development of heterogeneities in the sub-continental mantle: evidence from the Ferrar Group, Antarctica. *Contrib. Mineral. Petrol.* **73**; 89-104.
- KYLE, P.R., ELLIOT, D.H. & SUTTER, J.F. (1981) Jurassic Ferrar Supergroup tholeiites from the Transantarctic Mountains, Antarctica, and their relation to the initial fragmentation of Gondwana. In: Cresswell, M. & Vella, P. (eds). A. A. Balkema, Rotterdam **5**; 283-287.
- KYLE, P.R., PANKHURST, R.J. & BOWMAN, J.R. (1983) Isotopic and chemical variations in Kirkpatrick Basalt Group rocks from southern Victoria Land. In: *Antarctic Earth Science*. Aus. Acad. Sci.; 234-237.
- KYLE, P., PANKHURST, R., MOORBATH, S. & BOWMAN, J. (1987) Nature and development of an enriched mantle source for Jurassic Ferrar tholeiites, Transantarctic Mountains, Antarctica. *Terra Cognita* **7**; 614.
- LANGMUIR, C.H., BENDER, J.F., BENCE, A.E. & HANSON, G.N. (1977) Petrogenesis of basalts from the FAMOUS area: Mid-Atlantic Ridge. *Earth Planet. Sci. Lett.* **36**; 133-156.
- LEAMAN, D.E. (1972) Gravity survey of the Hobart district. *Geol. Surv. Bull. Tas.* **52**.
- LEAMAN, W.P., BUDAHN, J.R., GERLACH, D.C., SMITH, D.R. & POWELL, B.N. (1980) Origin of Hawaiian tholeiites: trace element constraints. *Am. J. Sci.* **280A**; 794-819.

- LE MAITRE, R.W. (1968) Chemical variation within and between volcanic rock series - a statistical approach. *J. Petrol.* 9; 220-252.
- LINDSLEY, D.H. (1965) Ferrosilite. *Carnegie Inst. Wash. Yearbook* 64; 148-149.
- LINDSLEY, D.H. (1981) The formation of pigeonite in the join hedenbergite-ferrosilite at 11.5 and 15kbar: experiments and a solution model. *Am. Mineral.* 66; 1175-1182.
- LINDSLEY, D.H. (1983) Pyroxene Thermometry. *Am. Mineral.* 68; 477-493.
- LINDSLEY, D.H. & MUNOZ, J.L. (1969) Subsolidus relations along the join hedenbergite - ferrosilite. *Am. J. Sci.* 267A (Shairer Volume); 295-324.
- MACDOUGALL, J.D. (1986) Isotopic composition of Deccan and ocean ridge basalts: implications for their mantle sources. *J. Geol. Soc. India.* 27; 38-46.
- MAHONEY, J.J., MACDOUGALL, J.D., LUGMAIR, G.W., GOPALAN, K. & KRISHNAMURTHY, P. (1985) Origin of contemporaneous tholeiitic and K-rich alkalic lavas: a case study from the northern Deccan Plateau, India. *Earth Planet. Sci. Lett.* 72; 39-53.
- MAHONEY, J.J., MACDOUGALL, J.D., LUGMAIR, G.W., MURALI, A.V., SANKAR, M. & GOPALAN, K. (1982) Origin of the Deccan Trap flows at Mahabaleshwar inferred from Nd and Sr isotopic and chemical evidence. *Earth Planet. Sci. Lett.* 60; 47-60.
- MANTOVANI, M.S.M., MARQUES, L.S., DE SOUSA, M.A., CIVETTA, L., ATALLA, L. & INNOCENTI, F. (1985) Trace element and strontium isotope constraints on the origin and evolution of Paraná continental flood basalts of Santa Catarina State (Southern Brazil). *J. Petrol.* 26; 187-209.
- MARSH, J.S. & EALES, H.V. (1984) The chemistry and petrogenesis of igneous rocks of the Karoo Central Area, southern Africa. *Spec. Publ. geol. Soc. S. Afr.* 13; 27-67.
- MCBIRNEY, A.R. & NOYES, R.M. (1979) Crystallization and layering of the Skaergaard intrusion. *J. Petrol.* 20; 487-554.
- MCDONOUGH, W.F., McCULLOCH, M.T. & SUN, S. -S. (1985) Isotopic and geochemical systematics in Tertiary-Recent basalts from southeastern Australia and implications for the evolution of the sub-continental mantle. *Geochim. Cosmochim. Acta* 49; 2051-2067.
- MCDUGALL, I. (1961) Optical and chemical studies of pyroxenes in a differentiated Tasmanian dolerite. *Am. Mineral.* 46; 661-687.
- MCDUGALL, I. (1962) Differentiation of the Tasmanian dolerites: Red Hill dolerite-granophyre association. *Geol. Soc. Am. Bull.* 73; 279-316.
- MCDUGALL, I. (1963) Potassium-argon age measurements on dolerites from Antarctica and South Africa. *J. Geophys. Res.* 68; 1535-1545.
- MCDUGALL, I. (1964) Differentiation of the Great Lake dolerite sheet Tasmania. *J. Geol. Soc. Aus.* 11; 107-132.
- MCDUGALL, I. & LEGGO, P.J. (1965) Isotopic age determinations on granite rocks from Tasmania. *J. Geol. Soc. Aust.* 12; 295-332.
- MCDUGALL, I. & LOVERING, J.F. (1963) Fractionation of chromium, nickel, cobalt and copper in a differentiated dolerite-granophyre sequence at Red Hill, Tasmania. *J. Geol. Soc. Aus.* 10; 325-338.
- MCDUGALL, I. & WELLMAN, P. (1976) Potassium-argon ages for some Australian Mesozoic igneous rocks. *J. Geol. Soc. Aust.* 23; 1-9.

- MCKELVEY, B.C. & WEBB, P.N. (1959) Geological investigations in South Victoria Land, Antarctica. Part 2- geology of Upper Taylor Glacier Region. *N.Z. J. Geol. Geophys.* 2; 718-728.
- MCLENNAN, S.M. & TAYLOR, S.R. (1981) Role of subducted sediments in island-arc magmatism: constraints from REE patterns. *Earth Planet. Sci. Lett.* 54; 423-430.
- MENSING, T.M., FAURE, G., JONES, L.M., BOWMAN, J.R. & HOEFS, J. (1984) Petrogenesis of the Kirkpatrick Basalt, Solo Nunatak, northern Victoria Land, Antarctica, based on isotopic compositions of strontium, oxygen and sulfur. *Contrib. Mineral. Petrol.* 87; 101-108.
- MILNES, A.R., COOPER, B.J. & COOPER, J.A. (1982) The Jurassic Wisanger Basalt of Kangaroo Island, South Australia. *Trans. Royal Soc. S. Aust.* 106; 1-13.
- MUIR, I.D. (1951) The clinopyroxenes of the Skaergaard intrusion, eastern Greenland. *Mineral. Mag.* 29; 690-714.
- MUTTER, J.C., HEGARTY, K.A., CANDE, S.C. & WEISSEL, J.K. (1985) Breakup between Australia and Antarctica: a brief review in the light of new data. *Tectonophysics* 114; 255-279.
- NAKAMURA, E., CAMPBELL, I.H. & SUN, S. -S. (1985) The influence of subduction processes on the geochemistry of Japanese alkaline basalts. *Nature* 316; 55-58.
- NASLAND, H.R. (1987) Lamellae of baddeleyite and Fe-Cr-Spinel in ilmenite from the Basistoppen Sill, East Greenland. *Can. Mineral.* 25; 91-96.
- NEWSOM, H.E., WHITE, W.M., JOCHUM, K.P. & HOFMANN, A.W. (1986) Siderophile and chalcophile element abundances in oceanic basalts, Pb isotope evolution and growth of the Earth's core. *Earth Planet. Sci. Lett.* 80; 299-313.
- NICHOLLS, I.A. (1974) Liquids in equilibrium with perioditic mineral assemblages at high water pressures. *Contrib. Mineral. Petrol.* 45; 289-316.
- NIELSON, R.L. & DUNGAN, M.A. (1983) Low pressure mineral-melt equilibria in natural anhydrous mafic systems. *Contrib. Mineral. Petrol.* 84; 310-326.
- NORRISH, K. & CHAPPELL, B.W. (1967) X-ray fluorescence spectrometry. In: *Physical Methods in Determinative Mineralogy*. Academic Press, London; 161-214.
- NORRISH, K. & HUTTON, J.T. (1969) An accurate X-ray spectrographic method for the analysis of a wide range of geological samples. *Geochim. Geophys. Acta.* 33; 431-453.
- O'REILLY, S.Y. & GRIFFIN, W.L. (1984) Sr isotopic heterogeneity in primitive basaltic rocks, southeastern Australia: correlation with mantle metasomatism. *Contrib. Mineral. Petrol.* 87; 220-230.
- OVERSBY, V.M. & EWART, A. (1972) Lead isotopic compositions of Tonga-Kermadec Volcanics and their petrogenetic significance. *Contrib. Mineral. Petrol.* 37; 181-210.
- PALACZ, Z.A. & SAUNDERS, A.D. (1986) Coupled trace element and isotope enrichment in the Cook-Austral-Samoa islands, southwest Pacific. *Earth Planet. Sci. Lett.* 79; 270-280.
- PAUL, D.K., KRESTEN, P., BARMAN, T.R., MCNUTT, R.H. & BRUNFELT, A.O. (1984) Geochemical and Petrological Relations in some Deccan basalts, Western Maharashtra, India. *J. Volcan. Geotherm. Res.* 21; 165-176.
- PHILPOTTS, J.A. & SCHNETZLER, C.C. (1968) Genesis of Continental Diabases and Oceanic Tholeiites considered in light of rare-earth and barium abundances and partition coefficients. In: *Origin and Distribution of the Elements*. L. H. Ahrens (ed) Pergamon

Press; 939-947.

- POLDERVAART, A. & HESS, H.H. (1951) Pyroxenes in the crystallization of basaltic magma. *J. Geol.* **59**; 472-489.
- POTTS, P.J., THORPE, O.W., ISAACS, M.C. WRIGHT, D.W. (1985) High-precision instrumental neutron-activation analysis of geological samples employing simultaneous counting with both planar and coaxial detector. *Chem Geol.* **48**; 145-155.
- PRESTVIK, T & GOLES, G.G. (1985) Comments in petrogenesis and the tectonic setting of Columbia River Basalts. *Earth Planet. Sci. Lett.* **72**; 65-73.
- REX, D.C. (1972) K-Ar age determinations on volcanic and associated rocks from the Antarctic Peninsula and Dronning Maud Land. In: *Antarctic Geology and Geophysics*. Adie, R.J. (ed). Oslo University; 133-136.
- RICHARDSON, S.H., ERLANK, A.J., DUNCAN, A.R. & REID, D.L. (1982) Correlated Nd, Sr and Pb isotope variations in Walvis Ridge basalts and implications for the evolution of their mantle source. *Earth Planet. Sci. Lett.* **34**; 327-342.
- RICHARDSON, R.G. (1980) Crustal Seismology. Unpublished PhD. Thesis. University of Tasmania.
- ROBINSON, E.S. & SPLETTSTOESSER, J.F. (1984) Structure of the Transantarctic Mountains determined from geophysical surveys. In: *Geology of the Central Transantarctic Mountains*. Turner, M.D. & Splettstoesser, J.F. (eds). Am. Geophys. Union; 119-162.
- ROEDER, P.L. & EMSLIE, R.F. (1970) Olivine-liquid equilibrium. *Contrib. Mineral. Petrol.* **29**; 275-289.
- RUDNICK, R.L., MCDONOUGH, W.F., MCCULLOCH, M.T. & TAYLOR, S.R. (1986) Lower crustal xenoliths from Queensland, Australia: Evidence for deep crustal assimilation and fractionation of continental basalts. *Geochim. Cosmochim. Acta* **50**; 1099-1115.
- SASS, J.H. & LACHENBRUCH, A.H. (1979) Thermal regime of the Australian continental crust. In: *The Earth - its origin, structure and evolution*. McElhinny, M.W. (ed). Academic Press; 301-347.
- SCHMIDT, P.W. & MCDUGALL, I. (1977) Paleomagnetic and potassium-argon dating studies of the Tasmanian Dolerites. *J. Geol. Soc. Aust.* **25**; 321-328.
- SEN, G. (1986) Mineralogy and petrogenesis of the Deccan Trap Lava flows around Mahabaleshwar, India. *J. Petrol.* **27**; 627-663.
- SHIMIZU, N. & HART, S.R. (1982) Applications of the ion microprobe to geochemistry and cosmochemistry. *Ann. Rev. Earth Planet. Sci.* **10**; 483-526.
- SIDERS, M.A. & ELLIOT, D.H. (1983) Intraflow variability in the Kirkpatrick Basalt, Northern Victoria Land, Antarctica. *Geol. Soc. Am. Abs. Prog.* **15**; 687.
- SIDERS, M.A. & ELLIOT, D.H. (1985) Major and trace element geochemistry of the Kirkpatrick Basalt, Mesa Range, Antarctica. *Earth Planet. Sci. Lett.* **72**; 54-64.
- SLAWSON, W.F. (1983) Isotopic composition of lead from a paleo-island arc: Shasta, California. *Can. J. Earth Sci.* **20**; 1521-1527.
- SOLOMON, M. (1962) The tectonic history of Tasmania. In: *Geology of Tasmania*. Spry, A. & Banks, M.R. (eds). ;311-339.
- SPARKS, R.S.J. & HUPPERT, H.E. (1984) Density changes during the fractional crystallization of basaltic magmas: fluid dynamic implications. *Contrib. Mineral. Petrol.* **85**; 300-309.

- SPARKS, R.S.J., HUPPERT, H.E. & TURNER, J.S. (1984) The fluid dynamics of evolving magma chambers. *Phil. Trans. Royal Soc. Lond.* 310A; 511-534.
- SPARKS, R.S.J., MEYER, P. & SIGURDSSON, H. (1980) Density variation amongst mid-ocean ridge basalts: implications for magma mixing and the scarcity of primitive lavas. *Earth Planet. Sci. Lett.* 46; 419-430.
- SPEER, J.A. (1980) Chapter 3: Zircon. *Rev. Mineral. Mineral. Soc. Am.* 5; 67-112.
- SPENCER, K.J. & LINDSLEY, D.H. (1981) A solution model for coexisting iron-titanium oxides. *Am. Mineral.* 66; 1189-1201.
- SPRY, A. (1962) Igneous Activity. In: *The Geology of Tasmania*. Spry, A. & Banks, M.R.; 255-284.
- STARIK, I. YE., RAVICH, M. G., KRYLOV, A. YA. & SILIN, YV. I. (1959) The absolute age of the rocks of the East Antarctic Platform. *Dokl. Akad. Nank. SSSR.* 126; 144-146.
- STEIGER, R.H. & JAGER, E. (1977) Subcommittee on geochronology: convention on the use of decay constants in geo- and cosmochemistry. *Earth Planet. Sci. Lett.* 36; 359-362.
- STUMP, E. WHITE, A.J.R. & BORG, S.G. (1986) Reconstruction of Australia and Antarctica: evidence from granites and recent mapping. *Earth Planet. Sci. Lett.* 79; 348-360.
- SUN, S.-S. (1980) Lead isotopic study of young volcanic rocks from mid-ocean ridges, ocean islands, and island rocks. *Phil. Trans. Royal Soc. Lond.* 297A; 409-445.
- SUN, S.-S. (1982) Chemical composition of the earth's primitive mantle. *Geochim. Cosmochim. Acta* 46; 179-192.
- SUN, S.-S. & MCDONOUGH, W.F. (1987) Composition of the Earth's primitive mantle and implications for its evolution. (Submitted for publication).
- SUN, S.-S. & NESBITT, R.W. (1978) Geochemical regularities and genetic significance of ophiolitic basalts. *Geology* 6; 689-693.
- SUN, S.-S., NESBITT, R.W. & SHARASKIN, A.Y. (1979) Geochemical characteristics of mid-ocean ridge basalts. *Earth Planet. Sci. Lett.* 44; 119-138.
- TAYLOR Jr., H.P. (1974) The application of oxygen and hydrogen isotope studies to problems of hydrothermal alteration and ore deposition. *Econ. Geol.* 69; 843-883.
- TAYLOR, S.R. & MCLENNON, S.M. (1985) The Continental Crust: its composition and evolution. Hallam, A. (ed). Blackwell Scientific Publications; 312pp
- THOMPSON, R.N., MORRISON, M.A., DICKIN, A.P. & HENDRY, G.L. (1983) Continental flood basalts... arachnids rule OK? In: *Continental Basalts and Mantle Xenoliths*. Hawkesworth, C.J. & Norry, M. J. (eds). Shiva Ltd.; 158-185.
- TURNER, J.S. & CAMPBELL, I.H. (1986) Convection and mixing in magma chambers. *Earth Sci. Rev.* 23; 255-352.
- TURNER, J.S. & GUSTAFSON, L.B. (1981) Fluid motions and compositional gradients produced fractional crystallization or melting at vertical boundaries. *J. Volcanol. Geothermal. Res.* 11; 93-125.
- VEEVERS, J.J., MACPOWELL, C. & JOHNSON, B.D. (1981) Seafloor constraints on the reconstruction of Gondwana. In: *Gondwana Five*. Crisswell, M.M. & Vella, P. (eds). A. A. Balkema, Rotterdam; 267.
- VIDAL, P., CHAUVEL, C. & BROUSSE, R. (1984) Large mantle heterogeneity beneath French

Polynesia. *Nature* 307; 536-538.

- WAGER, L.R. & BROWN, G.M. (1968) *Layered Igneous Rocks*. Oliver and Boyd, Edin. & Lond.; pp588.
- WALKER, D.A. & CAMERON, W.E. (1983) Boninite primary magmas: evidence from the Cape Vogel Peninsula, PNG. *Contrib. Mineral. Petrol.* 83; 150-158.
- WALKER, F. (1961) The causes of variation in dolerite intrusions. In: *Dolerite: a symposium*. Uni. Tas.; 1-25.
- WALKER, K.R., WARE, N.G. & LOVERING, J.F. (1973) Compositional variation of the pyroxenes of the differentiated Palisades Sill, New Jersey. *Geol. Soc. Am. Bull.* 84; 89-110.
- WATSON, E.B. & HARRISON, T.M. (1983) Zircon saturation revisited: temperature and composition effects in a variety of crustal magma types. *Earth Planet. Sci. Lett.* 64; 295-304.
- WEAVER, B.L. & TARNEY, J. (1981) The Scourie Dyke suite: petrogenesis and geochemical nature of the Proterozoic sub-continental mantle. *Contrib. Mineral. Petrol.* 78; 175-188.
- WEAVER, B.L. & TARNEY, J. (1984) Empirical approach to estimating the composition of the continental crust. *Nature* 310; 575-577.
- WEBB, P.N. (1962) Isotope ages of Antarctic rocks: a summary. *N.Z. J. Geol. Geophys.* 5; 790-796.
- WEGENER, A. (1912) Die Entstehung der Kontinente. *Petermanns Geogr. Mitt.* 58.
- WHITE, A.J.R. & CHAPPELL, B.W. (1983) Granitoid types and their distribution in the Lachlan Fold Belt, southeastern Australia. *Geol. Soc. Am. Mem.* 159; 21-34.
- WHITE, W.M. & HOFMANN, A.W. (1982) Sr and Nd isotope geochemistry of oceanic basalts and mantle evolution. *Nature* 296; 821-825.
- WILKINSON, J.F.G. (1986) Classification and average compositions of common basalts and andesites. *J. Petrol.* 27; 31-62.
- WILLIAMS, C.T. (1978b) Uranium-enriched minerals in mesostasis areas of the Rhum layered pluton. *Contrib. Mineral. Petrol.* 66; 29-39.
- WILLIAMS, E. (1978a) Tasman Fold Belt system in Tasmania. *Tectonophysics* 48; 159-205.
- WOOD, D.A. (1978) Major and trace element variations in the Tertiary lavas of Eastern Iceland and their significance with respect to the Iceland geochemical anomaly. *J. Petrol.* 19; 393-436.
- WOOD, D.A. (1979) A variably veined suboceanic upper mantle - genetic significance for mid-ocean ridge basalts from geochemical evidence. *Geology* 7; 499-503.
- WRIGHT, E. & WHITE, W.M. (1986/1987) The origin of Samoa: new evidence from Sr, Nd, and Pb isotopes. *Earth Planet. Sci. Lett.* 81; 151-162.
- WYBORN, L.A.I. & PAGE, R.W. (1983) The Proterozoic Kalkadoon and Ewen Batholiths, Mount Isa Inlier, Queensland: source, chemistry, age and metamorphism. *BMR J. Aust. Geol. Geophys.* 8; 53-69.